

# The landscape of QCD axion models

Luca Di Luzio

*Deutsches Elektronen-Synchrotron DESY, Notkestraße 85, D-22607 Hamburg, Germany*

Maurizio Giannotti

*Physical Sciences, Barry University, 11300 NE 2nd Ave., Miami Shores, FL 33161, USA*

Enrico Nardi\*

*INFN, Laboratori Nazionali di Frascati, C.P. 13, I-00044 Frascati, Italy*

Luca Visinelli

*Gravitation Astroparticle Physics Amsterdam (GRAPPA),  
Institute for Theoretical Physics Amsterdam and Delta Institute for Theoretical Physics,  
University of Amsterdam, Science Park 904, 1098 XH Amsterdam, The Netherlands*

*NOTE: First draft. We welcome comments, corrections, suggestions. For missing references we kindly ask to specify in relation to which topic and at which point of the review it would be appropriate to include a citation. We will not be able to address unspecifed requests. (Please email all the authors.)*

---

## Abstract

We review the landscape of QCD axion models. Theoretical constructions that extend the window for the axion mass and couplings beyond conventional regions are highlighted and classified. Bounds from cosmology, astrophysics and experimental searches are reexamined and updated.

*Keywords:* Axion phenomenology, axion cosmology and astrophysics, axion models

---

---

\*Corresponding author

*Email addresses:* `luca.diluzio@desy.de` (Luca Di Luzio), `MGiannotti@barry.edu` (Maurizio Giannotti), `enrico.nardi@lnf.infn.it` (Enrico Nardi), `l.visinelli@uva.nl` (Luca Visinelli)

## Contents

<b>1</b>	<b>Introduction</b>	<b>4</b>
<b>2</b>	<b>From the strong CP problem to the QCD axion</b>	<b>7</b>
2.1	QCD vacuum structure . . . . .	7
2.2	Dependence of the QCD vacuum energy on $\theta$ . . . . .	10
2.3	Neutron EDM and the strong CP problem . . . . .	12
2.4	Musings on the strong CP problem . . . . .	13
2.4.1	Solutions without axions . . . . .	13
2.4.2	Peccei Quinn mechanism . . . . .	14
2.5	Axion effective Lagrangian . . . . .	15
2.5.1	Axion potential and axion mass . . . . .	16
2.5.2	Axion-pion coupling . . . . .	17
2.5.3	Axion-photon coupling . . . . .	18
2.5.4	Axion-nucleon coupling . . . . .	18
2.5.5	Axion-electron coupling . . . . .	19
2.6	Origin of model-dependent axion couplings . . . . .	19
2.7	Benchmark axion models . . . . .	20
2.7.1	KSVZ axion . . . . .	21
2.7.2	DFSZ axion . . . . .	22
2.8	Summary of flavour and CP conserving axion couplings . . . . .	25
2.9	Flavour violating axion couplings . . . . .	26
2.10	CP-violating axion couplings . . . . .	27
2.11	The dirty side of the axion . . . . .	28
<b>3</b>	<b>Axion cosmology</b>	<b>31</b>
3.1	Basics of cosmology and thermodynamics in the early Universe . . . . .	31
3.2	The axion potential and the axion mass at finite temperature . . . . .	33
3.3	Vacuum realignment mechanism . . . . .	34
3.4	The contribution from topological defects . . . . .	38
3.4.1	Cosmic axion strings . . . . .	39
3.4.2	String populations . . . . .	39
3.4.3	Spectrum of radiated axions . . . . .	41
3.4.4	Cosmological domain walls . . . . .	42
3.5	Axion isocurvature fluctuations . . . . .	42
3.6	Cosmological bounds on the axion mass . . . . .	44
3.7	Benchmark axion mass region for $\Omega_a \simeq \Omega_{\text{CDM}}$ . . . . .	45
3.7.1	Post-inflationary scenario . . . . .	45
3.7.2	Pre-inflationary scenario . . . . .	45
3.7.3	Summary of cosmological axion bounds . . . . .	46
3.8	QCD axions as dark radiation . . . . .	48
3.9	Axion miniclusters and axion stars . . . . .	50
<b>4</b>	<b>Astrophysical signatures and bounds</b>	<b>52</b>
4.1	Axion-photon coupling . . . . .	53
4.2	Axion-electron coupling . . . . .	57
4.3	Axion-nucleon coupling . . . . .	60
4.4	Axion coupling to the neutron EDM . . . . .	62
4.5	Axion CP-odd couplings . . . . .	62
4.6	Axion coupling to gravity and black hole superradiance . . . . .	63
4.7	Summary of astrophysical bounds . . . . .	63

<b>5</b>	<b>Experimental Searches</b>	<b>67</b>
5.1	Solar axions and helioscopes . . . . .	67
5.2	Helioscopes sensitivity to $g_{a\gamma}$ and $g_{ae}$ . . . . .	68
5.3	DM axions and haloscopes . . . . .	71
5.4	Searches for axions produced in the laboratory . . . . .	73
5.5	Summary of experimental constraints . . . . .	74
<b>6</b>	<b>The axion landscape beyond benchmarks</b>	<b>78</b>
6.1	Enhancing/suppressing $g_{a\gamma}$ . . . . .	78
6.1.1	KSVZ-like scenarios . . . . .	79
6.1.2	DFSZ-like scenarios . . . . .	83
6.1.3	Enhancing $g_{a\gamma}$ above the KSVZ and DFSZ benchmarks . . . . .	85
6.2	Enhancing/suppressing $g_{ae}$ . . . . .	86
6.2.1	Enhancing $g_{ae}$ in KSVZ-like scenarios . . . . .	86
6.2.2	Enhancing $g_{ae}$ in DFSZ-like scenarios . . . . .	87
6.2.3	Suppressing $g_{ae}$ in DFSZ-like scenarios: the electrophobic axion . . . . .	88
6.3	Enhancing/suppressing $g_{aN}$ . . . . .	88
6.3.1	Enhancing $g_{aN}$ . . . . .	89
6.3.2	Suppressing $g_{aN}$ : the nucleophobic axion . . . . .	89
6.4	Enhanced axion couplings and astrophysics . . . . .	92
6.5	Flavour violating axions . . . . .	94
6.5.1	Generation dependent Peccei-Quinn symmetries . . . . .	96
6.5.2	Constraints on flavour violating axion couplings . . . . .	97
6.6	Extending the mass region region for dark matter axions . . . . .	99
6.6.1	Non-standard cosmological evolution . . . . .	100
6.6.2	Modifying the $m_a$ - $f_a$ relation or the axion mass function $m_a(T)$ . . . . .	101
6.6.3	Dark Matter from axion initial velocity . . . . .	104
6.7	Super-heavy axions . . . . .	104
<b>7</b>	<b>Axions and...</b>	<b>107</b>
7.1	Axions and neutrino masses . . . . .	107
7.2	Axions and baryon asymmetry . . . . .	107
7.3	Axions and inflation . . . . .	108
7.4	Solutions to the domain walls problem . . . . .	110
7.5	Solutions to the Peccei Quinn quality problem . . . . .	111
7.6	Axions and composite dynamics . . . . .	113
7.7	Axions and GUTs . . . . .	113
<b>8</b>	<b>Concluding remarks and <i>desiderata</i></b>	<b>115</b>
	<b>Acknowledgments</b>	<b>117</b>
	<b>Appendix A: Tables of notations and of acronyms</b>	<b>118</b>
	<b>References</b>	<b>121</b>

## 1. Introduction

At the dawn of the third decade of the third millennium, particle physics seems stranded in an awkward intrigue. The celebrated theoretical construction known as the Standard Model (SM) has been established as the correct description of fundamental phenomena down to scales of the order of  $10^{-16}$  cm. However, a certain number of observations including dark matter (DM), neutrino masses  $m_\nu$ , and the cosmological matter-antimatter asymmetry  $\eta_b$ , remain unaccounted within the SM, and constitute indisputable evidences that the present theory must be extended. Besides this, the SM discomfits particle physicists because of a certain number of theoretical distresses generically related with exceedingly small numbers, that are usually referred to as problems of naturalness, as for example the value of the cosmological constant (dark energy) in units of the Planck mass  $\Lambda \sim 10^{-31} m_{\text{Pl}}$ , the electroweak breaking vacuum expectation value (VEV)  $v \sim 10^{-17} m_{\text{Pl}}$ , the CP violating QCD angle  $\theta \lesssim 10^{-10}$ .<sup>1</sup>

Theoretical constructions that extend the SM are clearly more appealing when they are able to solve more than one of the previous issues with the same amount of theoretical input. A well known case is supersymmetry equipped with an  $R$ -parity symmetry to forbid fast proton decay, which protects the value of  $v/m_{\text{Pl}}$  from quantum corrections, and at the same time predicts that a new stable particle, which shares all the properties of a good DM candidate, must exist. Another example is the type-I seesaw model for neutrino masses which, besides accounting for the suppression of the neutrino mass scale [6–9], can also yield quite naturally a cosmological baryon asymmetry of the correct size [10]. The serious drawbacks of these two theories are that supersymmetry has not been found at the LHC, while the experimental verification of type-I seesaw leptogenesis remains well outside the reach of all current experiments [11–15].

A third example of a ‘two birds with one stone’ theory is provided by the axion [16, 17]. In an effective field theory (EFT) description, the SM is extended by introducing a single new massless pseudo-scalar particle  $a$ , the axion, for which only one coupling is mandatory, namely an effective coupling to the CP violating topological gluon density  $(a/f_a + \theta)G\tilde{G}$ , where  $f_a$  is the scale of the effective operator,  $G = G_{\mu\nu}$  is the gluon field strength tensor,  $\tilde{G}_{\mu\nu}$  its dual, and we have added to the axion-gluon operator the infamous CP violating  $\theta$  term. Such a simple extension has astonishingly far reaching consequences: the strong CP problem is solved because the minimum of the vacuum energy occurs when the coefficient of  $G\tilde{G}$  vanishes [18]. Thus, by acquiring a suitable VEV, the axion disposes of the perilous CP violating operator. In performing this task, the axion acquires a tiny mass, and in this process a cosmological population of zero momentum excitations, which nowadays still sums to the energy density of the Universe, is unavoidably produced. Hence axions definitely contribute to the DM. Whether they can wholly account for it remains, for the time being, an open question. Solving the strong CP problem and providing a natural DM candidate by no means exhausts the role of axions in fundamental physics. Axion phenomenology crosses boundaries between particle physics, astrophysics and cosmology, it is replete with interdisciplinary connections which have already provided fruitful insights into different domains of physics. Axions have unusually intriguing features, although deeply interwoven with QCD, they interact more feebly than all SM particles, and although their typical mass is much smaller than the mass of at least two types of neutrinos, they might dominate the matter content of our Universe. Moreover, differently from the case of supersymmetry, current experimental searches have so far only been able to cut out relatively small regions of the parameter space in which the QCD axion can naturally live, but differently from leptogenesis, the axion hypothesis is within the reach of experimental verification, and it is conceivable, for example, that the canonical axion DM mass window could be thoroughly explored within the next one or two decades. If ever discovered, there is little doubt that the existence of axions would reshape more than one branch of fundamental physics.

The axion has been so far introduced by postulating a non-renormalizable axion-gluon operator. In quantum field theory (QFT) there is a simple prescription for constructing a renormalizable completion whose low-energy limit matches the required form of the effective action density. What is needed is a

---

<sup>1</sup>These small number problems do not stand on the same footing. For example a tiny value of  $\theta$  is *technically natural*, in the sense that it does not get lifted by quantum corrections. On the other hand, while anthropic or environmental selection arguments can provide explanations for the values of  $\Lambda$  [1] and  $v$  [2, 3], a value of  $\theta_{\text{QCD}}$  many orders of magnitude larger than the experimental limit would still leave our Universe basically unaffected [4, 5].

Lagrangian equipped with a global  $U(1)_{\text{PQ}}$  symmetry, exact at the classical level but broken at the quantum level by a colour anomaly, that undergoes spontaneous breaking at some high energy scale. Such a symmetry is known as Peccei-Quinn (PQ) symmetry after its proposers [19, 20].<sup>2</sup> As we will see in the next sections, the pseudo-Nambu Goldstone Boson (pNGB) resulting from such a broken symmetry exhibits precisely the properties required for an axion.

The result of dressing the QFT prescription with a complete model is, however, far from being unique. For example, in many cases different realizations of the PQ symmetry give rise to axions that do not interact only with the gluons, but that couple also to other SM particles. This indeed enriches in many aspects the subject of axion phenomenology. In particular, it provides additional important channels for experimental axion searches. However, the continuous proliferation of new theoretical constructions, that has received a major boost especially in recent years, has brought to a state of affairs in which it is rather arduous for experimental and theoretical researchers to attain a sufficiently complete and reliable acquaintance with the vast literature on axion models. Hence, we believe that an updated account of new (and old) theoretical ideas in axion model building, which we feel is lacking in the literature, could be timely and useful.

The aim of this work is to review the landscape of QFT realizations of the PQ symmetry.<sup>3</sup> A reasoned classification of the babel of axion models is accomplished by pinpointing theoretical constructions that predict unusual properties of the axion, especially in relation to the different experimental approaches that could be pursued for their detection, as for example enhanced or suppressed couplings to specific SM states, or unconventional mass regions where the axion could saturate the DM density. Although presently axion searches rely almost exclusively on axion couplings to photons, a number of novel detection concepts which exploit cutting-edge techniques has been recently put forth with the aim of searching for axions through their couplings to nucleons or electrons. Even if in most cases only pathfinder or demonstrative small-scale setups have been commissioned, generally with projected sensitivities that hardly reach into the parameter space regions hinted by most popular axion models, other less known theoretical constructions could be probed, constrained or ruled out by these experiments, which can then effectively contribute to circumscribe the realm of viable axion models. We thus expect that the experimental community of axion hunters could benefit from the classification scheme that we have adopted.

This Review is self contained, it includes pedagogical, but at the same time sufficiently detailed introductions to axion theory, cosmology, astrophysics and experimental searches, that are intended to provide guidance to the neophyte, whether she is a young student planning to orient her researches towards axion physics, or an experienced colleague active in a different domain of physics, but willing to get insights in a field that is currently experiencing a blooming phase. Experts in the field can instead browse quickly through the most pedagogical parts, and focus directly on the sections of their interest.

We start in Section 2 with a description of the origin of the strong CP problem and of the PQ mechanism that solves it. We then review model-independent properties of the axion (mass and couplings) illustrating how they can be derived from a chiral Lagrangian formulation. Model-dependent features are addressed here only for two popular benchmark constructions, universally known as KSVZ and DFSZ axion models. An introduction to flavour violating axion couplings and a brief discussion of CP violating couplings are also included. We conclude this section with some remarks about possible sources of explicit breaking of the PQ symmetry and the way they could endanger the effectiveness of the PQ mechanism. Excellent reviews exist in the literature that address in more depth some of these topics. Coleman’s Erice lectures [21] contain an enlightening treatment of the QCD vacuum and of the strong CP problem. Early reviews on axion theory can be found in Refs. [22–24]. More recent accounts are given in Ref. [25] and in the review of Kim and Carosi [26].

Section 3 addresses axion cosmology. After a basic introduction to the physics of the early Universe, we recall the properties of the axion potential and of the axion mass at temperatures around the QCD

---

<sup>2</sup>Historically, axion theory developed in the reverse order: the PQ symmetry was invented first, and only subsequently it was realized that the PQ mechanism implied the existence of a very light pseudo-scalar boson [16, 17].

<sup>3</sup>We will only target genuine QCD axion models, that is, models that generate an effective axion-gluon operator and that solve the strong CP problem. Other types of very light pseudo-scalar particles that share some of the properties of the QCD axion, but do not solve the strong CP problem, and that are commonly denoted as axion-like particles (ALPs), are not touched on in this Review.

phase transition. Then we describe the vacuum realignment mechanism as a source of a relic density of axions. The issue of cosmic topological defects which arise during axion-related phase transitions is also briefly addressed, as well as the constraints from axion isocurvature fluctuations that apply when the PQ symmetry is broken before inflation. Next we discuss the canonical mass window within which axions can saturate the DM relic density. We conclude this section with a brief overview of axion miniclusters and axion stars. An excellent review on the theory and cosmology of axions can be found in Ref. [27]. Another review of the cosmological role of axions, which also addresses the cosmology of axions superpartners in supersymmetric models, is Ref. [28]. A more recent and rather complete account of axion cosmology can be found in Ref. [29].

Section 4 is devoted to a thorough description of the role of axions in astrophysics. The layout of the discussion analyzes axion couplings to SM states one at the time, and describes in which particular stellar environment and for which reasons each coupling becomes particularly relevant. This section also contains an updated summary of astrophysical bounds on the different types of couplings. The astrophysics of axions has been the subject of thorough investigations since the time the axion was invented. The early reviews of Turner [30] and Raffelt [31] are still actual as concerns many qualitative aspects of axion astrophysics, and remain important references. Two accounts of astrophysical axion bounds dating around year 2006 can be found in Refs. [32] and [33]. A recent review which also includes an assessment of the astrophysical hints for the existence of axions which can be inferred from some anomalies observed in specific phases of stellar evolution can be found in Ref. [34].

Section 5 contains an account of the status of axion experimental searches (helioscopes, haloscopes, light shining through wall) and a summary of existing experimental constraints and projected limits that, at the time of writing, is up to date. However, in view of the continuous and rapid evolution of the experimental landscape, this part will likely become outdated in the not too distant future. Early accounts of experimental searches for invisible axions have been presented in Refs. [35, 36] and more recently in Ref. [37]. At the time of this writing, the most recent review, which is also remarkably complete, is Ref. [38].

Section 6 contains the central part of this Review. We begin with a systematic classification of models that predict sizable enhancements in the axion coupling to photons, electrons and nucleons. We describe the mechanisms at the basis of these enhancements, and we confront the resulting enlarged parameter space with current bounds. We then focus on models that predict flavour violating axion couplings to quarks and leptons, and we review the role played by existing limits on Flavour Changing Neutral Currents (FCNC) in constraining constructions of this type. Mechanisms that allow to extend the mass region in which axions can account for the whole of DM deserve particular attention, in view of the fact that the best experimental sensitivities to the axion-photon coupling are attained by haloscope experiments, which however can only probe rather narrow and pre-defined axion-DM mass intervals. We review models that implement the possibility of saturating the DM energy density for values of the axion mass both larger and smaller than the conventional values, and we explain through which mechanisms this result can be obtained. For completeness, we include at the end of this section a review of models in which the axions are ‘super-heavy’, namely with masses in excess of 100 keV.

In Section 7, we extend the discussion to a different set of axion-related topics. We first review constructions that attempt to connect axion physics to other unsolved SM issues, like neutrino masses, the cosmological baryon asymmetry, and inflation. Next we discuss possible solutions to a couple of well known problems that can generally affect model realizations of the PQ symmetry, namely how to maintain under control dangerous sources of explicit PQ breaking, and how to ensure that axion-related domain walls will not represent cosmological threats. The possibility that axions are composite states arising from a new strong dynamics is an old idea that has been recently revived, hence we present a survey of the related literature. We include a brief account of attempts to embed axions in GUT theories.

In the Appendix the reader can find a table with the symbols and notations that have been used in the mathematical expressions including an explanation of their meaning, a table containing the definition of the acronyms used in the text, and a table containing a list of current and planned axion experiments, with the relevant reference where the experimental setup is described.

## 2. From the strong CP problem to the QCD axion

This Section is devoted to the physical foundations of the QCD axion as a solution of the strong CP problem. We start by reviewing the non-trivial vacuum structure of Yang-Mills theories in Section 2.1 and the  $\theta$  dependence of the QCD vacuum energy in Section 2.2. Next, we discuss the  $\theta$  contribution to the neutron electric dipole moment (nEDM) in Section 2.3 and give a critical assessment of the strong CP problem and its possible solutions in Section 2.4, among which the axion solution via the Peccei Quinn (PQ) mechanism. The rest of the Section is devoted to the study of standard axion properties, starting from the axion effective Lagrangian in Section 2.5, including a general description of model-dependent axion couplings in Section 2.6, and continuing with a pedagogical derivation of the so-called benchmark axion models in Section 2.7. In Section 2.8 we provide a concise summary of standard axion properties, while Sections 2.9–2.10 are devoted to a basic introduction to flavour and CP violating axions. We conclude in Section 2.11 with the so-called PQ quality problem.

### 2.1. QCD vacuum structure

Until the mid of the 70's, when the formulation of Quantum Chromodynamics (QCD) was being developed, the so-called  $U(1)$  problem [39] was thought to be one of its major difficulties, while the absence of strong CP violation was believed to be one of its main successes [40, 41]. Few years later, with the discovery of Yang Mills instantons [42] and the non-trivial QCD vacuum structure [43, 44], this point of view was unexpectedly turned around. The solution of the  $U(1)$  problem brought as a gift the so-called strong CP problem. In order to present this story, which also provides the physical foundations of axion physics, let us start from the QCD Lagrangian<sup>4</sup>

$$\mathcal{L}_{\text{QCD}} = \sum_q \bar{q} (i\not{D} - m_q e^{i\theta_q}) q - \frac{1}{4} G^{a\mu\nu} G_{\mu\nu}^a + \theta \frac{g_s^2}{32\pi^2} G^{a\mu\nu} \tilde{G}_{\mu\nu}^a. \quad (1)$$

This Lagrangian contains two potential sources of CP violation: the phases of the quark masses  $\theta_q$ , and the so-called topological term, proportional to  $\theta$  (in short  $G\tilde{G}$ ). In fact, both  $\theta_q$  and  $\theta$  violate P and T (and hence CP). On the other hand, the  $G\tilde{G}$  operator can be written as a total derivative

$$G^{a\mu\nu} \tilde{G}_{\mu\nu}^a = \partial_\mu K^\mu = \partial_\mu \epsilon^{\mu\alpha\beta\gamma} \left( A_\alpha^a G_{\beta\gamma}^a - \frac{g_s}{3} f^{abc} A_\alpha^a A_\beta^b A_\gamma^c \right), \quad (2)$$

in terms of the Chern-Simons current,  $K^\mu$ , and hence it bears no effects in perturbation theory. However, classical configurations do exist for which the effects of this term cannot be ignored. These configurations are topological in nature, and can be identified by going to Euclidean space and writing the volume integral of the  $G\tilde{G}$  term as

$$\int d^4x G_{\mu\nu}^a \tilde{G}_{\mu\nu}^a = \int d^4x \partial_\mu K_\mu = \int_{S_3} d\sigma_\mu K_\mu, \quad (3)$$

where  $S_3$  is the three-sphere at infinity and  $d\sigma_\mu$  an element of its hypersurface. In order for these configurations to contribute to the path integral, we require that the gauge potentials are such that the field strength tensor  $G_{\mu\nu}^a$  vanishes as  $|x| \rightarrow \infty$  so that the action is finite. Besides  $A_\mu^a|_{S_3} = 0$ , other configurations that can be obtained from this by a gauge transformation also satisfy  $G_{\mu\nu}^a = 0$  at the boundary. In terms of the Lie algebra valued potential  $A_\mu = A_\mu^a T^a$  where  $T^a$  are the group generators, they read  $A'_\mu = U^{-1} A_\mu U + i g_s^{-1} U^{-1} \partial_\mu U$ , so that at the boundary  $A'_\mu = i g_s^{-1} U^{-1} \partial_\mu U$ . Configurations of this type are called a *pure gauges*. We are interested in pure gauges for which  $U$  cannot be continuously deformed into the identity in group space. To argue that such configurations exist, let us consider an  $SU(2)$  subgroup of  $SU(3)$  and let us restrict the gauge potentials defining  $K_\mu$  in the surface integral in Eq. (3) to this subgroup. Since  $SU(2)$  has  $S_3$  as group manifold, these potentials provide a mapping  $S_3 \rightarrow S_3$ . It can be shown that

<sup>4</sup>We adopt the following conventions:  $D_\mu = \partial_\mu - i g_s T^a A_\mu^a$ ,  $G_{\mu\nu}^a = \partial_\mu A_\nu^a - \partial_\nu A_\mu^a + g_s f^{abc} A_\mu^b A_\nu^c$  and  $\tilde{G}_{\mu\nu}^a = \frac{1}{2} \epsilon_{\mu\nu\rho\sigma} G^{\rho\sigma a}$ , with  $\epsilon^{0123} = -1$ . The latter convention is used in [45], while for instance Ref. [38] employs  $\epsilon^{0123} = +1$ .



for mappings of non-trivial topology the integral in Eq. (3) counts the number of times the hypersphere at infinity is wrapped around the  $S_3$  group manifold. More precisely  $\int d^4x G_{\mu\nu}^a \tilde{G}_{\mu\nu}^a = \frac{32\pi^2}{g_s^2} \nu$ , where  $\nu \in \mathbb{Z}$  is called winding number or Pontryagin index. Thus, in Euclidean space  $SU(2)$  field configurations of finite action fall in homotopy classes of different winding number. An important point is that it is not possible to deform a field configuration into another of different winding number while maintaining the action finite. As regards general  $SU(3)$  gauge field configurations, they can be classified in the same  $SU(2)$  homotopy classes, the reason being that any mapping from  $S_3$  into any simple Lie group  $G$  can be deformed into a mapping to a  $SU(2)$  subgroup of  $G$  in a continuous way [46], hence with no change of homotopy class. Configurations of unit winding number were explicitly constructed by Belavin, Polyakov, Schwartz and Tyupkin [42] who also showed that their finite action  $S_1 = \frac{8\pi^2}{g_s^2}$  corresponds to a minimum, which implies that they are solutions of the classical equation of motion in Euclidean space. Being of finite action, these gauge configuration are localised in all the four dimensions, which justifies the name *instantons*.

To assess the relevance of instantons let us return to physical Minkowski space and let us consider a gauge field configuration of winding number  $\nu$ . Choosing the temporal gauge  $A_0^a = 0$  so that  $K_i = 0$  allows to rewrite Eq. (3) as

$$\nu = \frac{g_s^2}{32\pi^2} \int d^4x G_{(\nu)\mu\rho}^a \tilde{G}_{(\nu)}^{a\mu\rho} \rightarrow \frac{g_s^2}{32\pi^2} \int d^4x \partial_0 K_{(\nu)}^0 = \frac{g_s^2}{32\pi^2} \int d^3x K_{(\nu)}^0(\mathbf{x}, t) \Big|_{t=-\infty}^{t=+\infty} = \nu. \quad (4)$$

This shows that  $\int d^4x G_{(\nu)} \tilde{G}_{(\nu)}$  corresponds to an interpolation from a pure gauge with winding number  $n$  at  $t = -\infty$ , to a different pure gauge configuration at  $t = +\infty$  with winding number  $m = n + \nu$ . More precisely, one can interpret (multi)instanton solutions as tunnelling from one  $G_{\mu\nu}^a = 0$  vacuum state  $|n\rangle$  to a gauge-rotated one with different winding number  $|m\rangle$  [47, 48]. In the semiclassical approximation the tunnelling probability is given by the exponential of the (multi)instanton action  $e^{-S_\nu}$  where  $S_\nu = \frac{8\pi^2}{g_s^2} \nu$  [43, 44], so that the effects of solutions with higher winding number  $\nu > 1$  [49, 50] are strongly suppressed with respect to instanton effects with action  $S_1$ , and hence of little interest.

An important remark is now in order. While the integral in Eq. (4) is gauge invariant, and hence the difference  $m - n = \nu$  is a physically meaningful number, the Chern-Simons current  $K^\mu$  by itself is not gauge invariant, which means that  $n$  and  $m$  labelling the vacuum states have no real physical meaning. This is also evidenced by the fact that the action of a gauge transformation of non-trivial winding number amounts to a relabelling  $U_{(1)}|n\rangle = |n+1\rangle$ . Clearly a more consistent definition of the physical vacuum is called for. Let us consider the linear combination

$$|\theta\rangle = \sum_{n=-\infty}^{+\infty} e^{in\theta} |n\rangle, \quad (5)$$

where  $\theta \in [0, 2\pi)$  is an angular parameter, which is known as the  $\theta$  vacuum.<sup>5</sup>

This vacuum state has the important property of being an eigenstate of the unitary operator of the gauge transformation

$$U_{(1)}|\theta\rangle = \sum_{n=-\infty}^{+\infty} e^{in\theta} |n+1\rangle = e^{-i\theta} |\theta\rangle, \quad (6)$$

so that is physically well-defined. The introduction of the  $\theta$  vacuum is also necessary to preserve locality and cluster decomposition [43, 52]. To see this, let us consider the expectation value of a local operator  $\mathcal{O}$  within a large Euclidean volume  $\Omega$

$$\langle \mathcal{O} \rangle_\Omega = \frac{\sum_\nu f(\nu) \int_\nu \mathcal{D}\phi e^{-S_\Omega[\phi]} \mathcal{O}[\phi]}{\sum_\nu f(\nu) \int_\nu \mathcal{D}\phi e^{-S_\Omega[\phi]}}, \quad (7)$$

<sup>5</sup>A less conventional and more intuitive way of introducing the  $\theta$  vacuum that relies on general quantum-mechanical principles applied to a Yang-Mills theory can be found in Ref. [51].



where  $\phi$  denotes all the fields of the theory,  $S_\Omega$  is the integral of the Lagrangian restricted to the volume  $\Omega$  and we have included the sum over all topological sectors  $\nu$ , with a general weight factor  $f(\nu)$ . Suppose now the volume  $\Omega$  is split into two large regions,  $\Omega = \Omega_1 + \Omega_2$ , with  $\mathcal{O}$  localized in  $\Omega_1$ . The integral in Eq. (7) can hence be split into

$$\langle \mathcal{O} \rangle_\Omega = \frac{\sum_{\nu_1, \nu_2} f(\nu_1 + \nu_2) \int_{\nu_1} \mathcal{D}\phi e^{-S_{\Omega_1}[\phi]} \mathcal{O}[\phi] \int_{\nu_2} \mathcal{D}\phi e^{-S_{\Omega_2}[\phi]}}{\sum_{\nu_1, \nu_2} f(\nu_1 + \nu_2) \int_{\nu_1} \mathcal{D}\phi e^{-S_{\Omega_1}[\phi]} \int_{\nu_2} \mathcal{D}\phi e^{-S_{\Omega_2}[\phi]}}, \quad (8)$$

with the constraint  $\nu = \nu_1 + \nu_2$ . The principle of cluster decomposition (which states that distant enough experiments must yield uncorrelated results) requires that the physics in the volume  $\Omega_2$  cannot affect the average of an observable localized in  $\Omega_1$ . In order for this to be true one needs

$$f(\nu_1 + \nu_2) = f(\nu_1)f(\nu_2), \quad (9)$$

so that the volume  $\Omega_2$  cancels out in the ratio of Eq. (8). Remarkably, this fixes the form of  $f(\nu)$  to be

$$f(\nu) = e^{i\theta\nu}, \quad (10)$$

where  $\theta$  is a free parameter.

A notable property of  $\theta$  is the fact that its value cannot be changed via the action of a gauge invariant operator. This can be seen by considering the time ordered product of a set of gauge invariant operators  $\mathcal{O}_1 \mathcal{O}_2 \dots$  between two different vacuum states

$$\langle \theta' | T(\mathcal{O}_1 \mathcal{O}_2 \dots) | \theta \rangle = \sum_{m, n} e^{i(n\theta - m\theta')} \langle m | T(\mathcal{O}_1 \mathcal{O}_2 \dots) | n \rangle = \sum_{m, n} e^{i(n\theta - m\theta')} F(\nu), \quad (11)$$

where in the last step we have emphasized that the matrix element depends only on the difference  $\nu = n - m$ , because  $\Omega_1 T(\mathcal{O}_1 \mathcal{O}_2 \dots) \Omega_1^{-1} = T(\mathcal{O}_1 \mathcal{O}_2 \dots)$  and hence both  $n$  and  $m$  are shifted by the same amount under a large gauge transformation. Then Eq. (11) becomes:

$$\langle \theta' | T(\mathcal{O}_1 \mathcal{O}_2 \dots) | \theta \rangle = \sum_n e^{in(\theta - \theta')} \sum_\nu e^{i\frac{\nu}{2}(\theta + \theta')} F(\nu) = 2\pi\delta(\theta - \theta') \sum_\nu e^{i\nu\theta} F(\nu), \quad (12)$$

which is zero for  $\theta \neq \theta'$ . This property is referred to as a super-selection rule:  $\theta$  is a fundamental parameter that labels the Yang-Mills vacuum and each value of  $\theta$  labels a different theory.

To see explicitly how the  $\theta$  term enters the QCD Lagrangian, let us consider the vacuum-to-vacuum transition in the presence of an external source  $J$

$$\langle \theta_+ | \theta_- \rangle_J = \sum_{m, n} e^{in\theta} e^{-im\theta} \langle m_+ | n_- \rangle_J = \sum_\nu e^{i\nu\theta} \sum_m \langle m_+ | (\nu + m)_- \rangle_J. \quad (13)$$

The vacuum amplitude is a sum over different vacuum transitions in which  $\nu$  corresponds to the net change of winding number between  $t = -\infty$  and  $t = +\infty$ , weighted by the factor  $e^{i\nu\theta}$ . The latter can be replaced, thanks to Eq. (4), by an effective contribution to the Yang-Mills Lagrangian

$$\langle \theta_+ | \theta_- \rangle_J = \sum_\nu \int \mathcal{D}A e^{-\int d^4x \frac{1}{4} G\tilde{G} + i\theta \frac{g_s^2}{32\pi^2} \int d^4x G\tilde{G} + J\text{-term}} \delta\left(\nu - \frac{g_s^2}{32\pi^2} \int d^4x G\tilde{G}\right), \quad (14)$$

where the transition amplitude  $\sum_m \langle m_+ | (\nu + m)_- \rangle_J$  has been expressed in terms of a path integral over all gauge field configurations  $A$  with fixed  $\nu$  (hence the delta function) and the phase factor  $e^{i\nu\theta}$  has been replaced by a  $G\tilde{G}$  term in the Euclidean action.

In summary, the non-trivial structure of the Yang-Mills vacuum requires that the path integral is extended to include gauge field configurations with non-trivial winding number, and in turn this requires that the CP-violating  $G\tilde{G}$  term must be included in the effective action. A strong argument in support of the

correctness of this picture comes from the fact that in the hadronic spectrum there are no signs of a light state that could correspond to the Goldstone boson of a  $U(1)_A$  symmetry spontaneously broken by the quark condensates, a puzzle that was dubbed by Weinberg ‘the  $U(1)_A$  problem’ [39]. The topologically non-trivial gauge configurations responsible for the non-vanishing of the surface integral in Eq. (3) provide the solution: the complex nature of the QCD vacuum makes  $U(1)_A$  not a true symmetry of QCD [47, 48, 53], and this explains the heaviness of the  $\eta'$  meson compared to the other pseudo Goldstone bosons of the spontaneously broken chiral symmetry.

## 2.2. Dependence of the QCD vacuum energy on $\theta$

We are interested in determining the  $\theta$  dependence of the QCD vacuum energy density,  $E(\theta)$ . This is because the axion vacuum expectation value (VEV) can be treated as an effective  $\theta$  parameter, so that some exact results that can be established for the QCD  $\theta$  angle hold for the axion as well, and are especially important in the study of the axion potential. In the large 4-volume ( $V_4$ ) limit,  $E(\theta)$  is related to the Euclidean functional generator,  $Z(\theta)$ , via (see e.g. [21])

$$Z(\theta) = \lim_{V_4 \rightarrow \infty} e^{-E(\theta)V_4}. \quad (15)$$

The latter also admits a path integral representation given by<sup>6</sup>

$$Z(\theta) = \int \mathcal{D}A e^{-\frac{1}{4} \int d^4x GG + i\theta \frac{g_s^2}{32\pi^2} \int d^4x G\tilde{G}} \sim e^{-\frac{8\pi^2}{g_s^2} \theta} e^{i\theta}, \quad (16)$$

where in the last step we have taken the leading term in the semi-classical approximation  $\hbar \rightarrow 0$ , corresponding to the contribution of a  $\nu = 1$  instanton. Since the instanton is translational invariant one still needs to integrate over its center. This can be done within the dilute-instanton-gas approximation, which corresponds to summing-up the contribution of approximate solutions consisting of  $n$  instantons and  $\bar{n}$  anti-instantons with  $n - \bar{n} = 1$  and with their centers widely separated. Using this approximation one gets (see e.g. [21])

$$E(\theta) = -2K e^{-\frac{8\pi^2}{g_s^2} \theta} \cos \theta, \quad (17)$$

where  $K$  is a positive constant encoding Jacobian factors due to the instanton zero modes (translations and dilatations) and a functional determinant originating from the gaussian integration over the quantum fluctuations on the instanton background. The latter are actually crucial for stabilizing the zero mode associated to dilatations, since the integration over the instanton size  $\rho$  formally diverges (at short distances) at the classical level, due to the classical scale invariance of QCD which is broken via radiative corrections. In practice, the breaking of scale invariance can be approximated by taking a running coupling  $g_s(\mu = 1/\rho)$  in Eq. (17), with

$$g_s^2(\mu) = \frac{8\pi^2}{\beta_0 \log(\mu/\Lambda_{\text{QCD}})}, \quad (18)$$

in terms of the one-loop QCD beta-function  $\beta_0 = 11 - 2n_f/3$  with  $n_f$  active flavours and the integration constant  $\Lambda_{\text{QCD}} \approx 150$  MeV. Hence, the integration over the instanton sizes is dominated by values of  $\rho$  corresponding to an unsuppressed exponential factor

$$e^{-\frac{8\pi^2}{g_s^2(1/\rho)}} = (\rho\Lambda_{\text{QCD}})^{\beta_0}, \quad (19)$$

namely for  $\rho \sim 1/\Lambda_{\text{QCD}}$ , which corresponds to the so-called *large instantons*, in contrast to possible short-distance contributions which are exponentially suppressed due to the asymptotic freedom of the coupling

---

<sup>6</sup>In passing to the Euclidean,  $t = -it_E$ , the  $G\tilde{G}$  operator picks up an imaginary part, which eventually leads to the periodic  $\theta$ -dependence of the QCD vacuum energy.

$g_s$ . It should be noted that the semi-classical approximation breaks down for  $g_s(\mu = \Lambda_{\text{QCD}}) \rightarrow \infty$ , so that instanton calculus cannot be used for accurate predictions in QCD.<sup>7</sup>

An alternative way to systematically deal with the  $\theta$  dependence of the QCD vacuum is via chiral Lagrangian techniques, which will be reviewed in Section 2.5 for the case of the axion. Before that, however, one needs to include massive quarks. In order to understand the role of quark fields in the problem, let us perform a global chiral transformation on a single quark field

$$q \rightarrow e^{i\gamma_5 \alpha} q. \quad (20)$$

The associated axial current,  $J_\mu^5 = \bar{\psi} \gamma_\mu \gamma_5 \psi$ , is not conserved because of the quark mass term and the chiral anomaly (note that the latter has a structure similar to the topological term)

$$\partial^\mu J_\mu^5 = 2m_q \bar{q} i \gamma_5 q + \frac{g_s^2}{16\pi^2} G \tilde{G}. \quad (21)$$

Hence, we expect that both  $\theta_q$  (see Eq. (1)) and  $\theta$  are shifted upon the transformation in Eq. (20). One has  $\theta_q \rightarrow \theta_q + 2\alpha$ , while it is less trivial to show that  $\theta \rightarrow \theta - 2\alpha$ . This can be most easily understood in terms of the non-invariance of the path integral measure [55] under the transformation in Eq. (20)

$$\mathcal{D}q \mathcal{D}\bar{q} \rightarrow \left( e^{-i\alpha \frac{g_s^2}{16\pi^2} \int d^4x G \tilde{G}} \right) \mathcal{D}q \mathcal{D}\bar{q}. \quad (22)$$

Hence, only the linear combination

$$\bar{\theta} = \theta + \theta_q \quad (23)$$

is invariant under a quark chiral rotation, and hence physically observable. The generalization of the  $\bar{\theta}$  parameter in the electroweak theory (invariant under a generic chiral transformation involving an arbitrary set of quark fields) reads

$$\bar{\theta} = \theta + \text{Arg Det } Y_U Y_D, \quad (24)$$

in terms of the up and down Yukawa matrices.

Some exact results regarding the  $\theta$  dependence of the QCD vacuum energy density,  $E(\theta)$ , can be derived by using its path integral representation in the presence of fermions as well. Denoting collectively by  $\mathcal{D}\phi \equiv \mathcal{D}A \mathcal{D}q \mathcal{D}\bar{q}$  the functional integration variables comprising gluons, quarks and anti-quarks fields, recalling the expression of the QCD vacuum energy density in terms of the functional  $Z(\theta)$  defined in Eq. (15), and being  $\nu$  the winding number defined in Eq. (4), one can show the following properties:

- $E(0) \leq E(\theta)$

This is a special case of the Vafa-Witten theorem [18], which states that parity cannot be spontaneously broken in QCD. To prove that, one exploits the following inequality

$$Z(\theta) = \int \mathcal{D}\phi e^{-S_{\theta=0} + i\theta\nu} = \left| \int \mathcal{D}\phi e^{-S_{\theta=0} + i\theta\nu} \right| \leq \int |\mathcal{D}\phi e^{-S_{\theta=0} + i\theta\nu}| = \int \mathcal{D}\phi e^{-S_{\theta=0}} = Z(0), \quad (25)$$

where we crucially exploited the fact that the path integral measure is positive definite, which is true for a vector-like theory like QCD [56]. This, however, does not hold in chiral gauge theories like the SM. The consequences of this fact will be discussed in Section 2.10.

- $E(\theta) = E(\theta + 2\pi)$

This simply follows from the fact that  $\theta$  is a global phase and  $\nu$  an integer.

---

<sup>7</sup>On the other hand, large instantons at finite temperature are suppressed by electric screening so that the semiclassical approximation is increasingly reliable at high  $T \gg \Lambda_{\text{QCD}}$ , which serves as an infrared cut-off (see e.g. [54]).

- $E(\theta) = E(-\theta)$

To show this let us perform a field redefinition  $\phi \xrightarrow{\text{CP}} \phi'$  which leaves  $\mathcal{D}\phi$  invariant. Hence, we have

$$Z(\theta) = \int \mathcal{D}\phi e^{-S(\phi)_{\theta=0} + i\theta\nu(\phi)} = \int \mathcal{D}\phi' e^{-S(\phi')_{\theta=0} + i\theta\nu(\phi')} = \int \mathcal{D}\phi e^{-S(\phi)_{\theta=0} - i\theta\nu(\phi)} = Z(-\theta), \quad (26)$$

where in the last but one step we used the fact that  $S(\phi)_{\theta=0}$  is CP invariant, while the topological term is CP odd. Note, however, that  $S(\phi')_{\theta=0} \neq S(\phi)_{\theta=0}$  in the SM, due to the CKM phase, so  $E(\theta)$  picks up a small contribution odd in  $\theta$ .

### 2.3. Neutron EDM and the strong CP problem

Among the CP violating observables induced by  $\bar{\theta}$ , the neutron EDM (nEDM) stands out as the most sensitive one. The latter is defined in terms of the non-relativistic Hamiltonian

$$H = -d_n \vec{E} \cdot \hat{S}, \quad (27)$$

and the current experimental limit is  $|d_n^{\text{exp}}| < 3.0 \cdot 10^{-26} \text{ e cm} = 1.5 \cdot 10^{-12} \text{ e GeV}^{-1}$  (90% CL) [57].<sup>8</sup> A new round of searches are actively underway with the goal of improving the sensitivity to CP violation by up to two orders of magnitude (see e.g. [59]). Eq. (27) can be written in terms of a Lorentz invariant Lagrangian operator as follows

$$\mathcal{L} = -d_n \frac{i}{2} \bar{n} \sigma_{\mu\nu} \gamma_5 n F^{\mu\nu}. \quad (28)$$

Although the calculation of the nEDM presents several technical challenges [60–65] a crude estimate suffices in order to understand the natural size of the  $\bar{\theta}$  contribution to the nEDM. The operator in Eq. (28) is  $d = 5$  so one would naively expect its Wilson coefficient to be of  $\mathcal{O}(1/m_n)$  size. However, in order to contribute to the nEDM one needs to pick-up an imaginary part which can only originate from the phase of a light quark mass (working in the basis where the  $G\tilde{G}$  term is absent). Moreover, being a dipole, the operator must be generated via an EM loop. Hence, taking into account these two extra suppression factors, the effective contribution to  $d_n$  can be estimated as

$$\mathcal{L} \sim \frac{e}{16\pi^2} \frac{m_q}{m_n} \frac{e^{i\bar{\theta}}}{m_n} \bar{n} \sigma_{\mu\nu} \gamma_5 n F^{\mu\nu}, \quad (29)$$

Expanding linearly in  $\bar{\theta}$  one gets

$$|d_n| \sim \frac{1}{8\pi^2} \frac{m_q}{m_n} \frac{\bar{\theta} e}{m_n} \approx 10^{-4} \bar{\theta} \text{ e GeV}^{-1}. \quad (30)$$

In fact, this estimate yields a somewhat smaller value compared to the real calculation, since it is missing a chiral log enhancement coming from a charged pion loop [61]. The most precise calculation to date, based on QCD sum-rules, yields [63]

$$d_n = 2.4(1.0) \cdot 10^{-16} \bar{\theta} \text{ e cm} = 1.2(0.5) \cdot 10^{-2} \bar{\theta} \text{ e GeV}^{-1}, \quad (31)$$

thus implying the bound<sup>9</sup>

$$|\bar{\theta}| \lesssim 10^{-10}. \quad (32)$$

Understanding the smallness of  $\bar{\theta}$  consists in the so-called strong CP problem.

<sup>8</sup>In February 2020 the nEDM experiment at PSI has published a new improved limit  $|d_n^{\text{exp}}| < 1.8 \cdot 10^{-26} \text{ e cm}$  (90% CL) [58].

<sup>9</sup>Experiments searching for the EDM of the electron in paramagnetic systems have recently achieved a remarkable sensitivity and they can be used to obtain novel independent constraints on the QCD theta term at the level of  $|\bar{\theta}| \lesssim 3 \cdot 10^{-8}$  [66].

#### 2.4. Musings on the strong CP problem

The strong CP problem turns out to be qualitatively different from other “small value” problems in the SM. One first observation concerns the radiative stability of  $\bar{\theta}$ . Since CP is violated in the SM, one expects  $\bar{\theta}$  to receive an infinite renormalization due to the CKM phase [67, 68]. Based just on spurionic properties, the SM contribution to  $\bar{\theta}$  must be proportional to the Jarlskog invariant [69], which is given in terms of the following CP-odd, flavour singlet (lowest order) combination of the quark Yukawas

$$\text{Im Det}[Y_U Y_U^\dagger, Y_D Y_D^\dagger] = \frac{2^6 (m_t^2 - m_c^2)(m_t^2 - m_u^2)(m_c^2 - m_u^2)(m_b^2 - m_s^2)(m_b^2 - m_d^2)(m_s^2 - m_d^2)}{v^{12}} \times J_{\text{CKM}} \approx 10^{-20}, \quad (33)$$

where  $v = 246$  GeV and  $J_{\text{CKM}} = \text{Im } V_{ud} V_{cd}^* V_{cs} V_{us}^* \approx 3 \times 10^{-5}$ . Diagrammatically, this would correspond to the insertion of 12 Yukawas in the propagator of a quark mass and hence to a 6-loop diagram, whose imaginary part contributes to  $\bar{\theta}$ . On the other hand, the SM Yukawa Lagrangian features an accidental exchange symmetry:  $H \leftrightarrow \tilde{H}$ ,  $u_R \leftrightarrow d_R$ ,  $Y_U \leftrightarrow Y_D$ , under which  $\text{Im Det}[Y_U Y_U^\dagger, Y_D Y_D^\dagger]$  is odd. Hence, the 6-loop contribution must vanish, and in order to get a non-zero contribution one has to insert e.g. a  $U(1)_Y$  gauge boson which breaks the  $u_R \leftrightarrow d_R$  symmetry. Then a typical 7-loop contribution to the radiatively induced  $\bar{\theta}$  will look like

$$\delta \bar{\theta} \sim \frac{g'^2 (y_{u_R}^2 - y_{d_R}^2) \text{Im Det}[Y_U Y_U^\dagger, Y_D Y_D^\dagger]}{(4\pi^2)^7} \log \Lambda_{\text{UV}} \approx 10^{-33} \log \Lambda_{\text{UV}}, \quad (34)$$

where  $y_{u_R, d_R}$  denotes the hypercharge of a given SM chiral quark and  $\Lambda_{\text{UV}}$  is a UV cut-off. Thus if we take the tree-level value of  $\bar{\theta}$  to be small at some UV boundary (e.g. the Planck scale), it will remain radiatively small when run down to the QCD scale. This has to be contrasted instead with the hierarchy problem of the electroweak scale, for which the Higgs mass parameter is quadratically sensitive to threshold effects from UV physics,  $\delta \mu^2 \sim (\text{loop}) \times \Lambda_{\text{UV}}^2$ . Remarkably, the CP and flavour structure of the SM provides a non-trivial screening mechanism against radiative corrections to  $\bar{\theta}$ , which is not guaranteed in generic SM extensions.

Integrating out the SM quarks can also lead to finite threshold corrections to  $\bar{\theta}$ , which arise at lower orders in perturbation theory. The size of the largest contribution has been estimated to be [67]

$$\delta \bar{\theta}_{\text{fin.}} \sim \left(\frac{\alpha_s}{\pi}\right)^4 \left(\frac{\alpha_2}{\pi}\right)^2 \left(\frac{m_s^2 m_c^2}{m_W^4}\right) J_{\text{CKM}} \approx 10^{-18}, \quad (35)$$

where long-distance QCD effects are such that  $\alpha_s(\text{GeV})/\pi \approx 1$  at the scale relevant for the calculation of the nEDM. Although the contribution is practically of 2-loop order in the electroweak structure constant,  $\alpha_2$ , it is still well below the nEDM experimental sensitivity. Also in this case, generic SM extensions might spoil this conclusion.

Another fact that renders the strong CP problem different from other small value problems of the SM such as that of the light Yukawas ( $y_{u, d, e}$ ) or the cosmological constant, is the lack of an anthropic explanation. In fact, as long as  $\bar{\theta} \lesssim 1\%$ , nuclear physics and Big Bang Nucleosynthesis are practically unaffected [4], so that the value  $\bar{\theta} \sim 10^{-10}$  does not seem to be connected to any ‘catastrophic boundary’. See however [5, 70], for some attempts to relate the scanning of  $\bar{\theta}$  with that of the cosmological constant.

##### 2.4.1. Solutions without axions

Before introducing the axion solution of the strong CP problem, we discuss for completeness three classes of solutions which do not rely on the axion.<sup>10</sup>

<sup>10</sup>Besides the three possibilities outlined below, more speculative solutions that do not invoke an axion also exist, see for example [71].

- *Massless quark solution.* If one of the quark fields (say the up quark) were massless, the QCD Lagrangian would feature a global  $U(1)_u$  axial symmetry, which could be used to rotate the  $\theta$  term to zero (cf. the discussion below Eq. (20)). For some time this was believed to be a possible solution of the strong CP problem, due to the difficulty in extracting the value of  $m_u/m_d$  in chiral perturbation theory. Most notably, this was due to a second-order effect in the chiral Lagrangian, known as Kaplan-Manohar ambiguity [72]. Nowadays this possibility has been ruled out by the direct measurement of the up quark mass on the Lattice [73], which yields  $m_u^{\overline{\text{MS}}}(2 \text{ GeV}) = 2.32(10) \text{ MeV}$ , that is more than  $20\sigma$  away from zero. A variant of the  $m_u = 0$  solution was reconsidered recently in [74] (see also [75] for a similar idea), where it is assumed that the bare mass of the up quark is identically zero and that the apparent small up quark mass is generated via instanton effects, in analogy to second-order effects as for the Kaplan-Manohar ambiguity.
- *Soft P (CP) breaking.* It is conceivable that either P or CP are symmetries of the high-energy theory, thus setting  $\bar{\theta} = 0$  in the UV. Models of this type were first proposed in [76–78] and later on in [79, 80] in the context of grand-unified models. Eventually, P must be spontaneously broken in order to account for the SM chiral structure and similarly for CP in order to generate the CKM phase (and the extra CP violation that is needed for baryogenesis). In these setups the  $\bar{\theta}$  term becomes calculable and the main challenge consists in generating the observed CP violation in the quark sector in such a way that threshold contributions to  $\bar{\theta}$  are screened enough so that  $\delta\bar{\theta} \lesssim 10^{-10}$ . This can be done, however at the cost of some tuning or a somewhat exotic model building (for reviews, see e.g. [81, 82]).
- *QCD solutions.* It is conceivable, at least in principle, that the solution of the strong CP problem might be hidden in the IR dynamics of QCD. Attempts in this direction, e.g. by ‘trivializing’ the QCD vacuum by changing the topology of spacetime [83–86] or by invoking screening effects due to confinement [87–89], often fail to provide a simultaneous solution to the  $\eta'$  problem. Another interesting speculation is the possibility that non-perturbative renormalization effects drive  $\theta(\mu) \rightarrow 0$  in the IR [90–94].

It is fair to say that, while it is certainly worth looking for solutions of the strong CP problem within QCD, no commonly accepted framework has emerged so far. On the other hand, the most unsatisfactory aspect of the  $m_u = 0$  possibility is the lack of any particular theoretical motivation for why the mass of a single quark vanishes, while the mass of all the other quark species is clearly non-zero. Regarding the soft P (CP) breaking solutions, besides the model building complications involved, it is also unappealing the fact that the strong CP problem is solved by UV dynamics, without a clear experimental way to test the mechanism. From this point of view, the Peccei Quinn solution, which is reviewed in the next section, is crucially different, since it delivers a low-energy experimental handle in the form of the axion.

#### 2.4.2. Peccei Quinn mechanism

From a modern perspective, the basic ingredient of the Peccei Quinn (PQ) solution [16, 17, 19, 20] of the strong CP problem consists in the introduction of a new spin zero field  $a(x)$ , hereby denoted as the axion field, whose effective Lagrangian

$$\mathcal{L}_a = \frac{1}{2}(\partial_\mu a)^2 + \mathcal{L}(\partial_\mu a, \psi) + \frac{g_s^2}{32\pi^2} \frac{a}{f_a} G\tilde{G} \quad (36)$$

is endowed with a quasi shift symmetry  $a \rightarrow a + \kappa f_a$  that leaves the action invariant up to the term

$$\delta S = \frac{\kappa}{32\pi^2} \int d^4x G\tilde{G}. \quad (37)$$

The transformation parameter  $\kappa$  is arbitrary and can be chosen to remove the  $\bar{\theta}$  term, while the Vafa-Witten theorem [18] (see Eq. (25) for the proof) ensures that  $\langle a \rangle = 0$  in a vector-like theory like QCD,<sup>11</sup> thus solving

<sup>11</sup>A crucial step of the proof relies on the positive definiteness of the fermionic determinant in the background of the gauge fields, i.e.  $\det(\not{D} + m) > 0$ . This is not ensured for a chiral theory where  $m = 0$ , since it is not possible to write a bare mass term for fermions, and hence the Vafa-Witten theorem does not apply in such case. In fact, in the SM, which is chiral and contains an extra source of CP violation in the Yukawa sector, one expects an irreducible contribution to the axion VEV, as discussed in Section 2.10.

dynamically the strong CP problem. Alternatively, one can explicitly compute the axion potential  $V(a)$  with chiral Lagrangian techniques (which will be done in Section 2.5.1) and show that the absolute minimum is in  $\langle a \rangle = 0$ .

Since the Lagrangian Eq. (36) is non-renormalizable, it requires a UV completion at energies of the order of  $f_a$ . Historically, the first renormalizable model incorporating the axion solution of the strong CP problem was due to Peccei and Quinn [19, 20], which postulated the existence of a  $U(1)_{\text{PQ}}$  global symmetry, spontaneously broken and anomalous under QCD. The presence of a pseudo-Goldstone boson  $a(x)$  (dubbed axion, since it washes out the strong CP problem) was soon realized by Weinberg and Wilczek [16, 17]. However, before considering explicit models we will first discuss some general properties of the axion effective Lagrangian in Eq. (36), which is already sufficient for characterizing some general aspects of axion physics.

### 2.5. Axion effective Lagrangian

The effective operator  $aG\tilde{G}$  is the building block of the PQ solution of the strong CP problem, and provides some model-independent properties of the axion, which we discuss here with the help of the chiral Lagrangian [45, 95]. Let us consider for simplicity 2-flavor QCD, with  $q^T = (u, d)$  and  $M_q = \text{diag}(m_u, m_d)$ . The axion effective Lagrangian reads

$$\mathcal{L}_a = \frac{1}{2}(\partial_\mu a)^2 + \frac{a}{f_a} \frac{g_s^2}{32\pi^2} G\tilde{G} + \frac{1}{4} g_{a\gamma}^0 a F\tilde{F} + \frac{\partial_\mu a}{2f_a} \bar{q} c_q^0 \gamma^\mu \gamma_5 q - \bar{q}_L M_q q_R + \text{h.c.} \quad (38)$$

For later purposes, we have extended Eq. (36) to include two model-dependent couplings:  $g_{a\gamma}^0$  that couples the axion to  $F\tilde{F}$  and violates the shift symmetry, and  $c_q^0 = \text{diag}(c_u^0, c_d^0)$  that couples derivatively the axion to the quark axial current.<sup>12</sup> Their origin will be clarified in Section 2.6. It is convenient to first eliminate the  $aG\tilde{G}$  term via a field-dependent axial transformation of the quark fields:

$$q \rightarrow e^{i\gamma_5 \frac{a}{2f_a} Q_a} q, \quad (39)$$

where  $Q_a$  is a generic matrix acting on the quark fields. This transformation has the effect of generating a term  $-g_s^2 \text{Tr} Q_a / (32\pi^2) \frac{a}{f_a} G\tilde{G}$  which, by requiring that  $\text{Tr} Q_a = 1$ , precisely cancels the axion-gluon term. Since in general this transformation is anomalous under QED, it will also affect the  $F\tilde{F}$  term. Moreover, extra axion-dependent terms are generated by the quark mass operator and the quark kinetic term. Then Eq. (38) becomes

$$\mathcal{L}_a = \frac{1}{2}(\partial_\mu a)^2 + \frac{1}{4} a g_{a\gamma} F\tilde{F} + \frac{\partial_\mu a}{2f_a} \bar{q} c_q \gamma^\mu \gamma_5 q - \bar{q}_L M_a q_R + \text{h.c.}, \quad (40)$$

where we have defined axion-dressed parameters

$$g_{a\gamma} = g_{a\gamma}^0 - (2N_c) \frac{\alpha}{2\pi f_a} \text{Tr}(Q_a Q^2) \quad \text{with} \quad Q = \text{diag}(2/3, -1/3), \quad (41)$$

$$c_q = c_q^0 - Q_a, \quad (42)$$

$$M_a = e^{i\frac{a}{2f_a} Q_a} M_q e^{i\frac{a}{2f_a} Q_a}, \quad (43)$$

where  $N_c = 3$  is the number of colours. The axial quark current can be conveniently decomposed into an iso-singlet and an iso-triplet component

$$\bar{q} c_q \gamma^\mu \gamma_5 q = \frac{1}{2} \text{Tr}[c_q] \bar{q} \gamma^\mu \gamma_5 q + \frac{1}{2} \text{Tr}[c_q \sigma^a] \bar{q} \gamma^\mu \gamma_5 \sigma^a q, \quad (44)$$

<sup>12</sup>While the anomalous dimension of conserved currents vanishes, that is not the case for anomalous currents. In fact, as shown in Refs. [96, 97] the iso-spin singlet axial current,  $j_{\Sigma_q}^\mu = \sum_q \bar{q} \gamma^\mu \gamma_5 q$ , renormalizes multiplicatively. Taking this effect into account it is possible to connect the low-energy derivative axion couplings to quarks with their UV counterparts, which are understood to be the coefficients  $c_q^0$  (for details see [45]).



where we have used the Fierz identity for Pauli matrices,  $(\sigma^a)_{ij}(\sigma^a)_{kl} = 2\delta_{il}\delta_{kj} - \delta_{ij}\delta_{kl}$ . Eq. (40) should be compared with the chiral axion Lagrangian, including for simplicity only pions and axions<sup>13</sup>

$$\mathcal{L}_a^{\text{PT}} = \frac{f_\pi^2}{4} [\text{Tr}((D^\mu U)^\dagger D^\mu U) + 2B_0 \text{Tr}(UM_a^\dagger + M_a U^\dagger)] + \frac{\partial^\mu a}{2f_a} \frac{1}{2} \text{Tr}[c_q \sigma^a] J_\mu^a, \quad (45)$$

where we neglected the iso-singlet current since it is associated to the heavy  $\eta'$ .<sup>14</sup>  $B_0$  is related to the quark condensate and

$$J_\mu^a = \frac{i}{2} f_\pi^2 \text{Tr}[\sigma^a (U D_\mu U^\dagger - U^\dagger D_\mu U)], \quad (46)$$

is the pion iso-triplet axial-vector current (derived from the covariant derivative term in Eq. (45)) that has the same transformation properties under  $SU(2)_L \otimes SU(2)_R$  as the corresponding quark current in Eq. (44), and we have employed the standard parametrization

$$U = e^{i\pi^a \sigma^a / f_\pi} = \mathbb{I} \cos \frac{\pi}{f_\pi} + i \frac{\sigma^a \pi^a}{\pi} \sin \frac{\pi}{f_\pi}, \quad (47)$$

with  $\pi = \sqrt{(\pi^0)^2 + 2\pi^+ \pi^-}$ ,  $f_\pi = 92.3$  MeV and  $D_\mu U = \partial_\mu U + ieA_\mu[Q, U]$ . In the following, we discuss the various terms arising from the axion chiral Lagrangian.

#### 2.5.1. Axion potential and axion mass

Expanding the non-derivative part of the axion chiral Lagrangian, one obtains

$$\begin{aligned} 2B_0 \frac{f_\pi^2}{4} \text{Tr}(UM_a^\dagger + M_a U^\dagger) &= B_0 f_\pi^2 (m_u + m_d) - \frac{1}{2} B_0 (m_u + m_d) \pi^2 \\ &\quad - \frac{i}{4} B_0 \frac{f_\pi^2}{f_a} a \text{Tr}(U\{Q_a, M_q\}) + \text{h.c.} + \dots \end{aligned} \quad (48)$$

It is customary to choose  $Q_a = M_q^{-1} / \text{Tr} M_q^{-1}$ . Note that any linear coupling of the axion to an arbitrary number of pion fields is set to zero: for an odd number of pions because  $\text{Tr} \sigma^a = 0$ , while for an even number there is a cancellation with the hermitian conjugate. In particular, this sets to zero a mass mixing term between  $a$  and  $\pi^0$  (ignoring possible kinetic mixing between  $a$  and  $\pi^0$ , cf. Section 2.5.2), while from the second term in Eq. (48) we obtain  $m_\pi^2 = B_0(m_u + m_d)$  at the leading order in the chiral Lagrangian expansion. With the above choice of  $Q_a$  the axion-pion potential turns out to be

$$\begin{aligned} V(a, \pi^a) &= -2B_0 \frac{f_\pi^2}{4} \text{Tr}(UM_a^\dagger + M_a U^\dagger) \\ &= -\frac{m_\pi^2 f_\pi^2}{m_u + m_d} \left\{ \left[ m_u \cos\left(\frac{m_d}{m_u + m_d} \frac{a}{f_a}\right) + m_d \cos\left(\frac{m_u}{m_u + m_d} \frac{a}{f_a}\right) \right] \cos\left(\frac{\pi}{f_\pi}\right) \right. \\ &\quad \left. + \frac{\pi^0}{\pi} \left[ m_u \sin\left(\frac{m_d}{m_u + m_d} \frac{a}{f_a}\right) - m_d \sin\left(\frac{m_u}{m_u + m_d} \frac{a}{f_a}\right) \right] \sin\left(\frac{\pi}{f_\pi}\right) \right\}. \end{aligned} \quad (49)$$

Expanding for  $a/f_a \ll 1$  we obtain

$$V(a, \pi^a) = -m_\pi^2 f_\pi^2 \cos\left(\frac{\pi}{f_\pi}\right) + \frac{1}{2} \frac{m_u m_d}{(m_u + m_d)^2} \frac{m_\pi^2 f_\pi^2}{f_a^2} a^2 \cos\left(\frac{\pi}{f_\pi}\right) + \mathcal{O}\left(\frac{a^3}{f_a^3}\right), \quad (50)$$

<sup>13</sup>Nucleons can be included as well in chiral Lagrangian [95]. However, due to the lack of a mass gap between  $\Lambda_\chi = 4\pi f_\pi$  and  $m_N$ , the convergence of the EFT is not good. For this reason we are going to discuss axion-nucleon couplings separately, in the context of a non-relativistic EFT for nucleons [45] (cf. Section 2.5.4).

<sup>14</sup>Interactions between the axion and the  $\eta'$  meson can be taken into account in the large  $N$  approximation by using the formalism of Refs. [98, 99].

where linear terms in the axion field are absent by construction. The axion mass (squared) is then readily obtained by setting the pion on its ground state  $\pi = 0$ , which yields [16]

$$m_a^2 = \frac{m_u m_d}{(m_u + m_d)^2} \frac{m_\pi^2 f_\pi^2}{f_a^2} \longrightarrow m_a \simeq 5.7 \left( \frac{10^{12} \text{ GeV}}{f_a} \right) \mu\text{eV}. \quad (51)$$

An alternative expression for the axion-pion potential, corresponding to the choice  $Q_a = \frac{1}{2} \text{diag}(1, 1)$ , is given by [45, 99]

$$V(a, \pi^0) = -m_\pi^2 f_\pi^2 \sqrt{1 - \frac{4m_u m_d}{(m_u + m_d)^2} \sin^2 \left( \frac{a}{2f_a} \right) \cos \left( \frac{\pi^0}{f_\pi} - \phi_a \right)}, \quad (52)$$

with

$$\tan \phi_a = \frac{m_u - m_d}{m_u + m_d} \tan \left( \frac{a}{2f_a} \right), \quad (53)$$

which clearly shows that the absolute minimum is in  $(a, \pi^0) = (0, 0)$ .<sup>15</sup> In particular, on the pion ground state,  $\pi^0 = \phi_a f_\pi$ , the chiral perturbation theory ( $\chi$ PT) axion potential takes the form

$$V(a) = -m_\pi^2 f_\pi^2 \sqrt{1 - \frac{4m_u m_d}{(m_u + m_d)^2} \sin^2 \left( \frac{a}{2f_a} \right)}. \quad (54)$$

Note that this potential differs even qualitatively from the instanton potential in Eq. (17). This is not surprising given that the latter relies on a semi-classical approximation, which is not under control at the confinement scale. On the other hand, the chiral potential cannot be used above the chiral phase transition and the instanton potential becomes more reliable at  $T \sim 1 \text{ GeV}$ , which is the relevant regime for the calculation of the axion DM relic density (cf. Section 3).

### 2.5.2. Axion-pion coupling

Next we inspect the derivative part of the axion-pion Lagrangian. This is obtained by expanding the iso-triplet current term in Eq. (45):

$$\begin{aligned} \frac{\partial_\mu a}{2f_a} \frac{1}{2} \text{Tr} [c_q \sigma^a] J_a^\mu &\simeq -\frac{1}{2} \left( \frac{m_d - m_u}{m_u + m_d} + c_d^0 - c_u^0 \right) \frac{f_\pi}{f_a} \partial_\mu a \partial^\mu \pi^0 \\ &+ \frac{1}{3} \left( \frac{m_d - m_u}{m_u + m_d} + c_d^0 - c_u^0 \right) \frac{1}{f_a f_\pi} \partial_\mu a (2\partial^\mu \pi^0 \pi^+ \pi^- - \pi_0 \partial^\mu \pi^+ \pi^- - \pi_0 \pi^+ \partial^\mu \pi^-). \end{aligned} \quad (55)$$

Note that the first term in Eq. (55) represents a kinetic mixing between the axion and the pion fields, which needs to be diagonalized in order to define the canonical axion and pion fields. The quadratic part of the axion-pion Lagrangian reads

$$\mathcal{L}_a^{\text{quad.}} = \frac{1}{2} \begin{pmatrix} \partial_\mu a & \partial_\mu \pi^0 \end{pmatrix} \begin{pmatrix} 1 & \epsilon \\ \epsilon & 1 \end{pmatrix} \begin{pmatrix} \partial^\mu a \\ \partial^\mu \pi^0 \end{pmatrix} + \frac{1}{2} \begin{pmatrix} a & \pi^0 \end{pmatrix} \begin{pmatrix} m_a^2 & 0 \\ 0 & m_\pi^2 \end{pmatrix} \begin{pmatrix} a \\ \pi^0 \end{pmatrix}, \quad (56)$$

with  $\epsilon = -\frac{1}{2} \left( \frac{m_d - m_u}{m_u + m_d} + c_d^0 - c_u^0 \right) \frac{f_\pi}{f_a}$  and  $m_a/m_\pi = \mathcal{O}(\epsilon)$ . In order to work with canonical propagators one can perform: *i*) an orthogonal transformation to diagonalize the kinetic term, *ii*) a rescaling to make the kinetic term canonical and *iii*) an orthogonal transformation to re-diagonalize the mass term (which does not affect the canonical kinetic term). The net effect of these operations is to shift the current basis fields by  $a \rightarrow a - \epsilon \pi^0$  and  $\pi^0 \rightarrow \pi^0 + (m_a^2/m_\pi^2)\epsilon a$ . Since the axion component into the current pion field is

<sup>15</sup>QED corrections could in principle generate new minima [100]. However, this is prevented by the hierarchy  $m_q/f_\pi \gg \alpha/\pi$ , which makes the vacuum structure for the pion potential trivial.

suppressed at the level of  $\epsilon^3$ , this redefinition has no practical consequences for experimental sensitivities and astrophysical bounds, which are sensitive at most to  $\mathcal{O}(\epsilon^2)$  effects. This justifies the fact that the correction due to kinetic mixing is generally ignored in the literature.

The second addend in Eq. (55) gives instead the axion-pion coupling (see also [26, 101]), defined via the Lagrangian term

$$\mathcal{L}_a^{\text{int}} \supset \frac{C_{a\pi}}{f_a f_\pi} \partial_\mu a (2\partial^\mu \pi^0 \pi^+ \pi^- - \pi_0 \partial^\mu \pi^+ \pi^- - \pi_0 \pi^+ \partial^\mu \pi^-), \quad (57)$$

with

$$C_{a\pi} = -\frac{1}{3} \left( c_u^0 - c_d^0 - \frac{m_d - m_u}{m_u + m_d} \right). \quad (58)$$

Note that once the canonical axion and pion field are properly identified, the only linear coupling of the axion to the pions is the one in Eq. (57). The axion-pion coupling in Eq. (58) generalizes the expressions available in the literature in the case of KSVZ [101] and DFSZ [26] axions.

### 2.5.3. Axion-photon coupling

With the choice of  $Q_a = M_q^{-1} / \text{Tr } M_q^{-1}$  to ensure no axion-pion mass mixing, the LO axion-photon coupling in Eq. (41) becomes

$$g_{a\gamma} = \frac{\alpha}{2\pi f_a} \left[ g_{a\gamma}^0 - \frac{2}{3} \frac{4m_d + m_u}{m_u + m_d} \right]. \quad (59)$$

The same result can be obtained via another choice of  $Q_a$  (e.g. the one leading to the  $\chi$ PT potential in Eq. (54)), but requires the inclusion of a non-zero axion-pion mixing.

### 2.5.4. Axion-nucleon coupling

Following [45] we derive the axion coupling to nucleons (protons and neutrons), via an effective theory at energies  $\ll \Lambda_{\text{QCD}}$ , relevant for momentum exchanges of the order of the axion mass, where the nucleons are non-relativistic. This approach turns out to yield a more reliable approximation than current algebra techniques [102] or the chiral EFT for nucleons [95, 103]. Our goal is to match the quark current operator in Eq. (40) with a non-relativistic axion-nucleon Lagrangian. Using iso-spin as an active flavour symmetry and the axion as an external current, the leading order effective axion-nucleon Lagrangian reads

$$\begin{aligned} \mathcal{L}_N &= \bar{N} v^\mu \partial_\mu N + 2g_A \frac{c_u - c_d}{2} \frac{\partial_\mu a}{2f_a} \bar{N} S^\mu \sigma^3 N + 2g_0^{ud} \frac{c_u + c_d}{2} \frac{\partial_\mu a}{2f_a} \bar{N} S^\mu N + \dots \\ &= \bar{N} v^\mu \partial_\mu N + 2g_A \frac{c_u - c_d}{2} \frac{\partial_\mu a}{2f_a} (\bar{p} S^\mu p - \bar{n} S^\mu n) + 2g_0^{ud} \frac{c_u + c_d}{2} \frac{\partial_\mu a}{2f_a} (\bar{p} S^\mu p + \bar{n} S^\mu n) + \dots, \end{aligned} \quad (60)$$

where  $N = (p, n)^T$  is the iso-spin doublet field,  $v^\mu$  is the four-velocity of the non-relativistic nucleon and  $S^\mu$  the spin operator. The couplings  $g_A$  and  $g_0^{ud}$  correspond respectively to the axial iso-vector and axial iso-scalar combinations, while the dots in Eq. (60) denote higher order terms, including non-derivative axion couplings which for  $\langle a \rangle = 0$  (no extra sources of CP violation) are at least quadratic in  $a$ . Matching the two effective Lagrangians over a single-nucleon matrix element, for example  $\langle p | \mathcal{L}_a | p \rangle = \langle p | \mathcal{L}_N | p \rangle$ , at the leading order in the isospin breaking effects, we get

$$\frac{\partial_\mu a}{2f_a} c_u \underbrace{\langle p | \bar{u} \gamma^\mu \gamma_5 u | p \rangle}_{s^\mu \Delta u} + \frac{\partial_\mu a}{2f_a} c_d \underbrace{\langle p | \bar{d} \gamma^\mu \gamma_5 d | p \rangle}_{s^\mu \Delta d} = \frac{\partial_\mu a}{2f_a} g_A \frac{c_u - c_d}{2} \underbrace{2\langle p | \bar{p} S^\mu p | p \rangle}_{s^\mu} + \frac{\partial_\mu a}{2f_a} g_0^{ud} \frac{c_u + c_d}{2} \underbrace{2\langle p | \bar{p} S^\mu p | p \rangle}_{s^\mu}, \quad (61)$$

where we used the definition  $2\bar{p} S^\mu p = \bar{p} \gamma^\mu \gamma_5 p$ , and  $s^\mu$  is the spin of the nucleon at rest. Reshuffling the previous equation

$$g_A = \Delta u - \Delta d, \quad (62)$$

$$g_0^{ud} = \Delta u + \Delta d. \quad (63)$$

and substituting back into Eq. (60), we get

$$\mathcal{L}_N \supset \frac{\partial_\mu a}{2f_a} \left\{ \frac{c_u - c_d}{2} (\Delta u - \Delta d) (\bar{p} \gamma^\mu \gamma_5 p - \bar{n} \gamma^\mu \gamma_5 n) + \frac{c_u + c_d}{2} (\Delta u + \Delta d) (\bar{p} \gamma^\mu \gamma_5 p + \bar{n} \gamma^\mu \gamma_5 n) \right\}. \quad (64)$$

The axion-nucleon coupling is defined in analogy to the axion-quark ones as

$$\frac{\partial_\mu a}{2f_a} \bar{N} C_{aN} \gamma^\mu \gamma_5 N, \quad (65)$$

with  $C_{aN} = \text{diag}(C_{ap}, C_{an})$ , for which we get (recall that  $c_q = c_q^0 - Q_a$ )

$$C_{ap} = - \left( \frac{m_d}{m_u + m_d} \Delta u + \frac{m_u}{m_u + m_d} \Delta d \right) + c_u^0 \Delta u + c_d^0 \Delta d, \quad (66)$$

$$C_{an} = - \left( \frac{m_u}{m_u + m_d} \Delta u + \frac{m_d}{m_u + m_d} \Delta d \right) + c_d^0 \Delta u + c_u^0 \Delta d, \quad (67)$$

where  $\Delta u = 0.897(27)$ ,  $\Delta d = -0.376(27)$  and  $m_u^{\overline{\text{MS}}}(2 \text{ GeV})/m_d^{\overline{\text{MS}}}(2 \text{ GeV}) = 0.48(3)$  [45].

### 2.5.5. Axion-electron coupling

The axion-electron coupling is defined via the Lagrangian term

$$C_{ae} \frac{\partial_\mu a}{2f_a} \bar{e} \gamma^\mu \gamma_5 e, \quad (68)$$

where  $C_{ae} = c_e^0 + \delta c_e$ . In models where the tree-level contribution,  $c_e^0$ , is zero, the axion-electron coupling can still be generated radiatively. The relevant one-loop diagram is logarithmically divergent, and can be understood as an RGE effect on the  $c_e^0$  coefficient from the PQ scale down to the IR scale  $\mu_{\text{IR}}$  [95]. One finds [101, 102]<sup>16</sup>

$$\delta c_e = \frac{3\alpha^2}{4\pi^2} \left[ g_\gamma^0 \log \left( \frac{f_a}{\mu_{\text{IR}}} \right) - \frac{2}{3} \frac{4m_d + m_u}{m_u + m_d} \log \left( \frac{\Lambda_\chi}{\mu_{\text{IR}}} \right) \right]. \quad (69)$$

The part proportional to  $g_\gamma^0$  corresponds to the running between  $f_a$  and  $\mu_{\text{IR}} < \Lambda_\chi$ , while the second term arises from axion-pion mixing and is cut-off at the chiral symmetry breaking scale,  $\Lambda_\chi \simeq 1 \text{ GeV}$ , since for loop momenta larger than  $\Lambda_\chi$  the effect of the color anomaly is negligible. The IR parameter  $\mu_{\text{IR}}$  should be taken of the order of the energy scale relevant to the physical process under consideration, typically  $\mu_{\text{IR}} = m_e$ .

### 2.6. Origin of model-dependent axion couplings

Before discussing explicit axion models, it is useful to describe in a general way how the ‘model-dependent’ axion couplings  $g_\gamma^0$  and  $c_q^0$  introduced in the axion effective Lagrangian Eq. (38) arise from the point of view of a spontaneously broken  $U(1)_{\text{PQ}}$  symmetry. Let us denote by  $J_\mu^{\text{PQ}}$  the associated PQ current, which is conserved up to anomalies

$$\partial^\mu J_\mu^{\text{PQ}} = \frac{g_s^2 N}{16\pi^2} G\tilde{G} + \frac{e^2 E}{16\pi^2} F\tilde{F}, \quad (70)$$

where  $N$  and  $E$  are respectively the QCD and EM anomaly coefficients. From the Goldstone theorem  $\langle 0 | J_\mu^{\text{PQ}} | a \rangle = i v_a p_\mu$ , where the axion  $a$  is the pseudo Goldstone boson of  $U(1)_{\text{PQ}}$  breaking and we introduced the order parameter  $v_a$ . The axion effective Lagrangian contains the terms

$$\mathcal{L}_a \supset \frac{a}{v_a} \frac{g_s^2 N}{16\pi^2} G\tilde{G} + \frac{a}{v_a} \frac{e^2 E}{16\pi^2} F\tilde{F} + \frac{\partial_\mu a}{v_a} J_\mu^{\text{PQ}}, \quad (71)$$

<sup>16</sup>As pointed out by [101], the original expression in Ref. [102] contains a typo.

where the first two terms are required by anomaly matching and the PQ current depends on the global charges of the fields transforming under  $U(1)_{\text{PQ}}$ . E.g. for a chiral SM fermion  $f_L$  one has  $J_\mu^{\text{PQ}}|_{f_L} = \bar{f}_L \mathcal{X}_{f_L} \gamma^\mu f_L$ , where  $\mathcal{X}_{f_L}$  denotes its PQ charge. Using the standard normalization of the  $G\tilde{G}$  term in terms of  $f_a$  as in Eq. (38) yields

$$f_a = \frac{v_a}{2N}. \quad (72)$$

Hence Eq. (71) can be rewritten as (taking for illustrative purposes just two chiral fermions  $f_L$  and  $f_R$ )

$$\begin{aligned} \mathcal{L}_a &\supset \frac{a}{f_a} \frac{g_s^2}{32\pi^2} G\tilde{G} + \frac{a}{f_a} \frac{e^2}{32\pi^2} \frac{E}{N} F\tilde{F} + \frac{\partial_\mu a}{2f_a} \frac{1}{N} [\bar{f}_L \mathcal{X}_{f_L} \gamma^\mu f_L + \bar{f}_R \mathcal{X}_{f_R} \gamma^\mu f_R], \\ &= \frac{a}{f_a} \frac{g_s^2}{32\pi^2} G\tilde{G} + \frac{1}{4} g_{a\gamma}^0 a F\tilde{F} + \frac{\partial_\mu a}{2f_a} \bar{f} c_f^0 \gamma^\mu \gamma_5 f, \end{aligned} \quad (73)$$

where in the second step we have dropped the coupling with the conserved vector current since the corresponding term vanishes upon integration by part. The axion-photon couplings is thus defined as

$$g_{a\gamma}^0 = \frac{\alpha}{2\pi f_a} \frac{E}{N}, \quad (74)$$

and the axion coupling to the fermion  $f$  as

$$c_f^0 = \frac{\mathcal{X}_{f_R} - \mathcal{X}_{f_L}}{2N} = -\frac{\mathcal{X}_{H_f}}{2N}, \quad (75)$$

where in the last step, assuming a Yukawa term  $\bar{f}_L f_R H_f$ , we have replaced the fermion PQ charges with the charge  $\mathcal{X}_{H_f}$  of the corresponding Higgs. While the expressions above have a general validity in terms of the defining properties of the  $U(1)_{\text{PQ}}$  symmetry (i.e. its anomalous content and the global charge assignments), in the following we will illustrate how to derive them in the context of specific UV models.

## 2.7. Benchmark axion models

We now move to the discussion of explicit axion models, which provide a UV completion for the axion effective Lagrangian in Eq. (38). The simplest realization of the PQ mechanism is given by the Weinberg-Wilczek (WW) model [16, 17], in which the QCD anomaly of the  $U(1)_{\text{PQ}}$  current is generated by SM quarks charged under the PQ symmetry, while the scalar sector is extended via an extra Higgs doublet in order to enforce the additional  $U(1)_{\text{PQ}}$  symmetry. In the WW model the axion decay constant,  $f_a = (v/6) \sin 2\beta$ , with  $\tan \beta = v_u/v_d$ , is of the order of the electroweak scale  $v \simeq 246$  GeV. Hence, being the axion coupling to SM fields not sufficiently suppressed, the WW model was soon ruled out by laboratory searches.<sup>17</sup> This led to the so-called “invisible axion” models, in which the PQ symmetry breaking is decoupled from the electroweak scale via the introduction of a SM singlet scalar field, acquiring a VEV  $v_a \sim f_a \gg v$ . Axion’s interactions are then parametrically suppressed as  $1/f_a \ll 1/v$ .

UV completions of the axion effective Lagrangian can be divided in two large classes, according to the way the QCD anomaly of the  $U(1)_{\text{PQ}}$  current is realized. In models of the Dine-Fischler-Srednicki-Zhitnitsky (DFSZ) type [109, 110] the anomaly is carried by SM quarks (as in the WW model), while models of the Kim-Shifman-Vainshtein-Zakharov (KSVZ) type [111, 112] require new colored fermions. Since these two constructions provide the building blocks of most of the models considered in this report, we review them here in detail.

<sup>17</sup>The original WW model was ruled out by a combination of beam dump experiments [104] and rare meson decays such as  $K \rightarrow \pi a$  [105] and Quarkonia  $\rightarrow \gamma a$  [106]. For a historical account see for instance Sect. 3 in Ref. [107]. However, this was under the assumption of universality of the PQ charges. Variant axion models of the WW type (i.e. with non-universal PQ charges and the PQ breaking connected to the electroweak scale), took instead almost a decade to be ruled out from rare  $\pi$  and  $K$  meson decays [108].

### 2.7.1. KSVZ axion

The KSVZ model [111, 112] extends the SM field content with a vector-like fermion  $\mathcal{Q} = \mathcal{Q}_L + \mathcal{Q}_R$  in the fundamental of color, singlet under  $SU(2)_L$ , and neutral under hypercharge:  $\mathcal{Q} \sim (3, 1, 0)$ , and a SM-singlet complex scalar  $\Phi \sim (1, 1, 0)$ . In the absence of a bare mass term for  $\mathcal{Q}$ ,<sup>18</sup> the Lagrangian

$$\mathcal{L}_{\text{KSVZ}} = |\partial_\mu \Phi|^2 + \bar{\mathcal{Q}} i \not{D} \mathcal{Q} - (y_{\mathcal{Q}} \bar{\mathcal{Q}}_L \mathcal{Q}_R \Phi + \text{h.c.}) - V(\Phi), \quad (76)$$

features a  $U(1)_{\text{PQ}}$  symmetry

$$\Phi \rightarrow e^{i\alpha} \Phi, \quad \mathcal{Q}_L \rightarrow e^{i\alpha/2} \mathcal{Q}_L, \quad \mathcal{Q}_R \rightarrow e^{-i\alpha/2} \mathcal{Q}_R. \quad (77)$$

The potential

$$V(\Phi) = \lambda_\Phi \left( |\Phi|^2 - \frac{v_a^2}{2} \right)^2, \quad (78)$$

is such that the  $U(1)_{\text{PQ}}$  symmetry is spontaneously broken, with order parameter  $v_a$ . Decomposing the scalar field in polar coordinates

$$\Phi = \frac{1}{\sqrt{2}} (v_a + \rho_a) e^{ia/v_a}, \quad (79)$$

the axion field  $a$  corresponds to the Goldstone mode (massless at tree level), while the radial mode  $\rho_a$  picks up a mass  $m_{\rho_a} = \sqrt{2\lambda_\Phi} v_a$ . In the PQ broken phase also the fermion  $\mathcal{Q}$  gets massive, with  $m_{\mathcal{Q}} = y_{\mathcal{Q}} v_a / \sqrt{2}$ .

The Lagrangian term (where we neglected the heavy scalar radial mode)

$$\mathcal{L}_{\text{KSVZ}} \supset -m_{\mathcal{Q}} \bar{\mathcal{Q}}_L \mathcal{Q}_R e^{ia/v_a} + \text{h.c.}, \quad (80)$$

is responsible for the generation of the  $aG\tilde{G}$  operator in the effective theory below  $m_{\mathcal{Q}}$ . To see that, let us perform a field-dependent axial transformation:

$$\mathcal{Q} \rightarrow e^{-i\gamma_5 \frac{a}{2v_a}} \mathcal{Q}, \quad (81)$$

or, equivalently,  $\mathcal{Q}_L \rightarrow e^{i\frac{a}{2v_a}} \mathcal{Q}_L$  and  $\mathcal{Q}_R \rightarrow e^{-i\frac{a}{2v_a}} \mathcal{Q}_R$ . In the transformed variables the field  $\mathcal{Q}$  is now disentangled from the axion, so we can safely integrate it out. Moreover, being the transformation in Eq. (81) anomalous under QCD, one gets (e.g. from the non-invariance of the path integral measure [55]):

$$\delta \mathcal{L}_{\text{KSVZ}} = \frac{g_s^2}{32\pi^2} \frac{a}{v_a} G\tilde{G}, \quad (82)$$

where we have used the fact that  $\mathcal{Q}$  is in the fundamental of color. In such a case one can identify  $v_a = f_a$  (cf. Eq. (38)), and the only coupling of the axion with the SM fields is via the  $aG\tilde{G}$  term (model-independent contribution) discussed in Section 2.5.

For later purposes (cf. Section 6.1.1) we discuss the KSVZ model in the more general setup in which the heavy fermions  $\mathcal{Q}$  reside in a generic reducible representation  $\sum_{\mathcal{Q}} (\mathcal{C}_{\mathcal{Q}}, \mathcal{I}_{\mathcal{Q}}, \mathcal{Y}_{\mathcal{Q}})$  of the  $SU(3)_c \times SU(2)_L \times U(1)_Y$  gauge group. The only requirement for the PQ mechanism to work, is that at least one  $\mathcal{C}_{\mathcal{Q}}$  is a non-trivial representation. The PQ current will have in general both a QCD and EM anomaly, represented by the anomaly coefficients  $E$  and  $N$  (see definition in Eq. (70)) which read

$$N = \sum_{\mathcal{Q}} N_{\mathcal{Q}}, \quad E = \sum_{\mathcal{Q}} E_{\mathcal{Q}}, \quad (83)$$

<sup>18</sup>In the spirit of having the PQ to arise as an accidental global symmetry (cf. Section 2.11), this can be enforced e.g. via the discrete gauge symmetry [111]:  $\mathcal{Q}_L \rightarrow -\mathcal{Q}_L$ ,  $\mathcal{Q}_R \rightarrow \mathcal{Q}_R$ ,  $\Phi \rightarrow -\Phi$ .

with  $N_Q$  and  $E_Q$  denoting the contributions to the anomalies of each irreducible representation (all taken to be left-handed, so in particular  $\mathcal{X}_{Q_R^c} = -\mathcal{X}_{Q_R}$ )

$$N_Q = \mathcal{X}_Q d(\mathcal{I}_Q) T(\mathcal{C}_Q), \quad (84)$$

$$E_Q = \mathcal{X}_Q d(\mathcal{C}_Q) \text{Tr } q_Q^2 = \mathcal{X}_Q d(\mathcal{C}_Q) d(\mathcal{I}_Q) \left( \frac{1}{12} (d(\mathcal{I}_Q)^2 - 1) + \mathcal{Y}_Q^2 \right). \quad (85)$$

Here  $d(\mathcal{C}_Q)$  and  $d(\mathcal{I}_Q)$  denote the dimension of the colour and weak isospin representations,  $T(\mathcal{C}_Q)$  is the color Dynkin index (with standard normalization  $T(3) = 1/2$ ,  $T(6) = 5/2$ ,  $T(8) = 3$ ,  $T(15) = 10$ , etc.),  $q_Q = T_Q^{(3)} + \mathcal{Y}_Q$  denotes the  $U(1)_{\text{EM}}$  charge generator, and  $\mathcal{X}_{Q_R} = -\mathcal{X}_{Q_L} = \mp 1/2$  depending if in Eq. (76) the quark bilinear  $\bar{Q}_L Q_R$  couples to  $\Phi$  or  $\Phi^\dagger$ . Hence, after removing the axion field from the Yukawa Lagrangian via the transformation in Eq. (81), one gets the effective anomalous interactions

$$\delta \mathcal{L}_{\text{KSVZ}} = \frac{\alpha_s N}{4\pi} \frac{a}{v_a} G \tilde{G} + \frac{\alpha E}{4\pi} \frac{a}{v_a} F \tilde{F}. \quad (86)$$

It is customary to normalize the first term as in the axion effective Lagrangian Eq. (38), so that

$$\delta \mathcal{L}_{\text{KSVZ}} = \frac{\alpha_s}{8\pi} \frac{a}{f_a} G \tilde{G} + \frac{\alpha}{8\pi} \frac{E}{N} \frac{a}{f_a} F \tilde{F}, \quad (87)$$

where the relation between the coefficient of the EM term and the effective coupling introduced in Eq. (38) is  $g_{a\gamma}^0 = \frac{\alpha}{2\pi f_a} \frac{E}{N}$ , and we have further defined

$$f_a = \frac{v_a}{2N}. \quad (88)$$

The relation between  $f_a$  and  $v_a$  allows us to introduce the notion of Domain Wall (DW) number, which will be important in cosmology. From Eq. (79) we see that the axion is defined as an angular variable over the domain  $[0, 2\pi v_a)$ .<sup>19</sup> On the other hand, the QCD induced axion potential is periodic in  $[0, 2\pi f_a)$  (cf. Eq. (52) or Eq. (49)). We operatively define the DW number in terms of the QCD anomaly factor,  $N_{\text{DW}} \equiv 2N$ , as the number of inequivalent degenerate minima of the axion potential, that correspond to  $\theta = 2\pi n/N_{\text{DW}}$  with  $n \in \{0, 1, \dots, N_{\text{DW}} - 1\}$ . The consequences of domain walls in cosmology will be discussed in Section 3.4, while models characterised by  $N_{\text{DW}} = 1$ , a special value that allows to evade cosmological issues, are reviewed in Section 7.4. Here we just remark that the original KSVZ construction with one vector-like pair of heavy quarks, singlets under  $SU(2)_L$  ( $d(\mathcal{I}_Q) = 1$ ), in the fundamental of  $SU(3)$  ( $T(\mathcal{C}_Q) = 1/2$ ), and with PQ charges  $\mathcal{X}_{Q_L} = -\mathcal{X}_{Q_R} = 1/2$  as follows from Eq. (77), belongs to the class of  $N_{\text{DW}} = 1$  models.

### 2.7.2. DFSZ axion

The field content of the DFSZ model includes two Higgs doublets  $H_u \sim (1, 2, -\frac{1}{2})$  and  $H_d \sim (1, 2, +\frac{1}{2})$  and a SM-singlet complex scalar field,  $\Phi \sim (1, 1, 0)$ . The latter extends the WW model, allowing to decouple the PQ breaking scale from the electroweak scale. The renormalizable scalar potential

$$V(H_u, H_d, \Phi) = \tilde{V}_{\text{moduli}}(|H_u|, |H_d|, |\Phi|, |H_u H_d|) + \lambda H_u H_d \Phi^2 + \text{h.c.}, \quad (89)$$

contains all the moduli terms allowed by gauge invariance plus a non-hermitian operator which is responsible for the explicit breaking of the re-phasing symmetry of the three scalar fields into two linearly independent  $U(1)$ 's, to be identified with the hypercharge and the PQ symmetry<sup>20</sup>

$$U(1)_{H_u} \times U(1)_{H_d} \times U(1)_\Phi \rightarrow U(1)_Y \times U(1)_{\text{PQ}}. \quad (90)$$

<sup>19</sup>For  $\mathcal{X}_\Phi \neq 1$  the axion domain would be instead  $[0, 2\pi v_a/\mathcal{X}_\Phi)$ .

<sup>20</sup>This could also be achieved via the super-renormalizable operator  $H_u H_d \Phi$ . The latter choice is physically distinct from the one in Eq. (89), as e.g. it implies  $N_{\text{DW}} = 3$ , that is half of the one in standard DFSZ (cf. discussion below Eq. (102)).



The action of the PQ symmetry on the fermion fields is taken to be the same for all the generations and, in the case of the DFSZ-I model, is determined by the following Yukawa Lagrangian

$$\mathcal{L}_{\text{DFSZ-I}}^Y = -Y_U \bar{q}_L u_R H_u - Y_D \bar{q}_L d_R H_d - Y_E \bar{\ell}_L e_R H_d + \text{h.c.} . \quad (91)$$

Alternatively, one can couple  $\tilde{H}_u = i\sigma_2 H_u^*$  in the lepton sector, which goes under the name of DFSZ-II variant,

$$\mathcal{L}_{\text{DFSZ-II}}^Y = -Y_U \bar{q}_L u_R H_u - Y_D \bar{q}_L d_R H_d - Y_E \bar{\ell}_L e_R \tilde{H}_u + \text{h.c.} . \quad (92)$$

By means of a proper scalar potential in Eq. (89) one can ensure that all the three scalar fields pick up a VEV

$$H_u \supset \frac{v_u}{\sqrt{2}} e^{i\frac{a_u}{v_u}} \begin{pmatrix} 1 \\ 0 \end{pmatrix}, \quad H_d \supset \frac{v_d}{\sqrt{2}} e^{i\frac{a_d}{v_d}} \begin{pmatrix} 0 \\ 1 \end{pmatrix}, \quad \Phi \supset \frac{v_\Phi}{\sqrt{2}} e^{i\frac{a_\Phi}{v_\Phi}}, \quad (93)$$

where  $v_\Phi \gg v_{u,d}$  and we have neglected EM-charged and radial modes that do not contain the axion. Note that the parametrisation of the singlet field  $\Phi$  in the last relation differs from the one used in Eq. (79) in that  $a \rightarrow a_\Phi$  and  $v_a \rightarrow v_\Phi$ . This distinction is necessary whenever, as in DFSZ models, besides the singlet radial mode  $a_\Phi$ , Goldstone bosons of other scalar multiplets concur to define the physical axion  $a$ , and additional VEVs contribute to its dimensional normalization factor  $v_a$ . In order to identify the axion field  $a$  in terms of  $a_{u,d,\Phi}$  let us write down the PQ current

$$J_\mu^{\text{PQ}} = \mathcal{X}_\Phi \Phi^\dagger i \overset{\leftrightarrow}{\partial}_\mu \Phi + \mathcal{X}_{H_u} H_u^\dagger i \overset{\leftrightarrow}{\partial}_\mu H_u + \mathcal{X}_{H_d} H_d^\dagger i \overset{\leftrightarrow}{\partial}_\mu H_d + \dots \supset J_\mu^{\text{PQ}}|_a = \sum_{i=\Phi,u,d} \mathcal{X}_i v_i \partial_\mu a_i, \quad (94)$$

where the dots stand for the fermion contribution to the current, while in  $J_\mu^{\text{PQ}}|_a$  we have retained only the  $a_{u,d,\Phi}$  fields and defined  $\mathcal{X}_{u,d} = \mathcal{X}_{H_u,H_d}$  to compactify the result. The axion field is now defined as [102]

$$a = \frac{1}{v_a} \sum_i \mathcal{X}_i v_i a_i, \quad v_a^2 = \sum_i \mathcal{X}_i^2 v_i^2, \quad (95)$$

so that  $J_\mu^{\text{PQ}}|_a = v_a \partial_\mu a$  and, compatibly with Goldstone theorem,  $\langle 0 | J_\mu^{\text{PQ}} | a \rangle = i v_a p_\mu$ . Note, also, that under a PQ transformation  $a_i \rightarrow a_i + \kappa \mathcal{X}_i v_i$  the axion field transforms as  $a \rightarrow a + \kappa v_a$ . The PQ charges in the scalar sector can be determined by requiring: *i*) PQ invariance of the operator  $H_u H_d \Phi^2$ , which implies  $\mathcal{X}_{H_u} + \mathcal{X}_{H_d} + 2\mathcal{X}_\Phi = 0$ , and *ii*) orthogonality between  $J_\mu^{\text{PQ}}|_a$  in Eq. (94) and the corresponding contribution to the hypercharge current  $J_\mu^Y|_a = \sum_i Y_i v_i \partial_\mu a_i$ , which implies  $\sum_i 2Y_i \mathcal{X}_i v_i^2 = -\mathcal{X}_{H_u} v_u^2 + \mathcal{X}_{H_d} v_d^2 = 0$ . The latter condition ensures that there is no kinetic mixing between the physical axion and the  $Z$  boson.<sup>21</sup> All charges are hence fixed up to an overall normalisation<sup>22</sup> that can be fixed by choosing a conventional value for  $\mathcal{X}_\Phi$ :

$$\mathcal{X}_\Phi = 1, \quad \mathcal{X}_{H_u} = -2 \cos^2 \beta, \quad \mathcal{X}_{H_d} = -2 \sin^2 \beta, \quad (96)$$

where we have defined  $v_u/v = \sin \beta$ ,  $v_d/v = \cos \beta$ , with  $v \simeq 246$  GeV. Substituting these expressions into Eq. (95) we obtain:

$$v_a^2 = v_\Phi^2 + v^2 (\sin 2\beta)^2, \quad (97)$$

and given that  $v_\Phi \gg v$  we have  $v_a \simeq v_\Phi$ . The axion coupling to SM fermions can be derived by inverting the first relation in Eq. (95) to express  $a_{u,d}$  in terms of  $a$  and select the  $a$  dependent terms. This boils down to replace  $a_u/v_u \rightarrow \mathcal{X}_{H_u} a/v_a$ ,  $a_d/v_d \rightarrow \mathcal{X}_{H_d} a/v_a$  and yields

$$\mathcal{L}_{\text{DFSZ-I}} \supset -m_U \bar{u}_L u_R e^{i\mathcal{X}_{H_u} \frac{a}{v_a}} - m_D \bar{d}_L d_R e^{i\mathcal{X}_{H_d} \frac{a}{v_a}} - m_E \bar{e}_L e_R e^{i\mathcal{X}_{H_d} \frac{a}{v_a}} + \text{h.c.} . \quad (98)$$

<sup>21</sup>This canonical form is required in order to formally integrate out the  $Z$  boson, via a gaussian integration in the path-integral, when defining the axion EFT.

<sup>22</sup>Physical quantities such as axion couplings and the DW number do not depend from this normalization, as it can be readily verified by repeating all the steps above for a generic  $\mathcal{X}_\Phi$ .

The axion field can be now removed from the mass terms by redefining the fermion fields according to the field-dependent axial transformations:

$$u \rightarrow e^{-i\gamma_5 \mathcal{X}_{H_u} \frac{a}{2v_a}} u, \quad d \rightarrow e^{-i\gamma_5 \mathcal{X}_{H_d} \frac{a}{2v_a}} d, \quad e \rightarrow e^{-i\gamma_5 \mathcal{X}_{H_d} \frac{a}{2v_a}} e, \quad (99)$$

which, because of the QCD and EM anomalies, induce an axion coupling to both  $G\tilde{G}$  and  $F\tilde{F}$ . Let us note in passing that since the fermion charges satisfy the relations  $\mathcal{X}_{u_R} - \mathcal{X}_{u_L} = \mathcal{X}_{H_u}$ ,  $\mathcal{X}_{d_R} - \mathcal{X}_{d_L} = \mathcal{X}_{H_d}$ ,  $\mathcal{X}_{e_R} - \mathcal{X}_{e_L} = \mathcal{X}_{H_d}$  as dictated by PQ invariance of the Yukawa couplings, the transformations Eq. (99) are equivalent to redefine the LR chiral fields with a phase transformation proportional to their PQ charges. Specifying now Eqs. (84)–(85) to the DFSZ-I case, one obtains

$$N = -n_g \left( \frac{1}{2} \mathcal{X}_{H_u} + \frac{1}{2} \mathcal{X}_{H_d} \right) = 3, \quad (100)$$

$$E = -n_g \left( 3 \left( \frac{2}{3} \right)^2 \mathcal{X}_{H_u} + 3 \left( -\frac{1}{3} \right)^2 \mathcal{X}_{H_d} + (-1)^2 \mathcal{X}_{H_d} \right) = 8, \quad (101)$$

where  $n_g = 3$  is the number of SM fermion generations while  $\mathcal{X}_{H_{u,d}}$  are given in Eq. (96). The anomalous part of the axion effective Lagrangian then reads

$$\delta \mathcal{L}_{\text{DFSZ-I}} = \frac{\alpha_s}{8\pi} \frac{a}{f_a} G\tilde{G} + \frac{\alpha}{8\pi} \left( \frac{E}{N} \right) \frac{a}{f_a} F\tilde{F}, \quad (102)$$

with  $f_a = v_a/(2N) = v_a/6$  (hence the DW number is  $N_{\text{DW}} = 6$ ) and  $E/N = 8/3$ . The transformations in Eq. (99), however, do not leave the fermion kinetic terms invariant, and their variation corresponds to derivative couplings of the axion to the SM fermion fields:

$$\delta(\bar{u}i\not{\partial}u) = \mathcal{X}_{H_u} \frac{\partial_\mu a}{2v_a} \bar{u}\gamma^\mu\gamma_5 u = \left( -\frac{1}{3} \cos^2 \beta \right) \frac{\partial_\mu a}{2f_a} \bar{u}\gamma^\mu\gamma_5 u, \quad (103)$$

$$\delta(\bar{d}i\not{\partial}d) = \mathcal{X}_{H_d} \frac{\partial_\mu a}{2v_a} \bar{d}\gamma^\mu\gamma_5 d = \left( -\frac{1}{3} \sin^2 \beta \right) \frac{\partial_\mu a}{2f_a} \bar{d}\gamma^\mu\gamma_5 d, \quad (104)$$

$$\delta(\bar{e}i\not{\partial}e) = \mathcal{X}_{H_d} \frac{\partial_\mu a}{2v_a} \bar{e}\gamma^\mu\gamma_5 e = \left( -\frac{1}{3} \sin^2 \beta \right) \frac{\partial_\mu a}{2f_a} \bar{e}\gamma^\mu\gamma_5 e, \quad (105)$$

from which we can read out the effective axion-fermion couplings for DFSZ-I (cf. the definition of the axion effective Lagrangian Eq. (38) with an obvious extension to include the leptons):

$$c_{u_i}^0 = -\frac{1}{3} \cos^2 \beta, \quad c_{d_i}^0 = -\frac{1}{3} \sin^2 \beta, \quad c_{e_i}^0 = -\frac{1}{3} \sin^2 \beta, \quad (106)$$

where  $i = 1, 2, 3$  is a generation index. In the DFSZ-II model, the leptons couple to the complex conjugate up-type Higgs  $\tilde{H}_u$  instead than to  $H_d$ . This implies changing  $\mathcal{X}_{H_d} \rightarrow -\mathcal{X}_{H_u}$  in the last (leptonic) term in equations (98), (99) and (101) which yields  $E = 2$ ,  $E/N = 2/3$  and  $c_{e_i}^0 = \frac{1}{3} \cos^2 \beta$ .

For DFSZ phenomenological studies it is important to determine the allowed range for  $\tan \beta = v_u/v_d$ , which is set by the perturbative range of the top and bottom Yukawa couplings. A conservative limit is obtained by imposing a (tree-level) unitarity bound on Yukawa-mediated  $2 \rightarrow 2$  fermion scattering amplitudes at  $\sqrt{s} \gg M_{H_{u,d}}$ :  $|\text{Re } a_{J=0}| < 1/2$ , where  $a_{J=0}$  is the  $J = 0$  partial wave. Ignoring running effects, which would make the bound even stronger, and taking into account group theory factors [113, 114], one gets [115]:  $y_{t,b}^{\text{DFSZ}} < \sqrt{16\pi/3}$  (the strongest bound comes from the channel  $Q_L u_R(d_R) \rightarrow Q_L u_R(d_R)$ , with the initial and final states prepared into  $SU(3)_c$  singlets). These translate into a lower and upper bound on  $\tan \beta$ , that can be obtained via the relations  $y_t^{\text{SM}} = \sqrt{2}m_t/v = y_t^{\text{DFSZ}} \sin \beta$ ,  $y_b^{\text{SM}} = \sqrt{2}m_b/v = y_b^{\text{DFSZ}} \cos \beta$ . Using  $m_t = 173.1$  GeV,  $m_b = 4.18$  GeV and  $v = 246$  GeV yields the range

$$\tan \beta \in [0.25, 170]. \quad (107)$$

Note that the range in Eq. (107) holds both for DFSZ-I and DFSZ-II, since the  $\tau$  Yukawa plays a sub-leading role for perturbativity.

### 2.8. Summary of flavour and CP conserving axion couplings

Focussing on the most relevant axion couplings from the point of view of astrophysical constraints (see Section 4) and experimental sensitivities (see Section 5), we collect here their numerical values including available higher-order corrections. Flavour and CP violating axion couplings will be discussed instead in the next two Sections.

The relation between the axion mass and the axion decay constant (see Eq. (51) for a LO expression), has been computed including QED and NNLO corrections in the chiral expansion [116] and reads

$$m_a = 5.691(51) \left( \frac{10^{12} \text{ GeV}}{f_a} \right) \mu\text{eV}. \quad (108)$$

A direct calculation of the topological susceptibility via QCD lattice techniques finds a similar central value, with an error five time larger [117].

The axion interaction Lagrangian with photons, matter fields  $f = p, n, e$ , pions and the nEDM operator can be written as

$$\mathcal{L}_a^{\text{int}} \supset \frac{\alpha}{8\pi} \frac{C_{a\gamma}}{f_a} a F \tilde{F} + C_{af} \frac{\partial_\mu a}{2f_a} \bar{f} \gamma^\mu \gamma_5 f + \frac{C_{a\pi}}{f_a f_\pi} \partial_\mu a [\partial^\mu \pi \pi]^\mu - \frac{i}{2} \frac{C_{an\gamma}}{m_n} \frac{a}{f_a} \bar{n} \sigma_{\mu\nu} \gamma_5 n F^{\mu\nu}, \quad (109)$$

where we have schematically defined  $[\partial^\mu \pi \pi]^\mu = 2\partial^\mu \pi^0 \pi^+ \pi^- - \pi_0 \partial^\mu \pi^+ \pi^- - \pi_0 \pi^+ \partial^\mu \pi^-$ . The LO values of the  $C_{ax}$  coefficients have been derived in Section 2.5. Taking into account NLO chiral corrections for the axion-photon coupling and a LO non-relativistic effective Lagrangian approach for axion-nucleon couplings,<sup>23</sup> and including as well running effects, Ref. [45] finds

$$C_{a\gamma} = \frac{E}{N} - 1.92(4), \quad (110)$$

$$C_{ap} = -0.47(3) + 0.88(3) c_u^0 - 0.39(2) c_d^0 - C_{a,\text{sea}}, \quad (111)$$

$$C_{an} = -0.02(3) + 0.88(3) c_d^0 - 0.39(2) c_u^0 - C_{a,\text{sea}}, \quad (112)$$

$$C_{a,\text{sea}} = 0.038(5) c_s^0 + 0.012(5) c_c^0 + 0.009(2) c_b^0 + 0.0035(4) c_t^0, \quad (113)$$

$$C_{ae} = c_e^0 + \frac{3\alpha^2}{4\pi^2} \left[ \frac{E}{N} \log \left( \frac{f_a}{m_e} \right) - 1.92(4) \log \left( \frac{\text{GeV}}{m_e} \right) \right], \quad (114)$$

$$C_{a\pi} = 0.12(1) + \frac{1}{3} (c_d^0 - c_u^0), \quad (115)$$

$$C_{an\gamma} = 0.011(5) e, \quad (116)$$

where we have added to the list of [45] also  $C_{ae}$ ,  $C_{a\pi}$  (at the LO in the chiral expansion) and  $C_{an\gamma}$  (from the static nEDM result in Eq. (31)).

Sometimes the axion coupling to photons and matter field (first two terms in Eq. (109)) is written as

$$\mathcal{L}_a^{\text{int}} \supset \frac{1}{4} g_{a\gamma} a F \tilde{F} - i g_{af} a \bar{f} \gamma_5 f - \frac{i}{2} g_d a \bar{n} \sigma_{\mu\nu} \gamma_5 n F^{\mu\nu}, \quad (117)$$

where in the second term we have integrated by parts, applied the equations of motion (which is only valid for on-shell fermion states) and defined

$$g_{a\gamma} = \frac{\alpha}{2\pi} \frac{C_{a\gamma}}{f_a}, \quad g_{af} = C_{af} \frac{m_f}{f_a}, \quad g_d = \frac{C_{an\gamma}}{m_n f_a}. \quad (118)$$

The ‘model-independent’ predictions for the axion couplings (namely those exclusively due to the  $aG\tilde{G}$  operator) are obtained by setting  $E/N \rightarrow 0$  and  $c_i^0 \rightarrow 0$  in Eqs. (110)–(116). The latter also correspond

<sup>23</sup>Axion-nucleon couplings in the framework of the NNLO chiral Lagrangian have been recently considered in [118].

to the predictions of the simplest KSVZ model discussed in Section 2.7.1, while the two DFSZ variants of Section 2.7.2 yield

$$\text{DFSZ-I: } E/N = 8/3 \quad c_{u_i}^0 = -\frac{1}{3} \cos^2 \beta, \quad c_{d_i}^0 = -\frac{1}{3} \sin^2 \beta, \quad c_{e_i}^0 = -\frac{1}{3} \sin^2 \beta, \quad (119)$$

$$\text{DFSZ-II: } E/N = 2/3 \quad c_{u_i}^0 = -\frac{1}{3} \cos^2 \beta, \quad c_{d_i}^0 = -\frac{1}{3} \sin^2 \beta, \quad c_{e_i}^0 = \frac{1}{3} \cos^2 \beta, \quad (120)$$

with the index  $i = 1, 2, 3$  denoting generations and the perturbative unitarity domain  $\tan \beta \in [0.25, 170]$ . In Section 6 we will explore in depth how these ‘model-dependent’ coefficients can be modified compared to the standard KSVZ/DFSZ benchmarks.

For completeness, in the next two Sections we are going to discuss two other classes of model-dependent axion couplings which can be of phenomenological interest, although they do not arise to a sizeable level in the standard KSVZ/DFSZ benchmarks. These are namely flavour violating axion couplings (Section 2.9) and CP-violating ones (Section 2.10).

### 2.9. Flavour violating axion couplings

Relaxing the hypothesis of the universality of the PQ current in DFSZ-like constructions leads to flavour violating axion couplings to quarks and leptons. This option will be explored in detail in Section 6.5. Here, we preliminary show how such couplings arise in a generalized DFSZ setup with non-universal PQ charges. Let us assume that quarks with the same EM charge but of different generations couple to different Higgs doublets, for definiteness  $H_1$  or  $H_2$ , to which we assign the same hypercharge  $Y_{H_1} = Y_{H_2} = -\frac{1}{2}$  but different PQ charges  $\mathcal{X}_1 \neq \mathcal{X}_2$ . Let us start by considering the following Yukawa terms for the up-type quarks

$$\mathcal{L}_{12}^{Y_U} = -(Y_U)_{11} \bar{q}_{1L} u_{1R} H_1 - (Y_U)_{22} \bar{q}_{2L} u_{2R} H_2 - (Y_U)_{12} \bar{q}_{1L} u_{2R} H_1 + \dots \quad (121)$$

The quark bilinear  $\bar{q}_{1L} u_{2R}$  in the last term (or alternatively a similar term in the down-quark sector) is needed to generate the CKM mixing, and for the present discussion it is irrelevant whether it couples to  $H_1$  or  $H_2$ . Note, also, that from PQ charge consistency  $\mathcal{X}(\bar{q}_{2L} u_{1R}) = \mathcal{X}(\bar{q}_{2L} u_{2R}) - \mathcal{X}(\bar{q}_{1L} u_{2R}) + \mathcal{X}(\bar{q}_{1L} u_{1R}) = -\mathcal{X}_2$  it follows that the term  $\bar{q}_{2L} u_{1R} H_2$  is also allowed. However, being its structure determined by the first three terms we do not need to consider it explicitly. Projecting out from the Higgs doublets the neutral Goldstone bosons, as was done in Eq. (93), and identifying the axion field, we obtain the analogous of Eq. (98) in the form

$$\mathcal{L}_{12}^{m_U} = -(m_u)_{11} \bar{u}_{1L} u_{1R} e^{i\mathcal{X}_1 \frac{a}{v_a}} - (m_u)_{22} \bar{u}_{2L} u_{2R} e^{i\mathcal{X}_2 \frac{a}{v_a}} - (m_u)_{12} \bar{u}_{1L} u_{2R} e^{i\mathcal{X}_1 \frac{a}{v_a}} + \dots \quad (122)$$

Because of the presence of the mixing term, in this case it is not possible to remove the axion field from the mass terms with a pure axial redefinition of the quark fields as in Eq. (99), but it is necessary to introduce also a vectorial part in the field redefinition:

$$u_1 \rightarrow e^{-i(\gamma_5 \mathcal{X}_1 + \mathcal{X}_2) \frac{a}{2v_a}} u_1, \quad u_2 \rightarrow e^{-i(\gamma_5 \mathcal{X}_2 + \mathcal{X}_1) \frac{a}{2v_a}} u_2. \quad (123)$$

By introducing a vector of the two quark flavours  $u = (u_1, u_2)^T$  and the two matrices of charges  $\mathcal{X}_{12} = \text{diag}(\mathcal{X}_1, \mathcal{X}_2)$  and  $\mathcal{X}_{21} = \text{diag}(\mathcal{X}_2, \mathcal{X}_1)$  the variation of the fermion kinetic terms due to the redefinitions in Eq. (123) can be written as

$$\delta(\bar{u} i \not{\partial} u) = \frac{\partial_\mu a}{2v_a} \{ \bar{u} \mathcal{X}_{12} \gamma_\mu \gamma_5 u + \bar{u} \mathcal{X}_{21} \gamma_\mu u \} = \frac{\partial_\mu a}{2v_a} \{ \bar{u}_L \mathcal{X}_L \gamma_\mu u_L + \bar{u}_R \mathcal{X}_R \gamma_\mu u_R \}. \quad (124)$$

Clearly, since the matrices of charge  $\mathcal{X}_{L,R} = \mathcal{X}_{21} \mp \mathcal{X}_{12} = (\mathcal{X}_2 \mp \mathcal{X}_1) \begin{pmatrix} 1 & \\ & -1 \end{pmatrix}$  are not proportional to the identity, once the fermion interaction states are rotated into the mass eigenstates  $u'_{L,R} = U_{L,R}^u u_{L,R}$  flavour violating couplings, controlled by the matrices  $(\mathcal{X}_2 \mp \mathcal{X}_1) U_{L,R}^u \begin{pmatrix} 1 & \\ & -1 \end{pmatrix} U_{L,R}^{u\dagger}$  respectively for the L and R fields, unavoidably appear. We will see in Section 6.5 that interesting models which necessarily involve generation dependent PQ charges indeed share this feature.

### 2.10. CP-violating axion couplings

Under some circumstances, discussed below, the axion field can develop CP-violating (scalar) couplings to matter fields, which can be parametrized via the following Lagrangian term

$$\mathcal{L}_a^{\text{CPV}} = g_{af}^S a \bar{f} f. \quad (125)$$

In particular, CP-violating (scalar) axion couplings to nucleons  $N = p, n$ , mediate new forces in the form of scalar–scalar (monopole–monopole) or scalar–pseudo-scalar (monopole–dipole) interactions [119]. This terminology comes from the fact that in the non-relativistic limit the scalar coupling is spin-independent, contrary to the case of the pseudo-scalar density. Let us consider, for instance, the monopole-monopole interaction. The non-relativistic potential between two nucleons  $N_1$  and  $N_2$  can be calculated in the inverse Born approximation (with  $\vec{q}$  denoting the moment transferred)

$$V(r) = \int \frac{d^3 q}{(2\pi)^3} \frac{g_{N_1}^S g_{N_2}^S e^{i\vec{q}\cdot\vec{r}}}{\vec{q}^2 + m_a^2} = -\frac{g_{N_1}^S g_{N_2}^S e^{-m_a r}}{4\pi r}, \quad (126)$$

which for  $m_a \lesssim 1$  eV is subject to strong limits from e.g. precision tests of Newton’s inverse square law. Instead monopole-dipole interaction are at the base of new experimental setups that will be sensitive to either  $g_{aN}^S g_{an}$  or  $g_{aN}^S g_{ae}$ , as discussed in Section 5.4.

CP-violating scalar axion couplings are generated whenever the axion potential does not exactly relax the axion VEV to zero.<sup>24</sup> In the presence of extra sources of CP violation in the UV it is expected that  $\theta_{\text{eff}} = \langle a \rangle / f_a \neq 0$  and one finds [119]

$$g_{aN}^S = \frac{\theta_{\text{eff}}}{f_a} \frac{m_u m_d}{m_u + m_d} \langle N | (\bar{u}u + \bar{d}d) | N \rangle \sim \theta_{\text{eff}} \frac{f_\pi}{f_a}. \quad (127)$$

For instance, in the SM it is expected (based naive dimensional analysis [120])

$$\theta_{\text{eff}} \sim G_F^2 f_\pi^4 J_{\text{CKM}} \approx 10^{-18}, \quad (128)$$

(note that  $J_{\text{CKM}} = \text{Im } V_{ud} V_{cd}^* V_{cs} V_{us}^*$  has the same spurionic properties of  $\theta$ , being a CP-violating flavour singlet) which leads, however, to axion scalar couplings that are far from being experimentally accessible. New physics above the electroweak scale might provide extra sources of CP violation and be responsible for a sizeable  $\theta_{\text{eff}}$  which could bear some phenomenological consequences. Consider for definiteness the CP-violating operator (color EDM)

$$\mathcal{O}_{\text{CPV}} = \frac{i}{2} \tilde{d}_q g_s \bar{q} T^a G_{\mu\nu}^a \sigma^{\mu\nu} \gamma_5 q, \quad (129)$$

for any light quark flavour  $q = u, d, s$ , together with the QCD-dressed 1-point and 2-point axion functions, defined as

$$\chi' = i \int d^4 x \langle 0 | T \frac{\alpha_s}{8\pi} G \tilde{G}(x) \mathcal{O}_{\text{CPV}}(0) | 0 \rangle, \quad (130)$$

$$\chi = i \int d^4 x \langle 0 | T \frac{\alpha_s}{8\pi} G \tilde{G}(x) \frac{\alpha_s}{8\pi} G \tilde{G}(0) | 0 \rangle. \quad (131)$$

The latter is known as topological susceptibility (sometimes also denoted as  $K$  [112]) and can be also written as the second derivative of the QCD generating functional Eq. (16) (see also the QCD action density in Minkowski Eq. (1)) with respect to  $\theta$ . A comparison with the effective axion Lagrangian in Eq. (36) and the replacement  $\frac{\partial^2}{\partial \theta^2} \big|_{\theta=0} \rightarrow f_a^2 \frac{\delta^2}{\delta a^2} \big|_{a=0}$  highlights its relation with the axion mass:

$$\chi = f_a^2 m_a^2. \quad (132)$$

<sup>24</sup>Since electrons always couple derivatively to the axion, the VEV of the latter does not generate a scalar axion coupling to electrons. Hence, only scalar axion couplings to nucleons are relevant for the QCD axion.

A detailed computation that exploits chiral Lagrangian techniques, chiral fits and lattice QCD results gives the value  $\chi = (75.5(5) \text{ MeV})^2$  [45]. The two quantities  $\chi'$  and  $\chi$  enter the axion potential as

$$V(a) \approx \chi' \left( \frac{a}{f_a} \right) + \frac{1}{2} \chi \left( \frac{a}{f_a} \right)^2, \quad (133)$$

where we neglected higher orders in  $a/f_a \ll 1$ . Hence, the induced axion VEV is obtained by solving the tadpole equation

$$\theta_{\text{eff}} = -\frac{\chi'}{|\chi|}. \quad (134)$$

Using standard current algebra techniques one finds [121]

$$\theta_{\text{eff}} = -\frac{m_0^2}{2} \frac{\tilde{d}_q}{m_q}, \quad (135)$$

with  $m_0^2 = \langle 0 | g_s \bar{q} (T^a G_{\mu\nu}^a \sigma^{\mu\nu}) q | 0 \rangle / \langle 0 | \bar{q} q | 0 \rangle \approx 0.8 \text{ GeV}^2$ . This shows that it is possible to generate values of  $\theta_{\text{eff}}$  which saturate the nEDM bound  $|\theta_{\text{eff}}| \lesssim 10^{-10}$ , e.g. for  $\tilde{d}_q \sim 1/(10^{12} \text{ GeV})$ . In terms of a SM gauge invariant effective operator above the electroweak, the scale of new physics is given by  $v/\Lambda_{\text{NP}}^2 = \tilde{d}_q$ , which yields  $\Lambda_{\text{NP}} \sim 10^4 \text{ TeV}$ .

### 2.11. The dirty side of the axion

One of the most delicate aspects of the PQ mechanism is the fact that it relies on a global  $U(1)_{\text{PQ}}$  symmetry, which has to be preserved to a great degree of accuracy in order for the axion VEV to be relaxed to zero, a precision compatible with the non-observation of the neutron EDM. This issue is known as the *PQ quality problem* [122–127], and it is reviewed below.

Global symmetries are generally considered not to be fundamental features in a QFT, and this is particularly well justified in the case of anomalous symmetries which do not survive at the quantum level. However, in some cases the field content of the theory together with the requirement of Lorentz and local gauge invariance restricts the allowed renormalizable operators to a set which remains invariant under some global redefinition of the fields. These symmetries are thus *accidental* in the sense that they result from other first principle requirements. However, given that they are not imposed on the theory, in general are not respected by higher-order non-renormalizable operators. A well known example of an accidental global symmetry is baryon number ( $B$ ) in the SM: operators carrying nonzero baryon number must have at least three quark fields to be color singlets, and then at least four fermion fields to form a Lorentz scalar. Thus their minimal dimension is  $d = 6$ , whence the renormalizable Lagrangian conserves  $B$ . The high level of accuracy of baryon number conservation required to comply with proton decay bounds implies that  $B$ -violating effective operators must be suppressed by a rather large scale  $\Lambda_B \gtrsim 10^{15} \text{ GeV}$  which, however, can be considered natural when understood in terms of some GUT dynamics.

It would certainly be desirable to generate also the PQ symmetry as an accidental symmetry. The benchmark KSVZ and DFSZ constructions discussed in the previous sections do not address this issue and, in particular, there is no first principle reason that impedes writing in  $\mathcal{L}_{\text{KSVZ}}$  in Eq. (76) a quark mass term  $\mu_Q \bar{Q}_L Q_R$  or in  $\mathcal{L}_{\text{DFSZ}}$  in Eq. (89) a direct coupling  $\mu_H^2 H_u H_d$ , both of which would destroy PQ invariance of the renormalizable Lagrangians. The problem becomes even more serious once, after assuming that an accidental PQ symmetry can be enforced in some way, one proceeds to estimate at which operator dimension the symmetry can be first broken in order not to spoil the solution to the strong CP problem for a given value of the suppression scale. Let us consider the following set of effective operators of dimension  $d = 2m + n$  that violate the PQ symmetry by  $n$  units, and let us assume for definiteness that they are suppressed by the largest scale that can consistently appear in a QFT, the Planck scale  $m_{\text{Pl}}$ :

$$\begin{aligned} -V_{\text{PQ-break}}^n &= \frac{\lambda_n |\Phi|^{2m} (e^{-i\delta_n} \Phi^n + e^{i\delta_n} \Phi^{\dagger n})}{m_{\text{Pl}}^{d-4}} \supset \frac{\lambda_n f_a^4}{2} \left( \frac{f_a}{\sqrt{2} m_{\text{Pl}}} \right)^{d-4} \cos \left( \frac{na}{f_a} - \delta_n \right) \\ &\approx m_*^2 f_a^2 \left( \frac{\theta^2}{2} - \frac{\theta}{n} \tan \delta_n \right), \end{aligned} \quad (136)$$

with  $\lambda_n$  real and  $\delta_n$  the phase of the coupling,<sup>25</sup> and we have taken for simplicity a color anomaly factor  $2N = 1$  so that  $\Phi = \frac{1}{\sqrt{2}}(f_a + \rho_a)e^{ia/f_a}$ . In the last relation we have expanded for  $\theta = \frac{a}{f_a} \ll 1$  neglecting an irrelevant constant, and we have defined  $m_*^2 = \frac{\lambda_n f_a^2}{2} (f_a/(\sqrt{2}m_{\text{Pl}}))^{d-4} \cos \delta_n$ . The effect of the explicit breaking  $V_{\text{PQ-break}}^n$  is to move the minimum of the axion potential away from the CP conserving minimum  $\langle \theta \rangle = 0$  of the QCD induced potential  $V(\theta) = \frac{1}{2}m_a^2 f_a^2 \theta^2$  (see Eq. (50)) and shift it to

$$\langle \theta \rangle = \frac{m_*^2 \tan \delta_n}{n(m_a^2 + m_*^2)}. \quad (137)$$

Taking for example operators that violate PQ by one unit ( $n = 1$ ) and assuming  $\lambda_1 \sim \tan \delta_1 \sim 1$ , implies that to satisfy  $m_*^2/m_a^2 \lesssim 10^{-10}$  the dimension of these operators should be uncomfortably large:  $d \geq 8, 10, 21$  respectively for  $f_a \sim 10^8, 10^{10}, 10^{15}$  GeV.

Of course, in QFT it is always possible to assume that there are no heavy states mediating PQ-violating interactions, so that operators of the type Eq. (136) do not arise. However, there is a general consensus that quantum gravity effects violate all global symmetries at some level. The standard argument is that particles carrying global charges can be swallowed by black holes, which subsequently may evaporate by emitting Hawking radiation [128].<sup>26</sup> One can then speculate that non-perturbative quantum gravity formation of “virtual” black holes would eventually result in an effective theory containing all types of operators compatible with the local gauge symmetries of the theory, but violating global charge conservation, with suppression factors provided by appropriate powers of the cutoff scale  $m_{\text{Pl}}$ . This latter feature is often justified from the requirement that quantum gravity effects should disappear when sending  $m_{\text{Pl}} \rightarrow \infty$ . However, while this is indeed reasonable for perturbative quantum gravity corrections, global charge violation is intrinsically a non-perturbative phenomenon, and the assumption that the corresponding effects could be described only in terms of operators suppressed by powers of  $m_{\text{Pl}}$  is at least questionable. After all, non-perturbative QCD effects in the axion potential are approximately described by a cosine term  $V(a) \approx -\Lambda_{\text{QCD}}^4 \cos(a/f_a)$  with a positive power of  $\Lambda_{\text{QCD}}$ , rather than by effective operators suppressed by inverse powers of  $\Lambda_{\text{QCD}}$ . Similarly, one cannot exclude that gravity could give rise to operators like  $m_{\text{Pl}}^3(\Phi + \Phi^\dagger)$  or to other operators not containing  $m_{\text{Pl}}$  in the denominator [129–131].

In the absence of reliable ways to assess the validity of Eq. (136) for describing quantum gravity effects, other approaches have been pursued. Most noticeably, in scenarios in which Einstein gravity is minimally coupled to the axion field, non-conservation of global charges arises from non-perturbative effects related to wormholes that can absorb the global charge and consequently break the symmetry. These effects are to some extent computable and have been studied for example in Refs. [129–131] and, more recently, also in Ref. [132]. These studies indicate that in this setup global symmetries remain intact at any finite order in a perturbative expansion in  $1/m_{\text{Pl}}$  so that power-suppressed operators are not generated [132]. However, non-perturbative wormhole effects do generate additional cosine terms  $\sim \cos(a/f - \delta_1)$  similar to the last term in Eq. (136). However, they come with an exponential suppression factor  $e^{-S_{\text{wh}}}$  of the wormhole action. Then, if  $S_{\text{wh}}$  is sufficiently large, as it appears possible in many cases [131, 132], the axion solution to the strong CP problem would not be endangered.

The conclusions of this discussion are that, in a complete model, *i*) it would be highly desirable that the PQ symmetry could arise as an accidental symmetry of the fundamental Lagrangian, thus guaranteeing that at the QFT level it remains perturbatively unbroken; *ii*) it would be also desirable if some fundamental principle, like for example local gauge invariance, could impede writing down PQ violating effective operators of dimension  $d \leq 10$ , or if some mechanism could guarantee an appropriate strong suppression of the coefficient of any such operator. In this respect, different mechanisms in order to guarantee the quality of the PQ symmetry have been put forth. They can be conceptually divided in three different classes:

<sup>25</sup>Precisely because these operators are not PQ invariant, the PQ transformation required to remove  $\bar{\theta}$  from the QCD Lagrangian will in any case give a contribution  $n\bar{\theta}$  to  $\delta_n$ .

<sup>26</sup>Local charges, such as the electric charge, cannot disappear because Gauss law ensures that the electric field flux remains preserved when the charged particle falls into the black hole. Hence, charged black holes cannot evaporate entirely, but instead get stabilised as extremal black holes.



- *Low  $f_a$ .* For  $f_a \lesssim 10^3$  GeV, only  $d > 5$  is required in order not to generate a too large  $\langle\theta\rangle$  from Eq. (137). From this point of view the original WW axion model would have been perfectly natural, since in absence of SM-singlet fields the first gauge invariant PQ breaking operator that one can write in the scalar potential is  $(H_u H_d)^3$ , which is  $d = 6$ . Over the years, the increasing lower bounds on  $f_a$  let the PQ quality problem to emerge. In ‘super-heavy’ axion models, reviewed in Section 6.7, one can evade the astrophysical constraints on  $f_a \gtrsim 10^8$  GeV, e.g. by modifying the QCD relation between  $m_a$  and  $f_a$ . These models feature an axion decay constant of the order of  $10^{4\div 5}$  GeV, thus improving a lot on the PQ quality problem.
- *Gauge protection.* New local symmetries can lead to an accidental PQ symmetry protected from higher-order PQ breaking operators, up to some fixed order. Various mechanisms have been proposed, based on discrete gauge symmetries [133–136], Abelian [124, 126, 137, 138] and non-Abelian [139, 140] gauge symmetries or composite dynamics [141–145].
- *Small coupling.* There is the possibility that the overall coupling  $\lambda_n$  in Eq. (136) is extremely tiny, even though effective operators are generated at relatively low-dimension [146]. Another possibility that was already mentioned above, is that PQ breaking terms generated by quantum gravity come with a suppression factor  $e^{-S_{\text{wh}}}$  which is exponentially small for a sizeable wormhole action.

A more detailed account of all these mechanisms will be given in Section 7.5. Here we have recalled some aspects of the PQ solution to the strong CP problem which (in our opinion) have not yet found a fully satisfactory theoretical justification. Thus we believe that theoretical efforts to search for a compelling mechanism to generate accidentally a PQ symmetry of the required high quality keep being of primary importance. Meanwhile, this ‘incompleteness’ of a theory, that is otherwise quite elegant and particularly rich of phenomenological implications, should not discourage in any way experimental axion searches. Although theoretical UV completions of axion models and PQ protection mechanisms, for their very nature, tend to remain confined at high energy, thus challenging experimental tests, with the large number of ongoing and planned axion search experiments we are now entering a data driven era. If the axion will be discovered, probing its fine properties with good accuracy could hopefully provide the clues needed to unveil the fundamental origin of the PQ symmetry.

### 3. Axion cosmology

The main goal of this Section is to review the mechanisms through which axions contribute to the present DM energy density. In Section 3.1 we briefly recall some basic equations for cosmology and for early Universe thermodynamics, and we establish the notations. The temperature dependence of the axion potential and axion mass is reviewed in Section 3.2. In Section 3.3 we describe the mechanism of cold axions production from vacuum realignment. The contribution to the axion relic density from the decay of topological defects is reviewed in Section 3.4. Section 3.5 addresses the issue of isocurvature fluctuations in the axion field and of the related bounds that can be derived on the scale of inflation. Section 3.6 collects some bounds on the axion mass that can be obtained (mainly) from cosmological considerations. In Section 3.8 we address some issues related with the existence of a thermal population of relativistic axions. Finally, the role of axion-related substructures, in the form of axion miniclusters and axion stars, is reviewed in Section 3.9.

#### 3.1. Basics of cosmology and thermodynamics in the early Universe

Observations at scales larger than 100 Mpc support the evidence that the Universe is spatially homogeneous and isotropic. Our starting point is the description of such a Universe in terms of Einstein equations

$$\mathcal{G}^{\mu\nu} = 8\pi G_N \mathcal{T}^{\mu\nu}, \quad (138)$$

where the Einstein tensor  $\mathcal{G}^{\mu\nu}$  describes the geometry of the space-time and is defined in terms of (derivatives) of the metric tensor  $g_{\mu\nu}$  through the affine connection and its derivatives. The stress-energy tensor  $\mathcal{T}^{\mu\nu}$  describes the energy content of the Universe, and  $G_N$  is Newton constant. In the following we rewrite it as  $G_N = 1/m_{\text{Pl}}^2$  that defines the Planck mass with a value  $m_{\text{Pl}} = 1.221 \times 10^{19}$  GeV. The indices  $\mu, \nu$  run over the four space-time dimensions  $(t, x, y, z)$  where  $t$  is *cosmic* time (i.e. the time measured by a physical clock at rest in the comoving frame) which, for any given value, slices space-time into a three-dimensional homogeneous and isotropic space manifold  $\mathcal{M}_3$  with a constant curvature that can be positive, negative or zero, corresponding respectively to an open, closed or flat Universe. Observations and theoretical considerations support the last possibility (flat Universe) for which the line element is

$$ds^2 \equiv g^{\mu\nu} dx_\mu dx_\nu = dt^2 - R^2(t) (dx^2 + dy^2 + dz^2), \quad (139)$$

where  $R = R(t)$  is the cosmic scale factor. Eq. (139) defines the Friedmann-Lemaître-Robertson-Walker (FLRW) metric. Consistency with the symmetries of the metric (homogeneity and isotropy) requires  $\mathcal{T}_{\mu\nu}$  to be diagonal and with equal spatial components. A simple realisation is a perfect fluid at rest in the comoving frame with time dependent energy density  $\rho = \rho(t)$  and pressure  $P = P(t)$  for which the stress-energy tensor is  $\mathcal{T}_\nu^\mu = \text{diag}(\rho, -P, -P, -P)$ . The stress energy in the Universe is conveniently described by the simple equation of state  $P = w\rho$  so that a FLRW Universe remains completely characterised by the total energy density and by the fractional size and  $w$ -values of its components.

From the FLRW metric Eq. (139) the affine connection is computed, then the Einstein tensor, and inserting it into Einstein's field equations (138) with the stress-energy tensor for the perfect fluid on the right-hand-side, yields

$$H^2 \equiv \left( \frac{\dot{R}}{R} \right)^2 = \frac{8\pi}{3m_{\text{Pl}}^2} \rho, \quad (140)$$

$$\dot{H} + H^2 = \frac{\ddot{R}}{R} = -\frac{4\pi}{3m_{\text{Pl}}^2} (\rho + 3P), \quad (141)$$

where the first equation is obtained from the 0-0 component and the second from the spatial  $j$ - $j$  component after making use of Eq. (140) while, due to the symmetries of the system, all the other components vanish.  $H \equiv \dot{R}/R$  with the dot meaning derivation with respect to cosmic time, expresses the rate of the change

in the scale factor, and is called the Hubble rate. Combining the two Friedmann equations leads to the conservation law in an expanding Universe:

$$\dot{\rho} + 3H(P + \rho) = 0, \quad \text{or equivalently} \quad \frac{\partial}{\partial t}(\rho R^3) = -P \frac{\partial}{\partial t}(R^3). \quad (142)$$

The second form, whose physical meaning is that the change in energy in a comoving volume is equal to minus the pressure times the change in volume, is the first law of thermodynamics. This form is particularly useful for deducing the scaling of the energy density in matter and radiation with the expansion. Matter is pressureless ( $w = 0$ ) and immediately we obtain  $\rho_m \propto R^{-3}$ . For radiation  $P_{\text{rad}} = \rho_{\text{rad}}/3$  ( $w = -1/3$ ) and Eq. (142) can be recast as  $\partial(\rho_{\text{rad}} R^4)/\partial t = 0$ . Hence  $\rho_{\text{rad}} \propto R^{-4}$  where the additional factor of  $R^{-1}$  accounts for the redshift of radiation wavelength. Finally, from Eq. (141) we see that an accelerated expansion ( $\ddot{R}/R > 0$ ) requires  $\rho + 3P < 0$  that is, given that the energy density is always positive, acceleration requires a negative pressure  $P < -\rho/3$ . The simplest possibility is  $P_\Lambda = -\rho_\Lambda$  ( $w = -1$ ) in which case from the first relation in Eq. (142) we immediately obtain  $\rho_\Lambda = \text{const.}$  which corresponds to a Universe dominated by vacuum energy.

The FLRW metric Eq. (139) together with the Friedmann equation (140) and Eq. (142) provides the framework in which the so-called standard cosmological, or  $\Lambda$ CDM, model is defined. According to this model, the present Universe is dominantly filled with a mysterious vacuum energy component  $\rho_\Lambda$  which accounts for about 2/3 of the total energy density. The remaining 1/3 corresponds to a matter component, which is again dominated by an unknown type of dark matter (DM). Known particle species as baryons, electrons and (depending on their masses) neutrinos, contribute a subleading amount  $\rho_b \sim 0.2 \rho_{\text{DM}}$  while the photon contribution is even smaller  $\rho_{\text{rad}} \ll \rho_\Lambda, \rho_{\text{DM}}, \rho_b$ . However, in the early Universe, at temperatures above  $\sim 1$  eV, the Universe was dominated by radiation,  $\rho \simeq \rho_{\text{rad}}$ . The regime of radiation domination is the most relevant one for the topics that will be developed in the forthcoming Sections.

Let us now review some basic notions of thermodynamics in an expanding Universe. For particles in kinetic equilibrium with a thermal bath at temperature  $T$ , the phase space occupancy is given by the distributions  $f(E) = [\exp((E - \mu)/T) \pm 1]^{-1}$  with  $+1$  for fermions and  $-1$  for bosons, while  $\mu$  is the chemical potential of the particle species. If a certain number of species  $p = 1, 2, 3, \dots$  are in *chemical equilibrium*, then  $\sum_p \mu_p = 0$ . In the relativistic limit ( $T \gg m$ ) the contribution to the energy density of the thermal bath of a particle  $p$  with  $g_p$  internal degrees of freedom is

$$\rho_p = \frac{\pi^2}{30} \eta_p g_p T_p^4, \quad (143)$$

where the statistical factor  $\eta_p = 1$  (7/8) for bosons (fermions), and  $T_p$  is the temperature that characterises the  $p$ -particle distribution. If a species is kinetically decoupled from the thermal bath, then  $T_p$  might differ from  $T$ .<sup>27</sup> In the early Universe, a very important fiducial quantity is the total entropy in a comoving volume  $S = R^3(\rho + P)/T$ , and this is because entropy it is conserved, or approximately conserved, in most phases of the cosmological evolution.<sup>28</sup> For relativistic species  $P_p = \rho_p/3$  so that the contribution to the entropy density  $s = S/R^3$  of a relativistic particle is

$$s_p = \frac{2\pi^2}{45} \eta_p g_p T_p^3. \quad (144)$$

It is customary to write the energy and entropy densities of relativistic species in a compact form as

$$\rho_{\text{rad}} = \frac{\pi^2}{30} g_*(T) T^4, \quad s_{\text{rad}} = \frac{2\pi^2}{45} g_S(T) T^3, \quad (145)$$

<sup>27</sup>In the SM this occurs only for the neutrinos, and below  $T \sim 1$  MeV.

<sup>28</sup>This expression for  $S$  holds whenever all the particle chemical potentials are negligible  $|\mu| \ll T$ , which is generally true to an excellent approximation.

where the effective number of energy ( $g_*$ ) and entropy ( $g_S$ ) relativistic degrees of freedom are defined as

$$g_*(T) = \sum_p \eta_p g_p \left( \frac{T_p}{T} \right)^4, \quad g_S(T) = \sum_p \eta_p g_p \left( \frac{T_p}{T} \right)^3. \quad (146)$$

These expressions account for the possibility that for some species  $T_p \neq T$ , in which case  $g_S \neq g_*$ , while they are otherwise equal. Since we will mainly deal with the Universe history during the radiation dominated era ( $\rho \simeq \rho_{\text{rad}}$ ) in the following we will drop the subscript  $\text{rad}$  and simply use  $\rho$  and  $s$ . When  $g_S$  remains constant during the Universe evolution, entropy conservation  $dS \sim d(T^3 R^3) = 0$  implies  $T \propto 1/R \propto t^{-1/2}$ . Finally, from the Friedmann equation (140) and from the expression for the total energy density in the radiation dominated era Eq. (145), one obtains the following expression for the Hubble parameter:

$$H(T) = \left( \frac{4\pi^3 g_*(T)}{45} \right)^{1/2} \frac{T^2}{m_{\text{Pl}}} \simeq 1.66 g_*^{1/2} \frac{T^2}{m_{\text{Pl}}}. \quad (147)$$

In the early Universe, for  $T > m_t$  all the SM degrees of freedom are in the relativistic regime, and  $g_* = 106.75$ . Other relevant values are  $g_*(m_b > T > m_c) = 75.75$ ,  $g_*(T > \Lambda_{\text{QCD}}) = 61.75$  ( $\Lambda_{\text{QCD}}$  is the confinement scale),  $g_*(T > m_\pi) = 17.25$ ,  $g_*(T > m_e) = 10.75$ .

### 3.2. The axion potential and the axion mass at finite temperature

The dependence of the axion potential and mass on the temperature of the early Universe thermal bath is very important because it concurs to determine the present relic abundance of the axions generated through the vacuum realignment mechanism. Although this is not the only mechanism of production of cold relic axions, it is the most model independent and possibly the dominant one. However, deriving a reliable expression for  $V(a, T)$  is not an easy task. The chiral Lagrangian approach that in Section 2.5 proved to be a powerful tool to determine axion properties at zero temperature cannot be used, because convergence of the perturbative expansion deteriorates as the temperature approaches the critical temperature  $T_C \simeq 160$  MeV where QCD starts deconfining, and for  $T \simeq T_C$  the chiral approach is clearly inadequate to describe QCD. However, it is expected that at larger temperatures  $T \gg T_C$  QCD becomes perturbative, in which case perturbative computations, based for example on the so-called dilute instanton gas approximation (DIGA) [147] would represent a sensible approach. A perturbative computation of the axion potential around the background of a dilute instanton gas [54] results in a potential of the form

$$V(a, T)|_{T > T_C} = \chi(T) \left[ 1 - \cos \left( \frac{a}{f_a} \right) \right]. \quad (148)$$

The finite temperature QCD topological susceptibility  $\chi(T)$  is related to the temperature dependent axion mass as

$$\chi(T) = f_a^2 m_a^2(T). \quad (149)$$

The DIGA predicts a power-law dependence of the topological susceptibility on temperature with a rather large exponent  $\chi(T) \propto \chi(0) T^{-8}$ . However, the reliability of the DIGA estimate has been questioned because  $\chi(T)$  exhibits an exponential dependence on quantum corrections that are difficult to estimate perturbatively.<sup>29</sup> To tackle this problem different techniques have been used, as for example a semi-analytical approach based on the interacting instanton liquid model [149, 150] or non-perturbative QCD lattice methods. In particular several groups have carried out dedicated QCD simulations on the lattice in ranges of temperature relevant for the axion mass [117, 148, 151–153]. The results is that above some threshold temperature of the order of several 100 MeV a power-law dependence close to the DIGA prediction is found, although

<sup>29</sup>For example it was found in Ref. [148] that at temperature below  $\sim 4 T_C$  shifts in the axion mass of almost one order of magnitude are possible.

at lower temperatures sizeable deviations can appear. For definiteness we will assume in the following that well above  $T_C$  the temperature dependence of the axion mass can be parametrised as

$$m_a(T) \simeq \beta m_a \left( \frac{T_C}{T} \right)^\gamma, \quad (150)$$

where  $m_a$  is the zero-temperature axion mass, the exponent has a value  $\gamma \approx 4$ ,  $T_C \approx 160 \text{ MeV}$  (see e.g. [154]) while the parameter  $\beta$ , that depends on the number of quark flavours active at the temperature  $T$  and on other details of QCD physics, is found in the DIGA to be of the order of a few  $\times 10^{-2}$  [54] (we will adopt for numerical estimates  $\beta \approx 0.02$  as in Ref. [155]). Expanding Eq. (150) around  $a/f_a = 0$  gives

$$V(a, T)|_{T > T_C} \approx \frac{1}{2} m_a^2(T) a^2 \left[ 1 + b_2(T) \frac{a^2}{f_a^2} + \dots \right], \quad (151)$$

where the coefficient of the quadratic term in the expansion is identified with the square of the axion mass, while terms higher than quadratic, that correspond to higher momenta of the topological charge distribution  $(\alpha_s/8\pi)G\tilde{G}$ , describe self-interactions of the axion field. In particular, it is found in lattice simulations that the fourth order coefficient has a value  $b_2 \approx -\frac{1}{12}$ , as it would be expected from the cosine potential (that is in the DIGA). Being this coefficient negative, the interaction between axions is attractive.

### 3.3. Vacuum realignment mechanism

The contribution of the effective periodic potential  $V(a, T)$  leads to the formation of a cosmological population of cold axions, whose abundance has been first computed in Refs. [156–158]. In this so-called Vacuum Realignment Mechanism (VRM), the present energy density stored in the zero modes<sup>30</sup> of the axion field can be obtained by solving the equation of motion in an expanding Universe

$$\ddot{a} + 3H\dot{a} - \frac{1}{R^2(t)}\nabla^2 a + \frac{dV(a, T)}{da} = 0, \quad (152)$$

where the Hubble rate  $H$  has been defined in Eq. (140) and  $\nabla^2$  is the spatial Laplacian operator. Although a proper treatment would consist in solving Eq. (152) numerically in a given effective potential, for illustrative purposes and to better study the physics of the system, we focus for the moment on the quadratic form of the effective potential given in Eq. (148). We introduce the axion angle  $\theta(x) = a(x)/f_a$ , so that Eq. (152) in a quadratic potential reads

$$\ddot{\theta} + 3H\dot{\theta} - \frac{1}{R^2(t)}\nabla^2 \theta + m_a^2(t)\theta = 0, \quad (153)$$

where  $m_a(t) \equiv m_a(T(t))$ . In this approximation, the Fourier transform of the axion field follows a similar expression as in Eq. (152), with the replacement  $\nabla^2 \rightarrow -k^2$  in terms of the mode  $k^2 \equiv \mathbf{k} \cdot \mathbf{k}$  for each field decomposition. Hubble expansion implies that the wavelength of each mode  $k$  gets stretched as  $\lambda(t) = \frac{2\pi}{k} R(t)$ . There are two qualitatively different regimes in the evolution of a mode, depending on whether at a given time its wavelength is larger than the horizon  $\lambda(t) > t$ , or is inside the horizon  $\lambda(t) < t$ . Recalling that  $t = 1/(2H)$  super-horizon modes are then defined by the condition  $k \lesssim R(t)H(t)$ , while for  $k \gtrsim R(t)H(t)$  the mode is inside the horizon. For super-horizon modes the contribution from the spatial gradient in Eq. (153) can be neglected. If the mass term is also negligible, the solution for the mode goes to a constant as  $t^{-1/2}$  (see Eq. (155) below). For modes well inside the horizon, and for an adiabatic expansion, the solution to Eq. (153) conserves the number of axions in each mode. The number density of these higher frequency modes is suppressed with respect to the contribution from super-horizon modes so we neglect it. Additional details on higher modes can be found in Refs. [159–165].

When analysing Eq. (153), we see that the Hubble drag effectively damps the evolution of the axion field as long as the Hubble rate is significantly larger than the mass term. As the Universe cools and the

<sup>30</sup>The axion field can be expanded in terms of a linear superposition of eigenmodes with definite co-moving wavevector  $\mathbf{k}$   $a(\mathbf{x}, t) = \int d^3k a(\mathbf{k}, t) e^{i\mathbf{k} \cdot \mathbf{x}}$ , and the axion zero mode refers to the component  $a(\mathbf{k} = 0, t)$ .

expansion rate slows down, the mass term eventually begins to contribute to the evolution of the axion field once the condition

$$m_a(t_{\text{osc}}) \approx 3H(t_{\text{osc}}), \quad (154)$$

has been fulfilled.<sup>31</sup> Eq. (154) defines implicitly the time  $t_{\text{osc}}$  at which the axion mass becomes important, and from this moment on, the axion field begins to oscillate in the quadratic potential with oscillations that are damped by the expansion rate.<sup>32</sup>

For super-horizon modes  $k \lesssim RH$  ( $\nabla^2\theta \simeq 0$ ) and as long as  $t \ll t_{\text{osc}}$  ( $m_a(t) \simeq 0$ ), Eq. (153) reduces to  $\ddot{\theta} + (3/2t)\dot{\theta} = 0$ . Defining the initial conditions at the PQ symmetry breaking time as  $\theta(t_{\text{PQ}}) \equiv \theta_{\text{PQ}}$  and  $\dot{\theta}(t_{\text{PQ}}) \equiv \dot{\theta}_{\text{PQ}}$ , the solution to Eq. (153) reads

$$\theta(t) = \theta_{\text{PQ}} + \frac{\dot{\theta}_{\text{PQ}}}{H_{\text{PQ}}} \left( 1 - \frac{R_{\text{PQ}}}{R(t)} \right), \quad (155)$$

$$\dot{\theta}(t) = \dot{\theta}_{\text{PQ}} \left( \frac{R_{\text{PQ}}}{R(t)} \right)^3, \quad (156)$$

where  $H_{\text{PQ}} = H(t_{\text{PQ}})$  and  $R_{\text{PQ}} = R(t_{\text{PQ}})$ . At the time when the axion mass becomes relevant, defined by Eq. (154) as  $t_{\text{osc}}$ , we have

$$\frac{R_{\text{PQ}}}{R(t_{\text{osc}})} = \frac{T_{\text{osc}}}{T_{\text{PQ}}} \approx \frac{T_{\text{osc}}}{f_a} \lesssim 10^{-8}, \quad (157)$$

where we have used  $T_{\text{osc}} \equiv T(t_{\text{osc}}) \approx 1 \text{ GeV}$  and  $T_{\text{PQ}} \equiv T(t_{\text{PQ}}) \simeq f_a \gtrsim 10^8 \text{ GeV}$ . The ratio of the scale factors in parenthesis in Eq. (155) is thus a transient that rapidly decays after the PQ phase transition. We define the initial conditions at the onset of oscillations  $\theta(t_{\text{osc}}) \equiv \theta_i$  and  $\dot{\theta}(t_{\text{osc}}) \equiv \dot{\theta}_i$  as

$$\theta_i = \theta_{\text{PQ}} + \frac{\dot{\theta}_{\text{PQ}}}{H_{\text{PQ}}}, \quad (158)$$

$$\dot{\theta}_i = \dot{\theta}_{\text{PQ}} \left( \frac{H(t_{\text{osc}})}{H_{\text{PQ}}} \right)^{3/2}, \quad (159)$$

where in the second equation we have used  $R \propto 1/T$  and  $H \propto T^2/m_{\text{Pl}}$ . The combination in Eq. (158) is known in the literature as the *initial misalignment angle*. The effects of the initial velocity  $\dot{\theta}_i$  would be important if at  $t_{\text{osc}}$  the kinetic energy stored in the axion field  $\dot{a}^2/2$  exceeds the potential barrier  $2m_a^2 f_a^2$ , see Eq. (148), that is we would need  $\dot{\theta} > 2m_a$ . Using Eq. (154) we can rewrite Eq. (159) as

$$\dot{\theta}_i = m_a(t_{\text{osc}}) \frac{\dot{\theta}_{\text{PQ}}}{H_{\text{PQ}}} \frac{T_{\text{osc}}}{3T_{\text{PQ}}}, \quad (160)$$

so that we obtain the condition

$$\frac{\dot{\theta}_{\text{PQ}}}{H_{\text{PQ}}} > \frac{6}{T_{\text{osc}}} T_{\text{PQ}} \gtrsim 10^8. \quad (161)$$

where for the numerical value we have used Eq. (157). We can conclude that unless the axion velocity at the PQ breaking scale is at least eight orders of magnitude larger than the expansion rate of the Universe, the results for axion DM are indistinguishable from what is obtained by setting, as it is usually done,  $\dot{\theta}_i = 0$ . Some models that assume that at  $t_{\text{osc}}$  the axion kinetic energy dominates the potential energy are reviewed in Section 6.6.3.

Regarding the misalignment angle  $\theta_i$ , the possible initial values depend on the cosmological history of the axion field. To better see this, let us consider the following two conditions:

<sup>31</sup>The factor three appearing in Eq. (154) serves as a crude approximation to estimate the value of  $t_{\text{osc}}$ . In general, this factor should be matched to a numerical solution.

<sup>32</sup>The intuitive meaning of the condition Eq. (154) is the following: in radiation domination  $H(t) = 1/(2t)$ , hence the condition can be rewritten as  $m_a(t_{\text{osc}})t_{\text{osc}} \approx 1$ . In this regime, the angular frequency of the oscillations is  $\omega \approx m_a(t)$ . Therefore, requiring that the condition is satisfied amounts to require that the Universe is sufficiently old to host a sizeable fraction of one oscillation period.

- a) The PQ symmetry is spontaneously broken during inflation;
- b) The PQ symmetry is never restored after its spontaneous breaking occurs.

Condition **a)** is realised whenever the axion energy scale is larger than the Hubble rate at the end of inflation,  $f_a > H_I$ , while condition **b)** is realised whenever the PQ scale is larger than the maximum temperature reached in the post-inflationary Universe [166]. Broadly speaking, one of these two possible scenarios occurs:

**PreI scenario.** If both **a)** and **b)** are satisfied, inflation selects one patch of the Universe within which the spontaneous breaking of the PQ symmetry leads to a homogeneous value of the initial misalignment angle  $\theta_i$ . In this scenario, topological defects are inflated away and do not contribute to the axion energy density. However, other bounds that come from isocurvature modes [167–169] severely constrain these type of models, which require a relatively low-energy scale of inflation to be viable.

**PostI scenario.** If at least one of the conditions **a)** or **b)** is violated, the PQ symmetry breaks with different values of  $\theta_i$  taking different values in patches that are initially out of causal contact, but that today populate the volume enclosed by our Hubble horizon. In this scenario, isocurvature fluctuations in the PQ field randomise  $\theta$ , with no preferred value in the power spectrum. Moreover, modes with  $k \gtrsim RH$  decay because of the gradient term in the equation of motion. The proper treatment in this scenario is to solve numerically the equation of motion of the PQ field in an expanding Universe, in order to capture all features coming from VRM, including the contribution from topological defects, see Section 3.4. Here, we discuss how to approximate the computation of the relic density of cold axions, neglecting for the moment the important contribution from axionic strings and domain walls. In this scenario, the initial misalignment angle  $\theta_i$  at present time takes all possible values in the unit circle within a Hubble patch. The strategy to compute the present abundance relies on computing Eq. (153) many times, each time drawing the initial value  $\theta_i$  from a uniform distribution over the unit circle. For a quadratic potential, this is the same as assuming for the initial condition the value

$$\theta_i \equiv \sqrt{\langle \theta_i^2 \rangle} = \frac{\pi}{\sqrt{3}} \simeq 1.81, \quad (162)$$

where the angle brackets represent the value of the initial condition averaged over  $[-\pi, \pi)$ . For the periodic potential that defines the QCD axion this result is modified due to the presence of non-harmonic terms [155, 164, 170–173] which can be parametrised in terms of a function  $F(\theta_i)$  that accounts for the anharmonic corrections in the axion potential, so that

$$\langle \theta_i^2 \rangle = \frac{1}{2\pi} \int_{-\pi}^{\pi} d\theta_i F(\theta_i) \theta_i^2. \quad (163)$$

Including anharmonicities one finds  $\theta_i \approx 2.15$  [45], which is slightly larger than the value in Eq. (162).

In this scenario, topological defects form after inflation and remain within the horizon, contributing to the axion energy density as discussed in Section 3.4 below. In this scenario, the initial condition is thus fixed by the averaging of  $\theta_i$  over the Hubble patch, which leaves the present value of the axion mass as the sole unknown of the system. Demanding that the axion is the CDM particle today then pins down the value of  $m_a$ , as it has been recently assessed in various cosmological simulations of the axion field as discussed in Section 3.7 below. The detailed mechanism of cold axion production from topological defects needs still to be assessed with sufficient confidence and precision, and a general agreement within the community has not been achieved yet.

The evolution of the axion field can be described in terms of its effective equation of state  $w_a$ , which is defined as

$$w_a \equiv \left\langle \frac{\frac{1}{2}\dot{a}^2 - V(a, T)}{\frac{1}{2}\dot{a}^2 + V(a, T)} \right\rangle, \quad (164)$$



where the angle brackets stand for a temporal average over times larger than the oscillation period. The dependence of the axion energy density on the scale factor ranges from a dark energy-like solution,<sup>33</sup>  $w_a = -1$ , valid at  $t \lesssim t_{\text{osc}}$  (corresponding to an axion field at rest), to a DM-like solution,  $w_a = 0$ , for  $t \gtrsim t_{\text{osc}}$  (when, due to the oscillating behaviour, the average potential energy equals the average kinetic energy). The number of axions in a comoving volume is then frozen from about  $T_{\text{osc}}$  on, with a number density of axions at the onset of oscillations given by

$$n_a(T_{\text{osc}}) = \frac{b}{2} m_a(T_{\text{osc}}) f_a^2 \langle \theta_i^2 \rangle. \quad (165)$$

Here,  $b$  is a factor of order one [155] that captures the uncertainties derived from using the approximation in Eq. (154) to estimate the number density  $n_a(T_{\text{osc}})$ , instead of numerically solving Eq. (152). Assuming that entropy has been conserved within a comoving volume since the axion field has started to oscillate, the ratio of the axion number density to the entropy density has been conserved to any temperature  $T < T_{\text{osc}}$ ,

$$n_a(T) = n_a(T_{\text{osc}}) \left( \frac{s(T)}{s(T_{\text{osc}})} \right)^3. \quad (166)$$

where  $s(T)$  is given in Eq. (146). Neglecting the contribution from the topological defects discussed in Section 3.4, the present energy density of axions is then

$$\rho_a^{\text{VRM}}(T) = m_a n_a(T_{\text{osc}}) \frac{g_S(T)}{g_S(T_{\text{osc}})} \left( \frac{T}{T_{\text{osc}}} \right)^3. \quad (167)$$

In Fig. 1 we show the evolution of the axion angle  $\theta$  (blue solid line) and of the energy density of axions in units of the present CDM energy density (red dashed line), as a function of the inverse plasma temperature  $T_{\text{osc}}/T$ . We have set the initial misalignment angle  $\theta_i = 1$ . For  $T \gtrsim T_{\text{osc}}$  the axion field is frozen to the configuration  $\theta = \theta_i$  with zero energy density in cold axions from the VRM. The value of the axion mass has been fixed so that the present energy density matches the measured energy density in CDM. Using Eq. (167), we can express the energy density in cold axions expected from the VRM at present time, when the temperature of the CMBR photons is  $T_0 = 2.725 \text{ K}$ . It is customary to express the total energy density in one species as a fraction over the *critical* energy density of the Universe, which today is given by  $\rho_{\text{crit}} = 3m_{\text{Pl}}^2 H_0^2 / (8\pi) \approx (0.0805 \text{ eV})^4 h^2$ , where the numerical expression has been obtained using the value of the Hubble constant  $H_0 = 100 h \text{ km/s/Mpc}$  and the quantity  $h$  absorbs all uncertainty in the determination of the Hubble constant.

In the following, we have solved numerically for the equation of motion in Eq. (152) by coding a standard finite-difference method solver.<sup>34</sup> We have further used the QCD susceptibility  $\chi(T)$  obtained by lattice QCD methods [117] and the cosine potential in Eq. (148). Accounting for the change in the entropy and relativistic degrees of freedom with temperature, we finally obtain the present axion abundance

$$\Omega_a^{\text{VRM}} h^2 \equiv \frac{\rho_a^{\text{VRM}}(T_0)}{\rho_{\text{crit}}} h^2 = 0.12 \langle \theta_i^2 \rangle \left( \frac{f_a}{1.6 \times 10^{11} \text{ GeV}} \right)^{\frac{3+\gamma}{2+\gamma}} = 0.12 \langle \theta_i^2 \rangle \left( \frac{35.6 \text{ } \mu\text{eV}}{m_a} \right)^{\frac{3+\gamma}{2+\gamma}}, \quad (168)$$

where for the last relation we have used Eq. (108). The origin of the exponent in Eq. (168) can be understood in the following way: the condition for the start of oscillations Eq. (154) together with the mass-temperature relation in Eq. (150) and the Hubble-temperature relation  $H(T) = 1.66 g_*^{1/2} T^2 / m_{\text{Pl}}$  in Eq. (147) implies

$$T_{\text{osc}}^{2+\gamma} \simeq \left( \frac{b T_C^\gamma m_{\text{Pl}}}{4.98 g_*^{1/2}} \right) m_a. \quad (169)$$

<sup>33</sup>Due to this early dark energy-like behaviour, pseudo-scalars are often invoked when building models of quintessence [174–176] and inflation [177, 178].

<sup>34</sup>The code is available as a Mathematica package at the GIT repository <https://github.com/lucavisinelli>.

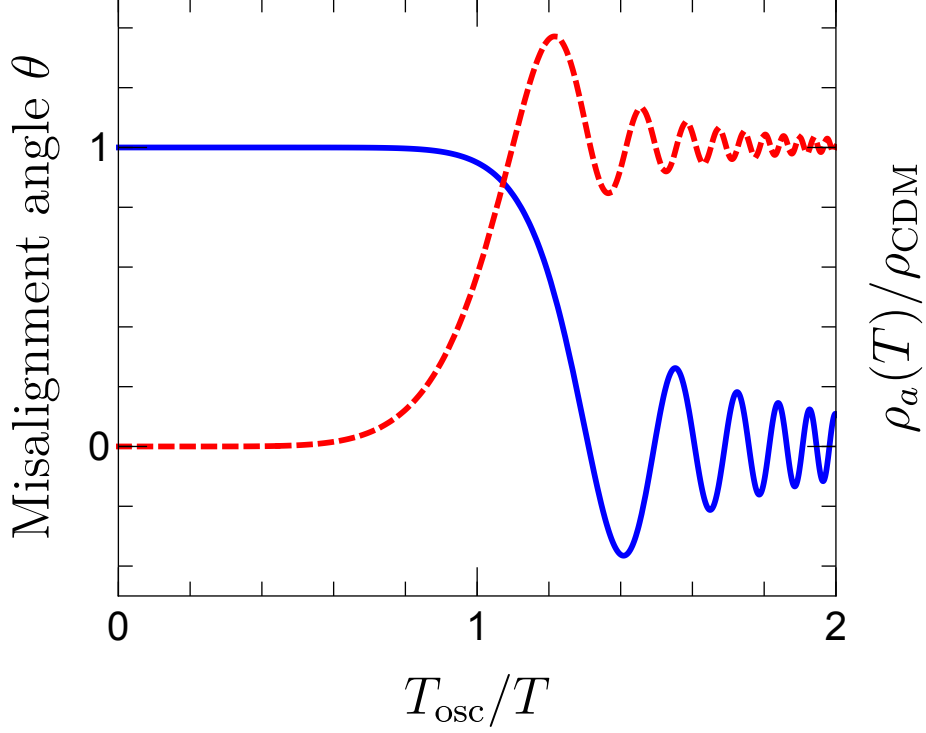


Figure 1: The axion angle  $\theta$  (blue solid line) and the energy density of axions in units of the present CDM energy density (red dashed line), as a function of the inverse plasma temperature  $T_{\text{osc}}/T$ . We set the initial misalignment angle  $\theta_i = 1$ .

Inserting Eq. (150) and Eq. (165) into Eq. (167) one obtains

$$\rho_a^{\text{VRM}}(T) \propto (m_a f_a)^2 \frac{T_C^\gamma T^3}{T_{\text{osc}}^{3+\gamma}}. \quad (170)$$

Since  $m_a f_a \approx m_\pi f_\pi$ , by substituting Eq. (169) for  $T_{\text{osc}}$ , the exponent in Eq. (168) follows.

For future reference it is worthwhile to give an approximate numerical value for  $T_{\text{osc}}$  in terms of  $m_a$ . With  $g_* = 61.75$  as it is appropriate for temperatures around 1 GeV,  $\gamma = 4$ ,  $T_C = 200$  MeV and  $\beta = 0.026$ , Eq. (169) gives

$$T_{\text{osc}} \approx 480 \text{ MeV} \left( \frac{m_a}{1 \mu\text{eV}} \right)^{1/6}. \quad (171)$$

In Section 6.6.1 we will challenge various conditions that have been assumed to hold in the derivation of Eq. (168) and we will argue that different ranges of mass values for CDM axions are possible.

### 3.4. The contribution from topological defects

The misalignment production discussed in the previous section is not the only axion production mechanism in the early universe. Competitive mechanisms are induced by the existence of topological defects<sup>(35)</sup> or a review, see Ref. [179]), specifically strings and domain walls (DW), associated with the axion field.

<sup>35</sup>q

In general, topological defects are inflated away and therefore are relevant only in the post inflationary scenario, **PostI**, introduced above.

Axion strings are formed, through the Kibble mechanism [180, 181], at the time of the spontaneous breaking of the PQ symmetry. Since the complex scalar PQ field must be single valued, its phase  $\theta$  must change by an integer multiple of  $2\pi$  on any closed loop. However, though  $\theta$  is homogeneous in each horizon volume, as dictated by its Goldstone nature, it has random values in different uncorrelated volumes and it is possible that the random phase changes from 0 to  $2\pi$  along a closed path stretching over multiple patches. Any closed loop over which the phase changes by  $2\pi$  must necessarily contain a point in which the PQ field vanishes, so that its phase is undefined.<sup>36</sup> It is evident that this region should be a string with no ends or closed, to avoid that the loop could be contracted in a topologically trivial manner. Crossing strings can form loops that decay, radiating low momentum (cold) axions. Estimating the contribution of the string decay to the axion abundance is a complex problem, not yet completely tackled. This will be the subject of Section 3.4.1.

Once the temperature of the Universe lowers to  $\sim 1$  GeV, non perturbative QCD effects become important and the PQ symmetry breaks down to a discrete  $\mathbb{Z}_{N_{\text{DW}}}$  symmetry. This is, in turn, spontaneously broken since in each casually disconnected patch the axion rests into one of the  $N_{\text{DW}}$  minima. DWs are field configurations that interpolate neighboring vacua. Such configurations have a very large energy density, surpassing the critical energy density of the universe, and are thus cosmologically problematic. The domain wall problem and its solutions are discussed in Section 7.4. Here we only mention that the problem does not subsist in the case of  $N_{\text{DW}} = 1$ , in which case the DW is unstable.

The cosmology of axion domain walls and of string-wall networks, which form after the axion acquires a mass, is discussed in details in Section 3.4.4. Since the following subsections are rather technical, the reader not interested in the details can skip directly to the final result for the axion number density in Eq. (183).

#### 3.4.1. Cosmic axion strings

As predicted by the Kibble mechanism [180, 181], a network of global strings originates whenever a global  $U(1)$  symmetry is spontaneously broken. In the case of the PQ symmetry, the Kibble mechanism produces *axionic* strings, which are vortex-like defects that form as soon as the symmetry is spontaneously broken. As we shall see below, the string population consists in long strings and in string loops. The last, formed by the continuous intersection of long intercommuting strings, contribute the majority of the radiated axions (see Section 3.4.3).

A fundamental aspect of axionic strings is that the explicit breaking of the  $U(1)$  symmetry, due to the QCD anomaly, leads to the dissipation of the string network at temperatures of the order of the QCD phase transition [182–184]. In fact, when the QCD axion acquires a mass, at the time  $t_{\text{osc}}$ , strings attach to surface-like defects corresponding to DWs [185], which, in the case of  $N_{\text{DW}} = 1$ , are unstable (see Section 3.4.4). The decay of the axionic string network contributes to the present abundance of cold axions [179, 182, 186–189], as confirmed by dedicated cosmological simulations [190–202].

#### 3.4.2. String populations

The population of strings can be neatly divided into two distinct subgroups:

1. **Long strings.** These are string-like defects, of size comparable to the horizon scale, that carry a net conserved topological charge and are stable, with energy density  $\rho_{\text{long}}$ . Long strings can be crudely approximated as thin curves with a string core of size  $\sim 1/f_a$  and a linear mass density  $\mu_{\text{eff}}(t)$  [182, 186, 203–205]. Assuming a linear realization of the  $U(1)_{\text{PQ}}$  symmetry with scalar potential given in Eq. (78) and  $f_a = v_a$  ( $N_{\text{DW}} = 1$ ), the linear mass density resulting from the string Lagrangian reads [184, 186]

$$\mu_{\text{eff}}(t) = \pi f_a^2 \ln(f_a t) . \quad (172)$$

<sup>36</sup>Since the loop can be shrunk to a point, there must exist a location where  $\theta$  has a discontinuous jump from 0 to  $2\pi$ . The only way this is allowed is if the phase is undefined, that is for a vanishing field.

The logarithmic correction in the energy density of long strings comes from the fact that, in a radiation-dominated cosmology, global strings have not completely straightened, so that short wavelengths also contribute to the total energy density [182]. A constant linear mass density is achieved when strings have completely stretched and modes smaller than the horizon at time  $t$  do not contribute significantly to the total energy density. The network of global strings relaxes into an approximately scaling solution characterised by a correlation length  $L = t/\sqrt{\xi}$ , where  $\xi$  is a dimensionless parameter describing the string stretching, and with an associated energy density that scales as

$$\rho_{\text{long}} = \xi(t) \frac{\mu_{\text{eff}}(t)}{t^2} = \frac{\mu_{\text{eff}}(t)}{L^2}. \quad (173)$$

Various levels of sophistications have been used to describe the dynamics of long strings. In the original formulation of the so-called one-scale model [206], the evolution of the network of long strings does not depend on the velocity of the string. A more complex parametrisation of the evolution is obtained by accounting for the dependence on the velocity of the centre of mass of the string [207–209] or when including the effects of friction due to interaction of the network of strings with surrounding matter and radiation [210, 211]. The mean-squared velocity of the long string gas  $\langle v^2 \rangle$  enters the equation of state  $w_{\text{str}}$  that describes the evolution of the energy density, namely [212]

$$w_{\text{str}} = \frac{2\langle v^2 \rangle - 1}{3}. \quad (174)$$

For ultra-relativistic strings,  $\langle v^2 \rangle \approx 1$  and a free network of long strings evolves as radiation, while in the case of slow-moving strings  $\langle v^2 \rangle \approx 0$  and  $w_{\text{str}} = -1/3$ . In general, we expect the equation of state for the string gas to vary within the range  $-1/3 \leq w_{\text{str}} \leq 1/3$ . Numerical simulations of long strings in a radiation-dominated cosmology show that  $\langle v^2 \rangle \approx 0.43$  [213]. A dissipative, velocity-dependent framework has been recently applied to study the evolution of axionic strings [214, 215].

2. **Loops.** The population of small closed loops, each of size  $\ell$  and energy density  $\rho_{\text{loop}}$ , forms from the continuous intersection of long intercommuting strings. Loops vibrate and shrink while releasing energy into a spectrum of radiated axions. The power loss of the network into radiation can be described through the dissipation of the energy of a closed loop  $E_{\text{loop}} = \mu_{\text{eff}}(t)\ell$  with length  $\ell$  into axions as [190, 211, 216],

$$\frac{dE_{\text{loop}}}{dt} = \kappa_s \mu_{\text{eff}}(t), \quad (175)$$

where  $\kappa_s \approx 0.15$  is a dimensionless quantity [212, 217, 218] computed at a fixed value of the string velocity  $\langle v^2 \rangle \approx 0.5$ . Solving Eq. (175), gives the length of the closed loop  $\ell = \ell(t, \ell_I)$  at time  $t$  and with initial length  $\ell_I$  at the time  $t_I$  at which the closed loop is formed. Although in principle, the length of loops formed could be ranging at any size, numerical simulations [191, 219–224] show that the initial length of the large loop at its formation tracks the time of formation as

$$\ell(t_I) = \alpha_{\text{loop}} t_I, \quad (176)$$

where  $\alpha_{\text{loop}}$  is an approximately constant loop size parameter which gives the fraction of the horizon size at which loops predominantly form. The loop spectrum is described in terms of a loop formation rate  $r_\ell(\ell_I, t_I)$ , which is related to the rate of the energy density dissipated into axions by [225, 226]

$$\frac{d\rho_{\text{loop}}}{dt} = \int_0^{+\infty} d\ell \mu_{\text{eff}}(t) \ell r_\ell(\ell, t). \quad (177)$$

The loop of initial size  $\ell_I$  shrinks and disappears by the time  $t_F$  defined implicitly as  $\ell(t_F, \ell_I) = 0$ . During this period, loops form at time  $t_I$  and evolve emitting cold axions in their spectra.

The total energy density of the string network is then  $\rho_{\text{str}} = \rho_{\text{long}} + \rho_{\text{loop}}$ . We neglect for simplicity additional features like kinks and cusps in the long strings, which would also dissipate energy during the evolution of the network. In the standard cosmology, it is expected that the majority of the energy density is in long strings, while the remaining part is distributed into small loops spanning all lengths from the string core  $\sim \pi/f_a$  to the horizon scale  $\sim \pi/H(t)$  [200].

### 3.4.3. Spectrum of radiated axions

In order to extract the energy density of the radiated axions from the simulation of the evolution of an axionic string network, the evolution of the energy density in the strings  $\rho_{\text{str}}$  is compared to what is obtained for a gas of free strings of energy density  $\rho_{\text{free}}$  that does not radiate [200]. The evolution of a free, non-intercommuting string gas is described by the kinetic equation

$$\frac{d\rho_{\text{free}}}{dt} + 3H(1 + w_{\text{str}})\rho_{\text{free}} = 0, \quad (178)$$

where  $w_{\text{str}}$  is given in Eq. (174). The solution to Eq. (178) is  $\rho_{\text{free}} \propto a^{-3(1+w_{\text{str}})}$  which, in the case of a radiation-dominated cosmology and fixing the proportionality constant to match the initial energy density of the string network in Eq. (173), gives

$$\rho_{\text{free}}(t) = \xi \frac{\mu_{\text{eff}}(t)}{t_{\text{PQ}}^2} \left( \frac{t}{t_{\text{PQ}}} \right)^{-\frac{3}{2}(1+w_{\text{str}})}. \quad (179)$$

When the axion emission is included, Eq. (178) is modified to include the effective energy lost in the emission of axions per unit time  $\Gamma_{\text{str} \rightarrow a}$ , defined as the difference in the rates at which the energy densities in the free string gas and the string network change,

$$\Gamma_{\text{str} \rightarrow a}(t) \equiv \dot{\rho}_{\text{free}}(t) - \dot{\rho}_{\text{str}}(t) = H(1 - 3w_{\text{str}})\rho_{\text{str}} - \frac{\rho_{\text{str}}}{\mu_{\text{eff}}} \frac{d\mu_{\text{eff}}}{dt}. \quad (180)$$

Once the power radiated by the string network  $\Gamma_{\text{str} \rightarrow a}$  has been obtained, the energy density of the radiated axions follows the evolution  $\rho_a^{\text{str}} + 4H\rho_a^{\text{str}} = \Gamma_{\text{str} \rightarrow a}$ ; the axion energy density from the decay of the string network contributes to an additional source on top of the abundance expressed in Eq. (167) obtained using the VRM. The number density of axions associated to this process is [200]

$$n_a^{\text{str}} = \int^t dt' \frac{\Gamma_{\text{str} \rightarrow a}(t')}{H(t')} \left( \frac{R(t')}{R(t)} \right)^3 \int \frac{dk}{k} F(k) = \frac{(1 - 3w_{\text{str}})\pi f_a^2}{t^{3/2}} \int^t dt' \frac{\ln(f_a t')}{(t')^{1/2}} \int \frac{dk}{k} F(k), \quad (181)$$

where the spectral energy density  $F(k) \propto k^{-q}$  has been explored in different regimes in the literature depending on the value of the spectral index  $q$ . A choice  $q > 1$  assumes that axions are radiated away on a timescale comparable to the Hubble time, and describes a power spectrum ranging over all modes from  $k \approx 1/\ell(t_I) \approx H(t_I)/\alpha_{\text{loop}}$  to infinity [190, 216]. On the other hand, assuming that strings efficiently shrink emitting all of their energy at once leads to a flat power spectrum per logarithmic interval with an infrared cutoff at the wave mode  $k \approx H$  and a ultraviolet cutoff at  $k = f_a$ , with a harder spectral index  $q = 1$  [188, 227, 228]. Demanding that the spectrum is normalised over the given interval results in

$$F(k) = \begin{cases} \frac{q-1}{\alpha_{\text{loop}}^{q-1}} \left( \frac{k}{H} \right)^{-q}, & \text{for } q > 1, \\ \frac{1}{\ln(f_a/H)} \frac{H}{k}, & \text{for } q = 1. \end{cases} \quad (182)$$

The integration of Eq. (181) with the spectrum in Eq. (182) and  $q > 1$  finally leads to

$$n_a^{\text{str}} \approx \frac{(1 - 3w_{\text{str}})\pi f_a^2}{2t_{\text{osc}}} \times \begin{cases} \alpha_{\text{loop}} \frac{q-1}{q} \ln(f_a t_{\text{osc}}), & \text{for } q > 1, \\ 1, & \text{for } q = 1. \end{cases} \quad (183)$$

This expression shows that most of the axions are radiated by loops right before  $t_{\text{osc}}$ , when DWs dissipate the network. The computation matches the estimation for the decay of the string network at the time of DW formation [184, 190]. The number density of axions at time  $t_{\text{osc}}$  from Eq. (183) results from a steeply falling integrand function of  $t$ , so that the dominant contribution comes from loops originating nearly instantaneously at values  $t_I \sim t_{\text{osc}}$  [184, 190, 191]. The use of the harder spectrum with  $q = 1$  generically leads to results for the string contributions which are smaller by a factor  $\log(f_a t_{\text{osc}}) \approx 70$ .

We will use the results of this Section in the discussion about the status of the computation of the present axion abundance in Section 3.7.

### 3.4.4. Cosmological domain walls

Cosmological DWs emerge with the spontaneous breaking of discrete symmetries [179, 186, 210]. When the PQ symmetry is explicitly broken by nonperturbative QCD effects, the axion acquires a periodic potential with  $N_{\text{DW}}$  equivalent minima. Thus, the original  $U(1)$  symmetry, which guaranties the equivalence of all values of  $\theta$ , is broken into a discrete  $\mathbb{Z}_{N_{\text{DW}}}$  symmetry. Evidently, it is not required that all space is in the same minimum. Uncorrelated patches may choose different ground states, randomly selecting one of the  $N_{\text{DW}}$  equivalent vacua. Axion DWs appear at the boundaries of physical regions that are in different minima, providing a smooth interpolation between the two vacua. Such configurations have a thickness  $\delta_{\text{wall}} \approx 1/m_a(t_{\text{osc}})$  and an energy per unit area  $\sigma_{\text{wall}} \approx 8m_a^2(t_{\text{osc}})v_a$ , for the cosine potential [45]. Notice that there are axion DWs even in the case of  $N_{\text{DW}} = 1$ , which have an interpolating field configuration starting and ending in the same vacuum, but winding around the bottom of the Mexican hat potential once [27].

As explained above, at the time when the axion acquires a mass, axion strings become the edge of DWs, forming a string-wall network [179, 210] whose dynamics depends on the value of  $N_{\text{DW}}$ . In the case of  $N_{\text{DW}} = 1$ , strings disrupt the DWs soon after their formation by separating them into smaller pieces [186, 229] and dissipating the network. The decay of these DWs produces a spectrum of radiated axions, obtainable with dedicated simulations.<sup>37</sup> On the other hand, DWs in theories with  $N_{\text{DW}} > 1$  are generally stable, eventually coming to dominate the expansion rate of the universe [230], a result in conflict with observations. A more detailed description of this DW problem and its possible solutions will be discussed in Section 7.4.

### 3.5. Axion isocurvature fluctuations

This topic is relevant in the **PreI** scenario. We consider an early inflationary period described by the quasi-de Sitter space-time metric, with a nearly-constant Hubble rate  $H_I$ . In this setting, the axion field is a massless spectator. Inflationary models generically predict the appearance of primordial scalar and tensor fluctuations, which redshift to super-horizon scales to later evolve into primordial curvature perturbations as well as primordial gravitational waves, leaving an imprint in the CMBR anisotropy and on the large-scale structure [231–236]. The CMBR features distinct peaks both in its angular power spectrum of temperature (TT) as well as in the temperature-polarisation cross-power spectrum (TE), with the first peak in TT measured at  $\ell = 220.6 \pm 0.6$  at 68% confidence level (CL) by the *Planck* collaboration [237]. Other information extracted from the CMBR include the polarisation angular power spectrum (EE).

Adiabatic curvature perturbations generated during inflation show a nearly scale-invariant dimensionless power spectrum of primordial curvature perturbations with amplitude  $\Delta_{\mathcal{R}}^2(k_0)$ , with a mild dependence on the co-moving wavenumber  $k$  which is parametrised by a scalar spectral index  $n_S$  around an arbitrary reference scale  $k_0$ <sup>38</sup> as [240–242]

$$\Delta_{\mathcal{R}}^2(k) \equiv \Delta_{\mathcal{R}}^2(k_0) \left( \frac{k}{k_0} \right)^{n_S-1}. \quad (184)$$

If the axion field  $a$  originated during inflation, it would have also inherited quantum fluctuations with the typical standard deviation  $\sigma_a$  of a massless scalar field in the accelerated expansion, see e.g. Ref. [243],

$$\sigma_a = \sqrt{\langle a^2 \rangle} \simeq \frac{H_I}{2\pi}, \quad (185)$$

and with a corresponding standard deviation for the distribution of the axion angle  $\sigma_\theta = \sigma_a/f_a$ . Since these axion fluctuations originated during inflation are independent of the quantum fluctuations of the inflaton field, they are of the isocurvature type. More in detail, the fluctuations in the axion field do not perturb the total energy density during inflation and change the value of the axion number density with respect

<sup>37</sup>Numerical simulations have mostly focused on the case of a KSVZ axion [197, 200–202], which is free of long-lived DWs.

<sup>38</sup>The reference scale  $k_0$  is also called the “pivot” scale in cosmology, and refers to the comoving scale at which measurements are taken. For example, the *Planck* mission often refers to the pivotal scale  $k_0 = 0.05 \text{ Mpc}^{-1}$  [238]. For isocurvature and tensor modes, the constraints are quoted at three different scales:  $k_{\text{low}} = 0.002 \text{ Mpc}^{-1}$ ,  $k_{\text{mid}} = 0.050 \text{ Mpc}^{-1}$ , and  $k_{\text{high}} = 0.100 \text{ Mpc}^{-1}$  [239].

Parameter	Prior	Reference
$\Omega_{\text{CDM}} h^2$	$0.1200 \pm 0.0012$	Base $\Lambda$ CDM, <i>Planck</i> TT, TE, EE + lowE + lensing [238]
$\ln(10^{10} \Delta_{\mathcal{R}}^2(k_0))$	$3.044 \pm 0.014$	Base $\Lambda$ CDM, <i>Planck</i> TT, TE, EE + lowE + lensing [238]
$n_S$	$0.9651 \pm 0.0041$	$\Lambda$ CDM+ $r$ , <i>Planck</i> TT, TE, EE + lowE + lensing+BK15 [239]
$r$	$< 0.056$ at 95% CL	$\Lambda$ CDM+ $r$ , <i>Planck</i> TT, TE, EE + lowE + lensing+BK15 [239]
$\beta$	$< 0.035$ at 95% CL	CDI $n_{\text{II}} = 1$ , <i>Planck</i> TT, TE, EE + lowE + lensing [239].

Table 1: Cosmological parameters used in this Review, obtained from the joint BICEP2/Keck Array (BK15) analysis of the combined dataset containing TT, TE, EE + lowE + lensing + BK15. The constraint on the axion isocurvature fraction  $\beta$  and the measurement of  $\Delta_{\mathcal{R}}^2(k_0)$  are based on the analysis of the TT, TE, EE + lowE + lensing dataset.

to entropy density,  $\delta(n_a/s) \neq 0$ . Axion isocurvature fluctuations convert into curvature perturbations at the time at which the axion mass becomes relevant, around the QCD phase transition [167–169], due to the feedback of isocurvature into curvature modes [244, 245]. Since the axion field behaves as CDM at recombination, these axion perturbations imprint into the temperature and polarisation fluctuations in the CMBR and, because of their isocurvature nature, they are completely uncorrelated with the adiabatic curvature perturbations.

Measurements of the anisotropies in the CMBR can be used to constrain this type of scenario, since data show that primordial fluctuations are predominantly adiabatic with little space left for fluctuations of the isocurvature type. The spectrum of the isocurvature perturbations in the axion energy density can be computed at a fixed scale as  $|\mathcal{S}_a|^2$ , where we define the amplitude

$$\mathcal{S}_a = \frac{\Omega_a}{\Omega_{\text{CDM}}} \frac{\partial \ln \Omega_a}{\partial \theta_i} \sigma_\theta. \quad (186)$$

This expression takes into account scenarios in which the axion could be a sub-dominant DM component and anharmonic terms are present in the potential [246]. In the illustrative case in which cosmic axions address the missing CDM mass,  $\Omega_a = \Omega_{\text{CDM}}$ , and in the case of a purely quadratic potential that ignores the anharmonic corrections from a more complicated shape of  $V(\theta)$ ,  $\Omega_a \propto \theta_i^2$ , the spectrum of axion isocurvature perturbations results in

$$\Delta_a^2(k) \simeq \left( \frac{H_I}{\pi \theta_i f_a} \right)^2. \quad (187)$$

The *Planck* mission constrains uncorrelated “axion” isocurvature fluctuations by placing an upper bound on the primordial isocurvature fraction,

$$\beta \equiv \frac{\Delta_a^2(k)}{\Delta_{\mathcal{R}}^2(k) + \Delta_a^2(k)}, \quad (188)$$

where the spectra are computed at a pivot scale  $k = k_0$ . Here, we have used the measurements of the CMBR temperature and polarisation anisotropies from the *Planck* satellite, jointly with the BICEP2/Keck Array (BK15) for the combined TT, TE, EE + lowE + lensing + BK15 dataset at 68% CL [238, 239, 247–252]. We report the values used in this Review in Table 1, where data in the form  $A \pm B$  are reported at 68% CL, while upper limits are reported at 95% CL.

Isocurvature bounds place a stringent constraint on the scale of inflation, so that models of axion DM that develop in the **PreI** scenario require a relatively low Hubble rate  $H_I$  compared to the scale  $H_I \lesssim 10^{13}$  GeV which has currently been probed using CMBR tensor modes. Using the results of the analysis we derive the constraint

$$\frac{H_I}{10^8 \text{ GeV}} \lesssim \left( \frac{\theta_i}{\pi} \right) \left( \frac{f_a}{10^{12} \text{ GeV}} \right). \quad (189)$$

This result has been computed using a quadratic potential for illustrative purpose. However, for the remaining of the Review we generally use the amplitude in Eq. (186) unless specified.



### 3.6. Cosmological bounds on the axion mass

Before addressing the upper bounds that can be set on the axion mass from early Universe and cosmological consideration, let us mention a generic (non cosmological) argument that is sometimes invoked to claim a *lower* limit on the axion mass. This argument is based on the belief that an axion decay constant  $f_a$  above the Planck scale is incompatible with an effective QFT description so that, according to Eq. (108),  $f_a \lesssim m_{\text{Pl}}$  would yield  $m_a \gtrsim 5 \times 10^{-13}$  eV. Note, however, that even this seemingly model-independent bound can be circumvented in a particular axion construction that exploits the Kim-Nilles-Peloso mechanism [253]. This mechanism requires the existence of at least two axions, and can produce an effective super-Planckian axion scale, although the original fundamental scale is sub-Planckian [253]. In any case this lower limit would not compete with the lower limit on the axion mass  $m_a \gtrsim 2 \times 10^{-11}$  eV that can be obtained from considerations of the super-radiance phenomenon (a topic that will be touched on in Section 4.6) and that as long as axion self interactions are sufficiently feeble, is truly model independent.

Moving now to review the cosmological arguments that allow to constrain from above the value of the axion mass, it should be mentioned from the start that altogether these bounds are much less constraining than the limits that can be inferred from astrophysical processes (discussed in Section 4), by translating the bounds on the different axion couplings  $g_{a\gamma}, g_{ae}, g_{aN}$  into lower bounds on the axion decay constant  $f_a$  and in turn on upper limits on  $m_a$ . Although the upper limits derived in this way are admittedly model dependent, and a precise number cannot be given without specifying the theoretical setup, the indication that  $m_a \lesssim 0.1$  eV is rather solid. In spite of this, the cosmological bounds are well worth mentioning because they rely on completely independent arguments.

*Hot dark matter.* Axions interact with pions ( $a + \pi \rightarrow \pi + \pi$ ) and nucleons ( $a + N \rightarrow \pi + N$ ) with a strength proportional to  $m_a$ . Then, for sufficiently large values of  $m_a$  a thermal population of axions arises, which would constitute a Hot Dark Matter (HDM) component. However, HDM abundance is severely constrained by data from cosmological surveys. Using WMAP-7 data Ref. [254] set the bound  $m_a \lesssim 0.72$  eV. More recently the bound was strengthened to  $m_a \lesssim 0.53$  eV using Planck 2015 results [255].

*Baryon to photon ratio from BBN and from CMB.* Axions decay to two photons with a lifetime inversely proportional to the fifth power of the mass,

$$\tau_a = \frac{64\pi}{g_{a\gamma}^2 m_a^3} \sim 10^{24} \left( \frac{\text{eV}}{m_a} \right)^5 \text{ s}. \quad (190)$$

For  $m_a \gtrsim 20$  eV the axion lifetime drops below the age of the Universe, hence, for a sufficiently large mass, the decay happens early enough and the HDM bound no longer apply. However, if axions decay not too early, non-thermal photons injected in the bath would produce a spectral distortion in the CMB, and this can be used to derive restrictive constraints [256]. However, if decays occur early enough, photons will have the time to thermalise and the CMB would not be affected. Nevertheless, the additional entropy injected into the bath increases the number of photons relative to that of baryons, decreasing the ratio  $\eta_b = n_b/n_\gamma$ . Nowadays we know with good precision the value of  $\eta_b$ , which is inferred independently from BBN and from CMB data, and there is a beautiful agreement between the two results. Since the relevant physics processes responsible for the primordial abundances of light elements and for the CMB occur in different cosmological eras that are characterised by temperatures that differ by about six orders of magnitude, the amount of entropy that can be injected in the thermal bath between  $T_{\text{BBN}} \sim 1$  MeV and  $T_{\text{CMB}} \sim 1$  eV is tightly constrained. This argument was used in Ref. [257] to exclude  $m_a \lesssim 300$  keV. A later study that used Planck data, together with new inferences of primordial element abundances, pushed the limit up to  $m_a \gtrsim 1$  MeV [258], while an assessment of the robustness of the bounds with respect to possible deviations in the standard cosmology was recently presented in Ref. [259]. These bounds nicely overlap with the constraints from beam dump and reactor experiments, which exclude axion (and ALP) masses up to several GeVs [260–266]. Altogether, these considerations allow to define  $m_a \lesssim 0.53$  eV as the cosmologically allowed axion mass window.

### 3.7. Benchmark axion mass region for $\Omega_a \simeq \Omega_{\text{CDM}}$

The present axion relic abundance  $\Omega_a$  depends on multiple production mechanisms that have been reviewed in the previous sections. Here, we discuss the benchmark axion DM mass regions both in the post- and pre-inflationary PQ breaking scenarios, including also the constraints coming from various cosmological considerations.

#### 3.7.1. Post-inflationary scenario

In the standard cosmological scenario, refined cosmological simulations yield to a large uncertainty in the determination of the DM axion mass, primarily due to the extrapolation of the string spectrum from the PQ scale down to the QCD phase transition. Assuming  $N_{\text{DW}} = 1$  leads to the range  $m_a \approx (10 - 100) \mu\text{eV}$  in which the QCD axion would account for all of the CDM observed in the Universe. The constraints from the non-observation of B-modes by the BICEP2/Keck Array, jointly with the measurements of the CMBR properties from the *Planck* collaboration allow to pin down the DM axion mass. For example, the work in Ref. [267] uses the energy contribution for  $\Omega_a h^2$  given in Refs. [173, 268] to obtain the value of the DM axion mass  $m_a = (82.2 \pm 1.1) \mu\text{eV}$  at a fixed value of the effective number of relativistic species  $N_{\text{eff}}^{\text{SM}} = 3.046$ .

These studies, however, did not properly account for the contribution of topological defects. As we have discussed in Section 3.4, the difficulty in this scenario arises precisely from the computations of the effects of the network of axionic strings, which has recently received attention. The recent literature has focused on models with  $N_{\text{DW}} = 1$ , which do not require additional assumptions about the dissipation of the domain wall network. Hiramatsu *et al.* [194] simulate the evolution of the axionic string network using an efficient identification scheme of global strings in order to assess the energy spectrum and the axion decay constant, which is found to be  $f_a \lesssim 3 \times 10^{11} \text{ GeV}$  or  $m_a \gtrsim 20 \mu\text{eV}$ , while the string stretching parameter appearing in Eq. (173) is found to be  $\xi = 0.87 \pm 0.14$ . Klaer and Moore [198] have used the expertise in Refs. [214, 269] and developed a numerical scheme that accounts for the large hierarchy of scales between the string core scale and the Hubble scale, with the quantity  $\log(f_a/H_{\text{QCD}}) \sim 70$  that directly enters the assessment of the string tension in Eq. (172). Using their technique along with the QCD susceptibility obtained in Ref. [117], Klaer and Moore find that the total axion production when strings are included is somewhat less efficient than in the angle-averaged misalignment case, with a value of the axion mass  $m_a = (26.2 \pm 3.4) \mu\text{eV}$  [199]. Gorghetto *et al.* [200] find an axion spectrum peaked at the energy of the order of the string core scale, which would correspond to a negligible number density of relic axions from strings. Buschmann *et al.* [202] have performed high-resolution simulations of the evolution of the PQ field starting at the epoch before the PQ phase transition and ending at matter-radiation equality, about the time at which axion miniclusters collapse. The value of the axion mass obtained from the simulations is  $m_a = (25.2 \pm 11.0) \mu\text{eV}$ . Both results in Refs. [200, 202] find a logarithmic deviation to the number of strings per Hubble patch from the scaling regime. Kawasaki *et al.* [270] estimate the abundance of CDM axions from both VRM and the decay of topological defects, obtaining the mass range  $m_a = (115 \pm 25) \mu\text{eV}$  for the models with the domain wall number  $N_{\text{DW}} = 1$ . The results for the present axion energy density as a function of the axion mass obtained in Refs. [199, 202] are consistent with each other, while the results in Ref. [270] are larger by a factor of order ten. Such a discrepancy could be partially due to the explicit separation of the VRM and string decay production mechanisms enforced in Ref. [270], which leads to an over-counting of the axion energy density [199]. The simulation by Vaquero *et al.* [201] differs from that in Ref. [202] for a number of details, including the use of the “fat” string scheme [271], initial condition, the measurement of the CDM energy density, the length and the details of the evolution to the matter-radiation equality. These results strongly depend on the choice of the temperature dependence of the QCD topological susceptibility. Refs. [194, 202, 270] have derived their results using a susceptibility with an index corresponding to  $2\gamma = 6.68$  in Eq. (150), using the parametrisation in the ILM [150]. This exponent is milder than what obtained in Ref. [117] for which  $2\gamma = 8.2$  at temperatures  $T \gg T_C$ .

#### 3.7.2. Pre-inflationary scenario

This scenario is realised whenever the PQ symmetry is spontaneously broken during inflation,  $H_I < f_a$ , and it is not restored afterwards [157]. In this scenario, the axion field is homogeneous through various

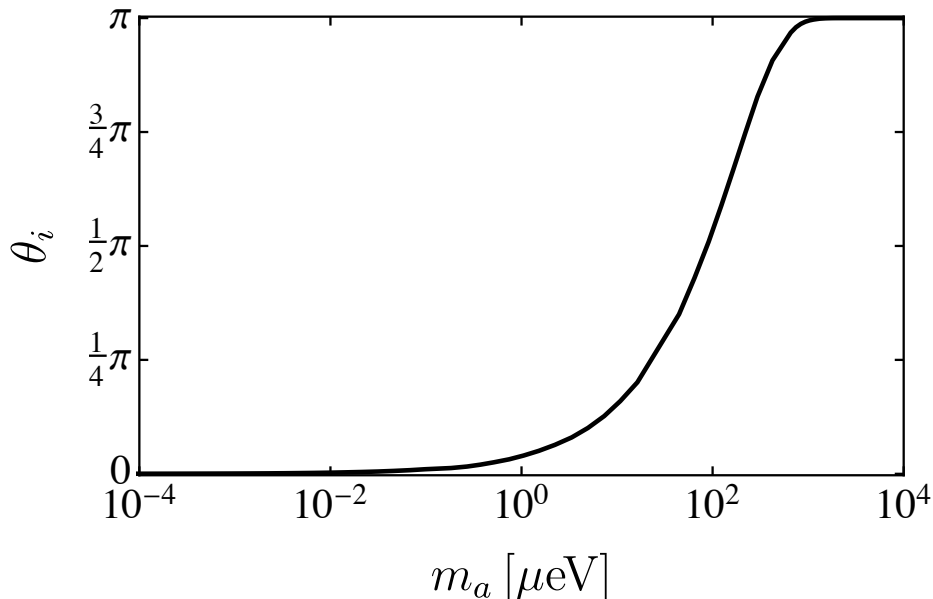


Figure 2: The relation between the DM axion mass and the initial misalignment angle in the **PreI** scenario.

Hubble patches, with a unique value of  $\theta_i$  observed over the whole observable universe. As shown in Fig. 2, each value of  $\theta_i$  is related to a unique value of the DM axion mass. A global fit of this scenario [272] performed using the DarkBit module [273] of the GAMBIT numerical code [274] yields the DM axion mass range  $0.12 \mu\text{eV} \leq m_a \leq 0.15 \text{ meV}$  at the 95% equal-tailed confidence interval of the marginalised posterior distribution accounting for the QCD axion (both the KSVZ and the DFSZ models) and taking into account results from various observations and experiments in the likelihood including the light-shining-through-wall experiments, helioscopes, cavity searches, distortions of gamma-ray spectra, supernovae, horizontal branch stars and the hint from the cooling of white dwarfs. An important assumption that impacts on the result is the choice for the prior on  $\theta_i$ , which in Ref. [272] is assumed to be uniform over the interval  $[-\pi, \pi)$ .

Small initial values of  $\theta_i$  might also occur naturally, i.e. without any fine tuning, in low-scale inflation models in which inflation lasts sufficiently long [275, 276]. If  $H_I \lesssim \Lambda_{\text{QCD}}$  the axion acquires a mass already during inflation, the  $\theta_i$ -distribution flows towards the CP conserving minimum and, for long durations of inflation, stabilises around sufficiently small  $\theta_i$  values. As a result the QCD axion can naturally give the DM abundance for axion masses well below the classical window, down to  $m_a \approx 10^{-12} \text{ eV}$  [275].

On the contrary, values of the initial misalignment angle that are close to the hilltop of the potential  $\theta_i \simeq \pi$  could drive the axion energy scale to values  $f_a \lesssim 10^{12} \text{ GeV}$  ( $m_a \gtrsim 10 \mu\text{eV}$ ), because of the importance of the non-harmonic terms in the axion potential. With the choice  $\pi - \theta_i \simeq 10^{-3}$ , one obtains  $f_a \approx 10^{10} \text{ GeV}$ . It is possible that the axion field has been driven to such a value of  $\theta_i$  during inflation [277].

### 3.7.3. Summary of cosmological axion bounds

The various constraints on the parameter space of the QCD axion can be summarised as in Fig. 3, in which we focus on the KSVZ model (with  $E/N = 0$  and  $N_{\text{DW}} = 1$ ), and we show the axion energy scale  $f_a$  (left Y axis) as a function of the Hubble rate at the end of inflation  $H_I$  (bottom X axis). The parameter space of the DM axion depends on four quantities, namely the axion energy scale  $f_a$ , the initial misalignment angle  $\theta_i$ , the Hubble rate during inflation  $H_I$ , and the contribution from topological defects to the total axion energy density  $\alpha_{\text{tot}} \equiv \rho_a / \rho_a^{\text{VRM}}$ . For the QCD axion, the axion mass  $m_a$  is related to  $f_a$  as in Eq. (108), see the different grids used on the Y axes. For single-field inflation, the tensor-to-scalar ratio

$r$  is proportional to  $H_I^2$ , as expressed in the top X axis. The parameter space is bound to the right by the non-detection of primordial gravitational waves by the *Planck*-BICEP2 collaborations, which set an upper limit on the scale of inflation  $H_I$ . The axion energy scale  $f_a$  is bound below by various astrophysical considerations, see Section 4.1, and translates into an upper bound on the mass of the QCD axion. The phenomenon of super-radiance excludes the portion of the axion mass given in Eq. (227) (see Section 4.6). The solid red line marks the watershed  $f_a = H_I$  and separates the region where the axion is present during inflation (top - left region, **PreI** scenario) from the region where the axion field originates after inflation (bottom - right region, **PostI** scenario). This line has to be thought as a qualitative bound between the two scenarios considered, since the exact details depend on the inflationary model, the preheating-reheating scenarios, and axion particle physics.

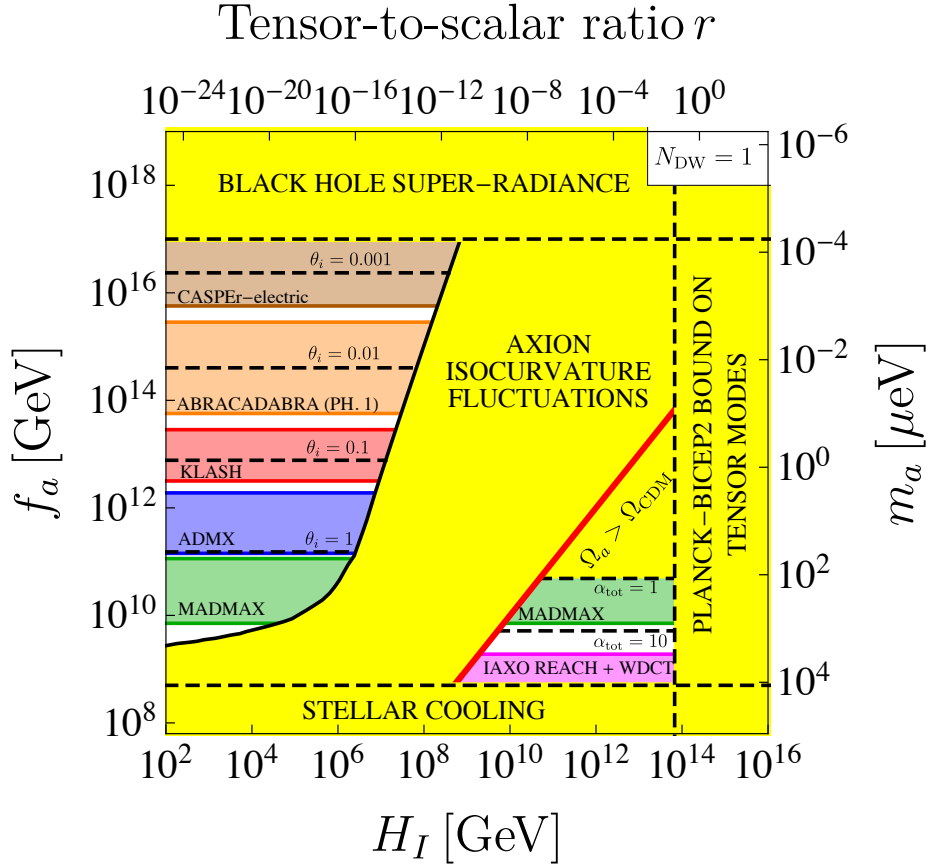


Figure 3: Region of axion parameter space where the axion constitutes the totality of the DM observed. The axion mass scale on the right corresponds to Eq. (51) for the case  $N_{\text{DW}} = 1$ . If the PQ symmetry breaks during inflation and the axion spectates inflation ( $f_a \gtrsim H_I$ , **PreI** scenario), axion isocurvature perturbations constrain the parameter space to the region on the top left, which is marked by the values of  $\theta_i$  necessary to achieve the observed CDM density for a given value of  $f_a$ . If the PQ symmetry breaks after inflation ( $f_a < H_I$ , **PostI** scenario), the axion is the CDM particle only for a specific value of  $f_a$ , which takes into account the contributions from the decay of topological defects  $\alpha_{\text{tot}}$ . The lower bound on  $f_a$  results from astrophysical considerations [32, 34, 278, 279], the upper bound on  $f_a$  relies on the non-detection in LIGO of gravitational waves associated with the super-radiance phenomenon from stellar-mass black holes [280, 281], the upper bound on  $H_I$  comes from the non-observation of tensor modes in the CMBR [238, 239, 282]. The coloured transparent bands indicate future reaches of planned or ongoing experiments covering the allowed regions of the parameter space: ABRACADABRA (orange), KLASH (red), ADMX (blue), MADMAX (green), and IAXO (magenta).

For  $f_a \gtrsim H_I$  (**PreI** scenario), we show the values  $\theta_i \in \{1, 0.1, 0.01, 0.001\}$ . The parameter space in this scenario is bound to the right by the non-observation of axion isocurvature fluctuations in the CMBR by

the *Planck* mission [238, 239, 282], subject to the requirement that axions constitute the DM. The change in the slope corresponds to the effect of the non-harmonic terms in the axion potential when  $\theta_i \gtrsim \mathcal{O}(1)$  [173]. The possible presence of axion isocurvatures in the spectrum of the CMBR relies on the fact that the PQ symmetry has never been restored after the end of inflation. For example, in the unified Standard Model–Axion–seesaw–Higgs portal inflation (SMASH) model of Refs. [283–285], although the axion energy scale can be as large as  $f_a \sim 4 \times 10^{16}$  GeV, the PQ symmetry is restored immediately after the end of inflation and isocurvature modes are absent. Caveats that allow to evade the bound from isocurvature fluctuations include the presence of more than one axion [286], or the identification of the inflaton with the radial component of the PQ field [287], see Section 7.3.

Note, that in single-field inflation models in which the axion constitutes the DM, the **PreI** scenario requires a value of the tensor-to-scalar ratio  $r$  which is well below the projected sensitivity of forthcoming cosmological surveys,  $r \sim 10^{-3}$ , which is forecast for example by the next-generation ground-based cosmic microwave background experiment CMB-S4 [288].<sup>39</sup> For example, an explicit realisation of an inflation model with an extremely low value of the tensor-to-scalar ratio  $r \sim 10^{-13}$  such that the axion is the DM has been recently presented in Ref. [289].

For  $f_a \lesssim H_I$  (**PostI** scenario), the axion is present during inflation as the Goldstone boson of the PQ field. The initial value of the misalignment angle is averaged out over many Hubble patches. We have used  $\langle \theta_i^2 \rangle \approx (2.15)^2$  as in Ref. [45], and we show results for two cases: 1)  $\alpha_{\text{tot}} = 1$  (no contribution from the decay of topological defects), and 2)  $\alpha_{\text{tot}} = 10$ , where the parameter  $\alpha_{\text{tot}} \equiv \rho_a / \rho_a^{\text{mis}}$  parametrises the ratio of the present energy density in axions  $\rho_a$  to that coming from misalignment only  $\rho_a^{\text{mis}}$ . We have also reported the forecasts for the sensitivities of various experiments, either planned or already running, including the Cosmic Axion Spin Precession Experiment (CASPER) [290], A Broadband/Resonant Approach to Cosmic Axion Detection with an Amplifying B-field Ring Apparatus (ABRACADABRA) [291, 292], the KLoe magnet for Axion Search (KLASH) [293, 294], the Axion Dark Matter Experiment (ADMX) [295–299], the MAgnetized Disc and Mirror Axion eXperiment (MADMAX) [300], and the International Axion Observatory (IAXO) [301–303]. Notice that we have chosen the bounds from laboratory searches by setting the ratio  $E/N = 0$  as in the original KSVZ model. Additional details on the experimental setups for axion helioscopes are given in Section 5.1, for axion haloscopes in Section 5.3, and for laboratory searches in Section 5.4.

### 3.8. QCD axions as dark radiation

So far, we have reviewed the coherent state of non-thermal axions that follows from the classical evolution of the axion field, and which might form the dominant component of the CDM in the universe. We now turn to the thermal axion population which, for the range of masses considered here, would contribute as a dark radiation component.

The addition of a new species that is relativistic at decoupling, such as thermal axions, would alter the number of effective neutrinos  $N_{\text{eff}}$ , which is defined from the contribution to the energy density in relativistic species as

$$\rho_r = \left[ 1 + \frac{7}{8} \left( \frac{4}{11} \right)^{4/3} N_{\text{eff}} \right] \rho_\gamma, \quad (191)$$

where  $\rho_\gamma$  is the energy density of the CMBR photons today, while the three active neutrinos in the SM contribute with a factor  $N_{\text{eff}}^{\text{SM}} = 3.045$  [304].<sup>40</sup> The energy density in radiation  $\rho_r$  contains the contributions from photons, SM neutrinos, as well as any other relativistic species, including relativistic axions, which bring an additional contribution  $\Delta N_{\text{eff}} \equiv N_{\text{eff}} - N_{\text{eff}}^{\text{SM}}$  into Eq. (191). So far, the current best-fit limits on  $N_{\text{eff}}$  coming from the *Planck* 2018 + BAO measurements agree with the SM prediction [254, 310, 311] and

<sup>39</sup>If the DM is in the form of QCD axions, a joint analysis of axion direct detection experiments and future CMB-S4 experiments is able to probe the range  $2.5 \times 10^6 \lesssim H_I/\text{GeV} \lesssim 4 \times 10^9$  [288], which is otherwise not accessible through CMBR tensor modes alone.

<sup>40</sup>See also Ref. [305] where the value  $N_{\text{eff}}^{\text{SM}} = 3.046$  is computed. See also Refs. [306–308] for earlier work. The value of  $N_{\text{eff}}$  can be considerably lower in low-reheating models [309].

lead to  $N_{\text{eff}} = 2.99 \pm 0.17$  at 68% CL, combining TT, TE, EE+lowE+lensing datasets plus Baryon Acoustic Oscillations (BAO) data [238], making a significant contribution from dark radiation still allowed within the 68% error bars. Depending on the nature of the interaction and the processes involved, axions in the form of dark radiation might lead to a sizeable contribution to  $\Delta N_{\text{eff}}$  [312, 313]. For example, setting the axion degree of freedom  $g_a = 1$  leads to the contribution

$$\Delta N_{\text{eff}} \equiv \frac{\rho_a}{\rho_\nu} = \frac{4}{7} \left( \frac{T_a}{T_\nu} \right)^4, \quad (192)$$

where  $\rho_\nu$  is the energy density in neutrinos at the CMBR decoupling and  $T_a$  is the temperature at which axions do not interact efficiently with the surrounding plasma and decouple. The contribution from dark radiation to the number of effective neutrinos is potentially detectable in future experiments such as the CMB-S4 mission [288], which targets to detect a variation  $\Delta N_{\text{eff}} \lesssim 0.03$ .

The production of axions in the primordial plasma proceeds through various interactions with SM particles, leading to a thermal population of axions with number density  $n_a^{\text{th}}(T)$  at temperature  $T$ , that inevitably accompanies the non-thermal populations described so far. The processes involved depend on the value of the decoupling temperature  $T_{\text{dec}}$ , with respect to the scale  $\Lambda_{\text{QCD}}$  at which the QCD phase transition occurs.

- $T_{\text{dec}} \gtrsim \Lambda_{\text{QCD}}$ . We first discuss the mechanisms occurring at temperatures well above the QCD confinement scale, when the plasma is composed of a soup of quarks  $q$  and gluons  $g$ . The relevant mechanism for axion production are processes involving QCD, namely 1)  $a + q \rightarrow g + q$ , 2)  $a + g \rightarrow q + \bar{q}$ , 3)  $a + g \rightarrow g + g$  [313–316]. Depending on the strength of the axion-photon coupling, the Primakoff process  $a + q \rightarrow \gamma + q$  and photo-production by a quark  $\gamma + q \rightarrow q + a$  might also contribute [317]. In all of these mechanisms, it is assumed that the axion population approaches a thermal equilibrium of relativistic particles, with number density

$$n_{\text{EQ}}(T) = \frac{\zeta(3)}{\pi^2} T^3, \quad (193)$$

where  $\zeta(z)$  is the Riemann zeta function of argument  $z$  and  $\zeta(3) \approx 1.2$ . In light of these production mechanisms, it is possible to write down the Boltzmann equation that follows the creation of the thermal axion relics. Defining the yield  $Y(T) = n_a^{\text{th}}(T)/s(T)$  in terms of the entropy density  $s(T)$  given in Eq. (146), the Boltzmann equation that regulates the number of thermal axions is given by

$$Y = Y_{\text{EQ}} \left[ 1 - \exp \left( - \int_0^x dx' \frac{\Gamma_a}{x' H} \right) \right], \quad (194)$$

where  $x = m_N/T$ ,  $\Gamma_a$  is the rate of axion production, and the population at thermal equilibrium is  $Y_{\text{EQ}} = \zeta(3)g_S(T_{\text{dec}})/\pi^2$ . Solving Eq. (194) with the assumption that axions mainly interact with the quark-gluon plasma, with cross-section  $\sigma_a \sim \alpha_s^3/(8\pi f_a^2)$  in terms of the strong coupling  $\alpha_s$ , gives a decoupling temperature

$$T_{\text{dec}} = 5 \times 10^{11} \text{ GeV} \left( \frac{f_a}{10^{12} \text{ GeV}} \right)^2, \quad (195)$$

which is generally well above the QCD scale. Demanding that these processes occur after the PQ symmetry is broken requires  $T_{\text{dec}} \lesssim f_a$ , which leads to the bound on the axion energy scale  $f_a \lesssim 2 \times 10^{12} \text{ GeV}$ . If the energy scale is higher than this value, the PQ symmetry has not undergone the spontaneous breaking at temperature  $T_{\text{dec}}$  and the axion field is not present in the plasma. In the opposite case, the population of thermal axions is formed with the present number density [314, 317]

$$n_a^{\text{th}}(T_0) = 7.5 \text{ cm}^{-3}. \quad (196)$$

Depending on the details of inflation and reheating, such a thermal population of axions might be washed out by a subsequent inflationary period, to be then re-established by other processes. If a new



heavy quark  $Q$  carrying a PQ charge is present, like it occurs in the KSVZ axion model, axions would be produced through Compton-like scattering processes  $Q + g \rightarrow Q + a$ .

In models where a direct coupling between axion and top quarks exists, the efficiency of the thermal production is enhanced by up to three orders of magnitude [316]. More generally, a direct coupling of the axion to quarks and leptons leads to significant enhancements in  $\Delta N_{\text{eff}}$  [313, 318], which might even alleviate the tension between the local direct measurement of  $H_0$  and the model-dependent value of  $H_0$  inferred from the CMBR [176, 312], which is currently existing between CMBR [238] and Supernovae measurements [319–321]. A prediction for  $\Delta N_{\text{eff}}$  is also useful to set a target for future CMB-S4 surveys [288].

- $T_{\text{dec}} \lesssim \Lambda_{\text{QCD}}$ . Since the axion mixes with the neutral pion  $\pi^0$  after the QCD phase transition, the leading mechanism for producing a thermal population at lower temperature occurs through pion-axion conversion  $\pi^\pm + \pi^0 \rightarrow \pi^\pm + a$  (whose interaction term is described by Eq. (57)), or by the conversion mediated by a nucleon  $N$  as  $\pi + N \rightarrow N + a$  [101, 254, 322, 323]. However, these processes are important only for relatively small axion energy scales, and would require to evade the constrain from the duration of the neutrino burst in SN 1987A,  $f_a \gtrsim 10^9$  GeV [324–327], which depends on the axion-nucleon interactions as we discuss in Section 4.3. Other processes, not discussed here, might involve the coupling of axions to charged leptons.

### 3.9. Axion miniclusters and axion stars

An important feature of the **PostI** scenario is the presence of ultracompact axion “miniclusters”, of masses of the order of  $M_{\text{MC}} \sim 10^{-10} M_\odot$  (here one solar mass is  $M_\odot$ ), that form from density perturbations at the time of the axionic string network collapse [328–331]. The existence of compact objects is a general feature [332], shared by other Goldstone bosons like ALPs [333] or Majorons [334], as well as by other scalar fields, with the size and mass of these objects depending on the specific model. Starting from the axion power spectrum, the collapse of non-linear density fluctuations during radiation domination that lead to the formation of axion miniclusters has been recently assessed through a semi-analytical Press-Schechter approach [335–337] or by numerical simulations [201, 202].

Axion miniclusters would lead to important detection features. First, in an encounter with the Earth, the local DM energy density  $\rho_{\text{loc}} \sim 0.4 \text{ GeV/cm}^3$  would temporarily be enhanced by a factor as large as  $10^6$  [27, 338], triggering the conversion of axions into photons in dedicated resonant cavities, see Section 4.1. The expected signal would be time-dependent due to the revolution and rotation motions of the Earth, which leads to a detectable annual modulation [339] and possibly even to a detectable diurnal modulation [340]. Since the cavity would have to be tuned to the correct frequency in order to capture the signal, a broadband axion cavity resonator has been proposed to exploit this possibility, see Ref. [38]. Second, the presence of axion miniclusters could be assessed through picolensing of individual clusters [341], or microlensing of a halo formed of axion miniclusters that hierarchically merge [335, 336]. This latter possibility could also be used to assess the fraction of cold axions that are bound into clumped objects, a fraction that can also be accessed through numerical simulations. Third, axion minicluster could be disrupted by the gravitational field of a nearby star encounter, or by the mean galactic gravitational field, leading to tidal streams of axions that would enhance the local CDM density by about one order of magnitude [342].

Axion stars [343] are oscillaton-like solutions of the Klein-Gordon equation associated with the axion potential in Eq. (50) and coupled to the Einstein or Poisson equation to account for the feedback into the gravitational field. Contrarily to axion miniclusters, the mass of the axion star is not fixed once setting the mass of the QCD axion. The typical mass of the axion star is fixed once a formation mechanism is imposed [344, 345]. Axion stars are described by a real pseudo-scalar field that oscillates with time, with a frequency that is related to the mass of the axion. This configuration is different from what is obtained from a self-gravitating condensate made of a *complex* boson field, which is known in the literature as a ‘boson star’ [346, 347]. Both configurations possess black hole-like solutions for a null field and, in the case of the complex scalar field of mass  $m_\phi$ , the boson star cannot grow to masses larger than the critical mass  $M_* = 0.633/(Gm_\phi)$  [348]. If the axion potential were quadratic as in Eq. (151), the axion star would also possess a slightly smaller critical mass  $M_* = 0.607/(Gm_a)$  [349], see also Ref. [350].



The formation of axion stars might proceed either by gravitational cooling out of the virialised minicluster or during a process of violent relaxation [345, 351–353], leading to a solution in the weak gravity regime [354, 355], with the mass and the radius of the axion star being related by [347, 356]

$$R_{\text{as}} = \frac{9.9}{Gm_a^2 M_{\text{as}}} . \quad (197)$$

This solution is known in the literature as the “dilute” regime, since the average energy density inside the axion star is much smaller than the energy scale  $\chi(0)$  at which the axion potential saturates. As the density of the star increases, self-interactions become more relevant and destabilise the equilibrium when the mass of the star approaches the critical value [350, 356, 357]

$$M_{\text{as,crit}} \approx 18.4 M_P \frac{f_a}{m_a} . \quad (198)$$

This result is valid for an axion field moving in the potential described in Eq. (54) with  $m_u/m_d = 0.48$ .

#### 4. Astrophysical signatures and bounds

Astrophysics, and stellar evolution in particular, offer powerful methods to probe the axion couplings to SM fields [31, 32, 358]. The observational properties of stars are conveniently shown in the Hertzsprung Russell (HR) or Color Magnitude Diagram (CMD), which shows the stellar luminosity (or magnitude) versus the surface temperature (expressed through the colour index).

No matter their initial mass, stars spend most of their life burning H into He in their core (main sequence). The post main sequence evolution depends on the stellar initial mass. A schematic picture of this evolution is shown in the left panel of Fig. 4. After the hydrogen in the core is exhausted, stars of roughly the same mass as our Sun enter the subgiant phase, burning hydrogen in a thick shell. It follows the Red Giant Branch (RGB) stage, with hydrogen burning in a thin shell surrounding an inert He core. The evolution in the RGB continues until the temperature in the core is high enough to ignite the He in the core (He-flash). Afterwards, the star moves to the Horizontal Branch (HB) region of the diagram. Such low mass stars never reach the conditions (temperature and density) required to ignite heavier elements and end up as carbon-oxygen White Dwarfs (WD).

Stars a few times the mass of the Sun do not undergo a He-flash and ignite helium soon after the end of the main sequence stage, transitioning to the cold (red) region of the HR diagram. The evolution during the He-burning stage may show a peculiar journey to the bluer region of the diagram and back, called the blue loop (see, e.g., the  $5 M_{\odot}$  track in the left panel of Fig. 4). Stars with an initial mass larger than about  $8 M_{\odot}$  do not become WD but undergo a core collapse, giving rise to a type II SN explosion and leaving a compact NS or, if very massive, a black hole.

The diagram in Fig. 4 is theoretical. It shows the evolutionary tracks of individual stars. Observationally, one extracts colour and magnitude of individual stars (at a fixed time) and shows the results in a diagram similar to the one shown in the right panel of Fig. 4. From the stellar population it is possible to reconstruct the evolutionary times of each stage (the longer the evolutionary time, the larger the stellar population

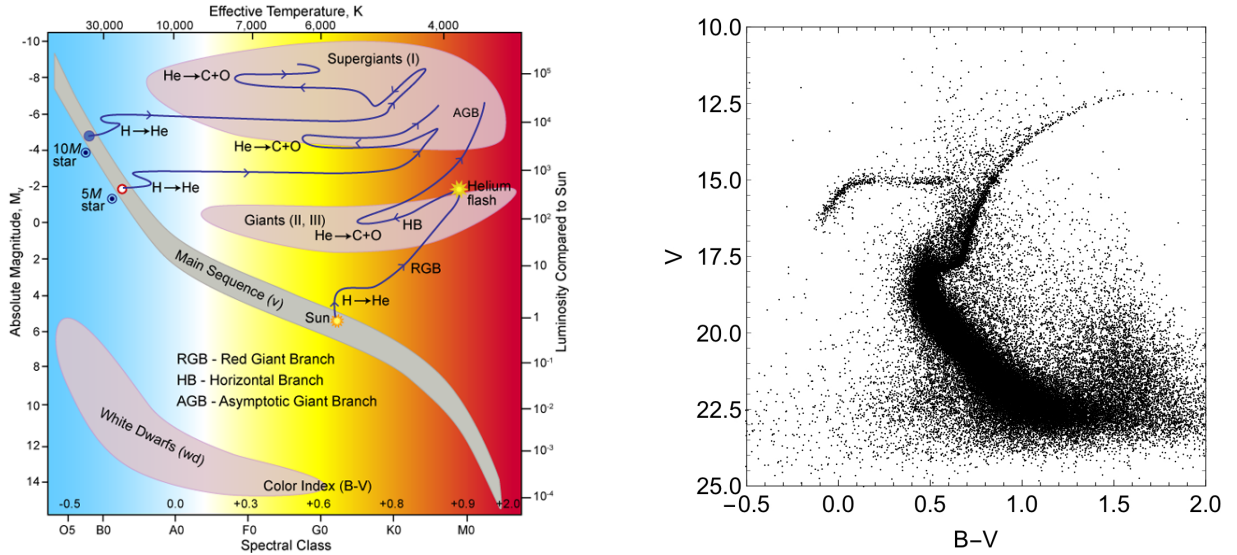


Figure 4: In the left panel, the theoretical Hertzsprung Russell (HR) or Color Magnitude Diagram (CMD), showing the evolution of luminosity and surface temperature of stars with different initial masses. To the right, the observational CMD of the M5 globular cluster, which shows the luminosity and surface temperature of stars at a fixed time (isochrones). More massive stars evolve more rapidly and are found in more advanced stages. The density of stars in different regions of the observational CMD reflects the duration of the corresponding evolutionary stage. The luminosity (energy emitted per unit time) is conventionally measured in magnitude. In the figures we show the magnitude in the visual (V) band. The surface temperature is shown as the B-V color, that is the difference between the blue (B) and visible (V) brightness. Note that, for historical reasons, the temperature increases toward the left of the diagram. So, stars with higher surface temperature (blue) are found to the left. See text for more details. The figure to the left is reproduced (with permission) from <https://physics.aps.org/articles/v2/69>.

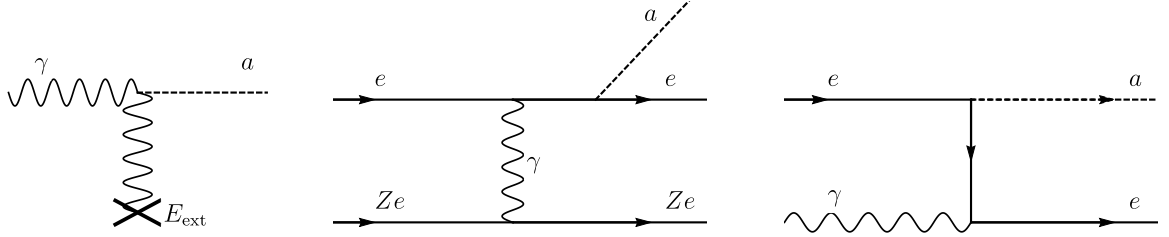


Figure 5: From left to right: axion Primakoff processes in an external electric field; axion bremsstrahlung process; and Compton processes. In the case of the bremsstrahlung process,  $Ze$  represents either an ion or an electron.

corresponding to that phase), which can then be compared with the theoretical predictions extracted from numerical stellar evolution codes.

The method presents evident difficulties related to statistics (particularly for fast evolutionary stages), stellar contamination, interstellar absorption of the stellar light, etc. Nevertheless, numerical simulations reproduce with a remarkable level of agreement the observed CMD of particular stellar populations and allow to set stringent bounds on new physics. The emission of axions (or other light particles) from stars might, in fact, impact their expected evolution and spoil the agreement with observations.

The aim of this section is to provide an updated summary of the bounds on axions derived from stellar astrophysics considerations. In addition, we will briefly present the results of the axion interpretation of some observations of anomalous stellar evolution that have been reported in the last two decades (see, e.g., references [34, 272, 359] for more detailed discussions). Our general approach will be to present first all the results in a model independent way. The impact on the axion benchmark models (KSVZ and DFSZ-type) will also be discussed at the end of the section.

#### 4.1. Axion-photon coupling

In the context of stellar evolution, the most relevant process induced by the axion-photon coupling,  $g_{a\gamma}$  (Section 2.5.3) is the Primakoff process (Fig. 5), consisting in the conversion of thermal photons in the electrostatic field of electrons and nuclei

$$\gamma + Ze \rightarrow a + Ze. \quad (199)$$

Neglecting degeneracy effects and the plasma frequency (a good assumption in plasma conditions when the Primakoff process is the dominating axion production mechanism), it is possible to provide a semi-analytical expression for the energy-loss rate per unit mass in axions [360]:

$$\varepsilon_P \simeq 2.8 \times 10^{-31} Z(\xi^2) \left( \frac{g_{a\gamma}}{\text{GeV}^{-1}} \right)^2 \frac{T^7}{\rho} \text{ erg g}^{-1} \text{ s}^{-1}, \quad (200)$$

where  $T$  and  $\rho$  are in K and in  $\text{g cm}^{-3}$  respectively. The coefficient  $Z(\xi^2)$  is a function of  $\xi^2 \equiv (\kappa_S/2T)^2$ , with  $\kappa_S$  being the Debye-Huckel screening wavenumber. It can be explicitly expressed as an integral over the photon distribution (see Eq. (4.79) in Ref. [31]). Ref. [360] proposed the analytical parametrization

$$Z(\xi^2) \simeq \left( \frac{1.037\xi^2}{1.01+\xi^2/5.4} + \frac{1.037\xi^2}{44+0.628\xi^2} \right) \ln \left( 3.85 + \frac{3.99}{\xi^2} \right), \quad (201)$$

which is better than 2% over the entire range of  $\xi$ . In general,  $Z(\xi^2)$  is  $\mathcal{O}(1)$  for relevant stellar conditions. For example, in the core of the Sun,  $\xi^2 \sim 12$  and  $Z \sim 6$  and in the core of a low-mass He burning star,  $\xi^2 \sim 2.5$  and  $Z \sim 3$  [31], while in a  $10M_\odot$  He burning star,  $\xi^2 \sim 0.1$  and  $Z \sim 0.4$  [360].

As shown in Fig. 6, the Primakoff process has a steep dependence on the stellar temperature, which controls the number of thermal photons, but is suppressed at high density because of the effects of a large plasma frequency and of the reduction of electron targets [365] (in such conditions, Eq. (200) ceases to be valid). Hence, this process is strongly suppressed in the degenerate core of WDs and RGB stars. Indeed,

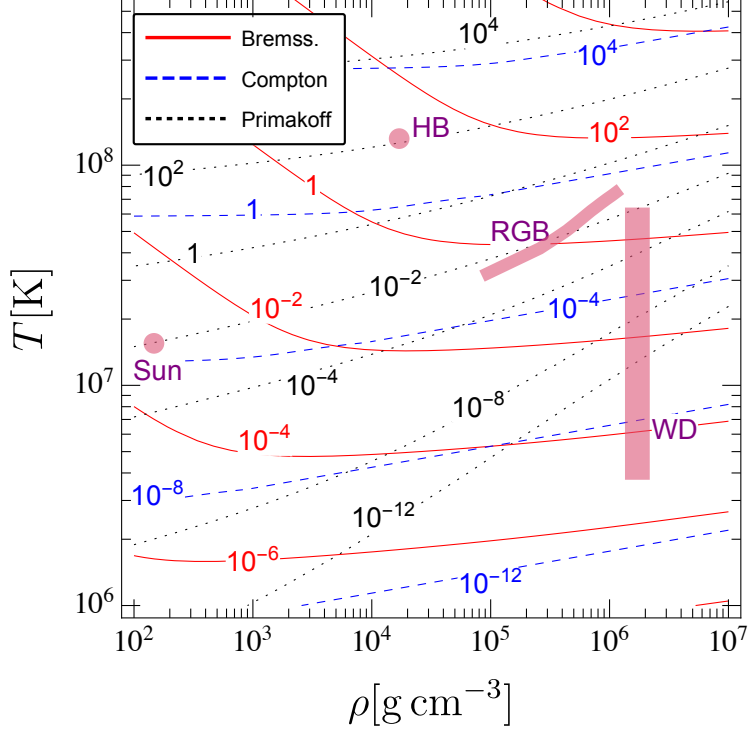


Figure 6: Contours of the axion energy-loss rates per unit mass,  $\epsilon_a$ , in  $\text{erg g}^{-1}\text{s}^{-1}$ , for a pure He plasma. Different lines represent different channels, as shown in the legend. The Primakoff process is calculated for  $g_{a\gamma} = 0.65 \times 10^{-10} \text{GeV}^{-1}$ , corresponding to the bound from HB stars [361, 362]. The Bremsstrahlung and Compton processes are calculated for  $g_{ae} = 4.3 \times 10^{-12}$ , corresponding to the RGB bound from M5 [279]. The onset of the degeneracy region is visible in the bending of the bremsstrahlung contours. The central temperature and density of the Sun [363], RGB stars, HB stars and WDs are also shown, for reference. In the case of HB and RGB, these are the result of a numerical simulation of a  $0.8 M_{\odot}$  model as obtained with the FuNS code [364]. The WD region is estimated using a polytropic model of WDs with mass from  $0.6$  to  $0.7 M_{\odot}$ , as discussed in Ref. [358], and spans luminosities in the range between  $0.5 \times 10^{-4}$  and  $0.5 L_{\odot}$ . Except for the WD case, the thickness of the lines has no significance.

the strongest bounds on the axion-photon coupling are derived from the analysis of stars with a low density and high temperature core. In the following, we present the relevant stellar arguments used to constrain this coupling.

**The Sun** - Given its low density and, more importantly, its proximity, the Sun provides a good environment to test the axion-photon coupling. Moreover, as we shall see, the Sun is an important source for axions to be detected in terrestrial experiments (see Section 5.1). The (number) spectrum of axions produced in the Sun is shown in the left panel in Fig. 7. Interestingly, the axion spectra produced by processes induced by the axion-photon and the axion-electron couplings are similar, if we consider couplings of the order of the current bounds (cfr. Section 4.2 for the astrophysical bounds on the axion-electron coupling). This is a very impactful result for experimental searches, as we discuss in Section 5.1. For considerations about stellar cooling, however, the relevant quantity is the axion luminosity, not the axion number, and this is dominated by Primakoff axions since they are, in average, more energetic (cfr. right panel of Fig. 7).

Strong bounds on exotic cooling processes in the Sun can be set from helioseismological considerations [366, 367]. The current bound is  $g_{a\gamma} \leq 4.1 \times 10^{-10} \text{GeV}^{-1}$  at  $3\sigma$  [367], which corresponds to  $g_{a\gamma} \leq 2.7 \times 10^{-10} \text{GeV}^{-1}$  at  $2\sigma$ . A somewhat weaker bound,  $g_{a\gamma} \leq 7 \times 10^{-10} \text{GeV}^{-1}$ , was inferred in

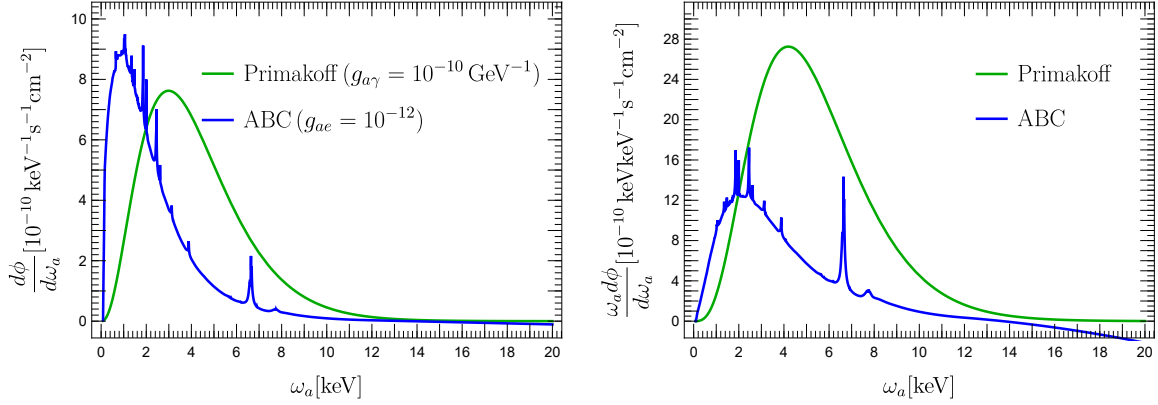


Figure 7: Solar axion spectrum. To the left shows the axion number and to the right the axion energy. The couplings are the same in both graphs.

Ref. [368] from the axion impact on solar neutrinos.

**R-parameter and HB stars** - The major problem with the Sun as a source for axions is the relatively low temperature of its core. This limits strongly the Primakoff emission rate. Stars in the HB stage, which follows the RGB phase, have a low core density of about  $10^4 \text{ g cm}^{-3}$  and a high temperature (see Fig. 6), providing excellent conditions to produce axions through the Primakoff process.

To assess the effects of axions on the evolution of HB stars, it is convenient to introduce the R-parameter, defined as the ratio of the number of stars in the HB and in the upper portion of the RGB:  $\mathcal{R} = N_{\text{HB}}/N_{\text{RGB}}$ . In the presence of axions, this parameter is expected to be

$$\mathcal{R} = \mathcal{R}_0(Y) - F_{a\gamma} \left( \frac{g_{a\gamma}}{10^{-10} \text{ GeV}^{-1}} \right) - F_{ae} \left( \frac{g_{ae}}{10^{-12}} \right), \quad (202)$$

where  $\mathcal{R}_0(Y)$  is a function of the helium abundance ( $Y$ ) in the GC and the  $F$  are some positive-defined functions of the axion couplings.<sup>41</sup> For completeness, we are including the contribution from processes induced by the axion coupling to photons,  $g_{a\gamma}$ , as well as the axion coupling to electrons,  $g_{ae}$ , which will be reviewed in more detail in Section 4.1. The positivity condition of the  $F$  insures that the axion emission can only lower the value of the  $R$ -parameter and that there could be a degeneracy between the effects of the axion couplings to electrons and photons. Although at the present a full numerical study that includes axions coupled to both electrons and photons does not exist, reference [369] provided approximate analytical expressions for the  $F$  in Eq. (202):

$$\mathcal{R}_0(Y) = 0.02 + 7.33 Y; \quad (203)$$

$$F_{a\gamma}(x) = 0.095 \sqrt{21.86 + 21.08 x}; \quad (204)$$

$$F_{ae}(x) = 0.53 x^2 + 0.039 \left( \sqrt{1.23^2 + 100 x^2} - 1.23 - 4.36 x^{3/2} \right). \quad (205)$$

<sup>41</sup>It is easy to infer that  $F_{a\gamma}$  must be positive. A finite axion-photon coupling would contribute to the stellar energy-loss, particularly in the HB stage, since Primakoff is suppressed in the degenerate plasma typical of the RGB core. Thus, a large  $g_{a\gamma}$  would shorten the life of HB stars and, consequently, their expected numbers in a cluster. The argument for the positivity of  $F_{ae}$  goes as follows. An efficient energy-loss channel, such as the one induced by a large coupling of axions to electrons, would delay the He-ignition in the RGB core (He-flash), allowing the core to grow more, and ultimately increasing the luminosity of the RGB tip and the number of RGB stars. The impact of a finite  $g_{ae}$  on the energy-loss in HB star is considerably less significant.

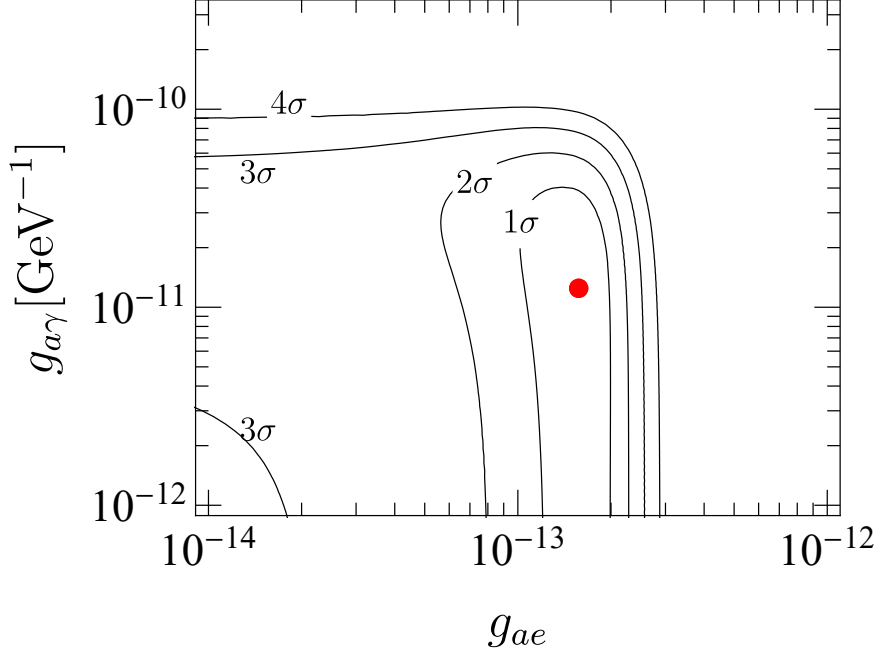


Figure 8: Stellar hints on general Axion Like Particles interacting with electrons and photons [359]. The hints are derived from the global analysis of WD pulsation, the WD luminosity function, RGB and HB stars. The best fit parameters are indicated with the red dot.

Neglecting the axion-electron coupling and adopting the value  $Y = 0.2535$  for the helium abundance [370], reference [361] derived the upper bound on the axion-photon coupling

$$g_{a\gamma} < 0.66 \times 10^{-10} \text{ GeV}^{-1} \quad (95\% \text{ CL}) . \quad (206)$$

This is known as the HB bound,<sup>42</sup> since by neglecting the axion-electron coupling we are essentially ignoring the RGB evolution. In addition to the result in Eq. (206), the analysis in [361] inferred an  $R$  parameter somewhat larger than observed, indicating a  $2\sigma$  preference for a small, non-vanishing axion-photon coupling, later confirmed in [362] using an updated value of the He abundance [371, 372]. The result,

$$g_{a\gamma} = (0.29 \pm 0.18) \times 10^{-10} \text{ GeV}^{-1} \quad (68\% \text{ CL}), \quad (207)$$

is known as the HB hint.

The combined  $2\sigma$  hints from the analysis of the WDLF, WD variables, the RGB tip and the  $R$ -parameter [34, 359] is presented in Fig. 8. The analysis shows a preference for an axion coupling to electrons at the level of  $3\sigma$ . The coupling to photons, however, is compatible with zero at  $1\sigma$ . Notice, however, that this conclusion cannot be drawn in the case of specific axion models, such as DFSZ I and II, which predict well defined relations among couplings.

**Massive Stars** - Further insights on the axion-photon coupling can be extracted from the analysis of intermediate mass stars,  $M \sim 8 - 12M_{\odot}$  [360, 373]. As discussed at the beginning of this section, the (core) He burning stage of these stars is characterized by a migration toward the blue (hotter) region of the CMD and back. This journey is known as the *blue loop*. The existence of the loop is corroborated by

<sup>42</sup>This bound was slightly updated in reference [362] to  $g_{a\gamma} < 0.66 \times 10^{-10} \text{ GeV}^{-1}$  (95% CL) .

many astronomical observations. In particular, this stage is essential to account for the observed Cepheid stars (see, e.g., [374]). The disappearance of the blue loop stage in the luminosity ranges where Cepheid stars are observed is forbidden [373]. A nonvanishing axion-photon coupling would reduce the time a star spends in the blue loop stage and, consequently, the number of *blue* versus *red* stars of a given luminosity. According to the analysis in [360], based on numerical simulations of solar metallicity stars in the  $8 - 12 M_{\odot}$  mass range, a coupling larger than  $\approx 0.8 \times 10^{-10} \text{GeV}^{-1}$  would cause the complete disappearance of the blue loop. The result is comparable to the globular cluster bound. Somewhat lower values of  $g_{a\gamma}$  might help explaining the observed deficiency of blue with respect to red supergiants discussed, e.g., in [375]. The numerous uncertainties in the microphysics and in the numerical description of the blue loop stage have not permitted a more quantitative assessment of this possibility [376].

More recently, the analysis of SN progenitors has also indicated a preference for additional cooling, in the form of axions or, possibly, other light particles [364]. Surveys show that in many cases the SN type II progenitors are red supergiants with a certain maximal (surface) luminosity. To stay below this luminosity, stars would need to be relatively light, contrary to observations. Standard modifications to the stellar codes, e.g., adding rotations, overshooting, etc., do not help but rather worsen the agreement with the observations. The addition of a novel cooling channel, however, might help reconciling the simulations with the observations. Because of the more efficient cooling, the development of the envelop would freeze at lower luminosities, allowing for more massive stars to end up with the required surface luminosity [364]. In the case of axions, the hint is to rather large couplings to both electrons and photons, close to the current HB and RGB bounds. However, the data sample is still too sparse to draw definitive conclusions and the identification of reliable axion couplings is prohibitive. The situation will largely improve with the data from the Large Synoptic Survey Telescope (LSST) [377, 378], which will likely identify a large number of SN progenitors (see Section 3 in Ref. [378]).

#### 4.2. Axion-electron coupling

The axion-electron coupling,  $g_{ae}$  (Section 2.5.5), induces several processes relevant for stellar evolution (see Ref. [358] for a comprehensive presentation). The most important are the Atomic recombination and de-excitation, the electron and ion Bremsstrahlung, and the Compton process, collectively known as the ABC processes.<sup>43</sup> The atomic recombination and deexcitation processes are an important contribution to the solar axion spectrum [380] (see Section 5.1) but can be ignored in numerical simulations of stellar evolution.

At high densities, particularly in electron degeneracy conditions, the most efficient axion production mechanism is the electron/ion bremsstrahlung process

$$e + Ze \rightarrow e + Ze + a, \quad (208)$$

shown in the central panel of Fig. 5. The axion energy-loss rates per unit mass for the case of a pure He plasma is shown in Fig. 6. As clear from the figure, at high density and relatively low temperature, when electrons become degenerate, the bremsstrahlung rate has a very mild dependence on the density. On the other hand, in nondegenerate conditions the rate depends linearly on the density. In both cases, there is also a dependence on the stellar chemical composition. Explicit expressions for the energy-loss rates per unit mass in the degenerate (d) and nondegenerate (nd) limits are provided in Ref. [381]. Approximately,

$$\varepsilon_{\text{ND}} \simeq 47 g_{ae}^2 T^{2.5} \frac{\rho}{\mu_e} \sum \frac{X_j Z_j}{A_j} \left( Z_j + \frac{1}{\sqrt{2}} \right) \text{erg g}^{-1} \text{s}^{-1}, \quad (209)$$

$$\varepsilon_{\text{D}} \simeq 8.6 \times 10^{-7} F g_{ae}^2 T^4 \left( \sum \frac{X_j Z_j^2}{A_j} \right) \text{erg g}^{-1} \text{s}^{-1}, \quad (210)$$

<sup>43</sup>Another astrophysical process discussed in the literature is the electron-positron annihilation,  $e^+e^- \rightarrow \gamma + a$  [379], which plays, however, a less significant role in stellar evolution.



Star	$P(\text{s})$	$\dot{P}_{\text{obs}}(\text{s/s})$	$\dot{P}_{\text{th}}(\text{s/s})$	$g_{ae}^{(\text{best})}$	$g_{ae}^{(\text{max})}(2\sigma)$
G117 - B15A	215	$(4.2 \pm 0.7) \times 10^{-15}$	$(1.25 \pm 0.09) \times 10^{-15}$	$4.9 \times 10^{-13}$	$6.0 \times 10^{-13}$
R548	213	$(3.3 \pm 1.1) \times 10^{-15}$	$(1.1 \pm 0.09) \times 10^{-15}$	$4.8 \times 10^{-13}$	$6.8 \times 10^{-13}$
PG 1351+489	489	$(2.0 \pm 0.9) \times 10^{-13}$	$(0.81 \pm 0.5) \times 10^{-13}$	$2.1 \times 10^{-13}$	$3.8 \times 10^{-13}$
L 19-2 (113)	113	$(3.0 \pm 0.6) \times 10^{-15}$	$(1.42 \pm 0.85) \times 10^{-15}$	$5.1 \times 10^{-13}$	$7.7 \times 10^{-13}$
L 19-2 (192)	192	$(3.0 \pm 0.6) \times 10^{-15}$	$(2.41 \pm 1.45) \times 10^{-15}$	$2.5 \times 10^{-13}$	$6.1 \times 10^{-13}$

Table 2: Hints,  $g_{ae}^{(\text{best})}$ , and bounds,  $g_{ae}^{(\text{max})}$ , on the axion-electron coupling from WD variable stars [382, 383].  $P$  is the period of the variable star and  $\dot{P}$  its time derivative. We report the measured (observed) values and the theoretical predictions.

where  $T$  and  $\rho$  are in K and in  $\text{g cm}^{-3}$  respectively,  $\mu_e = (\sum X_j Z_j / A_j)^{-1}$  is the mean molecular weight per electron,  $X_j$  is the relative mass density of the  $j$ -th ion, and  $Z_j$ ,  $A_j$  its charge and mass number respectively.<sup>44</sup> The mild density dependence of the degenerate rate is accounted for by the dimensionless function  $F$ . An explicit expression for this function can be found in [381] (see also section 3.5 of Ref. [358] for a pedagogical presentation). Numerically, it is of order 1 for the stellar plasma conditions,  $\rho \sim 10^5 - 10^6$  and  $T \sim 10^7 - 10^8$ , of interest for our discussion here, when the degenerate bremsstrahlung process dominates. The intermediate regime between degenerate and nondegenerate conditions in Fig. 6 is calculated as  $\varepsilon_B = (1/\varepsilon_B^{(\text{d})} + 1/\varepsilon_B^{(\text{nd})})^{-1}$ , following the prescription in Ref. [381].

The Compton process

$$\gamma + e \rightarrow \gamma + a \quad (211)$$

(right panel of Fig. 5) accounts for the production of axions from the scattering of thermal photons on electrons. The Compton axion emission rate is a steep function of the temperature

$$\varepsilon_C \simeq 2.7 \times 10^{-22} g_{ae}^2 \frac{1}{\mu_e} \left( \frac{n_e^{\text{eff}}}{n_e} \right) T^6 \text{ erg g}^{-1} \text{ s}^{-1}, \quad (212)$$

where  $n_e$  is the number density of electrons while  $n_e^{\text{eff}}$  is the effective number density of electron targets. At high densities, degeneracy effects reduce  $n_e^{\text{eff}}$ , suppressing the Compton rate (cfr. Fig. 6). The Compton process can effectively dominate over the bremsstrahlung only at low density and high temperature.

Below, we review the bounds on the axion-electron coupling derived by the most relevant stellar systems.

**White Dwarfs** - The strongest bounds on the axion-electron coupling are inferred from observations of stars with a dense core, where the bremsstrahlung is very effective. These conditions are realized in WD and RGB stars. As discussed above, the WD phase is the last stage of the evolution of a low mass star, after the nuclear energy sources are exhausted. Hence, the evolution of a WD is essentially a cooling process, governed by photon radiation and neutrino emission, with the possible addition of novel energy-loss channels, e.g. in axions.

There are at least two ways to test the cooling of WDs and, consequently, exotic cooling theories. First, one may study the WD Luminosity Function (WDLF), representing the distribution of WDs versus luminosity. While cooling, the WD luminosity decreases. Thus, the efficiency of the cooling reflects in the shape of the WDLF. Additionally, one can measure the secular drift of the oscillation period,  $\dot{P}/P$ , of WD variables, which is practically proportional to the cooling rate  $\dot{T}/T$ .

Let us begin with the WDLF. Current numerical analyses suggest the bound  $g_{ae} \gtrsim 2.8 \times 10^{-13}$  [383]. However, this result does not come with a credible confidence level because of the large theoretical and observational uncertainties (see, e.g., discussion in [384]). Moreover, the analyses show, fairly consistently (though not universally) an anomalously large energy-loss. In particular [384], using data from the Sloan

<sup>44</sup>In the typical plasma conditions where the bremsstrahlung is relevant, one finds  $Z_j/A_j \approx 1/2$ . So, the rate has a dependence on the chemical composition of the plasma and increases in the case of high  $Z$ . In particular, the rate is larger in a CO WD core than in the core of a RGB star, composed mostly of He.

Digital Sky Survey (SDSS) and the SuperCOSMOS Sky Survey (SCSS), showed that the axion coupling  $g_{ae} \simeq 1.4 \times 10^{-13}$  is favored with respect to the standard model case at about  $2\sigma$  confidence level.<sup>45</sup> A more recent analysis of the data in Ref. [384], found [34]

$$g_{ae} = 1.5^{+0.6}_{-0.9} \times 10^{-13} \quad (95\% \text{ C.L.}). \quad (213)$$

These results were confirmed in a later study [387], which attempted to reduce some systematic uncertainties, particularly those due to the star formation rate, by studying the WDLF of the thin and thick disk, and of the halo. A considerable improvement is expected from the next generation of astrophysical observations. Data from the GAIA satellite have already increased the catalog of WDs by an order of magnitude with respect to SDSS [388, 389]. The Large Synoptic Survey Telescope (LSST) is expected to detect even fainter WDs, ultimately increasing the census of WDs to tens of millions [377, 378].

An independent method to study the cooling of WDs is the analysis of the period change of the WD variables. Unfortunately, the period changes very slowly,  $\dot{P}/P \approx 10^{-18} \text{ s}^{-1}$  in most measured cases (see Table 2), and an accurate assessment of this change requires years of accurate data taking. Therefore, although there are many known WD variables,  $\dot{P}/P$  has been measured only for a handful of them (see Ref. [383] for an update review of this subject). Interestingly, in all cases the observed period change rate is always larger than the expected one,  $\dot{P}_{\text{th}} > \dot{P}_{\text{obs}}$ , hinting at an unexpected cooling channel. Such result could be attributed to an axion coupled to electrons with the couplings shown in Table 2. The highest level of discrepancy is observed in G117 - B15A but that may be due to some assumptions about the trapping mode and should perhaps be reconsidered [384]. The combined analysis of all other WD variables in the table gives a fairly good fit,  $\chi^2_{\text{min}}/\text{d.o.f.} = 1.1$ , for  $g_{ae} = 2.9 \times 10^{-13}$  and favors the axion (or ALP) interpretation at  $2\sigma$ .

**Red Giants** - Another strong bound on the axion-electron coupling is inferred from the luminosity of the tip of the RGB in Globular Clusters (GC). After the hydrogen in the core of a main sequence star is exhausted, the stellar core contracts and the star enters the RGB phase. During the RGB evolutions, the star expands, its surface cools down, and its luminosity increases (see Fig. 4). For sufficiently low mass stars, as those populating a GC, the electrons in the stellar core eventually become degenerate. Meanwhile, the core continues to contract and heat up, while its mass grows by the H-shell burn. The process continues until the core reaches the conditions necessary to ignite He. At this time, known as the He-flash, the star reaches the point of highest luminosity in the CMD, known as the RGB tip. The luminosity of the RGB tip is an excellent observable to probe the cooling of the star during the RGB phase, being the He ignition extremely sensitive to the temperature. Thus, any additional cooling, in the form of axions or other light, weakly interacting particles, can be effectively constrained by observations of the luminosity of the RGB tip. In the case of axions, the most efficient production mechanisms during the RGB production are the electron bremsstrahlung and the Compton processes. The two clusters studied so far,<sup>46</sup> M5 [279] and M3 [391], indicate fairly consistent, though not identical, results for the axion-electron coupling.<sup>47</sup> The combined analysis indicates the bound

$$g_{ae}^{(\text{best})} = 1.4 \times 10^{-13}, \quad (215a)$$

$$g_{ae} \leq 3.1 \times 10^{-13}, \quad \text{at } 95\% \text{ C.L.} \quad (215b)$$

<sup>45</sup>The additional energy can also be accounted for by hidden photons [369, 385] but not by anomalous neutrino electromagnetic form factors [386].

<sup>46</sup>We point out, however, that very recently, Ref. [390] considered 50 GC to find the upper bound  $g_{ae} = 2.5 \times 10^{-13}$  on the axion-electron coupling. The result is slightly more stringent than the one we discuss in this sections.

<sup>47</sup>In particular, the analysis of M5 [279] suggests a stronger hint to a non-vanishing axion-electron coupling

$$\begin{aligned} g_{ae} &= 1.88^{+1.19}_{-1.17} \times 10^{-13}, & \text{at } 68\% \text{ C.L.} \\ g_{ae} &\leq 4.3 \times 10^{-13}, & \text{at } 95\% \text{ C.L.}, \end{aligned} \quad (214)$$

while the observations of M3 are rather consistent with expectations ( $g_{ae}^{\text{best}} = 0.05 \times 10^{-13}$ ) and suggest a somewhat stronger bound  $g_{ae} \leq 2.6 \times 10^{-13}$  at 95% C.L. [391]. Reference [392] attributes the disagreement between theory and observations in [279], at least partially, to the convention used for the screening of the nuclear reaction rates.

Several uncertainties, including the cluster morphology and distance as well as uncertainties in the nuclear reaction rates, affect the exact determination of the RGB bound on the axion-electron coupling [279, 391, 393]. The use of multi-band photometry of multiple globular clusters would provide a substantial improvement (see, e.g., [390, 391]). The error in the globular cluster distance, currently the largest observational uncertainty, will be reduced considerably (perhaps by as much as a factor of 10) with the release of the GAIA data relevant for GCs, expected in 2022 [394].

The combination of hints from the WDLF, the WD pulsation, and RGB stars gives the  $1\sigma$  preferred interval

$$g_{ae} = 1.6^{+0.29}_{-0.34} \times 10^{-13}, \quad (216)$$

with  $\chi^2_{\min}/\text{d.o.f.} = 14.9/15 = 1.0$ , and favors the axion (or ALP) solution at slightly more than  $3\sigma$  [34].

#### 4.3. Axion-nucleon coupling

Finite axion-nuclei interactions allow for further ways axions may impact the evolution of stars. Non-thermal processes, such as nuclear transitions in stars (particularly, the Sun) with the emission of axions, provide an interesting channel to produce a possibly detectable axion flux. However, their impact on stellar evolution is minimal. Thermal processes turn out to be quite more relevant, in this respect.

The most relevant thermal process involving the axion-nucleon coupling is the nucleon bremsstrahlung

$$N + N' \rightarrow N + N' + a, \quad (217)$$

with  $N, N' = n, p$ , where  $n$  represents a neutron and  $p$  a proton. The Feynman diagram for these processes is shown in Fig. 9. One of the major difficulties in dealing with the nucleon bremsstrahlung is the description

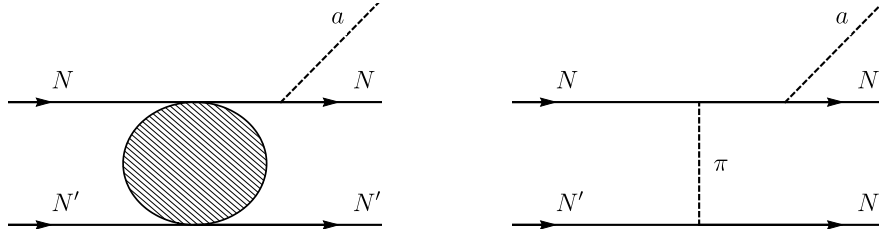


Figure 9: Axion nuclear bremsstrahlung (one of the possible diagrams).  $N, N'$  represent either a proton or a neutron. To the right is the Feynman diagram corresponding to the OPE approximation.

of the nuclear interaction, shown as a blob in figure 9. A substantial simplification, known as the One Pion Exchange (OPE) approximation, is to assume that the interaction is mediated by the exchange of a single pion, as shown in the right panel in figure 9. The OPE framework is not always justified (see, e.g., Ref. [31, 395]) but it does provide a starting point for more accurate computations (cfr. Ref. [396] for a recent review of the role of OPE and its corrections). Nevertheless, it is evident from the figure that the pion mass in the propagator is going to suppress the emission rate unless the temperature is such that the typical momentum exchanged in the collision, which is of the order of the nucleon momentum  $q_N \sim (3m_N T)^{1/2}$ , is larger than the pion mass. This demands  $T \gtrsim 10\text{MeV}$ , a temperature typical of the core of Supernovae (SNe) and Neutron Stars (NS). Therefore, only SNe and NS may (and, indeed, do) provide an environment to test the axion nucleon bremsstrahlung.

Approximate emission rates for the  $nn$  scattering (the  $pp$  scattering is similar) in the limit of nondegenerate and degenerate nuclei are given below [358]

$$\varepsilon_{\text{ND}} \approx 2.0 \times 10^{38} g_{an}^2 \rho_{14} T_{30}^{3.5} \text{erg g}^{-1} \text{s}^{-1}, \quad (218a)$$

$$\varepsilon_{\text{D}} \approx 4.7 \times 10^{39} g_{an}^2 \rho_{14}^{-2/3} T_{30}^6 \text{erg g}^{-1} \text{s}^{-1}, \quad (218b)$$

where  $T_{30} = T/30\text{MeV}$  and  $\rho_{14} = \rho/10^{14}\text{g cm}^{-3}$ . Notice that eqs. (218) are only a crude approximation of the emission rate, calculated in the OPE approximation and ignoring the pion mass and medium effects.

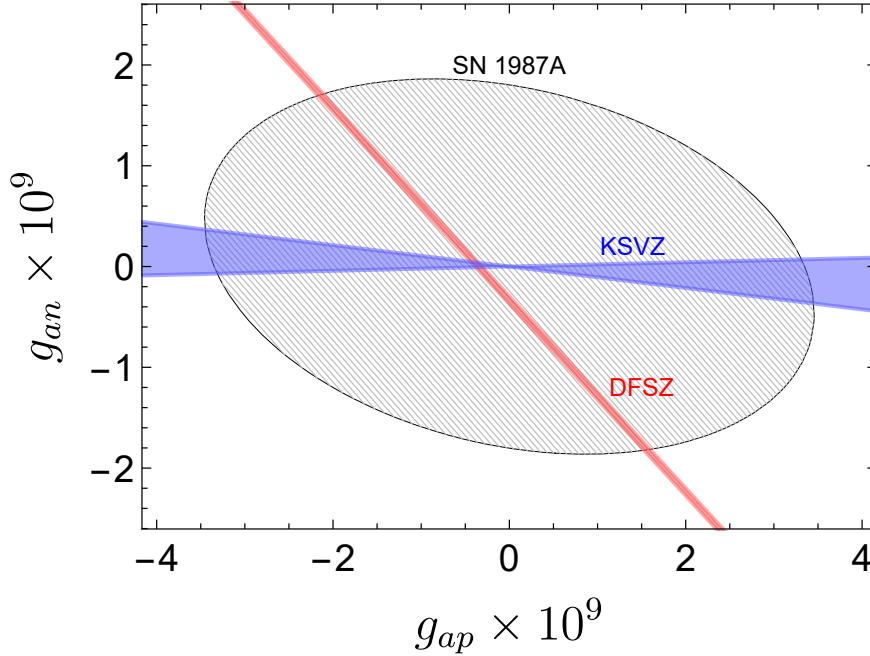


Figure 10: SN 1987A bound on the axion-nucleon couplings. In hatched gray, the region allowed by the SN 1987A bound derived in [396]. The parameter space for KSVZ and DFSZ axions is superimposed. The width of the lines represent the current uncertainties according to [45].

However, they do show the steeper temperature dependence of the degenerate emission rate and the stronger density dependence in the nondegenerate limit.

**SN 1987A** - The most well known argument to constraint the axion interaction with protons and neutrons is the one based on the observed neutrino signal from SN 1987A [31, 325, 326, 397]. The signal duration depends on the efficiency of the cooling and is compatible with the assumption that SN neutrinos carry about 99% of the energy released in the explosion. For a light, weakly interacting particle, a bound can be extracted from the requirement that it does not contribute more than neutrinos, about  $2 \times 10^{52}$  erg  $s^{-1}$ , to the cooling of the young SN, with a typical core conditions of  $T \sim 30$  MeV and  $\rho \sim 10^{14}$  g  $cm^{-3}$ . The most recent analysis for the axion case [396] derived the bound<sup>48</sup>

$$g_{an}^2 + 0.29 g_{ap}^2 + 0.27 g_{an} g_{ap} \lesssim 3.25 \times 10^{-18}, \quad (219)$$

shown in Fig. 10.

Strongly interacting axions may be trapped in the SN core. In this case the emission is reduced, as they thermalize and are effectively emitted from an *axiosphere*, similarly to what happens to neutrinos. The most recent analysis found that this condition is satisfied for  $g_{an} = g_{ap} \gtrsim 10^{-7}$ . However, even trapped axions may extract more energy than neutrinos from the young SN and couplings all the way to  $g_{an} = g_{ap} \approx 10^{-4}$  should be probably excluded [396].

**Neutron Stars** - Observations of the cooling of NS also provides information about the axion-nucleon coupling. In particular, the unexpectedly rapid cooling of the NS in CAS A was attributed to the presence

<sup>48</sup>Eq. (219) shows a surprisingly subdominant contribution of the proton scattering to the emission rate, quite more accentuated than what reported in previous analyses [31, 34]. The reason is that, besides being less abundant than neutrons, protons are nondegenerate while neutrons are partially degenerate and the emission rate in SN conditions is more efficient for degenerate nuclei, as evident from Eqs. (218).

of axions with coupling to neutrons [398]

$$g_{an} \simeq 4 \times 10^{-10}. \quad (220)$$

However, the anomalous rapid cooling may also be originated in the phase transition of the neutron condensate into a multicomponent state [399]. More recently, the data have been explained assuming a neutron triplet superfluid transition occurring at the present time,  $t \sim 320$  years, and that proton superconductivity is operating at  $t \ll 320$  years [400]. The neutron triplet superfluid transition accelerates the neutrino emission through the breaking and reformation of neutron Cooper pairs. Under these assumptions the data can be fitted well, leaving little room for additional axion cooling. Quantitatively,

$$g_{ap}^2 + 1.6 g_{an}^2 \leq 1.1 \times 10^{-18}. \quad (221)$$

An even stronger bound, though only on the axion-neutron coupling,

$$g_{an} \leq 2.8 \times 10^{-10}, \quad (222)$$

was inferred from observations of the NS in HESS J1731-347 [401].

#### 4.4. Axion coupling to the neutron EDM

As discussed in Section 2.8 a fundamental consequence of QCD axion models is that axions couple to the neutron EDM, effectively driving it to zero and solving the strong CP problem. The axion-neutron EDM vertex can be parameterized with the coupling  $g_d$  defined through the Lagrangian term (cf. Eq. (109))

$$\mathcal{L}_d = -\frac{i}{2} g_d a \bar{n} \sigma_{\mu\nu} \gamma_5 n F^{\mu\nu}. \quad (223)$$

This coupling induces the process  $n + \gamma \rightarrow n + a$ , allowing the production of axions that, in turn, contribute to the SN cooling. As discussed, observations of the SN 1987A neutrino burst limit the amount of possible exotic cooling rate to be less than the neutrino's. A rough estimate gives [402]

$$g_d \leq 4 \times 10^{-9} \text{ GeV}^{-2}. \quad (224)$$

We emphasize that the interaction in (223) is generic to any QCD axion model and does not demand any other assumption besides the solution of the strong CP problem. Therefore, the bound (224) is, effectively, a bound on the PQ constant or, equivalently, on the axion mass. If we express the coupling in terms of the axion mass,  $g_d \approx 6 \times 10^{-10} (m_a/\text{eV}) \text{ GeV}^{-2}$ , the SN bound implies  $f_a \gtrsim 9 \times 10^5 \text{ GeV}$  or, equivalently,  $m_a \lesssim 7 \text{ eV}$ .

#### 4.5. Axion CP-odd couplings

Stellar evolution provides also strong bounds on the axion CP odd couplings, discussed in Section 2.10. The axion scalar couplings to electrons  $g_{ae}^S$  can be constrained in globular cluster stars, where such particles can be produced through Compton scattering or bremsstrahlung [403]. The strongest bound is derived by the luminosity of the tip of the RGB. A semiquantitative argument, based on the assumption that any novel emission rate would spoil observations unless  $\varepsilon \lesssim 10 \text{ erg s}^{-1} \text{ g}^{-1}$ , gives the rather restrictive bound [404]

$$g_{ae}^S \leq 0.7 \times 10^{-15}. \quad (225)$$

HB stars provide a slightly less restrictive bound,  $g_{ae}^S \leq 3 \times 10^{-15}$ .

The scalar coupling to nuclei is likewise constrained in RGB stars [404]

$$g_{aN}^S \leq 1.1 \times 10^{-12}, \quad (226)$$

while HB stars provide the less restrictive bound  $g_{aN}^S \leq 6 \times 10^{-12}$ .

These astrophysics bounds are the dominant constraints on the coupling to nuclei for masses above 1 eV or so. However, for lower masses the experimental bounds on  $5^{\text{th}}$  force are much stronger (see Fig. 1 in Ref. [403]).

#### 4.6. Axion coupling to gravity and black hole superradiance

In some cases, astrophysical considerations can provide insights on the couplings of axions to gravity, without assuming any interaction with standard model fields. Such considerations are, therefore, completely model-independent. The case of black holes (BH) discussed below is particularly interesting since, just like in the case of the other bounds discussed in this section, there is no assumption that axions are initially present, i.e. there is no requirement for axions to be the DM.

Axions form gravitational bound states around black holes whenever their Compton length is of the order of the black holes radii. The phenomenon of *superradiance* [405] then guarantees that the axion occupation numbers grow exponentially, providing a way to extract very efficiently energy and angular momentum from the black hole [280, 281]. The rate at which the angular momentum is extracted depends on the black hole mass and so the presence of axions could be inferred by observations of black hole masses and spins. Current observations exclude the region [281]

$$3 \times 10^{17} \text{ GeV} \leq f_a \leq 10^{19} \text{ GeV}, \quad (227)$$

corresponding to the mass region  $6 \times 10^{-13} \text{ eV} \leq m_a \leq 2 \times 10^{-11} \text{ eV}$ .<sup>49</sup> We underline that superradiance can start from a quantum mechanical fluctuation and does not require the prior existence of an axion population.

The condition for the BH superradiance relies on the assumption that the axion self interaction is small, which is why the bounds concern such large values of  $f_a$ . For sufficiently large couplings, the axion cloud could collapse in what is known as a *bose nova*,<sup>50</sup> producing periodic bursts which should be observable by Advanced LIGO and VIRGO [281].

Other observational signatures of BH superradiance are the gravitational waves produced in the transition of axions between gravitational levels or from axions annihilation to gravitons [281, 407].

#### 4.7. Summary of astrophysical bounds

A summary of all the stellar evolution bounds on the axion couplings is shown in Table 3 where, whenever possible, we have reported the bounds at  $2\sigma$  and the hints at  $1\sigma$ . The bounds were derived without assuming any model dependence and are therefore quite general.

Particularly interesting among the astrophysical considerations are the bounds from BH superradiance and the SN 1987A bound on the neutron EDM, since they are the only ones that provide a bound on the axion mass rather than on the couplings.<sup>51</sup> Combined, they constrain the axion mass in the range  $2 \times 10^{-11} \text{ eV} \leq m_a \leq 7 \text{ eV}$ .

In the case of the other bounds, specific model-dependent relations connect the different couplings, as well as the axion mass. The astrophysical bounds for hadronic axion models are shown in Fig. 11. The models are parameterized in terms of the axion mass and  $E/N$ . We superimpose also the region excluded by the CERN Axion Solar Telescope (CAST) for reference. The astrophysical hinted region is not shown since hadronic axions cannot fit very well the required parameters [34].

Hadronic axions are naturally electrophobic. For axion masses between  $10^{-9}$  and  $1 \text{ eV}$ , and with  $E/N$  between 0 and 15, the parameter  $C_{ae}$ , defined in Eq. (118), which parameterize the interaction with electrons, is always confined in the range  $\approx 5 - 15 \times 10^{-3}$ . Consequently, the RGB bound is always suppressed with respect to the HB and the hot DM bounds for such axions.

The analogous plot for DFSZ axions is shown in Fig. 12. Again, we superimpose the region experimentally excluded, in this case by the Large Underground Xenon (LUX) experiment (CAST does not probe these

<sup>49</sup>A recent analysis [406] proposed a slightly more stringent upper bound on the axion mass,  $m_a \leq 10^{-11} \text{ eV}$ .

<sup>50</sup>Axion couplings to other fields, e.g. photons, would also induce an effective axion self-interaction. However, such couplings would need to be too large to have any significant effect. For example, the value of  $g_{a\gamma}$  required to induce a self-coupling as large as what expected from the axion potential in Eq. (50), for masses  $\sim 10^{-12} \text{ eV}$ , is several orders of magnitude larger than the value excluded by the HB bound. This justifies plotting  $E/N$  up to very large values, as we do in Section 5.

<sup>51</sup>Astrophysical considerations are, of course, affected by many uncertainties. In particular, the bound on the neutron EDM is based on a simple estimate and should probably be revised. Additionally, we are assuming a standard relation between the axion mass and the PQ scale as dictated by standard QCD. This relation can be modified in non-standard scenarios as discussed in Section 6.6.2.

Star	Hint ( $1\sigma$ )	Bound ( $2\sigma$ )
Sun	–	$g_{a\gamma} \leq 2.7 \times 10^{-10} \text{ GeV}^{-1}$
WDLF	$g_{ae} = 1.5_{-0.5}^{+0.3} \times 10^{-13}$	$g_{ae} \leq 2.1 \times 10^{-13}$
WDV	$g_{ae} = 2.9_{-0.9}^{+0.6} \times 10^{-13}$	$g_{ae} \leq 4.1 \times 10^{-13}$
RGB Tip	$g_{ae} = 1.4_{-1.3}^{+0.9} \times 10^{-13}$ (M3+M5)	$g_{ae} \leq 3.1 \times 10^{-13}$ (M3+M5)
	–	$g_{ae}^S \leq 0.7 \times 10^{-15}; \quad g_{aN}^S \leq 1.1 \times 10^{-12}$
HB	$g_{a\gamma} = (0.3 \pm 0.2) \times 10^{-10} \text{ GeV}^{-1}$	$g_{a\gamma} \leq 0.65 \times 10^{-10} \text{ GeV}^{-1}$
	–	$g_{ae}^S \leq 3 \times 10^{-15}; \quad g_{aN}^S \leq 6 \times 10^{-12}$
SN 1987A	–	$g_{an}^2 + 0.29 g_{ap}^2 + 0.27 g_{an} g_{ap} \lesssim 3.25 \times 10^{-18}$
	–	$g_d \lesssim 4 \times 10^{-9} \text{ GeV}^{-2} (\Rightarrow f_a \gtrsim 9 \times 10^5 \text{ GeV})$
NS in CAS A	–	$g_{ap}^2 + 1.6 g_{an}^2 \lesssim 1.1 \times 10^{-18}$
NS in HESS J1731-347	–	$g_{an} \leq 2.8 \times 10^{-10}$
Black Holes	–	$f_a \leq 3 \times 10^{17} \text{ GeV}$ or $f_a \geq 10^{19} \text{ GeV}$

Table 3: Summary of stellar hints and bounds on axions. The hints are all at  $1\sigma$  and the bounds at  $2\sigma$ , except for the case of SN 1987A and NS in CAS A, for which a confidence level was not provided. We have not reported the hint from the NS in CAS A [398] since it is in tension with the more recent bound in [400].

models). In this case, the stellar anomalous observations can be fitted quite well [34]. The hinted region is, however, quite difficult to explore experimentally and probably only the International AXion Observatory (IAXO) will be able to access parts of it in the near future [303].



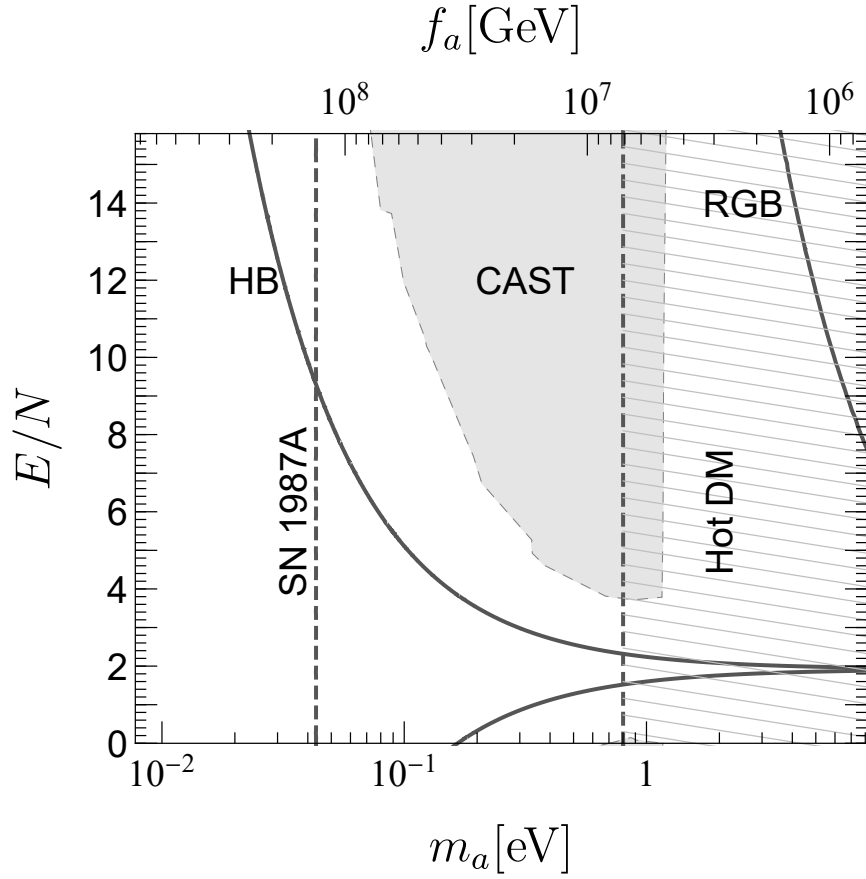


Figure 11: Astrophysical bounds on the hadronic axions (at  $2\sigma$ ). The region to the left of the curves are excluded by astrophysical considerations. The bound from SN 1987A is shown with dashed lines since the bound is less robust than the others [396, 408] and its statistical significance is not well defined. The area probed by CAST is shown in light gray. The lightly hatched region is excluded by the hot DM bound [409] (see Section 3.8).

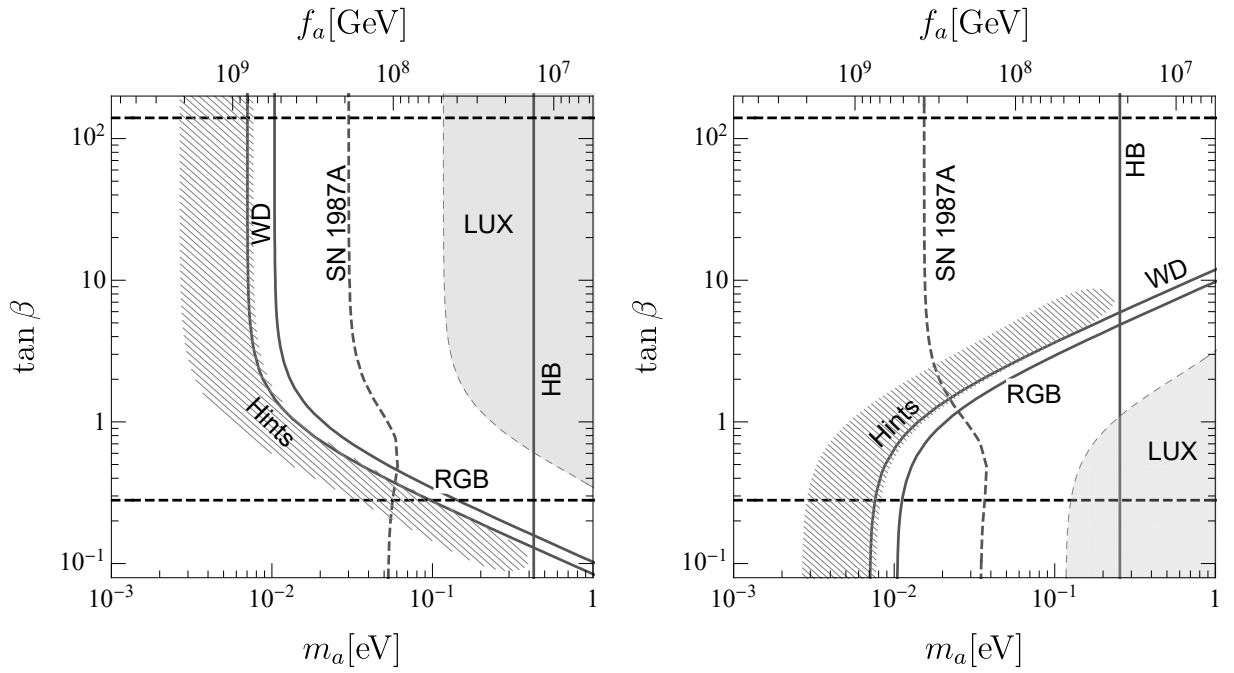


Figure 12: Astrophysical bounds on the DFSZ axions. The left panel represents the DFSZ I model. The right panel the DFSZ II. The region to the left of the curves are excluded by astrophysical considerations. The WD curve refers to the WD luminosity function bound (refer to the text for more information). The hatched region refers to the combined hints from the WD luminosity function, the WD pulsation, HB and RGB stars. The bound from SN 1987A is shown with dashed lines since the bound is somewhat less robust [396].

## 5. Experimental Searches

In the interest of keeping this review self-consistent, we briefly describe the status of the axion experimental searches. More complete reviews can be found in Refs. [26, 38].

### 5.1. Solar axions and helioscopes

The Sun is a natural source of axions. These are produced through Primakoff (Section 4.1) and ABC (Section 4.2) processes:

$$\frac{dN_a}{dt d\omega} = \left( \frac{g_{a\gamma}}{\text{GeV}^{-1}} \right)^2 n_{a\gamma}(\omega) + g_{ae}^2 n_{ae}(\omega), \quad (228)$$

where  $n_{a\gamma}$  represents the Primakoff contributions while  $n_{ae}$  gets contribution from atomic recombination and deexcitation, bremsstrahlung, and Compton processes,  $n_{ae} = n_{ae}^A + n_{ae}^B + n_{ae}^C$ . Good analytical approximations for these coefficients exist for all but the atomic recombination and deexcitation processes (see, e.g., Ref. [410] and [411]):

$$n_{a\gamma}(\omega) \approx 1.69 \times 10^{58} e^{-0.829 \omega} \omega^{2.45} \text{ keV}^{-1} \text{ s}^{-1}; \quad (229a)$$

$$n_{ae}^B \approx 7.4 \times 10^{62} \frac{\omega e^{-0.77 \omega}}{1 + 0.667 \omega^{1.278}} \text{ keV}^{-1} \text{ s}^{-1}; \quad (229b)$$

$$n_{ae}^C \approx 3.7 \times 10^{60} \omega^{2.987} e^{-0.776 \omega} \text{ keV}^{-1} \text{ s}^{-1}. \quad (229c)$$

The total number of axions emitted by the Sun per second is,

$$\frac{dN_a}{dt} = 1.1 \times 10^{39} \left[ \left( \frac{g_{a\gamma}}{10^{-10} \text{ GeV}^{-1}} \right)^2 + 0.7 \left( \frac{g_{ae}}{10^{-12}} \right)^2 \right] \text{ s}^{-1}. \quad (230)$$

Evidently, the axion flux gets a similar contribution from Primakoff and ABC axions for couplings of phenomenological interest (cfr. Fig. 7). Notice, however, that the ABC flux is peaked at slightly lower energies than the Primakoff, a fact that allows to distinguish between the two fluxes (and so infer some information about the underlying axion model) if enough data is collected in an helioscope experiment [412].<sup>52</sup>

The weight of the two contributions in Eq. (230) depends on the specific axion model. In terms of  $g_{e12} = g_{ae}/10^{-12}$  and  $g_{\gamma10} = g_{a\gamma}/10^{-10} \text{ GeV}^{-1}$ , we have

$$\text{KSVZ : } g_{e12}/g_{\gamma10} \approx 0; \quad (231a)$$

$$\text{DFSZ I : } g_{e12}/g_{\gamma10} = 20 \sin^2 \beta; \quad (231b)$$

$$\text{DFSZ II : } g_{e12}/g_{\gamma10} = 12 \cos^2 \beta. \quad (231c)$$

Experiments that aim at detecting the solar axion flux are known as axion helioscopes. The most notable example is the Sikivie helioscope [413], or simply helioscope, which adopts a strong laboratory magnetic field for the coherent conversion of solar axions into X-ray photons. However, the solar axion flux may be detected through other means, for example through the Primakoff-Bragg conversion [414] or the axio-electric effect [415, 416].

The Sikivie helioscope makes use of the axion coherent conversion in a transverse magnetic field  $B$ . The conversion probability is

$$P_{a \rightarrow \gamma} = \left( \frac{g_{a\gamma} B L}{2} \right)^2 \frac{\sin^2(qL/2)}{(qL/2)^2}, \quad (232)$$

<sup>52</sup>For example, the number of axions produced in the energy bin  $1 \leq \omega/\text{keV} \leq 2$  is 12.5% of the total, in the case of hadronic axions (no coupling with electrons) but it moves quickly to  $\sim 30\%$  if  $g_{ae}/g_{a\gamma} > 5 \times 10^{-2} \text{ GeV}$ , which is typical for DFSZ axions.

where  $q = q_\gamma - q_a$  is the momentum transfer provided by the magnetic field and  $L$  is the length of the magnet. Coherence is ensured whenever  $qL \ll 1$ . In this condition, the probability does not depend on the axion mass and energy. In vacuum, the relativistic approximation ( $\omega_a \gg m_a$ ) gives  $q \simeq m_a^2/2\omega$ . A small mass, therefore, ensures coherence on macroscopic scales.

Whenever the coherence condition is verified, the conversion probability scales as  $(g_{a\gamma}BL)^2$ , rapidly increasing with the magnetic field and the size of the magnet. When coherence is lost, the sensitivity is reduced proportionally to  $m_a^{-2}$ .<sup>53</sup> Since for QCD axion models  $g_{a\gamma}^2 \propto m_a^2$  the sensitivity line follows exactly the axion model line in the  $g_{a\gamma} - m_a$  plane once coherence is lost at large masses.

To regain sensitivity, the coherence can be restored using a buffer gas in the magnet beam pipes [418]. In this case the momentum transfer is  $q \simeq (m_a^2 - m_\gamma^2)/2\omega$ , where  $m_\gamma$  is the effective photon mass in the gas. Tuning the effective photon mass to the axion mass allows to effectively regain coherence.

The CERN Solar Axion Experiment (CAST) [419], a 3-rd generation and currently the most advanced running axion helioscope,<sup>54</sup> reported the bound  $g_{a\gamma} \leq 0.66 \times 10^{-10} \text{ GeV}^{-1}$  for masses  $m_a \leq 20 \text{ meV}$ , while reaching the  $m_a \sim \text{eV}$  range at high masses [420]. Going beyond that mass may be less interesting because of the hot DM bound [409, 421] (see Section 3.8).

The proposed International Axion Observatory (IAXO), a 4-th generation axion helioscope [422], is expected to increase the sensitivity by a factor of  $\gtrsim 10^4$ , probing the axion-photon coupling down to  $g_{a\gamma} \sim$  a few  $10^{-12} \text{ GeV}^{-1}$  at low mass and exploring significant regions of the KSVZ and DFSZ axion models [303]. A scaled down (and significantly less expensive) version of IAXO, called BabyIAXO, will likely start operations in the mid of the current decade, in DESY. Though considerably less powerful than its brother IAXO, BabyIAXO [303] will still be sensitive to DFSZ axion models, unique in this respect among the experiments probing the axion mass region above a few meV. The sensitivity of IAXO and BabyIAXO to hadronic and DFSZ axion models is shown in Figs. 13, 14, and 15.

There are other technologies to detect solar axions. One explored option is to exploit the coherent enhancement of the axion conversion into photons, via Primakoff effect, when the solar axion beam satisfies the Bragg condition of scattering with a crystal plane [423]. However, the sensitivity of these experiments is not competitive with the Sikivie helioscope or with the astrophysical bounds.

Large WIMP detectors such as LUX and XENON100 have the capability to detect solar axions through the axio-electric effect and do, in fact, provide bounds on the axion-electron coupling. Specifically, the XENON100 collaboration [424] reported  $g_{ae} < 7.7 \times 10^{-12}$  (90 % CL), LUX [425],  $g_{ae} < 3.5 \times 10^{-12}$ , and PandaX-II [426],  $g_{ae} < 4 \times 10^{-12}$ . These searches are particularly interesting since they permit the exploration of the axion-electron coupling in a very wide mass region. However, probing the parameter space allowed by the cooling of WDs and RGB may prove extremely challenging even for axio-electric helioscopes of the next generation of [38].

## 5.2. Helioscopes sensitivity to $g_{a\gamma}$ and $g_{ae}$

Here we provide simple, approximate expressions to extract the helioscope sensitivity to general axion models, accounting for the fact that axions can be produced in the Sun through processes induced by their couplings to electrons and to photons. By helioscope here we mean any instrument that can detect solar axions. In particular, we consider the standard Sikivie helioscope, which uses an external magnetic field to convert axions into photons, and the axioelectric helioscope, which operates through the axion interaction with electrons.

In the Sikivie helioscope, solar axions are converted into photons in a transverse magnetic field  $B$ . The conversion probability is given in Eq. (232), where we remind that  $q$  is the momentum transfer provided by the magnetic field. In vacuum,  $q \simeq m_a^2/2\omega$ . Whenever  $qL \ll 1$ , the probability does not depend on the energy.

<sup>53</sup>Given enough data (and a large enough axion mass), the spectral distortion induced by the loss of coherence may allow to pin down the axion mass [417].

<sup>54</sup>CAST is expected to stop operating in 2020.

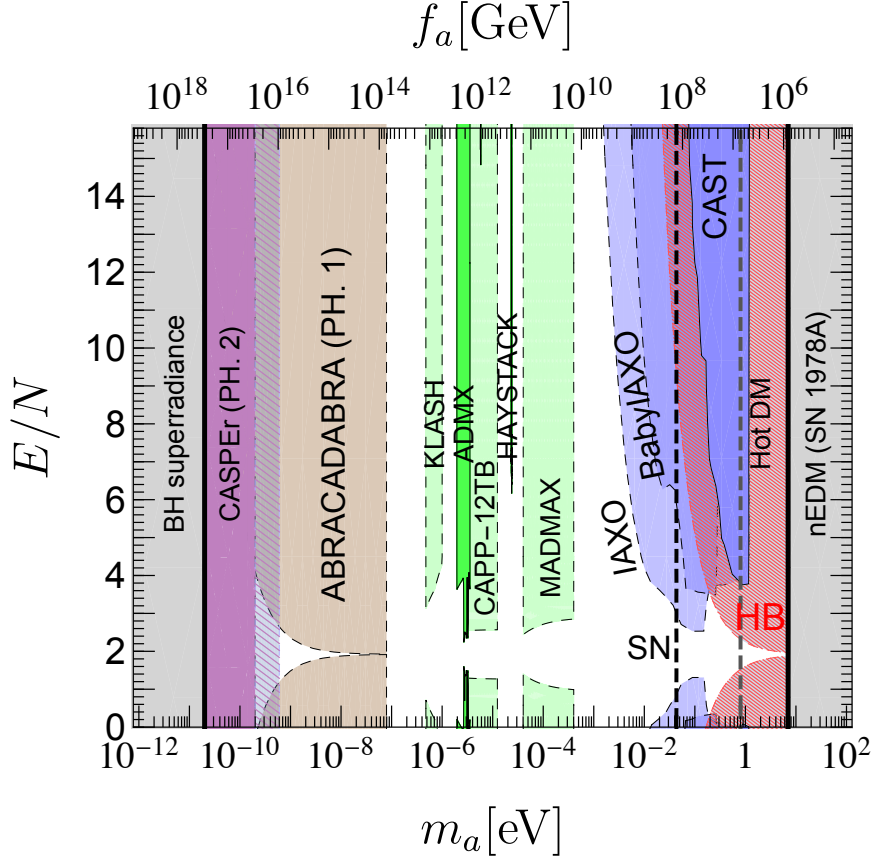


Figure 13: Hadronic axion parameter space. Interactions with electrons are neglected. Experimental bounds are shown with solid lines while projected sensitivity with dashed lines. The sensitivity of the haloscope experiments is calculated assuming that axions comprise the totality of the cold dark matter in the universe. In green are the cavity experiments. Darker colour corresponds to actual data while in lighter colour we show the sensitivity of proposed experiments. The sensitivity of ABRACADABRA refers to phase 1. CASPER refers to CASPER electric, phase 2. The hatched area next to the CASPER region indicates the error in the sensitivity due to QCD uncertainties in the calculation of the nEDM.

The expected number of events in the Sikivie helioscope is

$$N_\gamma - N_b = \frac{S\Delta t}{4\pi D_\odot^2} \int \frac{dN_a}{dt d\omega} P_{a\gamma} \epsilon d\omega \quad (233)$$

where  $N_b$  the total background,  $D_\odot \simeq 1.5 \times 10^{11}$  m is the distance to the Sun,  $S$  is the detector total area,  $\Delta t$  the exposure time, and  $\epsilon$  a parameter that measure the detection efficiency. In general, the integral should be restricted to some  $\omega$  region. We assume that these threshold values are accounted for by  $\epsilon$ .

Be  $\bar{g}_{a\gamma}$  the bound on the axion-photon coupling in the case of  $g_{ae} = 0$ . In the general case, we find

$$g_{a\gamma}^2 \int (g_{a\gamma}^2 n_\gamma + g_{ae}^2 n_e) \tilde{P}_{a\gamma} \epsilon d\omega \leq \bar{g}_{a\gamma}^4 \int n_\gamma \tilde{P}_{a\gamma} \epsilon d\omega \quad (234)$$

where  $g_{a\gamma}$  is given in units of  $\text{GeV}^{-1}$  and  $\tilde{P}_{a\gamma}$  is the oscillation probability divided by  $g_{a\gamma}$ . In the case of small axion mass, the factor  $qL$  in the expression for the probability is small and  $P_{a\gamma}$  does not depend on the axion energy. We can assume that the factor  $\epsilon$  is also roughly constant in the energy interval relevant for solar axions, if the experimental cuts in  $\omega$  are performed far from the regions where the two fluxes are

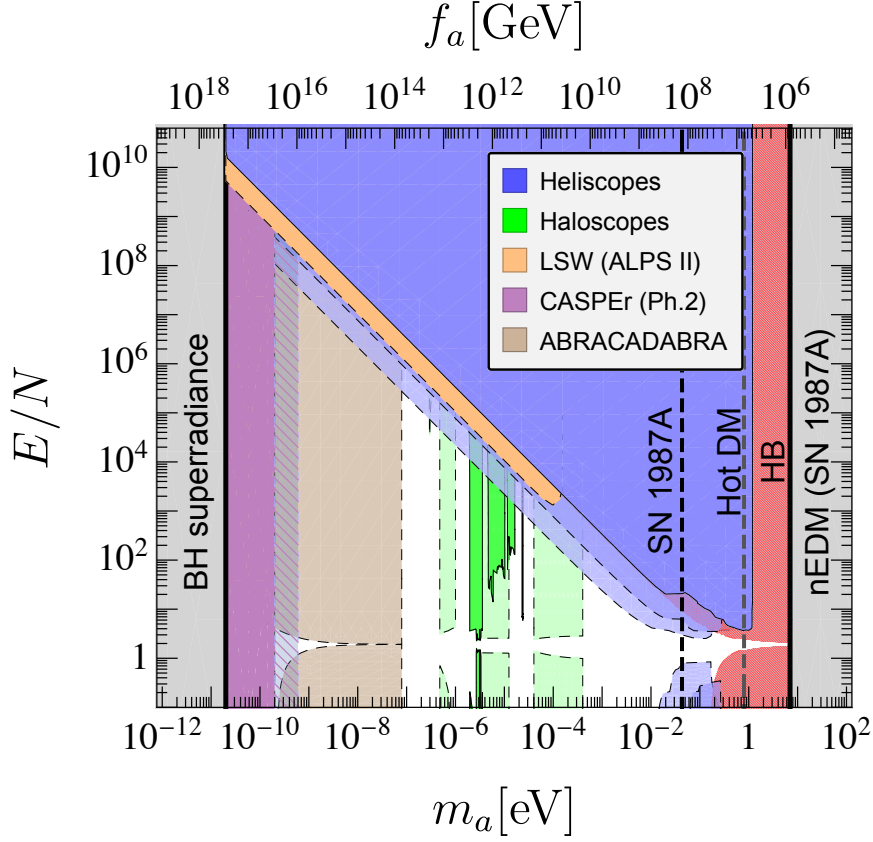


Figure 14: Phenomenological and experimental status for the hadronic axion. The experiments presented here are the same shown in Fig. 13. Experimental bounds are shown in solid lines while projected sensitivity in dashed lines. The Helioscope lines refer to the latest results from CAST [420] and to the expected sensitivity of BabyIAXO and IAXO [303]. For ABRACADABRA we are using the expected sensitivity in phase 1 ( $B_{\text{max}} = 5\text{T}$  and  $\text{Volume} = 1\text{ m}^3$  [291]) for the resonant case. The parameter space is constrained at low masses by the BH superradiance and at high masses by the SN 1987A bound on the nEDM (see text for more details).

large.<sup>55</sup> In this case, the integrals can be performed<sup>56</sup> and one finds the very simple relation

$$g_{\gamma 10}^2 (g_{\gamma 10}^2 + 0.7 g_{e 12}^2) \lesssim \bar{g}_{\gamma 10}^4, \quad (235)$$

where, we remind,  $g_{\gamma 10} = g_{a\gamma}/10^{-10}\text{GeV}^{-1}$  and  $g_{e 12} = g_{ae}/10^{-12}$ . At large masses, when coherence is lost, one cannot assume  $P_{a\gamma}$  constant anymore. Assuming a  $\omega^2$  dependence for  $P_{a\gamma}\epsilon$  we find that the coefficient 0.7 should be replaced with 0.3. Indeed, in this case Primakoff has a greater weight since it is peaked at higher energy. In this case, however, a gas can be used to restore coherence.

We turn now to the helioscopes based on the axio-electric effect. For nonrelativistic electrons and ultra-relativistic axions, the cross section for the axio-electric effect is [427–429] proportional to the photoelectric cross section

$$\sigma_{ae}(\omega) = \frac{g_{ae}^2}{8\pi\alpha} \left( \frac{\omega}{m_e} \right)^2 \sigma_{ph}(\omega) \simeq 2.1 \times 10^{-29} g_{e 12}^2 \omega_{\text{keV}}^2 \sigma_{ph}(\omega), \quad (236)$$

<sup>55</sup>This is not always the case. For example, in [411] the analysis is restricted to the energy range between 0.8 and 6.8 keV.

<sup>56</sup>We integrate between  $\omega = 100\text{eV}$  and  $\omega = 12\text{ keV}$ . Below 100 eV the emission rate is less clear and unaccounted processes may contribute [38].

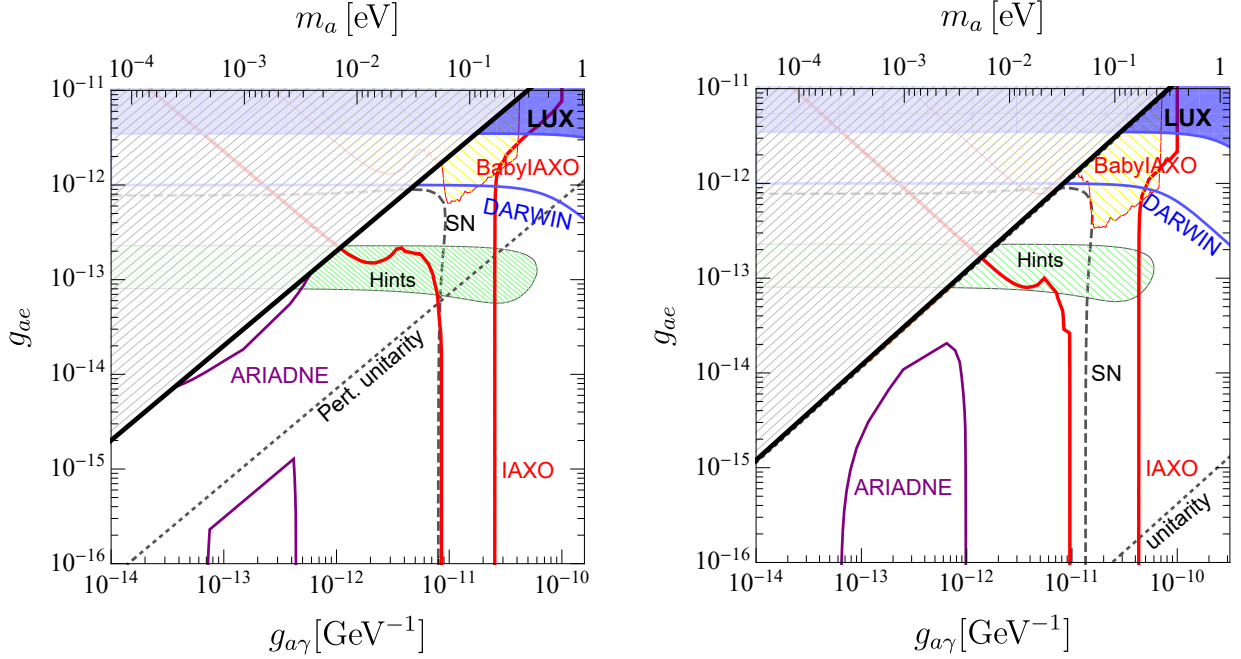


Figure 15: DFSZ axion I (left) and II (right) parameter space. The hatched region in the upper left corner is not accessible to such axions models. The green region represents the stellar evolution hints from HB, RGB and WD stars, as discussed in the text. The SN 1987A bound is shown with a dashed line to reflect the higher level of uncertainty with respect to other stellar bounds.

where  $\omega_{\text{keV}} = \omega/\text{keV}$ . The pronounced peak at low energy ( $\omega_a \sim 1 \text{ keV}$ ), characteristic of the photoelectric cross section, which would favor the ABC over the Primakoff flux, is compensated by the  $\omega^2$  term in the case of the axio-electric cross section. Therefore, in general the Primakoff flux is not negligible and should be included in the estimates of the experimental potential. For example, setting  $g_{ae} = 10^{-12}$  and  $g_{a\gamma} = 10^{-10} \text{ GeV}^{-1}$ , we find  $g_{a\gamma}^2 \int \sigma_{ae} n_\gamma d\omega \simeq 2g_{ae}^2 \int \sigma_{ae} n_e d\omega$ . Proceeding similarly to what done in the case of the Sikivie helioscopes, we set  $\bar{g}_{ae}$  to the experimental bound for a purely ABC spectrum and find the very simple relation for the axion couplings:

$$g_{ae}^2 \int (g_{a\gamma}^2 n_\gamma + g_{ae}^2 n_e) \tilde{\sigma}_{ae} \epsilon d\omega \leq \bar{g}_{ae}^4 \int n_\gamma \tilde{\sigma}_{ae} \epsilon d\omega, \quad (237)$$

where  $\tilde{\sigma}_{ae}$  is the axio-electric cross section for  $g_{ae} = 1$ . If we assume that  $\epsilon$  does not have a strong dependence on  $\omega$ , the integrals can be performed analytically and we find:

$$g_{e12}^2 (2g_{\gamma10}^2 + g_{e12}^2) \lesssim \bar{g}_{e12}^4 \quad (238)$$

### 5.3. DM axions and haloscopes

The local DM density is estimated to be about  $0.45 \text{ GeV}/\text{cm}^3$ . If the axion paradigm is correct and axions do make up the totality of the DM matter, we should expect (locally) about  $4.5 \times 10^{14} (\mu\text{eV}/m_a) \text{ cm}^{-3}$  non-relativistic axions, with energy  $\omega_a \sim m_a(1 + O(10^{-6}))$ , where the correction to the energy derives from the estimated axion velocity distribution ( $v \sim 10^{-3}$ ). Several experimental techniques have been developed to detect such a huge number of nonrelativistic axions. Collectively, such experiments are known as *axion haloscopes*.

The conventional haloscope technique is the resonant cavity haloscope [413], which employs the Primakoff conversion of DM axions in a strong magnetic field that permeates a resonant microwave cavity. The conversion is resonant if the axion energy  $\omega_a = m_a(1 + O(10^{-6}))$  matches a cavity mode. Cavity



experiments are well suited to search for axions in the  $\mu\text{eV}$  mass range, where they have reached extremely high sensitivities. In particular, the Axion Dark Matter eXperiment (ADMX), which is the most mature axion haloscope, has already reached into the KSVZ and DFSZ parameter space (under the assumption that axions are the totality of the DM) for masses  $m_a \sim 3\mu\text{eV}$  [299, 430]. A drawback is the slow mass-scanning time, which scales quadratically with the desired signal to noise level,  $\Delta t \propto (S/N)^2$ .<sup>57</sup> Furthermore, the cavity size has to match with great accuracy the axion Compton wavelength. Therefore, scanning higher masses requires smaller cavities with the consequent loss of sensitivity at fixed scanning time (the power of the signal scales linearly with the volume). A recent promising way-out consists in exploring higher order resonant modes [432].

Nevertheless, an intense program to probe the higher mass range is currently in place. The CAPP-8TB haloscope experiment, at IBS/CAPP, is designed to search for axions with mass 6.62 to 7.04  $\mu\text{eV}$ , with enough sensitivity to detect DFSZ or KSVZ axions [433]. Data taking is expected to start already in 2020 [434]. The operations of the more ambitious CAPP-12TB could also start in the 2020s. Its expected sensitivity is shown in Fig. 13.

The HAYSTACK experiment is probing masses about an order of magnitude larger than ADMX and recently reported the first results for a scan in the mass range 23.5 – 24  $\mu\text{eV}$ , with sensitivity down to  $g_{a\gamma} = 2 \times 10^{14} \text{ GeV}^{-1}$  [435]. At considerably higher masses, ORGAN [436] plans to probe the mass region  $\sim 60 - 210\mu\text{eV}$ .

A quite different haloscope concept, MADMAX [437] uses movable booster dielectric disks to enhance the photon signal and, as shown in Fig. 13 and 14, the projected sensitivity ranges from  $\sim 50$  to a few 100  $\mu\text{eV}$  [300]. A similar range of masses could be probed with tunable axion plasma haloscopes [438], which employ the axion coupling to plasmons. The resonance condition is induced by the matching of the axion mass with the plasma frequency and is, therefore, completely uncorrelated with the size of the experiment. Finally, the meV mass range might also become accessible using topological antiferromagnets [439]. The current study predicts enough sensitivity to probe, perhaps in its second stage, DFSZ axions in the 1 – 3 meV mass range.

Differently from the above experiments, the QUAX (QUaerere AXion) experiment [440] aims at detecting axion DM via the axion coupling to electrons. While the Earth moves through the cold axion halo, the coupling to the electron spins would induce spin flips in a magnetized material placed inside a static magnetic field. This effect can be detected using NMR techniques. The experiment aims at the mass range  $m_a \sim 100\mu\text{eV}$ , similar to the range of MADMAX. Recent experimental data [441] excluded the range of couplings  $g_{ae} > 4.9 \times 10^{-10}$  at 95% C.L., for an axion mass of 58  $\mu\text{eV}$ . This first bound is not yet comparable with the stellar constraints discussed in Section 4.2, and is still several orders of magnitude larger than what predicted in DFSZ axion models.

An intriguing proposal to test the axion DM paradigm in a wide mass range,  $\sim 0.2 - 40\mu\text{eV}$ , is through the detection of radio signals from the axion conversion into photons in NS magnetospheres [442]. The NS magnetosphere hosts a very intense magnetic field and a variable plasma frequency. If DM axions do exist, they would convert in such field at the radial distance where the plasma frequency matches the axion mass, and produce an observable flux. The detection potential of current and future radiotelescopes is discussed in [442] and expected to reach enough sensitivity to probe the DFSZ axion parameter region.

Probing lower masses is also quite challenging, requiring larger cavities and magnets. The KLASH (KLoe magnet for Axion Search) experiment aims at the mass region  $\simeq 0.3 - 1\mu\text{eV}$ , just below the ADMX range. According to the preliminary study, KLASH has the potential to probe axion-photon couplings close to the DFSZ benchmarks in the given mass range [294]. Experiments that aim at exploring even lower masses adopt different techniques to avoid the problem, inherent in all cavity searches, of matching the

---

<sup>57</sup>The rate at which a mass range can be scanned is controlled by the Dicke radiometer equation [431]:

$$S/N = \frac{P_a}{P_N} \sqrt{\Delta\nu t} = \frac{P_a}{T_S} \sqrt{\frac{t}{\Delta\nu}}, \quad (239)$$

where  $P_N = \Delta\nu T_S$  is the thermal noise power,  $\Delta\nu$  is the bandwidth and  $T_S$  is the system noise temperature (physical + receiver noise) (cfr., e.g., [38, 373]).

axion wavelength with extremely large cavity sizes. ABRACADABRA (A Broadband/Resonant Approach to Cosmic Axion Detection with an Amplifying B-field Ring Apparatus) uses a toroidal magnet and a pickup loop to detect the variable magnetic flux induced by the oscillating current produced by DM axions in the static (lab) magnetic field. The experiment can operate as a broadband or as a resonant experiment by using an untuned or a tuned magnetometer respectively. The aim is to probe a wide mass region below  $10^{-8}$  eV, with sensitivity to DFSZ axions for masses in the range  $0.1 - 10$  neV (cfr. Figs. 13 and 14). In the first data release, masses between  $10^{-12}$  eV and  $10^{-6}$  eV were explored, with slightly less sensitivity to the axion-photon coupling than CAST [292].

Another ingenious idea to probe low masses is to exploit the axion coupling to the neutron EDM, Eq. (223) [402]. The oscillating axion field generates an oscillating nEDM that can be detected using NMR techniques. The Cosmic Axion Spin Precession Experiment (CASPER), in its Electric version (CASPER-Electric), employs a ferroelectric crystal which posses a large, permanent internal electric field with which the axion field interacts. In phase 2, this experiment is expected to reach the sensitivity necessary to probe QCD axions [443], as shown in purple in Fig. 13 and 14.

CASPER Electric is particularly interesting from the modeling point of view, since it would effectively probe the axion-gluon coupling which, differently to the other couplings, is model independent. A consequence is that, in the case of a signal induced by a QCD axion, it may be possible to infer the (local) axion DM fraction. In fact, the value of  $g_d$  can be inferred, within the QCD uncertainties, from the value of the axion mass (identifiable since it sets the oscillation frequency) and the signal strength is a function only of  $g_d$  and of the (local) axion abundance. This possibility is unique among the axion haloscope experiments.

#### 5.4. Searches for axions produced in the laboratory

Pure laboratory searches are also emerging as powerful options to search for axions. Such methods avoid uncertainties related to the use of natural sources for the axion flux. However, the sensitivities of pure laboratory experiments are currently far from the benchmark QCD axion regions. However, they can test, more generically, the parameter space of ALPs.

One of the most mature experimental strategies to search for ALPs is the Light Shining Through a Wall (LSW) [444]. A powerful photon source, e. g. a laser beam, is used to produce axions, which are then reconverted into photons after crossing a *wall*, opaque to light but not to axions. In both cases, the conversion is induced by a strong laboratory magnetic field. The Any Light Particle Search (ALPS) experiment has probed the mass region  $m_a \lesssim 100 \mu\text{eV}$ , yet only for couplings not competitive with CAST. Its updated version ALPS II (data-taking expected starting from 2021) will surpass CAST and probe unexplored parameter space. However, the sensitivity is expected to be still far from the DFSZ and KSVZ regions and may be of interest for QCD axions only in the case of very photophilic models (see Fig. 14). Currently, the strongest existing limit on the axion-photon coupling using this technique is  $g_{a\gamma} < 3.5 \times 10^{-8} \text{ GeV}^{-1}$  (95% C.L.), for  $m_a \leq 0.3 \text{ meV}$ , achieved by the OSQAR experiment [445]. Similarly, polarization experiments use a laser beam in a strong magnetic field to search for axions or other light particles coupled to photons. The PVLAS experiment has been exploring this possibility for over a decade. The most recent reported constraints on the axion-photon coupling are comparable to the OSQAR bound but extend to slightly higher mass [446]. Some improvement is expected with the Vacuum Magnetic Birefringence experiment (VMB@CERN) [447].

Long range monopole-monopole and dipole-monopole interactions (cfr. Section 2.10), induced by CP-odd couplings, provide other possibilities to search for axions [119]. The CP-odd axion couplings expected in the SM are tiny, as evident from Eq. (128). However, additional contributions are allowed in theories beyond the SM and the current experimental bounds allow for considerably larger values. Long range forces are severely constrained by precision measurements of Newton's law and tests of the equivalence principle (see, e.g., [38] and references therein). A better strategy for axion detection consists in using NMR techniques to detect the axion field sourced by a macroscopic object. This program will be carried out by the ARIADNE experiment [448]. Interestingly, in the most optimistic scenario (largest allowed CP odd couplings), ARIADNE is expected to have enough sensitivity to probe the  $g_{aN}^S g_{an}$  combination of couplings down to values expected for the DFSZ axion [448, 449]. The forecasted sensitivity under these assumptions

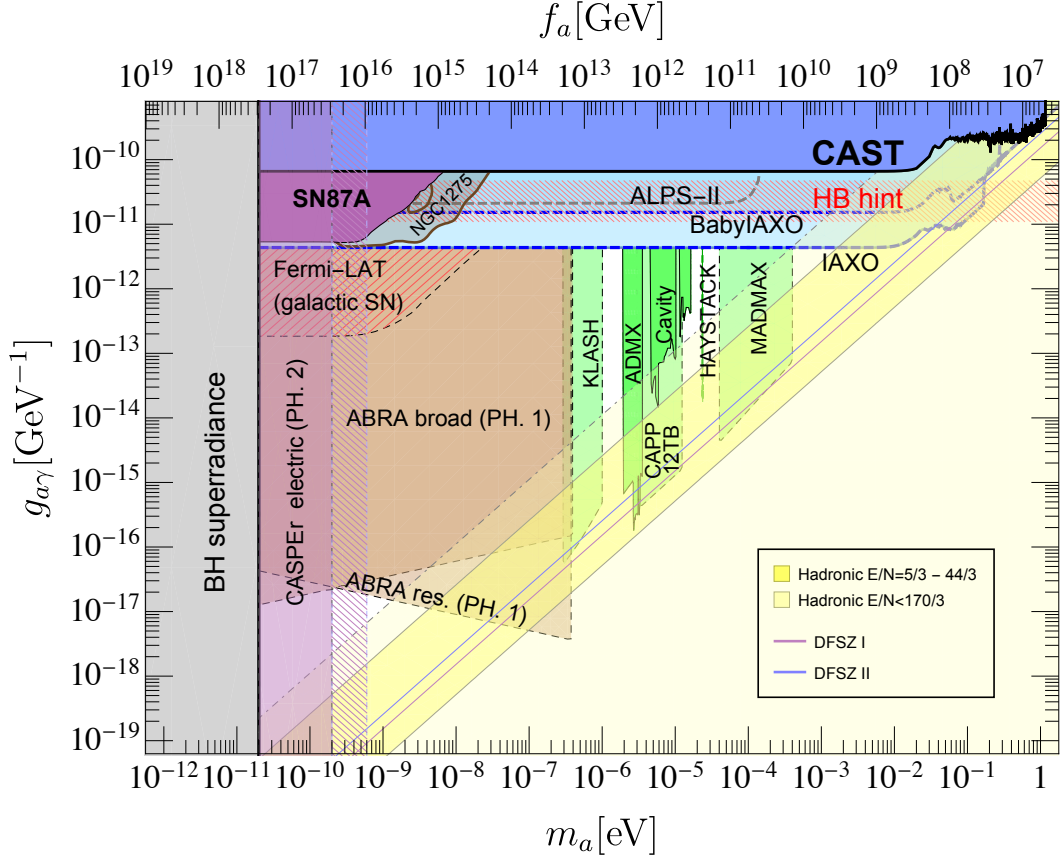


Figure 16: Phenomenological summary of the axion-photon interactions. We show also the region accessible to CASPER electric in phase II, when it will be able to probe the model independent axion coupling to gluons. The hatched region next to it represents the experimental uncertainty induced by the QCD error in the coupling. The region expected for hadronic axions for certain ranges of  $E/N$  is shown in yellow. The relevance of these particular ranges for  $E/N$  is discussed in Section 6. For completeness, we also show the position of the DFSZ I and DFSZ II axions. However, in the case of helioscope the figure does not take into account the possible contribution of  $g_a e$  to the axion production. Refer to Fig. 15 for a more comprehensive analysis of the DFSZ axion models.

is shown in Fig. 15. Standard KSVZ axions are not accessible to ARIADNE, since in that case the coupling to neutrons is vanishingly small.

Somewhat similarly, QUAX- $g_p g_s$  probes the  $g_{aN}^S g_{ae}$  combination. However, even in the most optimistic case, the expected sensitivity is still far from the coupling region expected in the case of KSVZ or DFSZ axions [450].

##### 5.5. Summary of experimental constraints

In this section we summarize the experimental and astrophysical bounds on the individual axion couplings. Table 4 provides a quick reference to the major probes for each coupling. More details can be found in Fig. 16, for what concerns the axion-photon coupling, Fig. 17 for the axion-electron coupling, and Fig. 18 for the axion couplings to protons and neutrons. Notice that, in all cases, we are assuming that the axion solves the strong CP problem. Hence, we show the CASPER electric potential in all cases since the experiment probes the model independent coupling to QCD gluons. However, we are not assuming any specific model and, hence, we are allowing for the couplings to be uncorrelated from the mass. The particular relation between mass and couplings depends on the specific axion model.

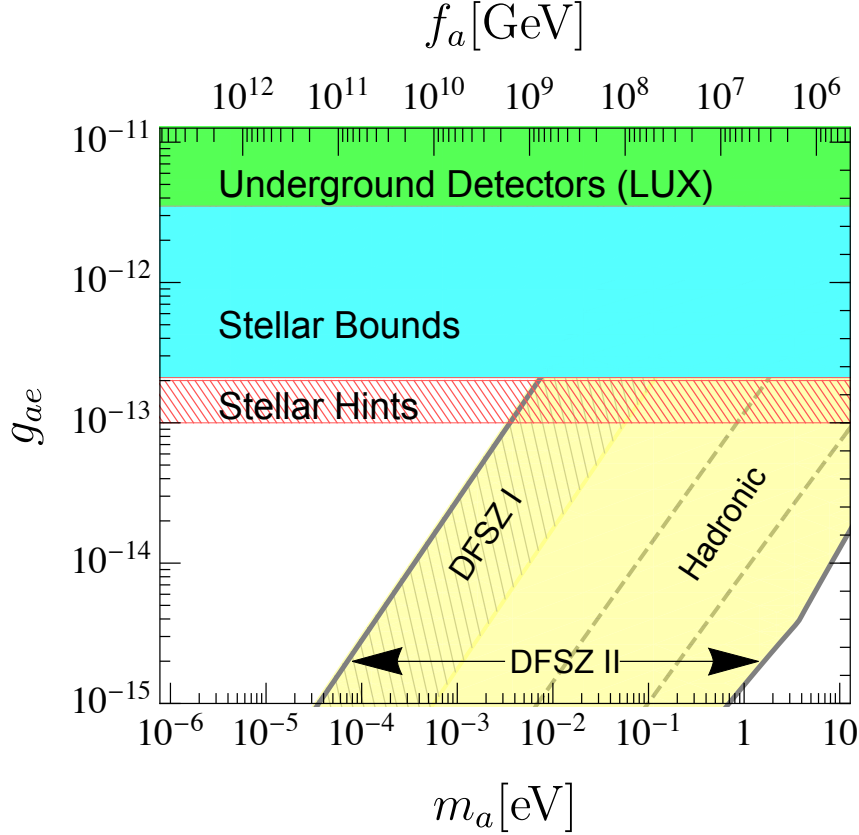


Figure 17: Phenomenological summary of the axion-electron interactions. The hadronic region is estimated for  $E/N$  between  $5/3$  and  $44/3$  (see Section 6). Notice the changing in the slope of the DFSZ II line at high mass. This happens when  $\tan \beta$  is such that the tree level coupling of the DFSZ II axion to electrons is subdominant with respect to the 1-loop contribution.

In the figures, we are showing the parameter space for DFSZ axions (I and II) and for hadronic axions within a specific range of  $E/N$  (cf. Section 6.1.1 and, in particular, Fig. 19). The reader should refer to Section 6 for a discussion of axion models beyond these benchmarks.

As evident from the figures, the axion-photon coupling is by far the most studied. Besides the experiments and bounds discussed in this section, we have added to the figure also the bound from the search for spectral irregularities in the gamma ray spectrum of NGC 1275 [451], from the non-observation of gamma rays from SN 1987A [452] and the Fermi Lat potential in the case of a future galactic SN [453]. Of course, such considerations apply to axions coupled to photons much more strongly than what expected in the benchmark axion models.

The axion-electron coupling is quite more difficult to probe, experimentally. The most efficient way is through helioscopes based on the axio-electric effect, discussed in Section 5.3. However, such experiments are still quite inefficient in the region below the astrophysical bounds. Given the very weak dependence of their potential on volume and observation time, this situation is not likely to change in the near future [38].

The strongest astrophysical constraints on the axion-nucleon coupling are derived from the cooling of NS and from SN 1987A (cf. Section 4.3). Experimentally, the couplings can be probed with NMR techniques. The experimental potential depends on the spin content of the nuclei adopted in the experiment. Our estimates for Fig. 18 are based on the single-particle Schmidt model [454], which predicts that only neutrons contribute to the nuclear spin of  $^3\text{He}$  (adopted in ARIADNE) and  $^{129}\text{Xe}$  (adopted in CASPER wind).<sup>58</sup> Thus,

<sup>58</sup>cf. Table 1 and 4 of Ref. [455].

Coupling	Source	Probes	Notes
$g_{a\gamma}$	Astro	Sun HB-stars SN 1987A	$g_{a\gamma} \leq 2.7 \times 10^{-10} \text{GeV}^{-1}$ for $m_a$ up to a few keV $g_{a\gamma} \leq 0.65 \times 10^{-10} \text{GeV}^{-1}$ for $m_a$ up to a few 10 keV $g_{a\gamma} \lesssim 6 \times 10^{-9} \text{GeV}^{-1}$ for $m_a \lesssim 100$ MeV $g_{a\gamma} \lesssim 5.3 \times 10^{-12} \text{GeV}^{-1}$ for $m_a \lesssim 4.4 \times 10^{-10}$ eV $m_a \sim 2 - 3.5 \mu\text{eV}$ . DFSZ for $m_a \sim 3 \mu\text{eV}$
	Cosmo	ADMX HAYSTACK MADMAX CULTASK KLASH ABRACADABRA  Radio astronomy	$g_{a\gamma} \sim (2 - 3) \times 10^{-10} \text{GeV}^{-1}$ for $m_a \sim (23 - 24) \mu\text{eV}$ DFSZ for $m_a \sim 0.04 - 0.4 \text{meV}$ ( <i>expected</i> ) DFSZ for $m_a \sim 3 - 12 \mu\text{eV}$ ( <i>expected, CAPP 12 T</i> ) $g_{a\gamma} \sim 3 \times 10^{-16} \text{GeV}^{-1}$ for $m_a \sim 0.3 - 1 \mu\text{eV}$ ( <i>expected, Ph. 3</i> ) $m_a \sim 2.5 \times 10^{-15} - 4 \times 10^{-7} \text{eV}$ ( <i>expected</i> ). DFSZ for $m_a \sim 40 - 400 \text{neV}$ ( <i>expected, ABRA res, Ph. 1</i> ) DFSZ for $m_a \sim 0.2 - 20 \mu\text{eV}$ ( <i>expected</i> )
	Sun	CAST BabyIAXO  IAXO	$g_{a\gamma} = 0.66 \times 10^{-10} \text{GeV}^{-1}$ for $m_a \lesssim 20 \text{meV}$ $g_{a\gamma} = 0.15 \times 10^{-10} \text{GeV}^{-1}$ for $m_a \lesssim 10 \text{meV}$ ( <i>expected</i> ) DFSZ for $m_a \sim 60 - 200 \text{meV}$ ( <i>expected</i> ) $g_{a\gamma} = 4.35 \times 10^{-12} \text{GeV}^{-1}$ for $m_a \lesssim 10 \text{meV}$ ( <i>expected</i> ) DFSZ for $m_a \gtrsim 8 \text{meV}$ ( <i>expected</i> )
	Lab	PVLAS OSQAR ALPS II	$10^{-7} \text{GeV}^{-1} \lesssim g_{a\gamma} \lesssim 10^{-6} \text{GeV}^{-1}$ for $m_a \sim 0.5 - 10 \text{meV}$ $g_{a\gamma} \simeq 4 \times 10^{-8} \text{GeV}^{-1}$ for $m_a \lesssim 0.4 \text{meV}$ $g_{a\gamma} \simeq 2 \times 10^{-11} \text{GeV}^{-1}$ for $m_a \lesssim 60 \mu\text{eV}$ ( <i>expected</i> )
$g_{ae}$	Astro	RGB-stars WDs	$g_{ae} \leq 3.1 \times 10^{-13}$ for $m_a$ up to a few 10 keV $g_{ae} \leq 2.1 \times 10^{-13}$ for $m_a$ up to a few keV
	Sun	LUX XENON100 PandaX-II LZ DARWIN	$g_{ae} \leq 3.5 \times 10^{-12}$ $g_{ae} \leq 7.7 \times 10^{-12}$ $g_{ae} \leq 4 \times 10^{-12}$ $g_{ae} \leq 1.5 \times 10^{-12}$ $g_{ae} \leq 1 \times 10^{-12}$
$g_{a\gamma} g_{ae}$	Sun	helioscopes (CAST, LUX,...)	Depends on explicit values of $g_{a\gamma}$ and $g_{ae}$ . Can be extracted from Eq. (235) and Eq. (238)
$g_{an}$	Astro	SN 1987A, NS	$g_{an} \leq 2.8 \times 10^{-10}$ (from NS in HESS J1731-347 )
	Lab	ARIADNE  CASPER wind	measures $g_{aN}^S g_{an}$ down to DFSZ for $m_a \sim 0.25 - 4 \text{meV}$ ( <i>expected for most optimistic choice</i> $g_{aN}^S = 10^{-12} \text{GeV}/f_a$ [448]). From $m_a \simeq 3.6 \times 10^{-12} \text{eV}$ ( $g_{an} \simeq 1.1 \times 10^{-14}$ ) and $m_a \simeq 9.5 \times 10^{-7} \text{eV}$ ( $g_{an} \simeq 5.1 \times 10^{-12}$ ) ( <i>expected, Ph. 2</i> ).
$g_{ap}$	Astro	SN 1987A	$g_{ap} \lesssim 3.3 \times 10^{-9}$ for $g_{an} = 0$ (hadronic axions).
$g_d$	Astro	SN 1987A	$g_d \leq 3 \times 10^{-9} \text{GeV}^{-2}$
	Lab	CASPER electric	QCD axion for $\log(\frac{m_a}{\text{eV}}) \simeq (-9.3 \pm 1.0)$ ( <i>expected, Ph. 2</i> )

Table 4: Summary of astrophysical and experimental probes on the axion couplings. For proposed experiments, in the notes column we indicate the expected mass range and potential, as extracted from the original literature. Whenever necessary, we also indicate the phase (Ph.) during which such results are expected. The haloscope potential reported assumes that the totality of the DM component in the universe is made of axions. Whenever an experiment can probe DFSZ axions, we have indicated the mass range using the sentence “DFSZ for  $m_a \dots$ ”. In the case of CASPER electric, we indicate the mass range in which the experiment may be sensitive to QCD axions. The error indicates the QCD uncertainty.

assuming the Schmidt model, neither ARIADNE nor CASPER wind can probe the axion-proton coupling, implying that they would be blind to, e.g., KSVZ axions. This result is not completely correct. The single-particle Schmidt model does not always reproduce the experimental results well [455]. In particular, in the case of  $^3\text{He}$  there is evidence of a small proton contribution to the nuclear spin [455]. Moreover, recently CASPER-ZULF-Comagnetometer used a mixture of  $^{13}\text{C}$  and  $^1\text{H}$  [456], which allows to access the axion-

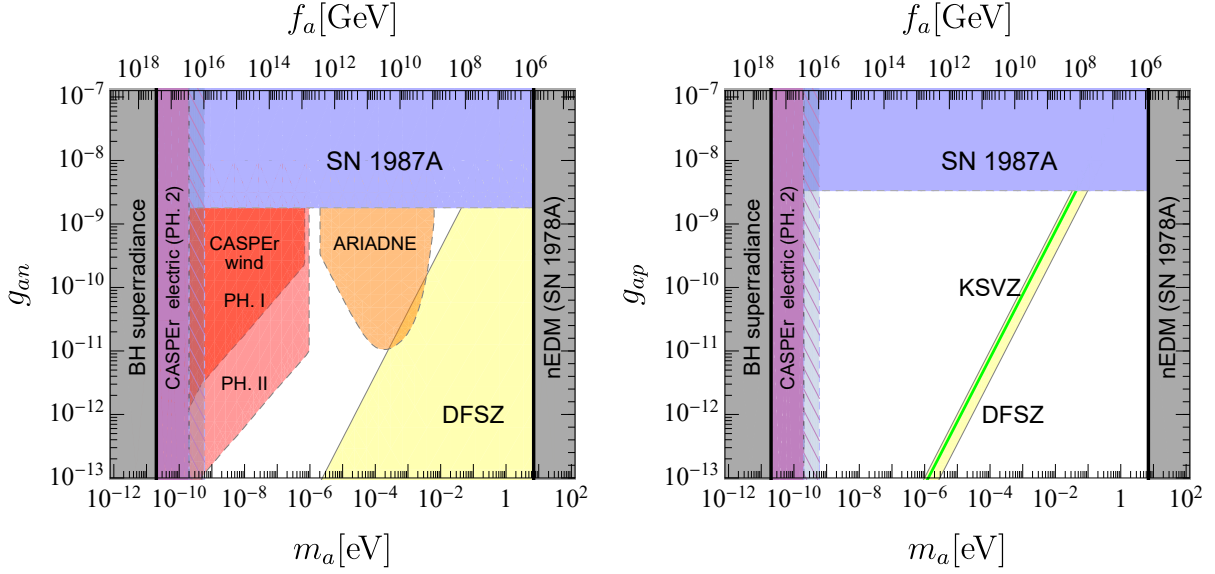


Figure 18: Phenomenological summary of the axion-nucleons interactions. In the case of the ARIADNE experiment, which measures the product  $g_{aN}^S g_{an}$ , the sensitivity is estimated for the most optimistic case of the scalar coupling,  $g_{aN}^S = 10^{-12} \text{ GeV}/f_a$  (see Ref. [448]). Notice that the axion-proton coupling remains largely unexplored. The hadronic axion coupling to neutrons is zero, within the errors [45]. Hence the absence of a KSVZ axion line in the left panel.

proton coupling. At any rate, the axion-proton coupling is significantly less probed experimentally and the current bounds on  $g_{ap}$  are not competitive with the astrophysical constraints.

In this section, we have focussed the attention to a subset of well known laboratory axion experiments, and more in general on experimental axion probes that either have already produced data, or that have passed some crucial step towards their realization, as for example having published a conceptual design report or having obtained funding to develop a R&D phase. In no way we have aimed to a complete review (a more comprehensive account of the experimental panorama, updated to the beginning of 2018, can be found in Ref. [38]). For example, recent results obtained by using superconducting LC circuit techniques at ADMX [457] or from the pathfinding run at the Western Australia haloscope ORGAN [436] have not been included. Most importantly, let us stress that the panorama of different proposals, that in many cases put forth originally new detection techniques, is much wider than what can be guessed from our brief review. To give a taste of the number of existing experimental projects and ideas, and to highlight the intellectual dynamism that permeates the community interested in axion searches, let us mention proposals for new helioscopes (TASTE) [458], or for variant haloscopes (ORPHEUS) [459], (RADES) [460], also including multilayers optical techniques [461] or the possibility of broadband axion searches (BEAST) [462], new LSW based experiments (STAX/NEXT) [463–465], detection techniques based on laser spectroscopy (AXIOMA) [466, 467], methods based on precision magnetometry [448], and on antiferromagnetically doped topological insulators (TOORAD) [439], or even more exotic ideas, like that of a global network of optical magnetometers sensitive to nuclear- and electron-spin couplings, that could reveal transient astrophysical events as the passage trough Earth of axion stars (GNOME) [468].



## 6. The axion landscape beyond benchmarks

Shortly after the KSVZ [111, 112] and DFSZ [109, 110] invisible axion models had been constructed, several variants started to appear in the literature. They were often motivated by the attempt of making more natural the preferred values of the axion decay constant  $10^8 \text{ GeV} \lesssim f_a \lesssim 10^{12} \text{ GeV}$  which does not match neither the electroweak nor the GUT scale, by constructing the axion as a composite state of a new non-abelian gauge interaction [103, 141, 469, 470] that becomes strong at the required scale.<sup>59</sup> At the same time, these constructions implied different properties for the axion, as for example sizeable differences in the strength of the axion coupling to the photon with respect to the KSVZ and DFSZ models. Thus, the idea that the *axion window*, i.e. the region in the  $(m_a, g_{a\gamma})$  plane predicted by QCD axion models could be sizeably larger than what suggested by canonical KSVZ/DFSZ constructions, was already contemplated as a likely possibility by some early phenomenological studies [103, 141, 471]. Recent years have witnessed a proliferation of proposals for axion experiments [37, 38] (see also Section 5) and, although at present all ongoing attempts to detect the axion rely on the axion-photon coupling, a certain number of new proposals, often based on cutting-edge experimental techniques, are also sensitive to the axion couplings to nucleons or electrons. In many cases the projected sensitivity of new proposals does not reach the level required to test the KSVZ and DFSZ models, and this is especially true for first generation experiments which, at least in their initial operational stages, mainly represent a proof-of-concept for the effectiveness of new axion searches techniques. For these experiments it is often understood that the explorable regions would at best test the possible existence of ALPs, that is particles that share some of the properties of the QCD axion, but that are not requested to solve the strong CP problem and, as a consequence, can exist within a much wider parameter space region.

The aim of this section is to carry out a thorough review of past and recent axion models, focussing on their predictions for the axion couplings to photons  $g_{a\gamma}$  (Section 6.1), to electrons  $g_{ae}$  (Section 6.2), to protons  $g_{ap}$  and neutrons  $g_{an}$  (Section 6.3), and their constraints from astrophysics and direct searches (Section 6.4). The highlight of this section is to specify under which conditions the values of these couplings can be either enhanced or suppressed with respect to their canonical values, and in which cases new features, like for example flavour changing axion couplings can emerge (Section 6.5). To classify the large number of possibilities, it turns out to be convenient to maintain a distinction between KSVZ-like and DFSZ-like scenarios. KSVZ-like refers to the class of models in which the SM fermions and the electroweak Higgs fields do not carry PQ charges, the axion-electron coupling vanishes at leading order, and the leading contribution to the axion-nucleon and axion-pion couplings only depends on the anomalous QCD term  $(a/f_a)G\tilde{G}$ . DFSZ-like instead broadly refers to the class of models in which the SM particles are charged under the PQ symmetry so that the couplings between the axion and the SM fermions acquire a contribution proportional to the quarks and leptons PQ charges.

In Section 6.6 we will address the issue of the range of axion masses  $m_a$  for which the axion can account for the whole cosmological density of DM. We will identify different variants in both the particle physics and in the cosmological model that allow to extend the canonical mass range towards smaller or larger values of  $m_a$ .

Finally, in Section 6.7, we will consider mechanisms to modify the  $m_a$ - $f_a$  relation while maintaining the solution of the strong CP problem, thus allowing for  $m_a \gtrsim 100 \text{ keV}$  axions that can avoid most astrophysical constraints.

### 6.1. Enhancing/suppressing $g_{a\gamma}$

In Eq. (59) we have given the general expression for the axion coupling to photons. Including NLO corrections, which were computed in Ref. [45], and using  $m_u/m_d \simeq 0.48(3)$ , one obtains the expression given in Eq. (110) that we repeat below for convenience:

$$g_{a\gamma} = \frac{\alpha}{2\pi f_a} \left[ \frac{E}{N} - 1.92(4) \right]. \quad (240)$$

<sup>59</sup>Composite axions will be the subject of Section 7.6.



We recall that  $E$  and  $N$  are respectively the coefficients of the PQ electromagnetic and colour anomalies whose general expression is given in Eq. (83). The original KSVZ model discussed in Section 2.7.1 adopted the simplest choice in which the QCD anomaly is induced by heavy exotic colored fermions  $\mathcal{Q}$  singlets under  $SU(2)_L \times U(1)_Y$ , so that  $E/N = 0$  and  $g_{a\gamma}$  is solely determined by the model-independent numerical factor “−1.92” that originates from the  $a/f_a G\tilde{G}$  term. This, however, implies that the  $\mathcal{Q}$ -baryon number, associated with the non-anomalous  $U(1)$  symmetry  $\mathcal{Q} \rightarrow e^{i\beta}\mathcal{Q}$ , is exactly conserved (being protected by the gauge symmetry) and hence, after confinement, the  $\mathcal{Q}$ ’s would give rise to stable fractionally charged hadrons which have not been observed [472]. Thus, charged  $\mathcal{Q}$ ’s that could mix with the light quarks and decay, and that would give rise to  $E/N \neq 0$ , should be considered phenomenologically preferred. For the DFSZ models discussed in Section 2.7.2 the SM quarks and leptons charges imply either  $E/N = 8/3$  or  $2/3$  depending on whether the leptons are coupled to the  $d$ -type (DFSZ-I) or to the  $u$ -type (DFSZ-II) Higgs. From Eq. (240) we see that large enhancements of the axion-photon coupling require  $E/N \gg 2$ , while the axion would approximately decouple from the photon if  $E/N \approx 2$ . Below we discuss several cases in which these possibilities can be realised.

### 6.1.1. KSVZ-like scenarios

The model dependence of the axion-photon coupling and the possibilities to arrange for large enhancements or for approximate decoupling, was first discussed by Kaplan in Ref. [103], where a variant of Kim’s composite axion model [470] (see also [473]) was put forth. Since composite axions will be the subject of Section 7.6, here we only provide the essential ingredients to explain the main features of the model. A gauge group factor  $SU(\mathcal{N})$  of metacolor (or axicolor) that becomes strongly interacting at a large scale  $\Lambda \sim f_a$  is added to the SM gauge group  $SU(3)_c \times SU(2)_L \times U(1)_Y$ , together with two multiplets of exotic Dirac fermions  $\psi$  and  $\xi$  that are  $SU(2)_L$  singlets and transform under  $SU(\mathcal{N}) \times SU(3)_c \times U(1)_Y$  as

$$\psi \sim (\mathcal{N}, 3)_{y_1}, \quad \xi \sim (\mathcal{N}, 1)_{y_2}, \quad (241)$$

where  $y_1, y_2$  denote hypercharges. The exotic quarks have no mass terms so that there is a  $U(1)^4$  global symmetry for the kinetic term corresponding to  $U(1)_{B_\psi} \times U(1)_{B_\xi} \times U(1)_{\bar{A}} \times U(1)_A$ . The first two factors are vector-like and correspond to  $\psi$  and  $\xi$  baryon number conservation. The remaining two axial symmetries get spontaneously broken by the condensates  $\langle \bar{\psi}_L \psi_R \rangle = \langle \bar{\xi}_L \xi_R \rangle \neq 0$  resulting in two NGBs that acquire masses due to the anomaly of the corresponding currents with the strongly interacting gauge groups. The current  $\tilde{J}_\mu^5 = \frac{1}{2} (\bar{\psi} \gamma_\mu \gamma_5 \psi + \bar{\xi} \gamma_\mu \gamma_5 \xi)$  has an anomaly with  $SU(\mathcal{N})$  hence the corresponding NGB acquires a large mass of order  $f_a$ . In contrast, the current  $J_\mu^5 = \frac{1}{\sqrt{24}} (\bar{\psi} \gamma_\mu \gamma_5 \psi - 3 \bar{\xi} \gamma_\mu \gamma_5 \xi)$  has only colour and electromagnetic anomalies:

$$\partial^\mu J_\mu^5 = \frac{g_s^2}{16\pi^2} \frac{\mathcal{N}}{2\sqrt{24}} G_{\mu\nu}^a \tilde{G}^{a\mu\nu} + \frac{e^2}{16\pi^2} \frac{3\mathcal{N}(y_2^2 - y_1^2)}{\sqrt{24}} F_{\mu\nu} \tilde{F}^{\mu\nu}, \quad (242)$$

so that the corresponding NGB, which is identified with the axion, acquires a tiny mass  $m_a \sim m_\pi f_\pi (N/f_a)$ . The axion coupling to photons involves the anomaly coefficient ratio  $E/N = 6(y_1^2 - y_2^2)$  and is thus proportional to  $g_{a\gamma} \propto 6(y_1^2 - y_2^2) - 1.92$ . As remarked in Ref. [103], by choosing  $(y_1, y_2) = (0, 1)$  one obtains an enhancement in  $g_{a\gamma}$  of a factor of ten with respect to the DFSZ model with  $E/N = 8/3$ , while  $(y_1, y_2) = (2/3, 1/3)$  give  $E/N - 1.92 = 0.08$  which corresponds to a factor of ten suppression. Although this composite axion model clearly relies on a different construction with respect to KSVZ models with fundamental scalars, it can still be classified as being of the KSVZ-type since the SM states do not carry PQ charges and at the leading order  $g_{ae} = 0$ . Models in which the axion does not couple directly to the leptons are also known as *hadronic* axion models. Note that similar constructions for composite axions always require at least two sets of massless exotic fermions in order to be able to generate a light axion that can solve the QCD  $\theta$  problem, since a single set would give rise to just one heavy axion for which the dominant potential term would drive  $\theta_{\mathcal{N}} \rightarrow 0$  leaving  $\theta$  at a generic  $O(1)$  value (unless an accurate alignment between the two angles is arranged for, see Section 6.7). Taken as a mechanism to enhance or suppress  $g_{a\gamma}$ , composite axion models are not particularly economical since, as we will see, KSVZ models involving two sets of exotic fermions allow for much larger enhancements of  $g_{a\gamma}$  as well as for more accurate cancellations between the two contributions to the coupling. Clearly in the first KSVZ construction the choice of a  $SU(2)_L \times U(1)_Y$

singlet representation for the heavy vector-like quarks  $Q$  represented the simplest possibility. Colour representations with nontrivial electroweak quantum numbers, as in the Kaplan model, would work as well, with the difference that at least some of the heavy quarks would be electrically charged yielding  $E/N \neq 0$ . While in principle any electroweak representation is equally good for implementing the PQ solution, not all are phenomenologically allowed, and only a few are in fact phenomenologically preferred. A systematic attempt of classifying the viable representations  $R_Q = (\mathcal{C}_Q, \mathcal{I}_Q, \mathcal{Y}_Q)$  under the  $SU(3)_c \times SU(2)_L \times U(1)_Y$  gauge group was carried out in Refs. [472, 474]. Four possible phenomenological criteria to classify the representations as *phenomenologically preferred* were identified:

- (i)  $R_Q$  should not induce Landau poles below a scale  $\Lambda_{LP}$  of the order of the Planck scale;
- (ii)  $R_Q$  should not give rise to cosmologically dangerous strongly interacting relics;
- (iii)  $R_Q$ 's yielding domain wall number  $N_{DW} = 1$  are preferred by cosmology;
- (iv) Improving gauge coupling unification can be an added value.

These four criteria have rather different discriminating power. Gauge coupling unification (iv) is a desirable feature for any particle physics model. However, improved gauge coupling unification for some  $R_Q$  might simply occur as an accident because of the many different representations that one can consider, as well as from the freedom in choosing the relevant mass scale  $m_Q$  between a few TeV (from exotic quark searches at the LHC) and  $\Lambda_{GUT}$ . Besides this, from the theoretical point of view envisaging a GUT completion of KSVZ axion models in which only a fragment  $R_Q$  of a complete GUT multiplet receives a mass  $m_Q \lesssim v_a \ll \Lambda_{GUT}$ , as is necessary to assist gauge coupling unification, while all the other fragments acquire GUT-scale masses, is not straightforward, and it appears especially challenging in all the cases in which the PQ symmetry commutes with the GUT gauge group (see Section 7.7 and in particular footnote 76). Difficulties in constructing explicit realisations of  $R_Q$  assisted unification thus suggest that discriminating the  $R_Q$  on the basis of the last property (iv) might be less meaningful than what one would initially guess. Axion models with  $N_{DW} > 1$  face the so called cosmological DW problem [230], while models with  $N_{DW} = 1$  are cosmologically safe [186, 229], hence motivating the criterium (iii) above. However, one can envisage various solutions of the DW problem based either on cosmology or model-building (which are reviewed in Section 7.4). Due to these considerations, in Refs. [472, 474] criteria (iii) ( $N_{DW} = 1$ ) and (iv) (improved gauge coupling unification) were only considered as desirable features of a KSVZ axion model, but not sufficiently discriminating to be used as criteria for identifying possibly pathological  $R_Q$ . The first two conditions are instead quite selective for discriminating among different representations, as it will be reviewed in the following.

(i) *Landau poles* (LP). Large representations can often induce LP in the hypercharge, weak, or strong gauge couplings  $g_1, g_2, g_3$  at some uncomfortably low-energy scale  $\Lambda_{LP} < m_{Pl}$ . In Refs. [472, 474], rather than  $\Lambda_{LP} \sim m_{Pl}$  a more conservative choice  $\Lambda_{LP} \sim 10^{18}$  GeV was made. This was justified by the fact that at energy scales approaching  $m_{Pl}$ , gravitational corrections to the running of the gauge couplings can become relevant, and explicit computations show that they go in the direction of delaying the emergence of LP [475]. Therefore a value of  $\Lambda_{LP}$  for which gravitational corrections are presumably negligible was chosen. The scale at which the LP arises was evaluated by using two-loops gauge beta functions<sup>60</sup> and by setting the threshold for including the  $R_Q$  representations in the running of the gauge couplings at  $m_Q = 5 \cdot 10^{11}$  GeV. By recalling that  $m_Q = y_Q N_{DW} f_a / \sqrt{2}$  (see Section 2.7.1), this value can be justified in post-inflationary scenarios in terms of the cosmological limit on  $f_a$  that follows from the requirement  $\Omega_a \lesssim \Omega_{DM}$ , and in pre-inflationary scenarios by demanding additionally that the initial value of the axion field is not tuned to be much smaller than  $f_a$ .

To see what is the maximum value of the  $g_{a\gamma}$  coupling allowed by the LP condition, one can start by considering a single representation  $R_Q = (\mathcal{C}_Q, \mathcal{I}_Q, \mathcal{Y}_Q)$  and look for the maximum allowed values of the  $E_Q/N_Q$  coupling factor. From Eq. (84) this factor can be written as

$$\frac{E}{N} = \frac{E_Q}{N_Q} = \frac{d(\mathcal{C}_Q)}{T(\mathcal{C}_Q)} \left[ \frac{1}{12} (d(\mathcal{I}_Q)^2 - 1) + \mathcal{Y}_Q^2 \right]. \quad (243)$$

<sup>60</sup>Accidental cancellations in the one-loop gauge beta function for higher-dimensional multiplets can lead indeed to erroneous estimates of the LP (see e.g. [476]).

The minimum value of the denominator is  $T(\mathcal{C}_Q) = \frac{1}{2}$  which corresponds to colour triplets. For a hyperchargless representation the LP condition in  $g_2$  is saturated with a fermion quadruplet  $R_Q(\mathcal{I}_Q^{\max}) = (3, 4, 0)$  while for an  $SU(2)_L$  singlet the LP condition in  $g_1$  is saturated by  $R_Q(\mathcal{Y}_Q^{\max}) = (3, 1, 5/2)$ , where the rational value  $5/2$  is a simple approximation to the real valued result. The maximum allowed hypercharge value  $\mathcal{Y}_Q = \frac{5}{2}$  in turn implies the condition  $\mathcal{Y}_Q \sqrt{d(\mathcal{I}_Q)} \leq \frac{5}{2}$ .  $E/N$  is then maximal for the value of  $d(\mathcal{I}_Q)$  that, within the allowed range  $1 \leq d(\mathcal{I}_Q) \leq 4$ , maximises the expression in square brackets in Eq. (243) subject to this condition, that is, it maximises the function  $d(\mathcal{I}_Q)^2 - 1 + 75/d(\mathcal{I}_Q)$ . The maximum is found for [474]

$$R_Q(\mathcal{Y}_Q^{\max}) = (3, 1, 5/2) \Rightarrow E/N = 75/2. \quad (244)$$

Larger values can be obtained by adding the two representations  $R_Q(\mathcal{Y}_Q^{\max}) \oplus R_Q(\mathcal{I}_Q^{\max})$  to maximise the numerator in Eq. (243) (this saturates the LP limits for  $g_1$  and  $g_2$ ) while the minimal possible value of the denominator  $\sum_Q \mathcal{X}_Q d(\mathcal{I}_Q) T(\mathcal{C}_Q) = \pm 1/2$  can be retained by adding a  $SU(2)_L \times U(1)_Y$  singlet in the adjoint of colour (with index  $T(8) = 3$ ) and with opposite sign of the PQ charge:  $(1 + 4) \times T(3) - T(8) = -1/2$ . In this way one obtains the maximum value of  $E/N$  compatible with the LP condition:

$$(3, 1, 5/2) \oplus (3, 4, 0) \ominus (8, 1, 0) \Rightarrow E/N = -135/2. \quad (245)$$

(Here and below the symbol  $\ominus$  will refer to an irreducible fragment of a reducible representation that has opposite sign of the PQ charge with respect to the other fragments, that is it couples to the Hermitian conjugate of the PQ field as  $y_Q \bar{Q}_L Q_R \Phi^\dagger$  rather than as in Eq. (76).) Equivalent possibilities can be obtained with different representations  $(3, 1, \mathcal{Y}_Q) \oplus (3, 4, \mathcal{Y}_{Q'})$  satisfying  $\mathcal{Y}_Q^2 + 4\mathcal{Y}_{Q'}^2 = (5/2)^2$ , as for example  $(3, 1, 3/2) \oplus (3, 4, 1)$ , etc.

(ii) *Cosmologically dangerous relics.* The transformation properties of  $R_Q$  under the SM gauge group constrain the type of couplings of the  $Q$ 's with SM particles, and in several cases this might result in stable or long-lived anomalously heavy ‘hadrons’. In post-inflationary scenarios this can represent a cosmological issue. In pre-inflationary scenarios instead they would be diluted away by the exponential expansion of the Universe and they would be harmless. Therefore, condition (ii) restricts the viable  $R_Q$  only under the assumption that  $U(1)_{PQ}$  is broken after inflation and that  $m_Q < T_{RH}$ . In this case the  $Q$ 's will attain, via their gauge interactions, a thermal distribution. This provides well defined initial conditions for their cosmological history, which depend only on their mass  $m_Q$  and representation  $R_Q$ .

For some  $R_Q$ , as for example the  $SU(2)_L \times U(1)_Y$  singlets of the original KSVZ model [111, 112] as well as for the three representations in Eq. (245),  $Q$  decays into SM particles are forbidden, and moreover the heavy quarks can only hadronize into fractionally charged hadrons by combining with light SM quarks (see the Appendix in Ref. [474]). These  $Q$ -hadrons must then exist today as stable relics. However, searches for fractionally charged particles in ordinary matter limit their abundance with respect to ordinary nucleons to  $n_Q/n_b \lesssim 10^{-20}$  [477] which is orders of magnitude below any reasonable estimate of the cosmological relic abundance of the  $Q$ 's and of their expected concentration in bulk matter. The set of viable  $R_Q$ 's is then restricted to the much smaller subset that allows for integrally charged or neutral color singlet  $Q$ -hadrons. In this case the limits on the relative abundance  $n_Q/n_b$  are less tight, and whether this type of  $Q$ -hadrons and the corresponding representations can be excluded crucially depends on the estimates of their cosmological abundance  $\Omega_Q$  and on whether they will concentrate in the galactic disc as normal baryons do, or if instead they will dominantly remain in the halo.

Obtaining reliable estimates of  $\Omega_Q$  is a non-trivial task though. At temperatures above the QCD phase transition the  $Q$ 's annihilate as free quarks, the annihilation cross section can be computed perturbatively for any representation with reliable results. One generally assumes a symmetric scenario  $n_Q = n_{\bar{Q}}$  since any asymmetry would eventually quench  $Q\bar{Q}$  annihilation resulting in stronger bounds. In this regime, one obtains that for all masses above a few TeV  $\Omega_Q \gg \Omega_{DM}$ . This would firmly exclude stable  $Q$ 's if it were not for the fact that after confinement,  $Q$ -hadrons can restart annihilating, and quite likely at a faster pace. Obtaining reliable estimates of  $\Omega_Q$  in this non-perturbative regime is a non-trivial task and a general consensus on the final result has not yet been achieved. A cross section typical of inclusive hadronic scattering  $\sigma_{ann} \sim (m_\pi^2 v)^{-1} \sim 30 v^{-1} \text{ mb}$  was assumed in Ref. [478] which can suppress the relic abundance down to  $n_Q/n_b \sim 10^{-11}$ . It was later remarked [479] that the relevant process is exclusive

containing no  $Q$ 's in the final state, and the corresponding cross section was estimated to be smaller by a few orders of magnitude. Ref. [480] suggested that annihilation could be catalysed by the formation of quarkonia-like bound states in the collision of a  $Q$ - and a  $\bar{Q}$ -hadron that, after losing energy and angular momentum, bring the  $Q$ ,  $\bar{Q}$  wavefunctions to overlap. Refs. [481, 482] reconsidered this mechanism arguing that  $\Omega_Q$  could indeed be efficiently reduced to the level that energy density considerations would not be able to exclude stable relics with  $m_Q \lesssim 5 \cdot 10^3$  TeV. Ref. [483] studied this mechanism more quantitatively. They remarked that Refs. [481, 482] did not consider the possible formation of  $QQ\ldots$  bound states which, contrarily to  $Q\bar{Q}$ , would hinder annihilation rather than catalyse it, preserving a sizeable fraction of the original  $Q$ 's in this type of states. Regardless of the fact that a clear picture is still missing, even assuming that  $\Omega_Q$  can be suppressed down to values safely below  $\Omega_{\text{DM}}$ , all estimates suggest that present cosmological concentrations would still be rather large, say at least  $10^{-8} \lesssim n_Q/n_b \lesssim 10^{-6}$ . Of course it can be questioned if relative concentrations of the same order had to be expected also in the Galactic disk [484, 485]. However, searches for anomalously heavy isotopes in terrestrial, lunar, and meteoritic materials, yield limits on  $n_Q/n_b$  many orders of magnitude below the numbers quoted above [486], and moreover even tiny amounts of heavy  $Q$ 's in the interior of celestial bodies (stars, neutron stars, Earth) would produce all sorts of effects like instabilities [487], collapses [488], anomalously large heat flows [489]. Therefore, unless an extremely efficient mechanism exists that keeps  $Q$ -hadrons completely separated from ordinary matter, cosmologically stable heavy relics of this type are excluded implying that, if they exist, they should decay.

As was shown in Ref. [474], for each of the  $R_Q$  considered above (i.e. those that allow for integrally charged or neutral color singlet  $Q$ -hadrons) it is always possible to construct gauge invariant operators of some dimension that can mediate their decay into SM particles. Then the issue is to see which range of lifetimes  $\tau_Q$  can be considered cosmologically safe. This can then be translated into an upper bound on the dimension of the relevant decay operators, given that the larger is the dimension, the longer is the lifetime, the more dangerous is the relic. The allowed values of  $\tau_Q$  are severely constrained by cosmological observations. For  $\tau_Q \sim (10^{-2} \div 10^{12})$  s the decays of superheavy quarks with  $m_Q \gg 1$  TeV would affect BBN [490–493]. Early energy release from heavy particles decays with lifetimes  $\sim (10^6 \div 10^{12})$  s is strongly constrained also by limits on CMB spectral distortions [494–496], while  $Q$ 's decaying around the recombination era ( $t_{\text{rec}} \sim 10^{13}$  s) are tightly constrained by measurements of CMB anisotropies. Decays after recombination would give rise to free-streaming photons visible in the diffuse gamma ray background [497], and tight constraints from Fermi LAT [498] allow to exclude  $\tau_Q \sim (10^{13} \div 10^{26})$  s. Note that these last constraints are also able to exclude lifetimes that are several order of magnitude larger than the age of the Universe,  $t_U \sim 4 \cdot 10^{17}$  s. The conclusion is that for the post-inflationary case cosmologically stable heavy  $Q$ 's with  $m_Q < T_{\text{RH}}$  are strongly disfavoured and likely ruled out, while for unstable  $Q$ 's the lifetime must satisfy  $\tau_Q \lesssim 10^{-2}$  s. Clearly, all  $R_Q$ 's which allow for decays via renormalizable operators easily satisfy this requirement, while for higher-dimensional operators suppressed by  $m_{\text{Pl}}$  only at  $d = 5$  and for  $m_Q \gtrsim 800$  TeV decays can occur sufficiently fast [472]. For  $d = 6$ , even for the largest values compatible with post-inflationary scenarios  $m_Q \sim f_a^{\text{max}} \sim 10^{12}$  GeV decays occur dangerously close to BBN, while operators of  $d = 7$  and higher are always excluded. Table 5 (adpted from Ref. [472]) collects the representations that satisfy both the LP and the cosmological constraints. The largest value  $E/N = 44/3$  is obtained for  $R_8$ , while the weakest coupling is obtained for  $R_3$  giving  $E/N - 1.92 \sim -0.25$ . These two values correspond to the two lines encompassing the green band in Fig. 19. Only the first two representations  $R_1$  and  $R_2$  have  $N_{\text{DW}} = 1$ , while out of all the representations listed in Table 5 only  $R_3 = (3, 2, 1/6)$  is able to improve considerably unification with respect to the SM [499], when a threshold  $m_Q = 2 \times 10^7$  GeV, as suggested by a two-loop analysis [472] is assumed.

With multiple representations sizeably larger values of  $E/N$  can be obtained. Saturating the LP condition using only cosmologically safe representations yields [472].

$$(3, 3, -4/3) \oplus (3, 3, -1/3) \ominus (\bar{6}, 1, -1/3) \quad \Rightarrow \quad E/N = 170/3. \quad (246)$$

which is only about 20% smaller than the value of  $E/N = -135/2$  in Eq. (245) obtained by imposing only the LP condition. This maximum value for the  $g_{a\gamma}$  coupling in KSVZ models is depicted with a dot-dashed line in Fig. 19. For  $f_a > 5 \times 10^{11}$  GeV we forcedly have to assume a pre-inflationary scenario were the

	$R_Q$	$\mathcal{O}_{Qq}$	$\Lambda_{\text{LP}}^{R_Q} [\text{GeV}]$	$E/N$	$N_{\text{DW}}$
$d \leq 4$	$R_1: (3, 1, -\frac{1}{3})$	$\overline{Q}_L d_R$	$9.3 \cdot 10^{38}(g_1)$	2/3	1
	$R_2: (3, 1, +\frac{2}{3})$	$\overline{Q}_L u_R$	$5.4 \cdot 10^{34}(g_1)$	8/3	1
	$R_3: (3, 2, +\frac{1}{6})$	$\overline{Q}_R q_L$	$6.5 \cdot 10^{39}(g_1)$	5/3	2
	$R_4: (3, 2, -\frac{5}{6})$	$\overline{Q}_L d_R H^\dagger$	$4.3 \cdot 10^{27}(g_1)$	17/3	2
	$R_5: (3, 2, +\frac{7}{6})$	$\overline{Q}_L u_R H$	$5.6 \cdot 10^{22}(g_1)$	29/3	2
	$R_6: (3, 3, -\frac{1}{3})$	$\overline{Q}_R q_L H^\dagger$	$5.1 \cdot 10^{30}(g_2)$	14/3	3
	$R_7: (3, 3, +\frac{2}{3})$	$\overline{Q}_R q_L H$	$6.6 \cdot 10^{27}(g_2)$	20/3	3
$d = 5$	$R_8: (3, 3, -\frac{4}{3})$	$\overline{Q}_L d_R H^{\dagger 2}$	$3.5 \cdot 10^{18}(g_1)$	44/3	3
	$R_9: (\overline{6}, 1, -\frac{1}{3})$	$\overline{Q}_L \sigma d_R \cdot G$	$2.3 \cdot 10^{37}(g_1)$	4/15	5
	$R_{10}: (\overline{6}, 1, +\frac{2}{3})$	$\overline{Q}_L \sigma u_R \cdot G$	$5.1 \cdot 10^{30}(g_1)$	16/15	5
	$R_{11}: (\overline{6}, 2, +\frac{1}{6})$	$\overline{Q}_R \sigma q_L \cdot G$	$7.3 \cdot 10^{38}(g_1)$	2/3	10
	$R_{12}: (8, 1, -1)$	$\overline{Q}_L \sigma e_R \cdot G$	$7.6 \cdot 10^{22}(g_1)$	8/3	6
	$R_{13}: (8, 2, -\frac{1}{2})$	$\overline{Q}_R \sigma \ell_L \cdot G$	$6.7 \cdot 10^{27}(g_1)$	4/3	12
	$R_{14}: (15, 1, -\frac{1}{3})$	$\overline{Q}_L \sigma d_R \cdot G$	$8.3 \cdot 10^{21}(g_3)$	1/6	20
	$R_{15}: (15, 1, +\frac{2}{3})$	$\overline{Q}_L \sigma u_R \cdot G$	$7.6 \cdot 10^{21}(g_3)$	2/3	20

Table 5:  $R_Q$  allowing for  $d \leq 4$  and  $d = 5$  decay operators ( $\sigma \cdot G \equiv \sigma_{\mu\nu} G^{\mu\nu}$ ) and yielding the first LP above  $10^{18}$  GeV in the gauge coupling given in parenthesis in the fourth column. The anomaly contribution to  $g_{a\gamma}$  is given in the fifth column, and the DW number in the sixth one. Table adapted from Ref. [472]

condition  $m_Q > T_{\text{RH}}$  could be easily fulfilled. In this case the limit from cosmological considerations does not apply, however, the limit from the LP analysis still holds, so that the bound is only mildly relaxed. The corresponding region lies on the left-hand side of the purple vertical line in Fig. 19 labelled  $f_a > 5 \times 10^{11}$  GeV.

Besides enhancing the axion-photon coupling, more  $R_Q$ 's can also weaken  $g_{a\gamma}$ , and even yield an approximate axion-photon decoupling. This requires an ad hoc choice of  $R_Q$ 's, but no numerical fine tuning. With two  $R_Q$ 's there are three such cases:  $R_6 \oplus R_9$ ;  $R_{10} \oplus R_{12}$  and  $R_4 \oplus R_{13}$  which give respectively  $E_c/N_c = (23/12, 64/33, 41/21) \approx (1.92, 1.94, 1.95)$  so that within theoretical errors even a complete decoupling is possible. In all these cases the axion could be eventually detected only via its coupling to nucleons that in KSVZ scenarios are model-independent, while the coupling to electrons is loop suppressed [102]. Finally, with multiple representations additional possibilities featuring  $N_{\text{DW}} = 1$  open up as for example  $R_{12} \ominus R_9$  or  $R_{12} \ominus R_{10}$  for which  $N = T(8) - T(6) = 3 - 5/2 = 1/2$  coincides with what would be obtained with a single fundamental of  $SU(3)_c$ .

### 6.1.2. DFSZ-like scenarios

As we have seen in Section 2.7.2 in DFSZ-type of models [109, 110] besides the SM-singlet field  $\Phi$ , two or more Higgs doublets  $H_i$  carrying PQ charges are introduced. The SM fermion content is not enlarged, but in general both quarks and leptons carry PQ charges since they are coupled to the Higgs fields. The electromagnetic and colour  $U(1)_{PQ}$  anomalies then depend on the SM fermions gauge quantum numbers as well as on their model dependent PQ charge assignments. Hence, several variants of DFSZ axion models are possible, some of which have been discussed, for instance, in Refs. [471, 506]. For most of these variants the axion-photon coupling remains within the KSVZ regions highlighted in Fig. 19, and only in some specific cases the KSVZ upper limit  $E/N = 170/3$  can be exceeded. We will now review under which conditions this can occur.

Let us assume  $n_H \geq 2$  Higgs doublets  $H_i$  coupled to quarks and leptons via Yukawa interactions, and to the singlet field  $\Phi$  through scalar potential terms. The kinetic term for the scalars carries a  $U(1)^{n_H+1}$  rephasing symmetry that must be explicitly broken to  $U(1)_{PQ} \times U(1)_Y$  so that the anomalous PQ current is unambiguously defined, and to avoid additional Goldstone bosons with couplings too mildly suppressed just



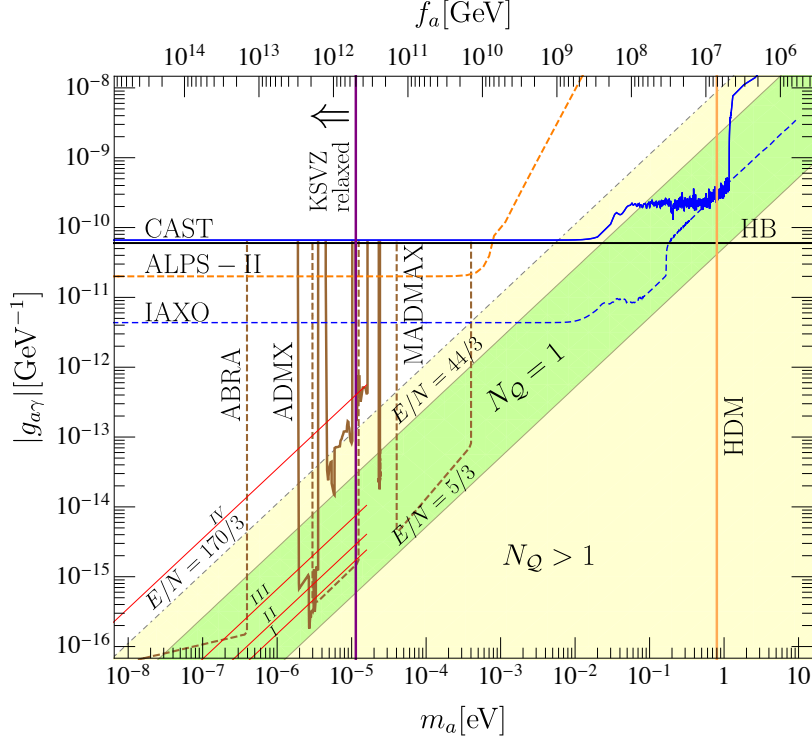


Figure 19: The  $g_{a\gamma}$ - $m_a$  window for preferred axion models. The two lines labeled  $E/N = 44/3$  and  $5/3$  encompass KSVZ models with a single  $R_Q$ , while the region below  $E/N = 170/3$  allows for more  $R_Q$ 's satisfying both the conditions on the absence of LP and of stable relics. The red lines labeled from I to IV (only partially drawn not to clutter the figure) indicate where the DFSZ-type of models lie (see Section 6.1.2). Current exclusion regions are delimited by solid lines. They correspond to the 2017 CAST results [420], to the ADMX limit [296, 373, 500–502], to the constraints from hot DM (HDM) [503] and from horizontal branch (HB) stars [361]. The expected sensitivities for ALPS-II [504], IAXO [373, 422], ADMX [505], MADMAX [300] and ABRACADABRA [291] are depicted with dashed lines. On the left side of the vertical violet line, corresponding to a pre-inflationary PQ breaking scenario, the upper limit on  $E/N$  for KSVZ models can get relaxed (see text).

by the electroweak scale. Renormalizable non-Hermitian monomials involving  $H_i$  and  $\Phi$  are then required to provide an explicit breaking  $U(1)^{n_H+1} \rightarrow U(1)_{PQ} \times U(1)_Y$ . This implies that the PQ charges of all the Higgs doublets, and hence also of the SM fermions, are interrelated and cannot be arbitrarily chosen. To keep the discussion as general as possible let us use a notation in which each fermion bilinear is coupled to a specific scalar doublet, so that  $\mathcal{X}(\bar{u}_{L_j} u_{R_j}) = -\mathcal{X}_{H_{u_j}}$ ,  $\mathcal{X}(\bar{d}_{L_j} d_{R_j}) = -\mathcal{X}_{H_{d_j}}$ ,  $\mathcal{X}(\bar{e}_{L_j} e_{R_j}) = -\mathcal{X}_{H_{e_j}}$  and we have taken the hypercharge of  $H_{d_j, e_j}$  opposite to that of  $H_{u_j}$ . The ratio of anomaly coefficients  $E/N$  can then be written as

$$\frac{E}{N} = \frac{\sum_j \left( \frac{4}{3} \mathcal{X}_{H_{u_j}} + \frac{1}{3} \mathcal{X}_{H_{d_j}} + \mathcal{X}_{H_{e_j}} \right)}{\sum_j \left( \frac{1}{2} \mathcal{X}_{H_{u_j}} + \frac{1}{2} \mathcal{X}_{H_{d_j}} \right)} = \frac{2}{3} + 2 \frac{\sum_j \left( \mathcal{X}_{H_{u_j}} + \mathcal{X}_{H_{e_j}} \right)}{\sum_j \left( \mathcal{X}_{H_{u_j}} + \mathcal{X}_{H_{d_j}} \right)}, \quad (247)$$

where the denominator, being proportional to the PQ-color anomaly, cannot vanish. The results for the two DFSZ models discussed in Section 2.7.2 are recovered from Eq. (247) by dropping the generation index and by setting for DFSZ-I  $H_e = H_d$  which yields  $E/N = 8/3$ , and for DFSZ-II  $H_e = \bar{H}_u$  which yields  $E/N = 2/3$ . In both cases the axion-photon couplings, that correspond to the oblique red lines labeled I and II in Fig. 19, fall inside the  $N_Q = 1$  KSVZ region.

Let us now consider the so called DFSZ-III variant [471] in which the leptons couple to a Higgs doublet  $H_e$  different from  $H_{u,d}$ . In order to enforce the breaking  $U(1)^4 = U(1)_e \times U(1)_u \times U(1)_d \times U(1)_\Phi \rightarrow U(1)_{PQ}$ ,

in the scalar potential the three doublets  $H_e$ ,  $H_u$  and  $H_d$  must be appropriately coupled among them and/or to  $\Phi^2$  or  $\Phi$ . To find which new values of  $E/N$  are allowed in DFSZ-III we follow Ref. [474]. Let us consider the mixed bilinear scalar monomials  $(H_e H_u)$ ,  $(H_e^\dagger H_d)$ ,  $(H_u H_d)$ . It is easy to see that these bilinear terms alone yield for  $E/N$  the same two possibilities obtained for DFSZ-I and II. Combining these bilinears among themselves or with their Hermitian conjugates to build quartic couplings two new possibilities arise:

$$\begin{aligned} (H_e H_u) \cdot (H_u H_d) &\implies \mathcal{X}_{H_e} = -(2\mathcal{X}_{H_u} + \mathcal{X}_{H_d}), & E/N = -4/3, \\ (H_e^\dagger H_d) \cdot (H_u H_d) &\implies \mathcal{X}_{H_e} = \mathcal{X}_{H_u} + 2\mathcal{X}_{H_d}, & E/N = 14/3. \end{aligned}$$

The largest coupling is obtained for the first possibility giving  $g_{a\gamma} \propto E/N - 1.92 \simeq -3.25$ . We see that the largest axion-photon coupling allowed in DFSZ-III still falls within the  $N_Q = 1$  band in Fig. 19.<sup>61</sup>

More possibilities in choosing the PQ charges become possible if we allow for generation dependent PQ charge assignments, a scenario that was already mentioned in Section 2.9 and that will be studied more extensively in Section 6.3. The maximum freedom corresponds to the case in which there are three Higgs doublets for each fermion species ( $H_{e_1}, H_{e_2}, H_{e_3}$ , etc.) so that the scalar rephasing symmetry is  $U(1)^{n_H+1}$  with  $n_H = 9$ , a scenario that was labeled DFSZ-IV in Ref. [474]. Differently from DFSZ-I, II and III, this scenario should not be understood as giving rise to realistic models, since it might be easily plagued by various phenomenological issues. However, it turns out to be useful to consider this construction since bounding from above the maximum possible  $E/N$  in DFSZ-IV automatically provides an upper bound on  $E/N$  for all cases with generation dependent PQ charges and  $2 \leq n_H \leq 9$  Higgs doublets coupled to the SM fermions. For the derivation of this upper bound we refer to Ref. [474], the result is that the maximum possible axion-photon coupling in DFSZ-IV models corresponds to

$$(E/N)_{\max}^{\text{DFSZ-IV}} = 524/3. \quad (248)$$

Although the value in Eq. (248) exceeds by a factor of three the maximum KSVZ value  $E/N = 170/3$  plotted in Fig. 19, the construction through which  $(E/N)_{\max}$  was obtained in Ref. [474] is sufficiently cumbersome to suggest that the  $N_Q > 1$  region in Fig. 19 can still be considered as representative also of most of DFSZ-IV type of models. In DFSZ-IV it is also possible to obtain axion-photon decoupling ensuring at the same time a correct breaking of the global symmetries  $U(1)^{9+1} \rightarrow U(1)_{\text{PQ}} \times U(1)_Y$ . One example is given by:

$$\mathcal{X}_{H_{u_j}} = (2, 4, 8) \mathcal{X}_\Phi, \quad \mathcal{X}_{H_{d_j}} = (0, -2, -4) \mathcal{X}_\Phi, \quad \mathcal{X}_{H_{e_j}} = (-1, -3, -5) \mathcal{X}_\Phi, \quad (249)$$

for which Eq. (247) yields  $E/N = 23/12 \approx 1.92$  and hence  $g_{a\gamma} \approx 0$  (within theoretical errors).

The values of  $E/N$  associated to the maximum and minimum of  $g_{a\gamma}$  for the different classes of models discussed so far are summarised in Table 6. Note that differently from the KSVZ models analysed in Section 6.1.1, the limits on the axion-photon coupling in DFSZ models do not depend on the details of the cosmological evolution of the Universe, and therefore hold also within the region on the left of the violet vertical line labeled  $f_a > 5 \times 10^{11}$  GeV in Fig. 19.

### 6.1.3. Enhancing $g_{a\gamma}$ above the KSVZ and DFSZ benchmarks

The anomalous triangle diagrams responsible for the axion-photon coupling depend on the gauge and global charges of the fermions running in the loops.  $E/N$  can then be boosted either by increasing the contribution of the gauge charges (subject to LP constraints) or by increasing the value of the global charges (not subject to LP constraints). In the previous sections we have given some examples that exploit the former possibility. More elaborated scenarios that rely on the second possibility allow to enhance the axion coupling to photons by much larger (exponentially enhanced) factors, via mechanisms loosely inspired by ‘clockwork’ type of constructions [507–509]. One of such possibilities was put forth in Ref. [510] and is based on a KSVZ type of model. Several singlet scalar fields  $\Phi_k$  ( $k = 0, 1, \dots, n$ ) are introduced, coupled among

<sup>61</sup>Note that the charges of the DFSZ-III variants in Ref. [471] do not allow to build PQ and gauge invariant mixed terms at the renormalizable level. Consequently,  $U(1)^4$  cannot get broken to a single  $U(1)_{\text{PQ}}$ .



	$E/N(g_{a\gamma}^{\max})$	$E/N(g_{a\gamma}^{\min})$
KSVZ ( $N_Q = 1$ )	44/3	5/3
KSVZ ( $N_Q > 1$ )	170/3	23/12
DFSZ-I-II ( $n_H = 2$ )	2/3	8/3
DFSZ-III ( $n_H = 3$ )	-4/3	8/3
DFSZ-IV ( $n_H = 9$ )	524/3	23/12

Table 6: Values of  $E/N$  corresponding to the maximum and minimum values of  $g_{a\gamma}$  for different classes of models. Only KSVZ models that satisfy the first two selection rules (i) and (ii) discussed in Section 6.1.1 are included.

them through non-Hermitian monomials  $\Phi_k^\dagger \Phi_{k+1}^3$  so that only a single global  $U(1)$  remains unbroken, and a charge relation  $\mathcal{X}_{\Phi_k} = 3^{-k} \mathcal{X}_{\Phi_0}$  is enforced. A vector-like representation of coloured quarks is coupled to  $\Phi_n$  while another pair of electromagnetically charged but colour neutral leptons is coupled to a different scalar  $\Phi_p$  with  $p < n$ . Hence the anomaly coefficient ratio  $E/N$  acquires from the ratio between the PQ charges of the coloured/uncoloured fermions an enhancement factor  $3^{n-p}$ . Cosmological constraints on clockwork axions have been analysed in Ref. [511].

A different possibility was proposed in Ref. [474]. This is based on a DFSZ type of construction and, for this reason, has the virtue of exponentially enhance also the axion-electron coupling (see Section 6.2). Let us consider a DFSZ-like scenarios with  $2 + 1 + (n - 1)$  Higgs doublets. The up and down Higgs scalars are coupled to the PQ symmetry breaking singlet through the term  $H_u H_d \Phi^2$  so that the PQ charge for  $H_u$  satisfies the relation  $\mathcal{X}_{H_u} = -2\mathcal{X}_\Phi - \mathcal{X}_{H_d}$ . Let us define  $H_1 = H_u$  and add  $n - 1$  additional scalar doublets  $H_k$  ( $k = 2, 3, \dots, n$ ) with the same hypercharge of  $H_1$  but whose couplings to the SM fermions are forbidden by the PQ symmetry. The additional doublets are coupled among each other via non-Hermitian quadrilinear terms  $(H_k^\dagger H_{k-1})(H_{k-1} H_d)$ , so that a single  $U(1)$  global symmetry survives, while their PQ charges satisfy  $\mathcal{X}_{H_k} = -2^k \mathcal{X}_\Phi - \mathcal{X}_{H_d}$ . Finally, let us couple the lepton Higgs doublet  $H_e$  as  $(H_e H_n)(H_n H_d)$  so that  $\mathcal{X}_{H_e} = 2^{n+1} \mathcal{X}_\Phi + \mathcal{X}_{H_d}$ . Inserting in Eq. (247) the expressions for  $\mathcal{X}_{H_u}$  and  $\mathcal{X}_{H_e}$  we readily obtain:

$$\frac{E}{N} = \frac{8}{3} - 2^{n+1}. \quad (250)$$

Since even in the most conservative case of doublets with electroweak scale masses,  $n$  can be as large as fifty before a LP is hit below the Planck scale, it is always possible to obtain exponentially large axion-photon couplings.

Other possibilities for large enhancement of  $g_{a\gamma}$  exist. Some examples that are qualitatively different from the ones sketched above can be found in Ref. [512].

## 6.2. Enhancing/suppressing $g_{ae}$

As discussed in Section 4.2, the axion-electron coupling  $g_{ae}$  can activate different processes that alter stellar evolution and that are particularly significant in the white dwarf and red giant evolutionary stages. The corresponding astrophysical bounds have been reviewed in Section 4.2. Although they are remarkably strong, translating them into constraints on fundamental parameters as the axion decay constant or the axion mass should be done with care, because the relation between  $g_{ae}$  and  $f_a$  (or  $m_a$ ) depends crucially on the specific model (cf. Eq. (114) for its general expression). For example, in the KSVZ scenarios electrons do not carry a PQ charge, and hence they couple to the axion only through a photon-electron loop generated by the axion-photon coupling, so that the resulting  $g_{ae}$  is loop suppressed and tiny (see Eq. (69)). For this reason astrophysical limits on  $g_{ae}$  provide only weak constraints on KSVZ models (cf. also Fig. 11).

### 6.2.1. Enhancing $g_{ae}$ in KSVZ-like scenarios

Large enhancements with respect to conventional KSVZ scenarios can be straightforwardly obtained by recalling that while in the original model  $E/N = 0$ , models that involve non-trivial heavy quarks representations like the ones discussed in Section 6.1.1, can yield particularly large  $E/N$  factors (see Table 5). In this

case  $g_{ae}$  gets enhanced by the same factor that enhances  $g_{a\gamma}$ . In another class of KSVZ models the one-loop induced axion-electron coupling can get an extra contribution from loops involving new particles. This is what happens for example in type-I seesaw scenarios for neutrino masses in which the heavy RH neutrinos  $N_R$  obtain their mass  $M_R$  from a coupling  $N_R N_R \Phi$  to the PQ symmetry breaking scalar singlet  $\Phi$ . These models are soundly motivated by the fact that the seesaw and the PQ symmetry breaking scales naturally fall in the same intermediate range  $M_R \sim f_a \sim 10^9 \div 10^{12}$  GeV so that an identification seems natural (see also Section 7.1). In this case, in order to acquire their mass, the RH neutrinos must carry a PQ charge, and their couplings to the axion give rise to new loops [513–515] that can enhance the axion-electron coupling by up to one or two orders of magnitude with respect to conventional hadronic axion models, see for example Refs. [136, 283, 513].

### 6.2.2. Enhancing $g_{ae}$ in DFSZ-like scenarios

In DFSZ scenarios the axion-electron coupling arises at the tree level and hence the astrophysical limits on  $g_{ae}$  are more effective in providing tight constraints on the fundamental axion parameters. Clearly, in the DFSZ variants reviewed in Section 6.1.2 in which  $g_{a\gamma}$  gets enhanced via an  $E/N$  value that is boosted by a large PQ electron charge, also  $g_{ae}$  is accordingly enhanced. However, defining correctly the coupling of electrons to the *physical* axion involves some subtleties. Let us consider for example the DFSZ construction with  $2 + 1 + (n - 1)$  Higgs doublets outlined in Section 6.1.3 that produces an exponential enhancement in  $E/N$ , see Eq. (250). The physical axion is identified by imposing the orthogonality condition between the PQ and hypercharge currents  $J_\mu^{\text{PQ}}|_a = \sum_i \mathcal{X}_i v_i \partial_\mu a_i$  and  $J_\mu^Y|_a = \sum_i Y_i v_i \partial_\mu a_i$ , where the sum runs over all the scalars  $\{\Phi, H_u, H_d, H_e, H_{k \geq 2}\}$ ,  $a_i$  are the scalar (neutral) orbital modes, and  $v_i$  are the corresponding VEVs. Note that since  $H_{u,d,e}$  need to pick-up a VEV to generate masses for the fermions, even in the case that all the  $H_{k \geq 2}$  have positive mass squared terms, non-vanishing  $v_{k \geq 2} \neq 0$  unavoidably arise because of the potential terms  $(H_k^\dagger H_{k-1})(H_{k-1} H_d)$  in which they appear linearly. The size of these VEVs is controlled by the size of the quadrilinear coupling constant, hence it is natural to expect  $v_k < v_u$  with a size that decreases with increasing  $k$ . To proceed, it is convenient to express the PQ charges  $\mathcal{X}_{H_d}, \mathcal{X}_{H_u}$ , and  $\mathcal{X}_{H_k}$  in terms of  $\mathcal{X}_{H_e}$  and  $\mathcal{X}_\Phi$  by using the relations given above Eq. (250) as

$$\mathcal{X}_{H_d} = \mathcal{X}_{H_e} - 2^{n+1} \mathcal{X}_\Phi, \quad \mathcal{X}_{H_k} = -\mathcal{X}_{H_e} + (2^{n+1} - 2^k) \mathcal{X}_\Phi, \quad (251)$$

where again we have defined  $H_u = H_1$ . Recalling that  $Y(H_e) = Y(H_d) = -Y(H_k) = \frac{1}{2}$  the orthogonality condition can be written as:

$$\sum_i 2Y_i \mathcal{X}_i v_i^2 = \mathcal{X}_{H_e} v^2 - \mathcal{X}_\Phi \left( 2^{n+1} v_d^2 + \sum_{k=1}^n (2^{n+1} - 2^k) v_k^2 \right) = 0, \quad (252)$$

where  $v^2 = v_e^2 + v_d^2 + \sum_{k=1}^n v_k^2$  is the electroweak VEV. The resulting PQ charge of the electron is:

$$\mathcal{X}_{H_e} = \frac{\mathcal{X}_\Phi}{v^2} \left( 2^{n+1} v_d^2 + \sum_{k=1}^n (2^{n+1} - 2^k) v_k^2 \right), \quad (253)$$

and the axion-electron coupling can be written as

$$g_{ae} = \frac{\mathcal{X}_{H_e}}{2N} \frac{m_e}{f_a} = -2^{n+1} \frac{m_e}{6f_a} \left[ \frac{v_d^2}{v^2} + \sum_{k=1}^n \left( 1 - \frac{1}{2^{n+1-k}} \right) \frac{v_k^2}{v^2} \right], \quad (254)$$

where we have used  $2N = 3(\mathcal{X}_{H_u} + \mathcal{X}_{H_d}) = -6\mathcal{X}_\Phi$ . For large  $n$  the size of  $g_{ae}$  is bounded from below by

$$|g_{ae}| \gtrsim 2^{n+1} \left( \frac{v_u^2}{v^2} + \frac{v_d^2}{v^2} \right) \frac{m_e}{6f_a}, \quad (255)$$

where the inequality is saturated when all the  $v_{k \geq 2}$  are negligible. Hence the axion coupling to the electrons is always exponentially enhanced.<sup>62</sup>

<sup>62</sup>Only for  $v_e = v$  one could have  $g_{ae} \rightarrow 0$ . However, the sum of the VEV ratios in Eq. (255) is bounded by the perturbativity of the top Yukawa coupling to be  $\gtrsim 0.1$ .

### 6.2.3. Suppressing $g_{ae}$ in DFSZ-like scenarios: the electrophobic axion

A more intriguing possibility within DFSZ-type of models is that of decoupling the axion from the electrons, especially if this could be done consistently with the conditions that enforce nucleophobia. In fact, in this case all the most stringent astrophysical limits would evaporate. Such an axion would be appropriately defined as *astrophobic* [516]. One might think that in order to decouple the electron from the axion it would be sufficient to introduce a third (leptonic) Higgs doublet neutral under the PQ symmetry, so that the leptons would not carry PQ charges either. However, perhaps a bit unexpectedly, this can work only for a few specific values of the VEVs ratios of the two hadronic Higgs [115]. To see this let us consider a model with three-Higgs doublets, that is now convenient to define having the same hypercharge, wherein  $H_{1,2}$  couple to quarks while  $H_3$  couples to the leptons. We need to require that the four  $U(1)$  rephasing symmetries of the kinetic term of the three scalar doublets  $H_{1,2,3}$  and of the PQ symmetry breaking field  $\Phi$  are broken by renormalizable potential terms so that  $U(1)^4 \rightarrow U(1)_Y \times U(1)_{PQ}$ . This can be done either by coupling the leptonic Higgs doublet  $H_3$  to both hadronic Higgses ( $H_{1,2}$ ), or by coupling one of the two hadronic Higgses to the other two doublets:

$$H_3^\dagger H_1 \Phi^m + H_3^\dagger H_2 \Phi^n \quad \text{or} \quad H_3^\dagger H_{1,2} \Phi^m + H_2^\dagger H_1 \Phi^n. \quad (256)$$

For renormalizable operators one has, without loss of generality,  $m = 1, 2$  and  $n = \pm 1, \pm 2$ , with the convention that negative values of  $n$  mean Hermitian conjugation  $\Phi^n \equiv (\Phi^\dagger)^{|n|}$ . This implies certain conditions for the PQ charges of the scalar, for example for the first pair of operators we have

$$-\mathcal{X}_3 + \mathcal{X}_1 + m = 0, \quad -\mathcal{X}_3 + \mathcal{X}_2 + n = 0, \quad (257)$$

where for simplicity we have set  $\mathcal{X}_\phi = 1$ . Similar relations hold if the second pair of operators in Eq. (256) is chosen. Besides these two conditions, orthogonality between the physical axion and the Goldstone boson of hypercharge implies:

$$\mathcal{X}_1 v_1^2 + \mathcal{X}_2 v_2^2 + \mathcal{X}_3 v_3^2 = 0. \quad (258)$$

To see under which conditions the leptons can be decoupled from the axion, let us set  $\mathcal{X}_3 \rightarrow 0$ . We obtain

$$\tan^2 \beta \equiv \frac{v_2^2}{v_1^2} = -\frac{\mathcal{X}_1}{\mathcal{X}_2} = -\frac{m}{n}, \quad (259)$$

so that with the constraints in Eq. (257),  $\mathcal{X}_3 \approx 0$  can be consistently enforced only for  $\tan^2 \beta \approx \frac{1}{2}, 1, 2$ . It can be verified that in the other two cases in Eq. (256)  $\tan \beta = 1$  is the only possibility. As it was remarked in Ref. [115], it is intriguing that the condition for nucleophobia Eq. (267) which, as we have seen in Section 6.3.2, requires  $\tan^2 \beta \approx \frac{m_d}{m_u} \approx 2$ , is consistent with one of the  $\tan \beta$  values that can enforce electrophobia or, said in another way, it is consistent with a suitable set of operators involving the three Higgs doublets, namely  $H_3^\dagger H_1 \Phi^2 + H_3^\dagger H_2 \Phi^\dagger$ .

### 6.3. Enhancing/suppressing $g_{aN}$

The defining property of axions is that they couple to gluons via the anomalous term, and hence they should couple as well to the nucleons  $N = n, p$ . In fact, from the model building point of view it is much more difficult to arrange for strong enhancements/suppressions of the axion-nucleon coupling  $g_{aN}$  than it is for  $g_{a\gamma}$  and  $g_{ae}$ . Nevertheless, a handful of working mechanisms has been put forth, and will be reviewed in this section. Of special interest is the possibility of approximate axion-nucleon decoupling, that will be reviewed in Section 6.3.2, because in this case the tightest constraints on  $f_a$  and  $m_a$ , inferred from astrophysical bounds on  $g_{aN}$  by assuming a conventional axion model, see Section 4.3, would be accordingly relaxed, and regions in the  $g_{a\gamma} - m_a$  plane that are generally considered excluded, would become allowed and thus worthwhile to be explored experimentally.

### 6.3.1. Enhancing $g_{aN}$

A possible way to enhance the axion coupling to nucleons is discussed in Ref. [517]. The idea is to uncorrelate the axion-nucleon coupling from the axion mass by assigning  $U(1)_{\text{PQ}}$  charges to SM quarks such that the latter do not contribute to the QCD anomaly. Effective dimension five operators are introduced that couple the axion multiplet  $\Phi$  to the light quarks and to the corresponding Higgs. Upon PQ symmetry breaking these terms give rise to the quark Yukawa couplings which, however, also involve the axion through a term  $e^{-ia/f}$ , where  $f$  is the  $U(1)$  symmetry breaking order parameter. As usual, by reabsorbing the axion via a quark field redefinition, derivative axion couplings are generated from the kinetic terms, and eventually an axion-nucleon interaction

$$\frac{\partial_\mu a}{f} \bar{N} \gamma^\mu \gamma_5 N \quad (260)$$

suppressed by the scale  $f$  results. The QCD anomaly of the PQ current is due instead to heavy vector-like fermions  $Q$  that couple to a scalar  $\Phi_k$  whose PQ charge is related to the charge of  $\Phi$  as  $\mathcal{X}_k = 3^{-k} \mathcal{X}_\Phi$ , as the result of a clockwork-type of potential  $\sum_j \Phi_j^\dagger \Phi_{j+1}^3 + \text{h.c.}$  (see Section 6.1.3). Hence the anomalous term reads

$$\frac{a}{3^k f} \frac{\alpha_s}{8\pi} G\tilde{G}, \quad (261)$$

where the factor  $3^k$  in the denominator is due to the exponential suppression of the heavy quarks PQ charges  $\mathcal{X}_Q \sim 3^{-k}$ . The axion decay constant is thus defined as  $f_a = 3^k f$ , so that the axion couplings to the nucleons in Eq. (260) is exponentially enhanced with respect to the usual  $1/f_a$  scaling.

A different, and possibly simpler way to exponentially enhance  $g_{aN}$  was recently proposed in [518]. It relies on clockworking directly a set of Higgs doublets in a DFSZ-type of construction. Let us take  $n+1$  doublets with hypercharge  $Y = -\frac{1}{2}$  and let us consider the following scalar terms:

$$H_0^\dagger H_1 \Phi^2, \quad \sum_{k=2}^n \left( H_{k-1}^\dagger H_k \right) \left( H_{k-1}^\dagger H_0 \right). \quad (262)$$

It is easy to verify the charge relation  $\mathcal{X}_k = \mathcal{X}_0 + 2^k \mathcal{X}_\Phi$  so that  $\mathcal{X}_n$  gets exponentially enhanced. Consider now the following generation dependent quark couplings:

$$\left( \bar{u}_{1L} u_{1R} H_n + \bar{d}_{1L} d_{1R} \tilde{H}_0 \right) + \left( \bar{u}_{2L} u_{2R} H_0 + \bar{d}_{2L} d_{2R} \tilde{H}_n \right) + \left( \bar{u}_{3L} u_{3R} H_1 + \bar{d}_{3L} d_{3R} \tilde{H}_0 \right), \quad (263)$$

where  $\tilde{H} = i\sigma_2 H^*$ . All CKM mixings can be generated by adding for example  $(\bar{u}_{2L} u_{1R} H_1) + (\bar{u}_{3L} u_{1R} H_n)$  together with all the additional terms consistent with the charge assignments implied by these two terms plus the terms in Eq. (263). The anomalies of the first two generations that contain the Higgs multiplet  $H_n$  with the ‘large charge’ cancel each other, so that the QCD (and QED) anomaly coefficient is determined only by the third generation:

$$2N = (\mathcal{X}_{u_{3R}} - \mathcal{X}_{u_{3L}}) + (\mathcal{X}_{d_{3R}} - \mathcal{X}_{d_{3L}}) = -\mathcal{X}_{H_1} + \mathcal{X}_{H_0} = 2\mathcal{X}_\Phi. \quad (264)$$

As a result, the axion coupling to the light up-quark gets exponentially enhanced as

$$c_{u1}^0 = \frac{-\mathcal{X}_{u_{1L}} + \mathcal{X}_{u_{1R}}}{2N} \approx 2^{n-1}, \quad (265)$$

which in turn gives rise to an exponentially enhanced  $g_{aN}$ , see Eqs. (66)–(67), while the axion-photon coupling  $g_{a\gamma}$  remains of standard size.

### 6.3.2. Suppressing $g_{aN}$ : the nucleophobic axion

Arranging for a strong suppressions of the axion-nucleon coupling  $g_{aN}$  is difficult. In KSVZ models in which the SM fermions do not carry PQ charges this is not possible, because  $g_{aN}$  remains determined by a

model-independent contribution that is induced by the axion coupling to the gluon fields. In DFSZ models the pathways to enforce  $g_{aN} \approx 0$  must comply with tight theoretical constraints. For example, a necessary (but not sufficient) condition is that the PQ-colour anomaly is only determined by the light quarks, that is, either the two heavier generations are not charged under PQ, or they have cancelling anomalies [516]. This unavoidably requires generation dependent axion couplings to the quarks, which in turn implies that nucleophobic axions are mediators of flavour changing interactions, see Section 6.5. An early study in the direction of suppressing  $g_{aN}$  was presented in Ref. [519], where some phenomenological aspects connected to nucleophobic axions were investigated, with the notable exception of SN1987A related limits, given that the Supernova explosion occurred only a few months before the completion of that paper. In another early reference [520] a class of models in which the axion couples to a single quark was studied, and it was found that when the coupling is only to the light up-quark it was possible to engineer for a strong suppression of  $g_{aN}$ . Clearly this is in agreement with the condition that to obtain  $g_{aN} \approx 0$  only the light quark generation is allowed to contribute to the PQ anomaly. More recently, a dedicated study of the various possibilities for constructing nucleophobic axion models was presented in Ref. [516]. We will now review the main results following this reference.

To identify which conditions must be satisfied to suppress both axion couplings to protons and neutrons it is convenient to recast Eq. (66) and Eq. (67) into the following isospin conserving and isospin violating linear combinations:

$$C_{ap} + C_{an} = (c_u^0 + c_d^0 - 1) (\Delta u + \Delta d) - 2C_{a,\text{sea}}, \quad (266)$$

$$C_{ap} - C_{an} = (c_u^0 - c_d^0 - f_{ud}) (\Delta u - \Delta d), \quad (267)$$

where we have defined  $f_{ud} = \frac{m_d - m_u}{m_d + m_u} \approx \frac{1}{3}$ . The last term in Eq. (266) accounts for the contribution to the nucleon couplings of the sea quarks, that has been neglected in the treatment of Section 2.5.4 (but included in the full expressions for the couplings Eqs. (111)–(112)) and that cancels out in Eq. (267). The leading contribution comes from the strange quark  $C_{a,\text{sea}} = 0.038 c_s^0 + \dots$ , and the overall value of the correction is less than 10% of the contribution of the valence quarks.<sup>63</sup> The (approximate) vanishing of Eqs. (266)–(267) can then be taken as the defining condition for the nucleophobic axion. Note, also, that since the axion-pion coupling  $C_{a\pi}$  is proportional to  $C_{ap} - C_{an}$ , see Eq. (58), nucleophobic axions are also pionphobic. In variant DFSZ models with two Higgs doublets  $H_{1,2}$  and non-universal PQ charge assignment [516] both conditions  $C_{ap} \pm C_{an} \approx 0$  can be realised [516]. To see this, let us focus on the first generation Yukawa terms

$$\bar{q}_{1L} u_{1R} H_1 + \bar{q}_{1L} d_{1R} \tilde{H}_2. \quad (268)$$

Neglecting the effects of flavour mixing, which are assumed to be small throughout this Section,<sup>64</sup> the axion couplings to the light quark fields are (cf. Eq. (75) for their UV origin in terms of PQ charges)

$$c_u^0 = \frac{1}{2N} (\mathcal{X}_{u_1} - \mathcal{X}_{q_1}) = -\frac{\mathcal{X}_1}{2N}, \quad (269)$$

$$c_d^0 = \frac{1}{2N} (\mathcal{X}_{d_1} - \mathcal{X}_{q_1}) = \frac{\mathcal{X}_2}{2N}. \quad (270)$$

Here  $\mathcal{X}_{u_1} = \mathcal{X}(u_1)$ , etc. denote the PQ charges of the fermion fields while  $\mathcal{X}_{1,2} = \mathcal{X}(H_{1,2})$ . The coefficient of the PQ colour anomaly is then

$$2N = \sum_{i=1}^3 (\mathcal{X}_{u_i} + \mathcal{X}_{d_i} - 2\mathcal{X}_{q_i}), \quad (271)$$

<sup>63</sup>Unless otherwise noticed, it is understood that axion-nucleon decoupling will refer to a suppression of  $\approx 10\%$  level compared to conventional KSVZ-like couplings.

<sup>64</sup>In the presence of flavour mixing,  $c_{u,d}^0 \rightarrow c_{u,d}^0 + \Delta c_{u,d}^0$ , where  $\Delta c_{u,d}^0$  involves quark mass diagonalization matrices. These effects will be discussed in Section 6.5, see also Ref. [516].

while the contribution to the colour anomaly from light quarks only can be written as:

$$2N_\ell = \mathcal{X}_{u_1} + \mathcal{X}_{d_1} - 2\mathcal{X}_{q_1} = \mathcal{X}_2 - \mathcal{X}_1. \quad (272)$$

Hence, the first condition for ensuring approximate nucleophobia reads (cf. Eq. (266))

$$c_u^0 + c_d^0 = \frac{N_\ell}{N} = 1. \quad (273)$$

This neatly shows that only models in which the color anomaly is determined solely by the light  $u, d$  quarks have a chance to be nucleophobic. This can be realised in two ways:

- (i) either the contributions of the two heavier generations vanish identically ( $N_2 = N_3 = 0$ );
- (ii) or they cancel each other ( $N_2 = -N_3$  and  $N_\ell = N_1$ ).

Assuming only two Higgs doublets, the first possibility can be easily realised by taking one Higgs doublet (say  $H_1$ ) with a vanishing PQ

The first possibility was for example realised in a scenario in which the axion couples only to the up quark [520] (see also [521]) so that  $2N = 2N_\ell$  is a straightforward result. Alternative possibilities in which the PQ charges for the two heavier generations are non-trivial were found in Ref. [522]. In the attempt of looking for connections between PQ symmetries and the quark flavour puzzle, with the aim of building predictive scenario for the quark masses and mixings, the authors of this last reference studied which PQ symmetries could force the vanishing of a certain number of entries in the Yukawa matrices, in such a way that a maximal parameter reduction consistent with observations is enforced.<sup>65</sup> Serendipitously, it was found that two specific PQ symmetries able to enforce maximal parameter reduction were also characterised by peculiar cancellations among the PQ charges of the heavier quarks resulting in  $N_2 = N_3 = 0$ .

The second possibility with non-vanishing anomaly coefficients for the heavier generations was thoroughly explored in Ref. [516].<sup>66</sup> With just two Higgs doublets, in order to have all three quark generations with different charges, some of the SM Yukawa operators are necessarily forbidden, so that zero textures are present in the quarks mass matrices [522]. In contrast, by imposing that the PQ symmetry does not forbid any of the SM Yukawa operators, then two quark generations must have the same charges, so that for example  $N_1 = N_2 = -N_3$ . The PQ charge assignments that satisfy this condition, and that can thus be compatible with nucleophobia, were classified in Ref. [516].

As regards the second condition, to enforce  $C_{ap} - C_{an} \approx 0$  in Eq. (267) we need  $c_u^0 - c_d^0 = f_{ud}$  where a value  $f_{ud} = \frac{m_d - m_u}{m_d + m_u} \approx \frac{1}{3}$  corresponds to  $\frac{m_d}{m_u} \approx 2$ . Let us denote by  $\tan \beta = v_2/v_1$  the ratio of the VEVs of  $H_{1,2}$ , and introduce the shorthand notation  $s_\beta = \sin \beta$ ,  $c_\beta = \cos \beta$ . The ratio  $\mathcal{X}_1/\mathcal{X}_2 = -\tan^2 \beta$  is fixed by the requirement that the PQ Goldstone boson is orthogonal to the Goldstone eaten up by the  $Z$ -boson, as in the standard DFSZ axion model (cf. Section 2.7.2). Labelling as  $H_1$  the Higgs doublet that couples to the up and charm quarks and considering the case in which all the generations have a non-vanishing anomaly but there is a cancellation  $N_2 + N_3 = 0$ . The anomaly coefficient of the light quarks can be written as  $2N_\ell = \mathcal{X}_2 - \mathcal{X}_1$ , and from this we obtain  $c_u^0 - c_d^0 = -\frac{1}{2N}(\mathcal{X}_1 + \mathcal{X}_2) = s_\beta^2 - c_\beta^2$ . The second condition for nucleophobia that requires  $c_u^0 - c_d^0 = f_{ud}$  is then realised for  $s_\beta^2 \approx 2/3$  that is  $\tan^2 \beta = \frac{m_d}{m_u} \approx 2$  (a value for which the top Yukawa coupling remains safely perturbative up to the Planck scale). In summary, while  $C_{ap} + C_{an} \approx 0$  is enforced just by charge assignments and does not require any tuning of the parameters,  $C_{ap} - C_{an} \approx 0$  requires a specific choice  $\tan \beta \approx \sqrt{2}$ .

<sup>65</sup>In fact the requirement of no massless quarks, no vanishing mixings and one CP violating phase in the CKM matrix implies that no-less than seven non-vanishing Yukawa entries are required, so that the matching between fundamental parameters and observables is one-to-one, but within the SM there are no predictions. Conversely, in the lepton sector equipped with the type-I seesaw for neutrino masses, the same strategy yields precise numerical predictions for the leptonic Dirac phase and for the absolute scale of neutrino masses [523].

<sup>66</sup>In this reference additional possibilities in which the contribution to the anomaly of two generations vanish identically were also identified.



It is also worthwhile mentioning that in nucleophobic models the requirement that a single generation of quarks contributes to the QCD anomaly also allows straightforwardly for  $N_{\text{DW}} = 1$ . There are in fact two ways in which  $H_{1,2}$  can be coupled to the PQ symmetry breaking field:  $H_2^\dagger H_1 \Phi$  in which case  $|\mathcal{X}_\Phi| = 2N_\ell = 2N$ , the axion field has the same periodicity than the  $\theta$  term, and the number of domain walls is  $N_{\text{DW}} = 1$ . The other possibility is  $H_2^\dagger H_1 \Phi^2$ , in which case  $|\mathcal{X}_\Phi| = N_\ell = N$  and  $N_{\text{DW}} = 2$ . In contrast, in conventional DFSZ models one gets respectively  $N_{\text{DW}} = 3$  and 6.

#### 6.4. Enhanced axion couplings and astrophysics

As seen in Section 4, limits from stellar evolution strongly constrain the allowed axion parameter space. The strongest astrophysical limit on the axion-photon coupling is derived from observations of the R-parameter in globular clusters. This is also known as the horizontal branch (HB) bound and constraints the axion-photon coupling down to  $g_{a\gamma} \lesssim 0.65 \times 10^{-10} \text{ GeV}^{-1}$  (cf. Section 4.1). The axion coupling to electrons is, instead, strongly constrained by red giant branch (RGB) stars and by white dwarfs (WD). As discussed in Section 4.2, these bounds amount to roughly  $g_{ae} \lesssim 2 - 3 \times 10^{-13}$ , depending on the particular observable and analysis.

Interestingly, these astrophysical bounds do not depend on the pseudoscalar mass and are valid up to masses of the order of the stellar interior temperature (several keV). Therefore, such bounds can be readily applied to axion models beyond benchmark, like the ones discussed above in this section.

Let us first notice that the WD/RGB bound dominates over the HB constraint in all models in which  $C_{ae}$  and  $C_{a\gamma}$ , defined in Eq. (118), satisfy the condition  $C_{ae}/C_{a\gamma} \gtrsim 10^{-2}$ . This is easily satisfied in the KSVZ-like model discussed in Section 6.1.3 and 6.2.1, in which the coupling with electrons is suppressed by a loop factor  $\sim 10^{-4}$  (cf. Eq. (114)). Hence, for such model the astrophysical bounds on the axion-electron coupling can be ignored, much the same as in the benchmark KSVZ axion. The parameter space is shown in Fig. 20. Notice that, thanks to the strong enhancement of the axion-photon coupling, the model is accessible to a large number of the axion experiments expected to take data in the near future, including ALPS II and BabyIAXO (cf. Section 5). The maximal value of  $n$  shown in figure can be easily accommodated and is well below the threshold required from the LP condition presented in Section 6.1.1.

A similar enhancement of the axion-photon coupling is expected in the DFSZ-type models discussed in Section 6.1.2. However, in this case the axion electron coupling is also naturally very large and the condition  $C_{ae}/C_{a\gamma} \gtrsim 10^{-2}$  is always expected, making the HB bound irrelevant. To see this, let us notice that from Eq. (250) and Eq. (253), it follows that (for large  $n$ )

$$\frac{C_{ae}}{C_{a\gamma}} \simeq \frac{1}{6} \left[ \frac{v_d^2}{v^2} + \sum_{k=1}^n \left( 1 - \frac{1}{2^{n+1-k}} \right) \frac{v_k^2}{v^2} \right], \quad (274)$$

where  $v^2 = v_e^2 + v_d^2 + \sum_{k=1}^n v_k^2$  is the square of the electroweak VEV and  $v_1 \equiv v_u$ . Mathematically, the minimum of Eq. (274) corresponds to the (unphysical) condition  $v_e = v$ , which implies that all the other VEVs are zero and  $C_{ae}/C_{a\gamma} = 0$ . However, perturbative unitarity bounds on the top Yukawa coupling (cf. Section 2.7.2), de facto require the term in parenthesis in Eq. (274) to be always larger than  $\sim 0.1$ , implying a finite lower bound on  $C_{ae}/C_{a\gamma} \gtrsim 10^{-2}$ . A lower value of  $C_{ae}/C_{a\gamma}$  for such models is, if mathematically possible, very unnatural. The axion parameter space for the case of minimal  $C_{ae}/C_{a\gamma}$  is shown in the left panel of Fig. 21. The potential of the axion helioscopes is minimally impacted. In fact, the increase of the RGB/WD bound is (partially) compensated by a more efficient production of solar axions, as discussed in Section 5.1. The predicted sensitivity of ALPS II is also sufficient to explore part of the region below the astrophysical bounds, though this section is clearly reduced with respect to the KSVZ-like model.

The axion parameter space for the higher coupling scenario, when the term in parenthesis in Eq. (274) is of order 1, is shown in the right panel of Fig. 21. In this cases, only a full scale IAXO (not BabyIAXO), among the planned future helioscopes, would have the capability to probe the axion parameter space allowed by the RGB/WD bounds. ALPS II would equally be unable to probe such model below the region excluded by astrophysics.

As evident from the figures, the large axion-photon couplings predicted in such models permit an almost complete exploration of their parameter space by the next generation of axion probes. In particular, several



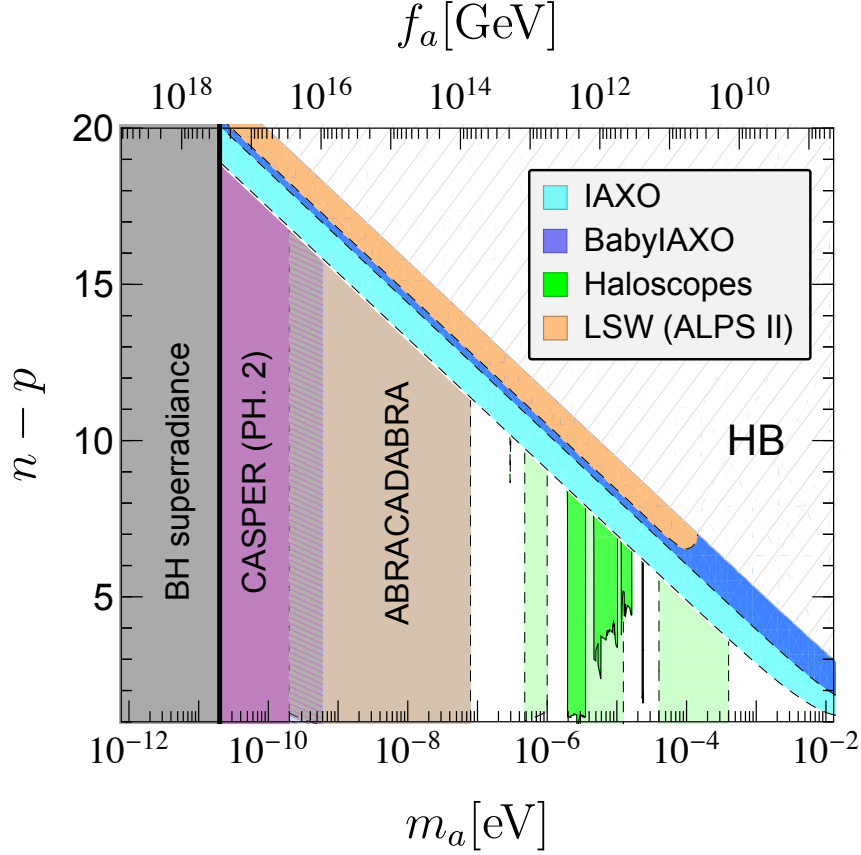


Figure 20: Parameter space (mass and  $n - p$ ) for the clockwork construction (KSVZ type) discussed in Section 6.1.3. We remind that  $3^n$  and  $3^p$  are, respectively, the PQ charges of the scalar singlets that give masses to the exotic quarks and exotic leptons. Notice that  $n - p$  is an integer  $\geq 1$ . Following the convention used in Section 5, we are shading with a lighter green the expected sensitivity of next generation axion haloscope and in darker green the reported results of current haloscopes. Moreover, we are using a dashed contour line for sensitivity and a continuous line for experimental results.

haloscope searches are expected to have enough sensitivity to probe the parameter region all the way to the minimal value of the axion-photon coupling (corresponding to  $n = 2$ ).

Nucleophobic axion models are also phenomenologically interesting, in particular in relation to the SN 1987A and various NS axion bounds, discussed in Section 4.3. Although the SN and NS constraints on the axion couplings are still uncertain, they seem to restrict efficiently the axion parameter space at masses higher than a few 10 meV, if the standard mass-coupling relation is assumed (see, e.g., Fig. 12 for DFSZ axions). These constraints show some tension with the axion interpretation of the stellar cooling anomalies, which favor slightly higher masses [34]. In this respect, nucleophobia would improve the significance of the interpretation of the stellar cooling anomalies in terms of axions. Moreover, experimentally, nucleophobia opens up large sections of the parameter space to experiments, primarily helioscopes, which are sensitive to the higher axion mass region.

Models that enhance the axion nucleon coupling may also find interesting phenomenological applications. A recent analysis [524], which ascribes the observed excess of X-rays from a few nearby neutron stars to ALPs coupled to nucleons and photons, could be interpreted in terms of nucleophilic QCD axions of the kind described in Section 6.3.1. The interpretation given in Ref. [524] asks for a mass below a few  $\mu\text{eV}$ , with  $g_{a\gamma}g_{aN} \sim$  a few  $10^{-21} \text{ GeV}^{-1}$ , a value several orders of magnitude larger than what expected, for example, in the DFSZ axion model. Such large couplings could, however, be possible in the case of the clockwork

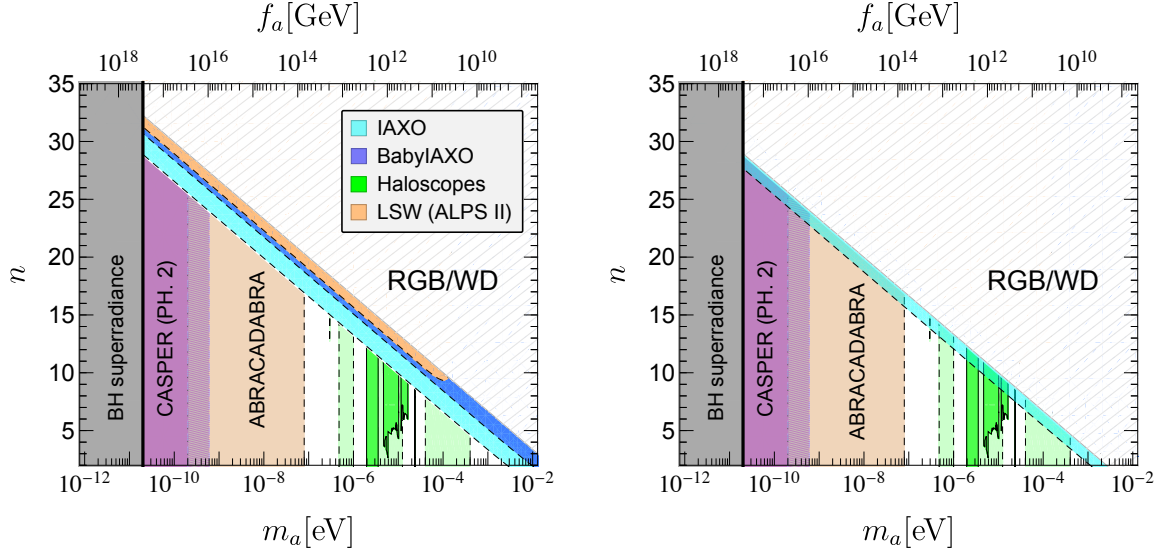


Figure 21: DFSZ model with enhanced axion-photon and axion-electron couplings, discussed in Section 6.1.2 and Section 6.2.2 for  $C_{ae}/C_{a\gamma}$  minimal (left) and maximal (right). Following the convention used in Section 5, we are shading with a lighter green the expected sensitivity of next generation axion haloscope and in darker green the reported results of current haloscopes. Moreover, we are using a dashed contour line for sensitivity and a continuous line for experimental results.

models described here, with enhanced coupling to photons and/or nucleons. Assuming, for example, a standard axion-photon coupling, the hinted region could be accessible to an axion of the kind presented in Section 6.3.1, with  $m_a \sim 1 \mu\text{eV}$  and  $n \sim 30$  (Cf. Eq. (265)), easily accessible to CASPER Electric (see Fig. 22).

Regardless of the phenomenological motivations, nucleophilic axions are viable axion models that could be probed in the near future, a fact that should encourage the exploration of the axion-nucleon parameter space, still quite poorly probed. An enhancement of the axion-neutron coupling by a factor larger than  $10^3$  with respect to the DFSZ axion, corresponding to  $n \sim 10$  in the model in Eq. (265), would make the model sensitive to CASPER wind in phase II.

### 6.5. Flavour violating axions

Assuming that axions exist and that the PQ symmetry acts on SM particles, the possibility that they couple differently to fermions of the same charge but of different generations is quite plausible. There is in fact no fundamental reason why the global and anomalous PQ symmetry should act universally in flavour space as the gauge interactions do. After all, this possibility is almost as old as the axion, as it was already contemplated in the Bardeen and Tye seminal paper [525] in 1978. This idea may then be daringly expanded to speculate whether the PQ symmetry can have something to do with flavour, that is with the pattern of fermions masses and mixing angles in the SM. The PQ symmetry could for example act as a flavour symmetry, or could emerge from a set of genuine flavour symmetries, a point of view that had been advocated by Wilczek already in the early 80's [526].

In the second half of the 80's the possibility of an axion coupled to the SM fermions in a generation dependent way was fired up by the observation in heavy ion collisions at GSI of a sharp peak at  $E(e^+) \sim 300 \text{ keV}$  in the positron spectrum [527–529]. The positron data were later found to be correlated with the simultaneous detection of electrons also featuring in their energy spectrum a narrow peak at the same energy [530]. The data were consistent with the production of a particle of mass  $1.6 - 1.8 \text{ MeV}$ , of probable pseudoscalar character [531], which then decayed into  $e^+e^-$ . Hence the characteristics of such a particle were well consistent with those of the original WW axion [16, 17]. However, this interpretation was challenged

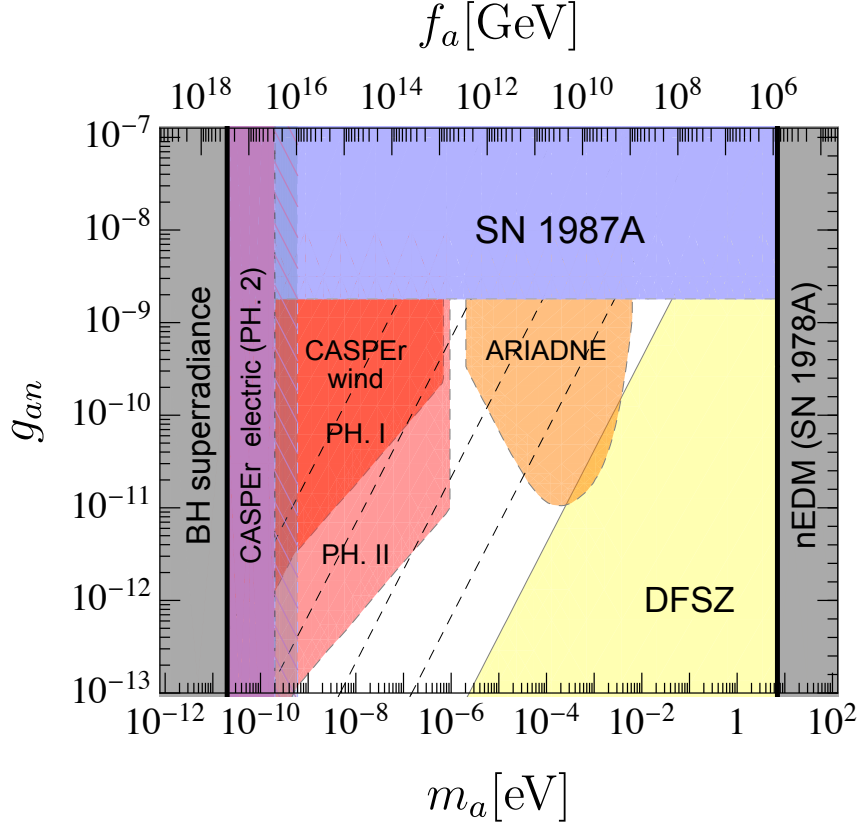


Figure 22: Current bounds and prospectives on the axion nucleon coupling. The black dashed lines correspond, from right to left, to  $n = 5, 10, 15$ , and  $20$  for the model discussed in Section 6.3.1 (see, in particular, Eq. (265)).

by the rather large value of the mass, which implied enhanced couplings, e.g. to either charm or bottom quarks, in conflict with limits from  $J/\psi \rightarrow \gamma a$  or  $\Upsilon \rightarrow \gamma a$ . These limits, however, required the axion to escape from the detectors with no deposit of energy, and could have been circumvented by short lived axions  $\tau_a \lesssim 6 \times 10^{-13} \text{ s}$  [532], due to very large values of the axion-electron coupling  $g_{ae}$ . However, for generation independent PQ symmetries the ratio of the axion-electron and axion-muon couplings is determined by the ratio of the lepton masses as  $g_{a\mu}/g_{ae} = m_\mu/m_e$ , see Eq. (118). This predicted a large enhancement of  $g_{a\mu}$ , in plain conflict with existing measurements of  $(g-2)_\mu$ . Generation dependent axion couplings remained the only way out, and a series of interesting papers analysing this possibility appeared [108, 519, 533–535]. While eventually new experimental results quickly ruled out the 1.8 MeV GSI axion [536–541], the road to further develop generation dependent PQ scenarios, and to explore axion-flavour interconnections was paved.

Recently, several models attempting to relate fermion family symmetries to the PQ symmetry have been put forth. Well motivated realisations identify the  $U(1)_{\text{PQ}}$  with the horizontal  $U(1)$  symmetry responsible for the Yukawa hierarchies [542–544]. Models of Froggatt-Nielsen [545] type have recently regained some attention (see e.g. Refs. [546, 547]), in relation to possible solutions to the strong CP problem. They typically predict axion flavour transitions controlled by the CKM matrix, although subject to built-in  $O(1)$  uncertainties, which are intrinsic to most flavour models based on  $U(1)$ . Models based on non-abelian horizontal symmetries like  $SU(3)_F$  can also lead to an almost<sup>67</sup> accidental global  $U(1)$ 's which can play the

<sup>67</sup>For three chiral families trilinear PQ symmetry breaking terms needs to be forbidden in the scalar potential, so although

role of a PQ symmetry [548, 549]. In both these types of constructions the resulting axion corresponds to a pseudoscalar ‘familon’ that can mediate flavour changing neutral currents (FCNC) transitions much alike the axions of  $U(1)$  flavour models. A different motivation for the non-universality of the PQ current, that was avocated in [115, 516], is that of constructing (nucleophobic) axion models in which the tightest astrophysical bounds can be circumvented, see the review in Section 6.3.2. A genuinely different approach is the attempt of maximize the predictive power of SM flavour data by searching for  $U(1)$  symmetries that would enforce the maximal number of textures zeros in the fermion mass matrices (compatibly with non-vanishing masses and mixings) [522, 523]. It was found in Ref. [522] that all  $U(1)$  symmetries suitable to realise this requirement in the quark sector have a QCD anomaly, and thus correspond to generation dependent PQ symmetries. The particular realisations based on this approach are interesting because, differently from most (if not all) other models, allow to fix the structure of the axion couplings to SM fermions in terms of the values of quark masses and mixings, including the off-diagonal flavour changing ones, up to the values of  $f_a$  and  $\tan\beta$ , as in conventional DFSZ models.

Clearly all the constructions listed above do not have ‘natural flavour conservation’, and thus predict new sources of FCNC processes. However, the latter may be still consistent with experiments if the scale  $f_a$  suppressing all axion couplings were sufficiently large or if flavour transitions mainly affected the second and third generation SM fermions.

#### 6.5.1. Generation dependent Peccei-Quinn symmetries

The important modifications in the structure of the axion couplings to the SM fermions, in the case when the PQ symmetry is generation dependent, was briefly addressed in Section 2.9. There it was shown that the consequences of dropping the assumption of generation independence of the PQ charges were twofold: firstly, flavour violating (FV) couplings arise, and secondly, besides coupling to axial-vector currents, ‘flavoured’ axions couple to vector currents as well. This latter point arises because the PQ charges of the fermions cannot maintain an exact chiral structure ( $\mathcal{X}_L = -\mathcal{X}_R$ ), while in general  $\mathcal{X}_L + \mathcal{X}_R \neq 0$  for the PQ symmetry to be anomalous.

Before discussing the existing bounds on axion FV interactions let us introduce some notations. In the simple scheme discussed in Section 2.9, with only two Higgs doublets and where only two generations were considered, the axion-fermion couplings could be easily expressed in terms of the PQ Higgs charges  $\mathcal{X}_{1,2}$ . Expressing the fermion couplings in terms of the charges of the (two or more) Higgs doublets is possible also in more complicated scenarios, however, the connection depends on the specific model. Hence, for the seek of generality, in this Section we will express the couplings simply in terms of the PQ charges of the SM fermions. Our starting point is the way the axion couples to the fermion current, as written in the first line of Eq. (73), except that  $f_{L,R}$  have now to be understood as vectors of SM fermions of the same electric charge (e.g.  $f = (u_1, u_2, u_3)^T$ ) while  $\mathbf{X}_f$  in the equation below is the diagonal matrix of the associated PQ charges. Going from the basis in which the PQ charges are well defined to the mass eigenstate basis  $f_{L,R} \rightarrow U_{L,R}^f f_{L,R}$ , with unitary matrices  $U_{L,R}^f$ , yields

$$\mathcal{L}_a = \frac{\partial_\mu a}{2f_a} \frac{1}{N} \left[ \bar{f}_L \left( U_L^{f\dagger} \mathbf{X}_{f_L} U_L^f \right) f_L + \bar{f}_R \left( U_R^{f\dagger} \mathbf{X}_{f_R} U_R^f \right) f_R \right]. \quad (275)$$

The light quarks mass eigenstates  $u, d$  can then be redefined as in Eq. (39) in order to remove the anomalous  $G\tilde{G}$  term from the Lagrangian, and again this results in adding to the couplings the model independent contribution in Eq. (42). The flavour-diagonal axion-fermion couplings receive corrections from the mixing:  $c_{f_i}^0 \rightarrow c_{f_i}^0 + \delta c_{f_i}^0$  where

$$\delta c_{f_i}^0 = \frac{1}{2N} (W_{f_{iR}} - W_{f_{iL}}), \quad \text{with} \quad W_{f_{iR}} = \left[ U_R^{f\dagger} (\mathbf{X}_{f_R} - \mathcal{X}_{f_{iR}} \mathbb{I}) U_R^f \right]_{ii}, \quad (276)$$

---

technically natural the PQ symmetry is still imposed by hand. On the other hand, in the presence of  $n_g$  chiral families the gauging of  $SU(n_g)$  would have delivered a truly accidental axion for  $n_g > 4$ , since the first operator breaking the PQ symmetry is of dimension  $n_g$ .

where  $\mathbb{I}$  is the identity matrix in generation space and a similar expression folds for  $W_{f_{iL}}$  upon swapping  $L \leftrightarrow R$ . Such a correction can be invoked to improve nucleophobia by tuning a cancellation against  $C_{a,\text{sea}}$  in Eq. (266), or to achieve electrophobia without recurring to a third Higgs by cancelling  $c_e^0$  against the correction from mixings, as it was done in Ref. [516]; but except for these two cases the  $\delta c_f^0$  contributions do not change much the overall picture. Of leading importance are instead the off-diagonal terms, that give rise to FV axial-vector and vector axion couplings:

$$\mathcal{L}_{af_i f_j} = \frac{\partial_\mu a}{2f_a} \left[ \bar{f}_i \gamma^\mu \left( C_{f_i f_j}^V - C_{f_i f_j}^A \gamma_5 \right) f_j \right], \quad (277)$$

$$C_{f_i f_j}^V = \frac{1}{2N} \left( U_L^{f\dagger} \mathbf{X}_{f_L} U_L^f + U_R^{f\dagger} \mathbf{X}_{f_R} U_R^f \right)_{ij}, \quad (278)$$

$$C_{f_i f_j}^A = \frac{1}{2N} \left( U_L^{f\dagger} \mathbf{X}_{f_L} U_L^f - U_R^{f\dagger} \mathbf{X}_{f_R} U_R^f \right)_{ij}. \quad (279)$$

The crucial point regarding these couplings is that, while the matrices of charges  $\mathbf{X}_{f_{R,L}}$  are presumably fixed in any specific model, little is known about the mixing matrices  $U_{R,L}^f$ .<sup>68</sup> In the quark sector, nothing is known about the RH matrices  $U_R^f$ , and their structure remains completely arbitrary. The LH mixings are instead constrained to satisfy  $V_{\text{CKM}} = U_{u_L}^\dagger U_{d_L} \approx \mathbb{I}$ . This, however, only implies  $U_{u_L} \approx U_{d_L}$  but does not provide additional information on the size of the off-diagonal entries, and in particular it does not forbid large flavour mixings. Differently from the quark sector, the lepton sector is characterised by large mixings, but one does not know if they originate from the neutrino or from the charged lepton rotation matrices (or from both), so that for example also  $U_L^\ell \approx \mathbb{I}$  remains a viable assumption.

### 6.5.2. Constraints on flavour violating axion couplings

Searches for FV decays involving invisible final states are the main experimental tool to probe the off-diagonal axion couplings  $C_{f_i f_j}^{A,V}$ . A general analysis of such flavour-changing processes involving a generic massless NGB, which holds also for FV axion, can be found in Ref. [550]. A recent thorough collection of limits on the FV couplings can be found in Ref. [551], and brief reviews about the status of the art are presented in Refs. [552, 553].<sup>69</sup> The currently best limits for each type of FV transition are listed in Table 7. They coincide with the limits given in Ref. [551] after the correspondence between their and our notations ( $V_{ij}^f/v_{\text{PQ}} \equiv C_{f_i f_j}^V/(2f_a)$ ) is accounted for.

The strongest bounds on FV axion couplings to quarks come from meson decays into final states containing invisible particles. Note, however, that decays involving initial and final pseudo-scalar mesons like  $P = K, B, D, \pi$  are only sensitive to the vector part of the FV quark current, since  $\langle P' | J_\mu^5 | P \rangle = 0$  by the Wigner-Eckart theorem. Searches for  $K^+ \rightarrow \pi^+ a$  decays provide the tightest limits. The current bound from E949/E787 [555] (see Table 7) implies  $m_a < 17 \cdot |C_{sd}^V|^{-1} \mu\text{eV}$  which, if one assumes that  $C_{sd}^V$  is not particularly suppressed, is about three orders of magnitude stronger than typical astrophysical bounds. In the next future, NA62 is expected to improve the limit on  $\text{Br}(K^+ \rightarrow \pi^+ a)$  by a factor of  $\sim 70$  [556, 557], thus strengthening the axion mass bound by a factor  $\sim 8$ . The most sensitive processes involving a quark of the third generation are  $B^\pm \rightarrow \pi^\pm a$  and  $B^\pm \rightarrow K^\pm a$ . Present limit from CLEO [558] imply respectively  $m_a < 11.4 \cdot 10^{-2} \cdot |C_{bd}^V|^{-1} \text{eV}$  and  $m_a < 9.5 \cdot 10^{-2} \cdot |C_{bs}^V|^{-1} \text{eV}$  which, for maximal mixing, are close to the astrophysics bounds. Note that the latter bound could be presumably strengthened by a factor  $\sim 6$  at BELLE II [559]. Processes involving FV transitions between up-type quarks are much less constrained. Decays of charmed mesons of the form  $D \rightarrow \pi a$  are only subject to the trivial requirement  $\text{Br}(D \rightarrow \pi a) < 1$ , which can be translated into weak bounds, which are at least two orders of magnitude worse than the ones for down-type quarks and not competitive with limits from astrophysics.

<sup>68</sup> The models discussed in in Ref. [522] are a remarkable exception since, thanks to the maximal reduction in the number of free parameters, both the quark mixing matrices remain fixed in terms of measured quantities.

<sup>69</sup> Close to the completion of this review, Ref. [554] appeared, where the importance of flavour violating transitions for axion searches was reiterated, and additional limits on FV axion couplings from three-body meson decays and baryonic decays, including the decay  $\Lambda \rightarrow n a$  that would represent a new cooling mechanism for the SN1987A, were derived.

As we have said meson decays can only constrain FV vector couplings. In order to set bounds on the axial-vector FV couplings one has to resort to other flavour changing processes, as for example neutral meson ( $K^0, D^0, B_d^0, B_s^0$ ) mixing, since meson mass splittings receive from axion interactions an additional contribution  $(\Delta m)_a$ . However, in spite of the fact that, for example, the measurement of the mass difference in the neutral kaon system  $\Delta m_K/m_K \simeq 0.7 \times 10^{-14}$  gives a number that is four orders of magnitude smaller than the limit from kaon decays  $\text{Br}(K^+ \rightarrow \pi^+ a) \lesssim 0.7 \times 10^{-10}$ , the sensitivity to this type of new physics of the former observable is not competitive with the sensitivity of the latter. To understand the reasons for this, let us write the approximate expressions for the relevant quantities in the game:

$$\frac{(\Delta m_K)_a}{m_K} \simeq \frac{f_K^2}{f_a^2} |C_{sd}^A|^2, \quad (280)$$

$$\Gamma(K^+ \rightarrow \pi^+ a) \simeq \frac{m_K^3}{16\pi f_a^2} |C_{sd}^V|^2, \quad (281)$$

$$\Gamma(K^+ \rightarrow \mu^+ \nu) \simeq \frac{m_K}{8\pi} (G_F f_K m_\mu |V_{us}|)^2, \quad (282)$$

where  $f_K$  is the kaon decay constant,  $G_F$  the Fermi constant, and  $V_{us}$  the relevant element of the CKM matrix. The leptonic decay in Eq. (282) has the largest branching ratio  $\simeq 63.4\%$ , so we approximate  $\Gamma_K^{\text{tot}} \approx \Gamma(K^+ \rightarrow \mu^+ \nu)$  and we obtain:

$$\text{Br}(K^+ \rightarrow \pi^+ a) \simeq (G_F f_K m_\mu |V_{us}|)^{-2} \times \frac{m_K^2}{f_a^2} |C_{sd}^V|^2. \quad (283)$$

The prefactor in the RHS of this equation accounts for chirality (and Cabibbo) suppression of the SM decays, and it is not present for  $K^+ \rightarrow \pi^+ a$  decays. This factor is huge  $\sim 5 \times 10^{14}$ , and enhances the effects of  $C_{sd}^V$  largely overcompensating for the better precision of  $\Delta m_K$ . As a result the limits on  $f_a/|C_{sd}^V|$  are more than five order of magnitude better than the corresponding limits on  $f_a/|C_{sd}^A|$ .

Differently from pseudoscalar mesons, for two-body charged lepton decays  $\ell_i \rightarrow \ell_j a$  both vector and axial-vector couplings contribute because the decaying particle has non-zero spin. Experimentally it is more convenient to search for decays of anti-leptons. The angular differential decay rate for two-body decays is

$$\frac{d\Gamma(\ell_i^+ \rightarrow \ell_j^+ a)}{d\cos\theta} = \frac{m_{\ell_i}^3}{128\pi f_a^2} \left[ |C_{\ell_i \ell_j}^V|^2 + |C_{\ell_i \ell_j}^A|^2 + 2\text{Re}(C_{\ell_i \ell_j}^A C_{\ell_i \ell_j}^{V*}) P_{\ell_i} \cos\theta \right], \quad (284)$$

where  $P_{\ell_i}$  is the polarisation vector of the decaying particle. Strong bounds have been obtained from searches for  $\mu^+ \rightarrow e^+ a$  decays, the best of which was obtained more than thirty years ago at TRIUMF, giving  $\text{Br}(\mu^+ \rightarrow e^+ a) < 2.6 \cdot 10^{-6}$  [560]. This bound, however, was obtained by exploring a kinematical region forbidden for  $\mu^+ \rightarrow e^+ \nu \bar{\nu}$  SM decays. Namely, the bound holds only if the decay is purely vector or purely axial-vector, implying in this case  $m_a < 2.5 \cdot |C_{\mu e}^{V(A)}|^{-1} \text{ meV}$ . However, the bound would evaporate for axion interactions with a SM-like  $V - A$  structure. Slightly weaker bounds, which however do not depend on the chirality properties of the coupling, were obtained by the Crystal Box experiment by searching for the radiative decay  $\mu^+ \rightarrow e^+ \gamma a$  [561, 562], see Table 7.

Assuming the decays are isotropic, or in case anisotropic decays are explicitly searched for, it is convenient to express the limits in terms of an effective coupling

$$C_{\ell_i \ell_j} = \left( |C_{\ell_i \ell_j}^V|^2 + |C_{\ell_i \ell_j}^A|^2 \right)^{1/2}. \quad (285)$$

Recent searches that explicitly evaluate limits for anisotropic two body muon decays have been carried out by the TWIST collaboration [563], and yield  $f_a < (1.0 - 1.4) \cdot C_{\mu e}$  depending on the anisotropy of the decay. These bounds are slightly less stringent than the old limits from Crystal Box. In the next future, the MEG [564] and Mu3e [565] experiments at PSI are expected to improve the bounds on  $\mu$ - $e$  transitions by about one order of magnitude. Bounds on  $\tau^+ \rightarrow \mu^+ a$  and  $\tau^+ \rightarrow e^+ a$  FV decays have been obtained by the ARGUS collaboration [566], and are also reported in Table 7. However, they imply limits on the axion mass which remain well below the astrophysical limits.



Decay	Branching ratio	Experiment/Reference	$f_a$ (GeV)
$K^+ \rightarrow \pi^+ a$	$< 0.73 \times 10^{-10}$	E949+E787 [555]	$> 3.4 \times 10^{11}  C_{sd}^V $
$B^\pm \rightarrow \pi^\pm a$	$< 4.9 \times 10^{-5}$	CLEO [558]	$> 5.0 \times 10^7  C_{bd}^V $
$B^\pm \rightarrow K^\pm a$	$< 4.9 \times 10^{-5}$	CLEO [558]	$> 6.0 \times 10^7  C_{bs}^V $
$D^\pm \rightarrow \pi^\pm a$	$< 1$		$> 1.6 \times 10^5  C_{cu}^V $
$\mu^+ \rightarrow e^+ a$	$< 2.6 \times 10^{-6}$	TRIUMF [560]	$> 4.5 \times 10^9  C_{\mu e}^{V(A)} $
$\mu^+ \rightarrow e^+ \gamma a$	$< 1.1 \times 10^{-9}$	Crystal Box [562]	$> 1.6 \times 10^9 C_{\mu e}$
$\tau^+ \rightarrow e^+ a$	$< 1.5 \times 10^{-2}$	ARGUS [566]	$> 0.9 \times 10^6 C_{\tau e}$
$\tau^+ \rightarrow \mu^+ a$	$< 2.6 \times 10^{-2}$	ARGUS [566]	$> 0.8 \times 10^6 C_{\tau \mu}$

Table 7: Limits on FV axion couplings to the SM fermions. The TRIUMF limit on  $\mu^+ \rightarrow e^+ a$  holds only for purely vector or purely axial-vector interactions. For the other leptonic transitions the total coupling  $C_{\ell_i \ell_j}$  is defined in Eq. (285).

### 6.6. Extending the mass region region for dark matter axions

As we have discussed in Section 3.3, the contribution to DM from the axion misalignment mechanism is evaluated by solving a second order differential equation for the misalignment angle  $\theta(t)$  with time dependent coefficients  $H(t)$  and  $m_a(t)$ . In pre-inflationary scenarios the axion field is homogenised over distances much larger than the horizon, and the spatial derivative term in Eq. (153) can be dropped. In post-inflationary scenarios field modes with wavelength  $\lambda(t) \ll t$  are quickly redshifted away, and restricting to the relevant super-horizon modes we can again drop spatial derivatives, so that Eq. (153) becomes

$$\ddot{\theta}(t) + 3H(t)\dot{\theta}(t) + m_a^2(T(t))\theta(t) = 0. \quad (286)$$

If the coefficients  $H(t)$  and  $m_a(t)$  have a power-law dependence on time, then Eq. (286) admits an exact solution. For example, let us assume that  $R(t) \propto t^p$ , where  $p > 0$  is a new constant describing the cosmological model ( $p = 1/2$  for radiation-domination). We also assume that  $m_a(T) \propto T^{-\gamma}$ , see Eq. (150), and  $\gamma$  is related to the exponent governing the temperature dependence of the topological susceptibility. Assuming that the entropy (see Eq. (145)) is conserved within a comoving volume,  $d(sR^3)/dt = 0$ , and neglecting the change in the number of degrees of freedom  $g_S(T)$ , we have  $T \propto 1/R \propto t^{-p}$  and  $m_a(t) \propto t^{\gamma p}$ . Under these conditions, the general solution of Eq. (286) is

$$\theta(t) = \left( \frac{m_a t^\alpha}{2\alpha} \right)^\beta \left[ C_1 \Gamma(1 + \beta) J_\beta \left( \frac{m_a t^\alpha}{\alpha} \right) + C_2 \Gamma(1 - \beta) J_{-\beta} \left( \frac{m_a t^\alpha}{\alpha} \right) \right], \quad (287)$$

where  $\alpha = (2 + \gamma p)/2$ ,  $\beta = (1 - 3p)/(2 + \gamma p)$ ,  $\Gamma(x)$  is the Euler gamma function of argument  $x$ ,  $J_\kappa(x)$  is the Bessel function of the first kind of order  $\kappa$ , and  $C_{1,2}$  are integration constants. The case studied in Section 3 corresponds to a cosmological evolution during radiation domination, that is  $p = 1/2$ , with the topological susceptibility obtained from lattice simulation, which roughly corresponds to  $\gamma \approx 4$  for  $T > T_C$  and  $\gamma \approx 0$  for  $T \ll T_C$ , see the discussion below Eq. (150). We have also set the initial conditions  $\dot{\theta} = 0$  and  $\theta = \theta_i$  at the time at which the PQ symmetry breaking occurs, see Section 3.3. Several studies have been carried out under these assumptions, which suggest that the DM energy density is saturated for an axion mass lying within a window  $m_a \sim (10 - 100) \mu\text{eV}$ . This mass window can be significantly altered by various non-standard conditions:

1. Assuming  $\theta_i \ll O(1)$  in pre-inflationary PQ breaking scenarios. This possibility has been already discussed in Section 3.3;
2. Assuming a non-standard cosmological evolution, that is by modifying the evolution of the Hubble parameter  $H(t)$ . This possibility will be explored in Section 6.6.1;
3. Altering the functional dependence of  $m_a(t)$  by appealing to beyond-the-SM particle physics. Some examples that exploit this possibility will be reviewed in Section 6.6.2;
4. Assuming a sufficiently large  $\theta_i \neq 0$ , see Eq. (161). This possibility will be reviewed in Section 6.6.3.



### 6.6.1. Non-standard cosmological evolution

The evolution of the Hubble parameter in the early Universe can be modified in different ways, and this can alter the mass region in which the relic density of axions saturates the DM density with respect to the conventional scenario reviewed in Section 3.6. We will now review some of these possibilities.

*Entropy generation:* The standard computation of the present axion energy density relies on the conservation of the entropy in a comoving volume, see Eq. (166). Suppose now that a new species  $X$ , like a massive scalar field with  $g_X$  degrees of freedom, is present in the early Universe and decays into thermalised products after the axion field starts to oscillate at  $T_{\text{osc}}$ , but prior to BBN. The present amount of entropy is increased by a factor  $\Delta \equiv 1 + g_X/g_S$ , where  $g_S$  is the number of entropy degrees of freedom in the SM at  $T_{\text{osc}}$ . In this scenario, the present axion energy density in Eq. (167) would be lowered by the entropy injection [567–570] by the same factor  $\Delta$ . If we demand that the axion energy density matches that of CDM in spite of entropy dilution, then from Eq. (168) we obtain that the mass of the axion has to be lower with respect to the conventional value derived in Section 3.3 as

$$m_a \rightarrow m_a \Delta^{-\frac{2+\gamma}{3+\gamma}}. \quad (288)$$

*Unconventional cosmologies:* If the evolution of the Universe at temperatures around or below  $\sim 1$  GeV is characterised by a period of non-canonical expansion, the onset of axion oscillations would be altered and that would lead to a different axion relic density today. Thus, non-standard cosmologies can enlarge the mass range for axion DM.

Such a scenario might occur for example if the evolution of the Universe is described by a scalar-tensor gravity theory [571–573] rather than by general relativity. Scalar-tensor theories benefit from an attraction mechanism which at late times makes them flow towards standard general relativity, so that discrepancies with direct cosmological observations can be avoided. Some consequences of a modified expansion rate due to a scalar-tensor theory have already been discussed in the literature in relation to a possible large enhancements of the WIMP DM relic density [574–578], or to lower the scale of leptogenesis down to the TeV range [579].

Another possibility consists in enlarging the particle content of the SM, by including a new particle which at early times dominates the expansion rate of the Universe. This possibility also results into a modification of the cosmic evolution that departs from the  $\Lambda$ CDM predictions. Scenarios of this type have been extensively discussed in the literature, in relation to the expected abundance of WIMPs [580–585] and their free-stream velocity [586]. A similar possibility has been explored in relation to axion physics both for hot [587] and cold relics [588–592]. In brief, we assume that a new field  $\phi$  coexists along with the SM particles and comes to dominate the energy density in the early Universe, down to a decay temperature  $T_{\text{dec}}$  that marks the transition to the standard cosmological scenario. If we assume that the new particle has an equation of state  $w_\phi$  and energy density  $\rho_\phi$ , and decays generating an extra radiation density  $\rho_r^{\text{ex}}$  at a rate  $\Gamma_\phi$ , the transition can be modelled as [591]

$$\dot{\rho}_\phi + 3(1 + w_\phi)H\rho_\phi = -\Gamma_\phi\rho_\phi, \quad (289)$$

$$\dot{\rho}_r^{\text{ex}} + 4H\rho_r^{\text{ex}} = \Gamma_\phi\rho_\phi, \quad (290)$$

where a dot indicates a derivation with respect to cosmic time  $t$ . If it is assumed that the decay products are light SM particles, then the energy density of the surrounding plasma is increased.

A non-standard cosmology evolution alters the moment at which the coherent oscillations of the axion field commence and possibly dilutes their energy density thereafter, modifying the present axion energy density for a given axion mass and initial misalignment angle. Models that have been considered in the literature include an early matter-dominated period [157, 567, 593, 594], for which  $w_\phi = 0$ , and a period of dominance by a “fast-rolling” kination field [595, 596], with  $w_\phi = 1$ . We have summarised these modifications in Fig. 23, where we show the effects of an early matter-dominated period (left) or a kination domination (right) on the axion parameter space, assuming a decay temperature  $T_{\text{dec}} = 100$  MeV. These results have to be compared with what has been obtained for the standard cosmological model in Fig. 3. In the **PreI**

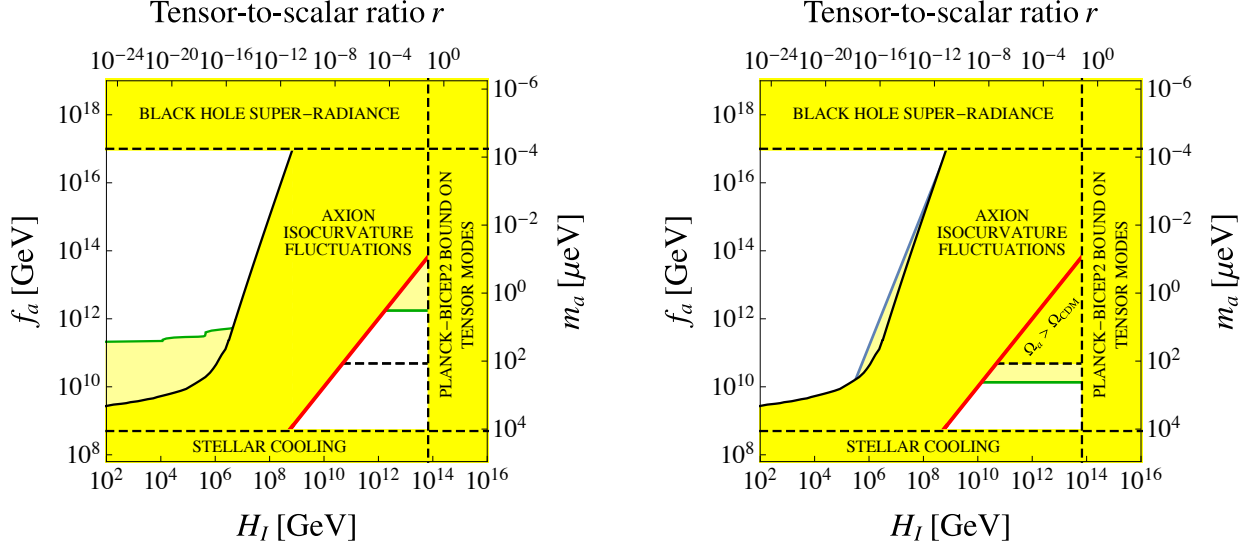


Figure 23: Region of axion parameter space where the axion constitutes the totality of the DM observed for an early matter-dominated period (left) and for an early kination period (right), see text for additional details. For each figure, axes and bounds have been described in Fig. 3.

scenario described in Section 3.3, the bounds from the non-detection of axion isocurvature fluctuations give more stringent constraints on the allowed parameter space with respect to the result in the standard cosmology, bound in each of the figure by the contour in green and with additional yellow shading where excluded. For the matter-dominated scenario with  $\theta_i \simeq 1$  and for a decay temperature  $T_{\text{dec}} \ll 1$  GeV, the axion can be the DM for values of the axion decay constant that are generally larger than what obtained in the standard scenario, that is  $f_a \gg 10^{11}$  GeV for a decay temperature  $T_{\text{dec}} \ll 1$  GeV. Comparing to the standard scenario, the value of the DM axion mass is generally larger when an early kination period occurs, and smaller when in the presence of an early matter-dominated period. These changes are ultimately due to the effects of entropy dilution and to the production of a different number of axions from the altered  $T_{\text{osc}}$  in Eq. (154), as explained in detail in Ref. [588].

#### 6.6.2. Modifying the $m_a$ - $f_a$ relation or the axion mass function $m_a(T)$

The axion abundance would also change if the axion mass/decay constant or the mass dependence on the temperature were modified. We will now explore some scenarios that realise this possibility.

*Axion dark matter with a non-conventional  $m_a$ - $f_a$  relation:* The estimate of the axion energy density due to the VRM carried out in Section 3.3 led to Eq. (168), which shows that besides a dependence on the value of the initial misalignment angle, the axion contribution to the CDM crucially depends on the value of the axion mass. In the conventional axion model of Section 2, the product of the zero temperature axion mass  $m_a$  and the PQ constant  $f_a$  is fixed by the value of the QCD topological susceptibility at zero temperature,  $(m_a f_a)^2 = \chi(0)$  for which the standard value is  $\chi(0) = (75.5 \text{ MeV})^4$ . However, it is possible to conceive models in which the relation between the axion mass and its decay constant is modified, a condition that can be conveniently expressed as  $(m_a f_a)^2 = \alpha_\chi \chi(0)$ , with  $\alpha_\chi \neq 1$ . This would change the fraction of axion DM for a given mass and initial misalignment angle or, equivalently, the value of the mass required for the axion to account for all of the DM. Assuming that the misalignment mechanism dominates the cosmological axion production, to keep the energy density in axions constant it is easy to see from Eqs. (169)–(170) that the mass should be rescaled by the factor  $\alpha_\chi^{(2+\gamma)/(3+\gamma)} \simeq \alpha_\chi^{6/7}$ , where the numerical exponent in the last

relation corresponds to the canonical value  $\gamma = 4$ . Hence, if  $\alpha_\chi > 1$  a larger axion mass is needed to account for the totality of CDM in axions, while the opposite is true if  $\alpha_\chi < 1$ .

An example of a model in which  $m_a$  is decreased from its standard value was proposed in Ref. [597]. This model relies on a  $Z_N$  symmetry under which  $a \rightarrow a + \frac{2\pi f_a}{N}$ , and furthermore the axion interacts with  $N$  copies of QCD whose fermions transform under  $Z_N$  as  $\psi_k \rightarrow \psi_{k+1}$ . Surprisingly, adding up the contributions of all the sectors one finds that cancelations occur in the axion potential with a high degree of accuracy. As a result, the axion mass gets exponentially suppressed with respect to the standard case, and in the large  $N$  limit one obtains

$$m_a^{(N)} \approx \frac{m_a}{2^{(N-4)/2}}, \quad (291)$$

which corresponds to  $\alpha_\chi \approx 2^{-N} < 1$  and, at constant relic density, to a rescaled axion mass  $m_a \rightarrow 2^{-\frac{6N}{7}} m_a$ . This result is particularly relevant for axion searches in the very low mass region.

*Axion dark matter with a modified mass function  $m_a(T)$ :* Another interesting possibility are scenarios in which the zero temperature axion mass is unchanged but its temperature dependence is non-standard. In this case, the temperature at which the axion field oscillation commence differs from Eq. (171). Since the axion energy density scales as<sup>70</sup>

$$\rho_a \propto m_a T_{\text{osc}}^{-1}, \quad (292)$$

shifting the temperature at which the oscillations start would change the energy density yield in axions even if the axion mass is unchanged. This effect is expected in the cosmological scenario predicted by the theory of the *mirror world* [598], extended to include the axion [599].

The mirror world idea is very old [600–603] and based on the assumption that the gauge group is the product of two identical groups,  $G \times G'$ . In the simplest possible model,  $G$  is the SM gauge group and  $G'$  an identical copy of it. Standard particles are singlets of  $G'$  and mirror particles are singlets of  $G$ . This implies the existence of mirror particles, identical to ours and interacting with our sector only through gravity (and possibly via other renormalizable portal couplings, which are assumed to be small). Since the gravitational interaction is very weak, mirror particles are not expected to come into thermal equilibrium with ordinary particles. Hence, there is no reason to expect that the standard and mirror universe have the same temperature.<sup>71</sup> In fact, cosmological observations require a colder mirror universe in order to reduce the radiation energy density at the time of the BBN [598, 604]. Denoting with  $x = T'/T$  the ratio of the mirror and standard temperatures, one finds that  $x \lesssim 0.4$  is needed to accomodate the most recent combined analysis of the Cosmic Microwave Background from the Planck collaboration and observations of the Baryon Acoustic Oscillations [238].

The possibility to implement the PQ mechanism in the mirror world scenario was proposed in Refs. [605–607]. The general feature is that the total Lagrangian must be of the form  $\mathcal{L} + \mathcal{L}' + \lambda \mathcal{L}_{\text{int}}$ , where  $\mathcal{L}$  represents the ordinary Lagrangian,  $\mathcal{L}'$  is the Lagrangian describing the mirror world content, and  $\mathcal{L}_{\text{int}}$  is an interaction term with a coupling  $\lambda$  which is taken to be small enough to ensure that the two sectors do not come into thermal equilibrium. The simplest realisation of the mechanism restricts the interaction to the Higgs sector. Ordinary and mirror world have each two Higgses, which interact with each other. The axion emerges as a combination of their phases in a generalization of the Weinberg-Wilczek mechanism. For  $\lambda = 0$ , the total Lagrangian contains two identical  $U(1)_{\text{axial}}$  symmetries, while the  $\mathcal{L}_{\text{int}}$  term breaks them into the usual  $U(1)_{\text{PQ}}$ , so that only one axion field results.

As long as the mirror-parity is an exact symmetry, the particle physics is exactly the same in the two worlds, and so the strong CP problem is simultaneously solved in both sectors. In particular, the axion couples to both sectors in the same way and their non-perturbative QCD dynamics produces the same

<sup>70</sup>This can be seen as follows:  $\rho_a = m_a n_a$  with  $n_a \propto m_a(T_{\text{osc}}) T_{\text{osc}}^{-3} \propto H(T_{\text{osc}}) T_{\text{osc}}^{-3} \propto T_{\text{osc}}^{-1}$ .

<sup>71</sup>In the exact  $Z_2$  symmetric case this requires an inflationary dynamics yielding different reheating temperatures in the standard and mirror sectors [598].

contribution to the axion effective potential. Hence, the total zero temperature axion mass, which includes the mirror world contributions, is  $m_{\text{tot}}(0) = \sqrt{2} m_a$ , only slightly larger than the standard zero temperature axion mass  $m_a$ , given in Eq. (51). However, at temperature  $T \sim 1$  GeV the axion mass could be considerably larger than its standard value. Assuming the same confinement temperature  $T_C$  in the two sectors, and neglecting a possible dependence of the exponent  $\gamma$  on the temperature so that  $\gamma(T) \approx \gamma(xT) = \gamma \approx 4$ , the expression in Eq. (150) for  $T \gtrsim T_C$  gives

$$m_{\text{tot}}^2(T) = m_a^2 \left[ \left( \frac{T_C}{T} \right)^{2\gamma} + \left( \frac{T_C}{xT} \right)^{2\gamma} \right] = m_a^2(T) \left( 1 + \frac{1}{x^{2\gamma}} \right), \quad (293)$$

where  $m_a(T)$  is the standard temperature dependent axion mass. Of course, this different temperature dependence implies a different value for  $T_{\text{osc}}$ . To estimate the contribution of the axion energy density, let us neglect the first term in the parenthesis in Eq. (293). This approximation is justified for  $x \ll 1$ . In this case, it is easy to see that the oscillation temperature in the mirror world scenario,  $T'_{\text{osc}}$ , is related to the standard oscillation temperature as

$$T'_{\text{osc}} \simeq x^{-\gamma/(\gamma+2)} T_{\text{osc}}. \quad (294)$$

The effect of this on the expected axion abundance can be inferred from Eq. (292):

$$\rho_a^{\text{mirror}} \simeq \sqrt{2} x^{\gamma/(\gamma+2)} \rho_a, \quad (295)$$

where the  $\sqrt{2}$  accounts for the modification of the zero temperature axion mass. Although in this case the modification to the zero temperature axion mass is only a minor effect, corresponding to a factor  $\alpha_\chi = 2$ , the above result shows that in the mirror world scenario the present energy density in axions can be considerably smaller than expected, and this allows to saturate  $\Omega_{\text{DM}}$  for large values of the PQ constant, a result that can be of interest for experiments searching for DM axions in mass regions well below the conventional window.

A different way to deplete the energy density of the QCD axion, thus allowing for larger  $f_a$  and smaller axion DM masses, was put forth in Ref. [608]. It is assumed that the axion couples to a massless  $U(1)'$  dark photon via an  $aF'\tilde{F}'$  term similar to the axion-photon coupling. The dark photon, however, is decoupled from the SM and does not interact with the thermal bath, a condition that has to be enforced to maintain it massless also at finite temperature. When the axion starts oscillating certain modes of the dark photon become tachyonic and start growing exponentially, and in this regime energy is efficiently transferred from the axion into the dark photons, leading to an exponential suppression of the axion density and drastically reducing its contribution to the DM, and opening a window for low mass values as small as  $m_a \sim 10^{-10}$  eV.

Another mechanism that brings in a hidden Abelian gauge field exploits the Witten effect [609] of hidden monopoles on the QCD axion dynamics. Long time ago Witten has shown that in the presence of a CP violating  $\theta$ -term, monopoles acquire a non-zero electric charge and become dyons. When a dynamical axion field replaces  $\theta$ , its potential receives additional contributions from interactions with the monopoles [610] and because of this the field oscillations begin much before the epoch of the QCD phase transition. This scenario does not work with QED monopoles, because of the extremely tight observational constraints on their abundance. For this reason Refs. [611, 612] attempted to implement the same mechanism exploiting monopoles of a hidden  $U(1)'$  symmetry. The axion abundance turns out to be inversely proportional to the abundance of hidden monopoles, and when the density of monopoles is sufficiently large to make up a significant fraction of the DM, the abundance of axions with decay constant smaller than about  $10^{12}$  GeV gets suppressed. While this mechanism does not seem to be able to extend by much the axion window towards low mass values, and moreover predicts that DM is accounted for by hidden monopoles, rather than by axions, it has some interesting features, as for example that of suppressing axion isocurvature perturbations, and of disposing of the domain wall problem.

### 6.6.3. Dark Matter from axion initial velocity

As we have seen in Section 3.3, oscillations of the axion field can start when the age of the Universe  $t_U \sim H^{-1}$  is of the order of the oscillation period  $\sim m_a^{-1}$ . However, one additional condition must also be satisfied: at  $t_{\text{osc}}$ , as defined by Eq. (154), the axion kinetic energy  $\dot{a}^2/2$  should not exceed the potential barrier  $2m_a^2 f_a^2$ , otherwise the axion field keeps rotating and oscillations are prevented. This implies that if  $\dot{\theta}_i \gtrsim 2m_a(t_{\text{osc}})$ , which in terms of quantities defined at the PQ scale translates into the condition  $\dot{\theta}_{\text{PQ}} > 10^8 H_{\text{PQ}}$ , see Eq. (161), the conventional misalignment scenario is not realised. Such large values of  $\dot{\theta}_{\text{PQ}}$  seem rather unnatural and difficult to achieve. However, given that an axion DM scenario in which this condition is realised would be genuinely different from the conventional misalignment scenario, it is worthwhile to investigate in some detail the consequences of this possibility, a task that was carried out in Refs. [613, 614].

The axion velocity  $\dot{\theta}$  can be related to the density of the PQ charge associated with the symmetry  $\Phi \rightarrow e^{i\alpha}\Phi$  of the field  $\Phi$  introduced in Eq. (79):

$$n_\theta = i \left( \Phi \dot{\Phi}^\dagger - \Phi^\dagger \dot{\Phi} \right) = \dot{\theta} f_a^2, \quad (296)$$

where the last expression holds after replacing  $\Phi \rightarrow f_a/\sqrt{2}$ . The charge density in a comoving volume is conserved, hence the scaling  $\dot{\theta} \sim R^{-3}$  in Eq. (156), and it is convenient to introduce the (constant) comoving density  $Y_\theta = n_\theta/T^3$ . Saturating the condition  $\dot{\theta} \sim m_a$  at  $T_{\text{osc}}$  we obtain the critical value for departing from the conventional misalignment scenario:

$$Y_\theta^c = \frac{n_\theta}{T^3} \simeq \frac{m_a(T_{\text{osc}}) f_a^2}{T_{\text{osc}}^3} \simeq \frac{f_a^2}{m_{\text{Pl}} T_{\text{osc}}}, \quad (297)$$

where we have used  $m_a(T_{\text{osc}}) \sim H(T_{\text{osc}}) \sim T_{\text{osc}}^2/m_{\text{Pl}}$ . The energy density in axions can be written as  $\rho_a = m_a Y_\theta^c T^3$  with  $m_a$  the zero temperature axion mass, and it saturates the DM density if at the temperature  $T_e$  of matter-radiation equality  $\rho_a \sim T_e^4$ , which yields  $m_a f_a^2 \sim T_e T_{\text{osc}} m_{\text{Pl}}$ . For  $Y_\theta > Y_\theta^c$  oscillations are delayed until some lower temperature  $T_* < T_{\text{osc}}$  when the kinetic energy is insufficient to overcome the potential barrier. In this case relic axions are overproduced and one has to lower the scale  $f_a$  to match  $\rho_a \approx \rho_{\text{DM}}$ . The numerical studies in Refs. [613, 614] indeed confirm that at fixed values of  $f_a$  the axion kinetic mechanism can produce more DM than the conventional misalignment scenario, and this opens up an interesting mass window for axion DM in the range  $m_a \in [10^2, 10^5] \mu\text{eV}$ .

The issue regarding how a large velocity  $\dot{\theta}_{\text{PQ}}$  can be generated was also addressed in Ref. [613], where a few possibilities were put forth. The basic idea is to introduce at the high scale an explicit breaking of the PQ symmetry via higher dimensional operators similar to the ones discussed in Section 2.11. In this way the potential gets tilted, and the axion starts moving towards the potential minimum acquiring a velocity. Of course an explicit breaking can shift the axion from the CP conserving minimum, so that while it must be effective in the early Universe, it must become negligible at lower temperatures. This can be arranged by assuming very flat potentials, so that the expectation value of the radial mode is initially large  $\langle \rho_a \rangle \gg f_a$  enhancing the effects of the operators that at later times, when eventually  $\rho_a$  relaxes to  $f_a$ , become sufficiently suppressed.

### 6.7. Super-heavy axions

In Sections 6.1–6.3, we showed how axions can be made more or less strongly coupled to SM fields through the dynamics of additional fields. In such models, the modification of the interaction strength was realized by altering the  $C_{af}$  parameters, defined in Eq. (109), while preserving the relation between the axion mass and decay constant  $f_a$  given in Eq. (108). In this Section we consider instead the possibility that the  $m_a$ – $f_a$  relation is modified (still keeping the solution of the strong CP problem), thus allowing for  $m_a \gtrsim 100$  keV axions (the 100 keV threshold is actually needed in order to evade (most) of the astrophysical constraints). We denote the latter *super-heavy* axions, in contrast to the canonical heavy axion regime up to  $m_a \lesssim 0.1$  eV. It should be first noted that such super-heavy axions are cosmologically unstable. For instance, the decay channel  $a \rightarrow \gamma + \gamma$  yields

$$\Gamma(a \rightarrow \gamma + \gamma) = \frac{g_{a\gamma}^2 m_a^3}{64\pi} = \frac{E/N - 1.92}{0.318 \text{ s}} \left( \frac{m_a}{100 \text{ keV}} \right)^5, \quad (298)$$

where in the last step we used the numerical values of the axion-photon coupling and the standard QCD  $m_a$ – $f_a$  relation<sup>72</sup> (cf. Eq. (118), (108) and (116)). Hence, barring an unrealistic cancellation in the axion-photon coupling, an axion with  $m_a \gtrsim 100$  keV cannot be DM.

Relaxing the relation between  $m_a$  and  $f_a$  requires some modifications of the gauge structure of the SM, particularly of the strong interaction sector. Yet, models which envisioned a large axion mass for some fixed couplings appeared early on (see, e.g., Refs. [123, 615–619]). The reason can be perhaps traced, at least in part, in the desire of avoiding the requirements of extremely small (experimentally prohibitive) axion couplings, which seemed an inevitable consequence of the experimental and astrophysical constraints. Early experimental tests of the original WW axion model (cf. footnote (17) in Section 2.7) ruled out the range  $f_a \lesssim 10^4$  GeV. According to the standard QCD relation in Eq. (108), this constraint implies an axion mass below 0.1 keV. However, light axions with masses below a few keV, can be easily produced in stars and impact their evolution possibly beyond what is observationally allowed (cf. Section 4). As it turns out, astrophysical constraints are considerably more restrictive than the original bounds, pushing the range of excluded couplings all the way up to  $f_a \sim 10^8$  GeV, implying extremely weakly interacting axions. Hence, somewhat surprisingly, the relatively weak bounds that ruled out the WW model brought to a rather dramatic result. The only two viable options left were either to make the axion extremely weakly coupled (invisible axion) or to make it heavier.<sup>73</sup> Either way, the axion could avoid the astrophysical bounds. Both roads were pursued. Models with a larger mass for fixed coupling have the additional appeal to be more easily tested in the laboratory while invisible axions were, at the time, truly thought to be beyond the foreseeable experimental potential (this, of course, before the seminal paper of Sikivie [413]).

Additional motivations for super-heavy axions can be found in connection with the PQ quality problem [122–127] (cf. Section 2.11), since explicit PQ-breaking terms would produce a shift, in some cases very large, to the axion mass (for an application in the context of Gamma Ray Bursts see [621]). This, however, would generically also shift the minimum of the axion potential away from its CP conserving point, thus spoiling the solution of the strong CP problem.<sup>74</sup> Indeed, some of the original models did not satisfy this condition.

An even earlier strategy to raise the axion mass was put forth by Holdom and Peskin [618], which pointed out that the contribution of the small color instantons to the axion potential could be made sizable by some nontrivial dynamics above the electroweak scale which reversed the sign of the color  $\beta$  function at some mass above 1 TeV or so. This idea was later reconsidered in Refs. [123, 619] in the context of GUTs, where it was argued that in the presence of new sources of chiral symmetry breaking at high energies there is no generic reason for the small instanton contribution to the axion potential to be aligned to the long-distance QCD contribution. Hence, also in this case raising the axion mass could have spoiled the solution to the strong CP problem.

Another, perhaps less economic, strategy is to assume that additional mass contribution emerges from the  $U(1)_{\text{PQ}}$  current anomaly, related to some hidden gauge sector with a confinement scale larger than  $\Lambda_{\text{QCD}}$ . One of the earliest attempts in this direction is the mirror world axion scenario, already introduced in Section 6.6.2. In this case, a whole new SM sector is introduced, with mirror and ordinary particles interacting with each other only gravitationally and, possibly, through some other very weak couplings, insufficient to bring the two sectors in thermal equilibrium during the cosmological evolution (cf. Section 6.6.2). The first example of such models [605] was based on a mirror extended GUT theory, with gauge group  $SU(5) \times SU(5)'$ , each one with its own PQ symmetry. A  $Z_2$  symmetry (*mirror parity*) for exchange of ordinary and mirror

<sup>72</sup>For fixed  $f_a$ , this provides a lower bound on the decay rate, compared to the case where  $m_a$  is enhanced.

<sup>73</sup>Another non-trivial option would have been to relax the hypothesis of the universality of the PQ current (see for instance the discussion at the beginning of Section 6.5). More recently, it was shown in Ref. [620] that an  $\mathcal{O}(10$  MeV) axion with the standard  $m_a$ – $f_a$  QCD relation could still be viable under the following conditions: *i*) the axion couples only to first generation fermions, with dominant decaying channel into electrons *ii*) the axion-pion coupling is suppressed (pion-phobia) and *iii*) large hadronic uncertainties in rare  $K$  decays are invoked. The UV completion of such an axion is however non-trivial, and it requires several extra fields beyond those of benchmark axion models.

<sup>74</sup>Turning up the argument, one can observe that generic PQ-breaking effective operators would spoil the axion solution for  $f_a$  above a few GeV or, if we forbid  $d = 5$  operators, for  $f_a$  a few TeV. Hence, such scales are interesting for a theoretical point of view. However, unless we make the axions super-heavy,  $f_a \sim 1$  TeV implies  $m_a \sim 1$  keV which is excluded by stellar argument. This is a strong motivation to consider super-heavy axions [622].



particles guaranties the equality of the  $\theta$  parameters in the two sectors. The  $U(1) \times U(1)'$  symmetry is reduced to just one PQ symmetry through the introduction of an  $SU(5) \times SU(5)'$  singlet complex scalar field, of PQ charge different from zero, that interacts with both ordinary and mirror Higgs. As explained in Section 6.6.2, in such a symmetric model the contribution to the axion mass from the hidden mirror sector would be a factor of  $\sqrt{2}$  larger than in the standard case. To have a larger mass gain, one has to assume a breaking of the mirror symmetry which does not, however, spoil the solution of the strong CP in both sectors. The way to do that is to have the mirror parity broken softly in the Higgs sector, without affecting the structure of the Yukawa couplings which has to remain the same in the two sectors (so that  $\arg \det Y_u Y_d = \arg \det Y'_u Y'_d$ ). In Ref. [605], it was assumed that the mirror parity is broken by soft terms and that the breaking of  $SU(5)'$  to the mirror SM happens at a much lower scale than in the ordinary sector. Since the coupling constant of  $SU(5)$  runs faster than that of  $SU(3)$ , it results that  $\Lambda'_{\text{QCD}} \gg \Lambda_{\text{QCD}}$ . Hence, the axion mass takes most of its contribution from the mirror sector.

Somewhat simpler models, which did not require a GUT but just a  $\text{SM} \times \text{SM}'$  gauge group, were considered in Ref. [606] and in its supersymmetric extension [607]. The mirror parity is spontaneously broken and induces a larger electroweak scale in the mirror sector, without affecting the Yukawa sectors. The higher mirror Higgs VEV generates heavier mirror fermions and, consequently, a faster renormalization group evolution and a larger confinement scale  $\Lambda'_{\text{QCD}} \gg \Lambda_{\text{QCD}}$ . These constructions were also motivated by the need to avoid Planck induced corrections which afflicted the model in Ref. [605] and could hence spoil the solution of the strong CP.

In recent times, several more models (see e.g. [623, 624]) reconsidered the  $Z_2$  symmetry to ensure CP conservation in super-heavy axion models with couplings all the way down to the TeV scale, hence accessible to detector searches such as ATLAS and CMS [624]. For instance, in the latter construction there is only one massless exotic quark transforming under  $SU(\mathcal{N})$  and an axion whose mass is induced by  $SU(\mathcal{N})$  instantons, so that in the limit of vanishing QCD coupling it remains massive. The problem with the two vacuum angles  $\theta_{\text{QCD}}$  and  $\theta_{\mathcal{N}}$  is again solved by imposing a  $Z_2$  symmetry that implies vacuum angles alignment. Another proposal that avoids the introduction of the discrete  $Z_2$  symmetry was put forth in [625] (see also [626, 627]). At high energies the gauge group is a product of factors  $SU(3)^{\mathcal{N}}$  and  $SU(3)_c$  is the diagonal subgroup that survives at low energies. Non-perturbative effects in each individual  $SU(3)$  factor generate a potential for the corresponding axion. The vacuum is naturally aligned to ensure  $\theta = 0$ , while the masses of these axions can be much larger than for the standard QCD axion, reaching values well above the GeV. Gaillard et al. [628] also consider a solution with massless new fermions. The solution is based on an enlarged but *unified* color sector, where unification solves the issue of the different  $\theta$  parameters that arise in the presence of two or more individual confining groups. The unified color group breaks spontaneously to QCD and to another confining group. Instantons of the unified group with a large characteristic scale contribute to breaking of a PQ symmetry and provide a source of large masses for the axions, so that no light pseudoscalar particles remain at low scales. This construction can yield both, dynamical and fundamental axions, with masses that can lie in the several TeV range.



## 7. Axions and...

This Section is devoted to the collection of various topics in which axion physics can be related to other open issues of the SM, such as massive neutrinos (Section 7.1), the baryon asymmetry (Section 7.2) and inflation (Section 7.3). We also discuss possible solutions of the DW issue (Section 7.4) as well as of the PQ quality problem (Section 7.5) and the embedding of axions in UV motivated frameworks, such as composite dynamics (Section 7.6) and grand unified theories (GUTs) (Section 7.7). Every topic is briefly sketched, with the scope of mainly redirecting to the relevant literature.

### 7.1. Axions and neutrino masses

Axions and neutrinos share various properties: they are both extremely lighter than charged leptons and possess a feeble coupling to SM fermions. In fact, the idea of connecting massive neutrinos with a spontaneously broken  $U(1)_{\text{PQ}}$  comes a long way. Early studies (such as [548, 629–631]) were actually motivated by the natural emergence of intermediate mass scales in grand-unified theories. In particular, the axion-neutrino connection has been largely explored in the context of the type-I seesaw [136, 283–285, 513, 631–636], in which the heavy RH neutrinos  $N_R$  obtain their mass  $M_R$  from a coupling  $N_R N_R \Phi$  to the PQ symmetry breaking scalar singlet  $\Phi$ . This connection is soundly motivated by the fact that the RH neutrino and the PQ symmetry breaking scales naturally fall in the same intermediate range  $M_R \sim f_a \sim 10^9 \div 10^{12}$  GeV, and further supported by the possibility of naturally producing a cosmological baryon asymmetry of the correct size via leptogenesis [632]. Considering instead only scalar extensions of the SM a simple setup based on the Zee model for radiative neutrino masses was discussed in Refs. [637, 638], while extensions based on the type-II (III) seesaw and other radiative neutrino mass models were explored later on [639–641]. Scenarios implementing Dirac neutrinos have also been discussed [642–645]. The latter, however, miss the main motivation behind the axion-neutrino connection, that is the identification of the PQ scale with the scale suppressing neutrino masses.

The constructions above often aim at providing a minimal SM extension addressing most of the shortcomings of the SM. It is fair to say, however, that they often lack in predictivity being the collection of somewhat orthogonal ingredients. The most genuine signature of the axion-neutrino connection would in fact be an axion coupling to neutrinos, of the type  $\mathcal{L} \supset (m_\nu/f_a) a \bar{\nu} i \gamma_5 \nu$ , which is clearly beyond any experimental accessibility due to the huge  $m_\nu/f_a$  suppression. Hence, any chance for predictivity beyond the single ingredients in isolation (e.g. Type-I seesaw and PQ mechanism) can only arise indirectly as a self-consistency of the whole setup.

A non-trivial step in this direction was achieved recently, in the context of the Standard Model–Axion–Seesaw–Higgs inflation portal (SMASH) model [283–285], in which the modulus of the PQ scalar is also the key ingredient for successful inflation. A robust prediction of this setup is that the PQ symmetry is broken after inflation and never restored after it, thus making the range for axion DM in principle calculable.

A different predictive approach, involving also flavour, was instead pursued recently in Ref. [523], which classified all the generation dependent  $U(1)$  symmetries which, in the presence of two leptonic Higgs doublets, can reduce the number of independent high-energy parameters of type-I seesaw to the minimum number compatible with non-vanishing neutrino mixings and CP violation in the leptonic sector. This setup leads to definite predictions for the charged leptons and neutrino mass matrices and, if extended to the quark sector, necessarily leads to a QCD anomalous  $U(1)_{\text{PQ}}$  [522], thus predicting the existence of a QCD axion, with couplings to SM fermions fixed in terms of SM fermion masses and mixings.

### 7.2. Axions and baryon asymmetry

The strong CP-violating parameter must be extremely small today, as required by the non-observation of the nEDM. However, if the smallness of the theta angle were due to the cosmological evolution of an axion field, it is plausible that  $\theta$  was  $\mathcal{O}(1)$  in the early Universe and, conceivably, such source of CP violation could have played a role for baryogenesis. This idea was first put forth by Kuzmin, Tkachev and Shaposhnikov in Ref. [646], which considered the possible effects on electroweak baryogenesis of strong CP-violation related to an axion field with a large background value. The conclusions of this work were, however, negative: SM baryon number violating processes are only effective at temperatures above  $T_{\text{EW}} \sim 100$  GeV, however, at

these temperatures strong CP violating effects are suppressed by an exceedingly small exponential factor  $\exp(-8\pi^2/g_s^2)$  where  $g_s$  is the strong gauge coupling. They concluded that the only possibility was to diminish the temperature of the electroweak phase transition down to  $\Lambda_{\text{QCD}}$ , and to require that no entropy was injected in the plasma after the phase transition to avoid diluting the baryon asymmetry. This, however, also implied that the Universe got over-dominated by axion DM, contrary to observations.

More recently, this problem was reconsidered in Ref. [647] in the context of cold electroweak baryogenesis (see e.g. Refs. [648, 649]), a scenario that can lead to a very efficient production of baryon number if the electroweak symmetry breaking is triggered through a fast tachyonic instability (‘Higgs quenching’) and if it occurs in a range of temperatures  $10 \text{ MeV} \lesssim T_{\text{EW}} \lesssim 1 \text{ GeV}$ . In this scenario baryon production occurs strongly out of equilibrium so that there are no washout effects and the efficiency can be very large. The corresponding rates can be described in terms of an effective equilibrium temperature  $T_{\text{eff}}$  much larger than  $T_{\text{EW}}$  and one or two orders of magnitude larger than the reheating temperature of the plasma after the phase transition  $T_{\text{RH}}$ . The baryon-to-photons ratio scales as  $(T_{\text{eff}}/T_{\text{RH}})^3$  so that it can easily reach the observed value. Axion oscillations start well after reheating, and are not delayed with respect to the conventional scenario, so that the cold DM energy density from axion misalignment remains as in the standard case.

A different approach to overcome the no-go of Ref. [646] was put forth more recently in Refs. [650, 651]. Instead of delaying the electroweak phase transition down to 1 GeV or below, the idea is to increase the QCD confinement scale  $\Lambda_{\text{QCD}} \gtrsim T_{\text{EW}}$ . This is achieved by promoting the strong coupling to a dynamical quantity, which evolves through the vacuum expectation value of a singlet scalar field that mixes with the Higgs field. QCD confinement and electroweak symmetry breaking occur simultaneously close to the TeV scale, providing large CP violation from an axion field value  $\theta(T)$  of  $\mathcal{O}(1)$  together with baryon number violation and the out-of-equilibrium condition from the phase transitions, which are expected to be first order.

Finally, Ref. [652] proposed a mechanism wherein the cosmological matter-antimatter asymmetry stems from initial conditions in which the axion field is fast rotating. A  $\dot{\theta} \neq 0$  corresponds to an asymmetry-density of the PQ charge, which is converted into the baryon asymmetry via QCD and electroweak sphalerons. This rotation can be induced at the PQ scale by effective operators that break explicitly the symmetry, tilting the bottom of the mexican-hat potential. However, these operators must fade away rapidly enough at lower temperatures not to spoil the solution of the strong CP problem, that is the zero temperature minimum of the axion potential must remain determined by the QCD non-perturbative effects. The mechanism encounters difficulties because to preserve the baryon asymmetry from being washed out,  $\dot{\theta}$  must remain large down to the temperature when sphaleron transitions get out of equilibrium. This, however, implies that at the QCD phase transition the axion kinetic energy would dominate the potential energy, thus delaying the onset of oscillations which results in an unacceptable overproduction of DM. The proposed way out is to engineer a way to increase the temperature of the electroweak phase transition in order to suppress sphalerons transitions at much earlier times. It should also be noted that the initial velocity required by this mechanism is extremely large. In terms of the relevant time scale at PQ symmetry breaking,  $H_{\text{PQ}}^{-1}$ , values of  $\dot{\theta}_{\text{PQ}} \gtrsim 10^8 H_{\text{PQ}}$  are required. It remains to be seen if axion potentials that can realise this condition at  $T_{\text{PQ}}$ , without incurring into problems at lower temperatures, can be constructed.

### 7.3. Axions and inflation

A period of accelerated expansion in the very early universe called *inflation* [653, 654] is usually invoked to address various problems of the standard cosmology, namely the absence of monopoles [205, 654, 655] and domain walls [656], the fact that the universe appears to be homogeneous and isotropic (the *horizon problem*) [657], and the fact that the universe appears to possess fine-tuned initial conditions that lead to its exceptionally flatness already at recombination (the *flatness problem*). One class of inflationary models relies on the dynamics of a field that is responsible for the inflationary period, the *inflaton*, which evolves under the influence of a nearly flat potential. The equation of motion for the inflaton field (denoted by  $\phi$ )

evolving under the potential  $V(\phi)$  is similar to Eq. (152),

$$\ddot{\phi} + 3H\dot{\phi} + \frac{1}{R^2}\nabla^2\phi + \frac{dV(\phi)}{d\phi} = 0, \quad (299)$$

giving the simplest model of *single field* inflation. For super-horizon modes, the spatial derivative can be neglected. A nearly flat potential grants an inflationary period in which the inflaton evolves under a *slow-roll* dynamics if i)  $\ddot{\phi} \ll H\dot{\phi}$ , and ii)  $\dot{\phi}^2 \ll V(\phi)$ . Condition i) leads to  $3H\dot{\phi} \simeq -dV(\phi)/d\phi$ , while condition ii) gives the equation of state

$$w_\phi = \frac{\frac{1}{2}\dot{\phi}^2 - V(\phi)}{\frac{1}{2}\dot{\phi}^2 + V(\phi)} \simeq -1. \quad (300)$$

If both conditions i) and ii) are satisfied, the energy density of the  $\phi$  field is constant during inflation, which grants a quasi-exponential growth of the scale factor according to Eq. (140).

Different models have been considered in order to embed the inflation mechanism into an axion framework. One possibility consists in identifying the inflaton field with the radial mode of the PQ field  $\rho_a$ , see Eq. (79), assuming a non-minimal coupling of the PQ field with gravity [287]. This model circumvents the problem that for relatively high values of the Hubble rate during inflation  $H_I$ , axion isocurvature fluctuations during inflation are too large with respect to what is allowed by measurements [239], see Section 3.5. In fact, in this model the radial field has not yet relaxed to its minimum value and evolves in the regime  $\rho_a \gg f_a$ , suppressing isocurvature fluctuations. At sufficiently high temperatures, the PQ potential in Eq. (78) can be approximated by a quartic potential: such a form of inflaton potential has been excluded to a high level of confidence by the measurements of the CMBR spectra by the *Planck* mission [309, 658, 659]. For this reason, a non-minimal coupling to gravity  $\xi$  is introduced to circumvent the bounds from the *Planck* mission, so that the potential at large values of  $\rho_a$  is flattened out and the model reconciles with observations [660]. A different kind of embedding has been carried out in the SMASH model [283–285], in which the Lagrangian (in the Jordan frame) contains a term which elaborates over the Higgs inflation model [661] to include a mixture of the PQ complex multiplet  $\Phi$  and of the Higgs field doublet  $H$ ,

$$S \supset \int d^4x \sqrt{-g} \left[ \frac{\bar{M}^2}{2} + \xi_H |H|^2 + \xi_\Phi |\Phi|^2 \right] \mathcal{R}, \quad (301)$$

where  $\bar{M}$  is a mass scale related to the Planck mass, and  $\xi_H, \xi_\Phi$  are dimensionless non-minimal couplings to the curvature scalar  $\mathcal{R}$ . Having the inflaton direction as a mixture of the radial modes of  $H$  and  $\Phi$  provides a solution of the unitarity problem of standard Higgs inflation [662, 663].

Within the single field slow-roll inflation model, it is possible to obtain predictions for the scalar and tensor power spectra on super-horizon scales. As discussed in Section 3.5, tensor modes for single-field inflation are defined in terms of the tensor-to-scalar ratio  $r$  which, if measured in the future at  $r \sim 10^{-3}$ , would shut off the **PreI** scenario completely [173, 268, 287, 664–666], see also Fig. 3. It has recently been shown [289] that a model of inflation with the SM Higgs field, in which the Higgs field is coupled non-minimally to *Palatini* gravity [667] leads to an inflation energy scale  $H_I \sim 10^8$  GeV and a low tensor-to-scalar ratio  $r \sim 10^{-13}$ . In this model, axion isocurvature fluctuations that would evade the current bounds can be accommodated, and it is then possible to realise axion DM in the **PreI** scenario with a value of the axion energy scale of the order of  $\sim 10^{14}$  GeV.

The QCD axion itself could have driven inflation, evolving via a series of tunnelling events in the so-called chain inflation model [668, 669]. Assuming an axion model in which the continuous shift symmetry is broken down to a discrete  $\mathbb{Z}_{N_{\text{DW}}}$  symmetry, with a large number of local minima  $N_{\text{DW}}$ , and an additional soft breaking term with height  $\eta$ , the potential reads

$$V(a) = V_0 \left[ 1 - \cos \left( \frac{N_{\text{DW}} a}{v_a} \right) \right] + \eta \cos \left( \frac{a}{v_a} \right). \quad (302)$$

The axion evolves in one of the false vacua described by the potential in Eq. (302), providing about one  $e$ -fold of inflation before tunnelling to the next false vacuum and approaching the true vacuum of the theory. Chain

inflation is a viable model for solving the horizon, entropy and flatness problem of standard cosmology and for generating the right amount of adiabatic cosmological perturbations [670, 671], although a considerable effort in model building is necessary since a large number of tunnelling events,  $\gtrsim 10^8$  per Hubble volume per  $e$ -fold, are required [672].

#### 7.4. Solutions to the domain walls problem

The DW problem arises from the fact that the axion field  $a$ , being an angular variable, takes values in the interval  $[0, 2\pi v_a)$ . The axion potential is periodic in  $a$  with period  $\Delta a = 2\pi v_a/N_{\text{DW}}$ , and thus it enjoys an exact  $\mathbb{Z}_{N_{\text{DW}}}$  discrete symmetry. Once at  $T \sim \Lambda_{\text{QCD}}$  the non-perturbative QCD effects lift the axion potential,  $N_{\text{DW}}$  degenerate vacua appear. In general the initial value of  $a$  at the bottom of the originally flat potential is randomly selected and it differs in different patches of the Universe, so that in each patch the axion will eventually flow towards a different minimum, breaking spontaneously  $\mathbb{Z}_{N_{\text{DW}}}$ . DWs will then form at the boundaries between regions of different vacua. The cosmological DW problem [230] consists in the fact that the energy density of the DWs would largely overshoot the critical density of the Universe. There are, however, two scenarios in which this there is no DW problem: (i) The first corresponds to the pre-inflationary scenario in which an initial patch characterised by some value of  $\theta_i$  gets exponentially inflated to super-horizon scales, so that after inflation the whole observable Universe is characterised by a unique minimum of the axion potential, and is thus free from topological defects. (ii) The second scenario encloses the models in which  $N_{\text{DW}} = 1$ , so that there is a single value of  $\theta$  where the potential has a minimum. Although the vacuum is unique, a particular type of DWs still form, but they are harmless. The reason can be pictured as follows: when  $U(1)_{\text{PQ}}$  gets broken, strings form, and in circulating around a string  $\theta$  changes by  $2\pi$ . When the temperature approaches the QCD scale and the axion potential gets tilted, the unique minimum  $\theta = 0$  is selected. Still, in a two dimensional region attached to the string the phase must jump from 0 to  $2\pi$  and back to 0, and this region corresponds to a wall with one edge attached to the string. However, a configuration of walls bounded by strings tends to rapidly collapse [210], and eventually the whole system of walls and strings disappears without ever coming to dominate the energy density of the Universe. Hence, axion models with  $N_{\text{DW}} = 1$  are safe with respect to the DW problem also in post-inflationary scenarios.

A first example of a construction with  $N_{\text{DW}} = 1$  is the original KSVZ model [111, 112] that we have reviewed in Section 2.7.1, where a single pair of electroweak singlet exotic quarks in the fundamental of  $SU(3)_c$  yields a colour anomaly  $2N = N_{\text{DW}} = 1$ . Georgi and Wise [673] considered instead the possibility of canceling part of the QCD anomaly of DFSZ-type of models by introducing suitable representations of exotic quarks of KSVZ-type with PQ charge of the opposite sign, so that a total anomaly  $2N = 1$  eventually results.

A different kind of construction features an apparent value  $N_{\text{DW}} > 1$ , while the physical number of DW is in fact  $N_{\text{DW}} = 1$ . These constructions rely on the introduction of extra symmetries, in such a way that the degenerate vacua of the axion potential are connected by symmetry transformations. The first realisation of this mechanism is due to Lazarides and Shafi (LS) [674] which observed that the DW problem does not exist if the discrete subgroup  $\mathbb{Z}_{N_{\text{DW}}}$  in  $U(1)_{\text{PQ}}$  can be embedded in the center of a continuous gauge group, and they provided a neat example based on the GUT symmetry  $SO(10) \times U(1)_{\text{PQ}}$ . A different possibility was proposed in Ref. [139]. The axion arises from an accidental  $U(1)$  enforced on the potential of a scalar multiplet  $Y_{\text{LR}}$  by a gauge symmetry  $SU(\mathcal{N})_L \times SU(\mathcal{N})_R$ .  $Y_{\text{LR}}$  transforms under the group as  $(\mathcal{N}, \overline{\mathcal{N}})$  and is responsible for the spontaneous breaking of the gauge group down to  $SU(\mathcal{N})_{L+R}$ . Although the construction gives a QCD anomaly with coefficient  $N = \mathcal{N}/2$ , all the minima can be connected by gauge transformations corresponding to the center  $\mathbb{Z}_{\mathcal{N}}$  of the unbroken group, and hence they are gauge equivalent. While in the original LS model  $\mathbb{Z}_{N_{\text{DW}}}$  was embedded into a local group, embedding in global groups can also yield the same result. For example, models with global family groups were considered in Ref. [675].

A different type of constructions in which  $N_{\text{DW}} = 1$  can be engineered, rely on the presence of more than one global  $U(1)$  symmetry [676]. The anomalous PQ will in general correspond to a combination of the various Abelian groups, and it can be arranged so that QCD effects break this specific combination to the trivial subgroup  $\mathbb{Z}_1$ .

A horizontal realisation of the PQ-symmetry that, together with  $B - L$  global invariance, can solve the DW problem for any arbitrary number of fermion generations was discussed in Ref. [677]. Other models enforce  $N_{\text{DW}} = 1$  making use in different ways of generation dependent PQ symmetries. For example a partial cancellation of the anomaly contributions between different generations can be arranged [115, 516], or the PQ charges are chosen in such a way that two generations give vanishing contributions to the anomaly [522], or more in general it can be assumed that some SM quark flavours have a special status with respect to the PQ symmetry [535], for example it can happen that only one or two out of all the SM quarks contribute to the anomaly [520]. Of course, as was discussed in Section 6.5, all these models feature flavour violating axion couplings, and can be thoroughly tested by searching for flavour changing processes.

Models for which none of the above two conditions (i) and (ii) are satisfied, that is the PQ symmetry is broken after inflation, and  $N_{\text{DW}} > 1$  gives rise to the same number of physically inequivalent degenerate vacua, can also remain viable, but additional assumptions are needed. The DW problem can be disposed of in a simple way by introducing an explicit breaking of the PQ symmetry so that the degeneracy between the different vacua is removed and there is a unique minimum of the potential [230]. Breaking explicitly the PQ symmetry is, however, a delicate issue: sufficiently large breaking effects are needed to guarantee that regions trapped in false vacua will cross over to the true vacuum before DWs start dominating the Universe energy density. However, at the same time they should not be too large, otherwise they would spoil the PQ solution. The present limit  $\theta \lesssim 10^{-10}$  still leaves a viable region in parameter space where these two conditions can be simultaneously matched [27, 29].

#### 7.5. Solutions to the Peccei Quinn quality problem

As we have discussed in Section 2.11 in order to ensure the effectiveness of the PQ mechanism in solving the strong CP problem a strong requirement needs to be satisfied: the PQ symmetry must remain a good symmetry well beyond the level of renormalizable operators, and arguably up to effective operators of dimensions  $d > 10$ . However, the PQ symmetry is a global symmetry, and in QFT global symmetries are not deemed to be fundamental or exact. Moreover, the PQ symmetry is anomalous, and as such at the quantum level it is not even a real symmetry. Analogies with baryon and lepton  $U(1)$  symmetries in the SM, which are also global and anomalous, but whose origin as accidental symmetries is well understood, naturally lead to speculate whether the PQ symmetry might also arise accidentally, in the sense that other fundamental symmetries (gauge and Lorentz) might forbid, up to the required dimension, operators that do not conserve the PQ charge. Several constructions have been put forth to realise this idea. Probably the simplest possibility is that of a discrete gauge symmetry. For instance a  $\mathbb{Z}_n$  acting on  $\Phi$  as  $\Phi \rightarrow e^{i2\pi/n}\Phi$  would forbid all effective operators  $(\Phi^\dagger\Phi)^m\Phi^k$  with  $k < n$ . A possible way to generate discrete gauge symmetries in 4-dimensional QFT was suggested in Ref. [678]. Consider a  $U(1)$  gauge symmetry under which the axion multiplet  $\Phi$  carries charge 1, while a second field  $\xi$  carries charge  $n$ :  $\Phi \rightarrow e^{i\alpha}\Phi$ ,  $\xi \rightarrow e^{in\alpha}\xi$ . Suppose that  $\xi$  undergoes condensation at some high-energy scale  $\langle\xi\rangle \gg f_a$ . The invariance of the VEV  $\langle\xi\rangle \rightarrow e^{in\alpha}\langle\xi\rangle$  with  $\alpha = 2\pi/n$  corresponds to a  $\mathbb{Z}_n$  discrete gauge symmetry, unbroken above  $f_a$ , under which  $\Phi$  transforms as  $\Phi \rightarrow e^{i\alpha}\Phi = e^{i2\pi/n}\Phi$ . This ensures that the first allowed operator breaking PQ explicitly is  $\Phi^n$ . Mechanisms with large local discrete symmetries have been for example invoked in Ref. [133–136].

Other models rely on the introduction of a new local Abelian symmetry  $U(1)'$  that, as in Ref. [124], can be directly added to enlarge the SM gauge group. In this reference two singlet scalars  $\Phi$  and  $S$  are also introduced, with  $U(1)'$  charges respectively  $p$  and  $q$ , and these charges are chosen in such a way that the lowest order effective operator that breaks the PQ symmetry, namely  $(S^\dagger)^p\Phi^q$ , is of the required high dimension  $d = p + q$ . Ref. [126] considers instead a supersymmetric GUT extension  $E_6 \times U(1)'$ , where the usual trilinear superpotential Yukawa coupling  $\mathbf{27}^3$  is forbidden by the new Abelian symmetry, and is replaced by a coupling involving a new unconventional representation  $\mathbf{27}_1\mathbf{27}_{-1}\overline{\mathbf{351}}_0$ , where subscripts refers to the  $U(1)'$  gauge charges. A global PQ symmetry under which with  $\mathcal{X}(\mathbf{27}) = 1$  and  $\mathcal{X}(\overline{\mathbf{351}}) = -2$  arises accidentally, and the lowest order gauge invariant PQ violating operators  $\mathbf{27}^6$  or  $\overline{\mathbf{351}}^6$  are of the required large dimension. Soft supersymmetry breaking effects might, however, endanger this solution [142]. Ref. [137] considers instead the possibility of embedding the PQ symmetry into a gauged  $U(1)'$ , which is rendered non anomalous by adding exotic fermions coupled to the SM only via gauge interactions, so that



the subset of gauge rotations acting only on the SM quarks can be interpreted as an accidental (global and anomalous)  $U(1) \subset U(1)'$ . Ref. [138] promotes baryon number to a local gauge symmetry by canceling the anomaly via the introduction of exotic fermions which play the role of KSVZ exotic quarks. The authors show that the PQ symmetry remains sufficiently protected by this gauged baryon number.

Other approaches exploit instead new non-Abelian gauge groups. Georgi, Hall and Wise [122] provided the first example<sup>75</sup> of an accidental PQ symmetry arising from a grand-unified gauge group based on  $SU(9)$ , which incorporates the usual  $SU(5)$  GUT as a subgroup. The construction is non-trivial, since it involves several  $SU(9)$  representations (left-handed fermions in a  $\mathbf{36} \oplus 5 \times \bar{\mathbf{9}}$  and scalar fields in a  $\mathbf{80} \oplus 5 \times \mathbf{9} \oplus \mathbf{126}$ ). Writing the most general renormalizable Lagrangian allowed by the  $SU(9)$  gauge symmetry enforces a QCD anomalous  $U(1)$  symmetry that is spontaneously broken at the unification scale. Although in this work the authors did not explicitly address the question of at which operator level the PQ breaking is explicitly broken, one can see that this happens due to the “baryon-like” invariant  $\epsilon_{ijk\dots} \mathbf{9}^i \mathbf{9}^j \mathbf{9}^k \dots$  and hence at  $d = 9$ . The complexity of this construction shows that it is highly nontrivial to get an accidental PQ symmetry in GUTs (without resorting to extra gauged  $U(1)$ ’s) and we are not aware of other successful attempts, apart for the original one in Ref. [122]. Instead the construction discussed in Ref. [139] takes inspiration from a type of flavour models in which the SM Yukawa couplings are promoted to dynamical scalar fields  $Y(x)$  transforming in the bi-fundamental of a gauge group  $SU(3)_L \times SU(3)_R$ . As it was remarked in Ref. [679], gauge invariant operators in the scalar potential for  $Y(x)$  are Hermitian and thus respect an accidental  $U(1)$  rephasing invariance, with the sole exception of  $\det Y(x)$  which is non-Hermitian and of dimension  $d = 3$ . Then, generalising the construction to an  $SU(\mathcal{N})_L \times SU(\mathcal{N})_R$  invariant potential with  $\mathcal{N} > 4$ , the dimension of the symmetry breaking operator is promoted to  $d = \mathcal{N}$ , so that the quality of the accidental  $U(1)$  remains determined by the dimension of the gauge group which can be arbitrarily chosen. Scalar-gauge theories in which  $Y(x)$  transforms as the symmetric (anti-symmetric) of  $SU(\mathcal{N})$  broken into  $SO(\mathcal{N})$  ( $Sp(\mathcal{N})$ ) also lead to an accidental Goldstone for  $\mathcal{N} > 4$  [680], and they might be used to construct models for the PQ protection along the lines of [139].

Ref. [140] introduces an exotic sector equipped with an  $SU(\mathcal{N})$  gauge symmetry where a hidden baryon number  $U(1)_{B_{\mathcal{N}}}$  appears accidentally, similarly to what happens in the SM with ordinary  $U(1)_B$ . However, differently from the SM where  $B$  violating effective operators are allowed already at  $d = 6$ , the  $B_{\mathcal{N}}$  violating operators of lowest dimension are the gauge (and, assuming  $\mathcal{N}$  even, also Lorentz) invariant  $SU(\mathcal{N})$  singlets  $\epsilon_{\alpha_1 \alpha_2 \dots \alpha_{\mathcal{N}}} Q^{\alpha_1} Q^{\alpha_2} \dots Q^{\alpha_{\mathcal{N}}}$  with dimension  $d = 3\mathcal{N}/2 \gg 3$ . In the presence of fermion species chiral under  $SU(\mathcal{N}) \times SU(2)_C$  a  $U(1)_{B_{\mathcal{N}}}$ - $SU(3)_C^2$  anomaly can arise, so that the new baryon symmetry can act in the SM as a PQ symmetry. In Ref. [146] instead the SM quark flavour symmetry has been used directly, and the required level of suppression for the PQ breaking operators is obtained by assuming that quark masses are generated radiatively, so that the Yukawa couplings do not correspond to fundamental symmetry breaking scalars, but result from a more complicated set of spurions that allow to keep the PQ symmetry exact up to  $d = 12$ .

Composite axion models (reviewed in Section 7.6) are also well suited to arrange for approximate PQ symmetries preserved up to operators of high dimension. One of the first constructions exploiting compositeness with this aim was the Randall model [141]. The relevant gauge symmetry is  $SU(\mathcal{N}) \times SU(m) \times SU(3)_C$ . Exotic fermions transform under the group factors with suitable chiral assignments in such a way that an accidental global  $U(1)$  arises, which is non-anomalous with respect to the first two factors but has an  $SU(3)_C$  anomaly.  $SU(\mathcal{N})$  becomes strong at a large scale breaking spontaneously  $SU(m)$  (much alike  $SU(3)_C$  condensates in the SM break spontaneously  $SU(2)_L$ ) and breaking also the global  $U(1)$ , but not  $SU(3)_C$ . In this model the lowest dimensional operator consistent with the gauge and Lorentz symmetries, but not respecting the  $U(1)$ , can be built with  $2m$  uncoloured fermions. Hence the quality of the PQ symmetry is controlled by the dimension of the  $SU(m)$  group. Other composite models for PQ symmetry protection exploiting similar ideas can be found in Refs. [142–145].

---

<sup>75</sup>Incidentally, this is also the first paper where the issue of the PQ quality problem was clearly laid down.

### 7.6. Axions and composite dynamics

Composite axion models were originally motivated by the possibility of dynamically explaining the hierarchy  $f_a \ll m_{\text{Pl}}$ , as a consequence of a confining non-abelian gauge theory, largely inspired by pions and chiral symmetry breaking in QCD as well as technicolor models for the electroweak scale.

For instance, the original model of Kim [470] (see also [473]) was based on a new gauge group  $SU(\mathcal{N})$  that confines at a scale  $\Lambda_{SU(\mathcal{N})} \sim f_a$ , and comprises the following vector-like fermion content with transformation properties under  $SU(\mathcal{N}) \times SU(3)_c$ :  $\psi_{L,R} \sim (\mathcal{N}, 3)$  and  $\xi_{L,R} \sim (\mathcal{N}, 1)$ . In the limit of zero fermion masses and for  $g_s \rightarrow 0$  the model has an  $SU(4)_L \times SU(4)_R \times U(1)_V$  global symmetry, which is spontaneously broken down to  $SU(4)_{L+R} \times U(1)_V$  by the fermion condensates  $\langle \bar{\psi}_L \psi_R \rangle = \langle \bar{\xi}_L \xi_R \rangle \sim \Lambda_{SU(\mathcal{N})}^3$ . The resulting 15 NGB transform as  $1 + 3 + \bar{3} + 8$  under  $SU(3)_c$ . The color singlet, with a  $(\bar{\psi}_L \psi_R - 3 \bar{\xi}_L \xi_R)$  content, is identified with the composite axion and  $U(1)_{\text{PQ}}$  corresponds to the  $[(T^{15})_L \times \mathbb{I}_R + \mathbb{I}_L \times (T^{15})_R]/\sqrt{2}$  broken generator of  $SU(4)_L \times SU(4)_R$ , with  $T^{15} = \frac{1}{2\sqrt{6}} \text{diag}(1, 1, 1, -3)$  belonging to the  $SU(4)$  Cartan sub-algebra, so that the  $U(1)_{\text{PQ}}$  is anomalous under QCD but not under  $SU(\mathcal{N})$ . When  $g_s$  is turned on, the  $SU(4)_{L+R}$  global symmetry is explicitly broken down to the gauged  $SU(3)_c$ . The axion gets a tiny mass from QCD instantons, since the associated current is QCD anomalous

$$J_{\text{PQ}}^\mu = \frac{1}{2\sqrt{6}} [\bar{\psi} \gamma^\mu \gamma_5 \psi - 3 \bar{\xi} \gamma^\mu \gamma_5 \xi] \quad \implies \quad \partial_\mu J_{\text{PQ}}^\mu = \frac{g_s}{16\pi^2} \frac{\mathcal{N}}{2\sqrt{6}} G\tilde{G}, \quad (303)$$

while the other pseudo NGB in non-trivial color representations get masses of order  $g_s \Lambda_{SU(\mathcal{N})}/(4\pi)$  via perturbative gluon loops (similarly to the QED contribution to the mass of the charged pion of order  $e \Lambda_{\text{QCD}}/(4\pi)$ ). The axion couplings to SM fields in Kim's composite axion model follow from the expression of the PQ current in Eq. (303) and from the definition of the 'axi-pion' constant [103]  $\langle 0 | J_{\text{PQ}}^\mu | a \rangle = i F_a p^\mu$  (with  $F_a$  of order  $\Lambda_{SU(\mathcal{N})}$ , analogously to  $f_\pi \sim \Lambda_{\text{QCD}}$ ). Matching with the axion effective Lagrangian in Eq. (36) one gets  $f_a = \sqrt{6} F_a / \mathcal{N} \sim \sqrt{6} \Lambda_{SU(\mathcal{N})} / \mathcal{N}$ . Note that similarly to KSVZ-like models where SM fields ( $f$ ) are uncharged under the PQ, the model-dependent axion coupling to SM fermions vanish,  $c_f^0 = 0$ , and also  $g_{a\gamma}^0 = 0$ . The latter actually depends on the specific choice of the exotic fermion representations in Kim's model. By assigning to them non-trivial electroweak quantum numbers one can also get direct EM anomaly contributions to  $g_{a\gamma}^0 \neq 0$  [103], as discussed in Section 6.1.1.

It should be noted that in Kim's original composite axion model, similarly to standard KSVZ constructions, vector-like exotic fermion masses need to be forbidden in order not to spoil the whole framework. In fact, bare mass terms,  $m_{\psi, \xi}$ , even if  $\ll \Lambda_{SU(\mathcal{N})}$ , would still misalign the minimum of the QCD axion potential unless extremely suppressed, since they contribute to the composite NGB axion mass as  $m_a \sim \sqrt{\Lambda_{SU(\mathcal{N})} m_{\psi, \xi}}$ . The model is also prone to the PQ quality problem (see Section 2.11), since Planck-suppressed  $U(1)_{\text{PQ}}$  breaking operators, which are in principle allowed by gauge symmetries, could spoil the solution of the strong CP problem. This motivated the construction of composite axion models in which an extra, chiral gauge symmetry avoids the presence of exotic fermion mass terms and protects as well from higher-order PQ symmetry breaking operators. Models of this type are briefly reviewed at the end of Section 7.5.

### 7.7. Axions and GUTs

Grand Unified Theories (GUTs) provide a rationale for the large value of the axion decay constant  $f_a$ , which for phenomenological reasons must lie between  $10^8$  GeV and the Planck scale. In fact, if the axion field is embedded into a scalar representation responsible for the breaking of the GUT symmetry (e.g. in the global phase of a complexified adjoint representation) one has  $f_a = v_a / N_{\text{DW}} \approx M_G / N_{\text{DW}}$ , where  $M_G \gtrsim 10^{15}$  GeV denotes the scale of GUT breaking, which is bounded from below by the non-observation of proton decay. Models of this type, in which the global  $U(1)_{\text{PQ}}$  commutes with the GUT group, were first proposed in the context of  $SU(5)$  [681] and  $SO(10)$  [682] (for modern variants see also [683–686]). A remarkable feature of these models is the connection between proton decay and standard axion searches, which will start to probe the GUT-scale axion in the coming decade (cf. the reach of Casper-Electric and ABRACADABRA in Section 5.3). For instance, the minimal  $SU(5) \times U(1)_{\text{PQ}}$  model of Ref. [684], based on the original Georgi-Glashow [687] field content plus a  $24_F$  representation that fixes both neutrino masses and gauge coupling



unification [688–690], provides a rather sharp prediction (arising from gauge coupling unification and proton decay constraints) for the value of the axion mass  $m_a \sim 5 \text{ neV}$ , setting a well-definite target for axion DM experiments. Regarding the connection with axion DM let us recall that, in order not to over-produce axion DM, GUT-scale values of  $f_a$  require the PQ symmetry to be broken before inflation (pre-inflationary PQ breaking scenario) together with a certain tuning of the initial misalignment angle to small values (for  $f_a \sim 10^{15} \text{ GeV}$ ,  $\theta_i \sim 1\%$ ). Note that values of  $f_a \ll M_G$  can still be obtained for  $v_a \sim M_G$ , but these require values of  $N_{\text{DW}}$  is unrealistically large. Another class of models which allows for  $f_a \ll M_G$  and that at the same time can be compatible with post-inflationary PQ breaking scenarios is based on  $SO(10)$  GUTs in which the axion is embedded into a representation responsible for an intermediate symmetry breaking stage, possibly related to the scale of right-handed neutrinos [630, 683, 691–694]. In such a case, however, the scale  $f_a$  turns out to be “sliding”, since it is only weakly constrained by gauge coupling unification [683].

Regarding the structure of axion couplings in GUTs, these are fixed up to some minor model-dependent factors, thus providing a well-defined and motivated benchmark for axion searches. Most notably, the value of the group theory factor that determines the axion coupling to photons is fixed to be  $E/N = 8/3$ . This can be seen from the explicit expression

$$\frac{E}{N} = \frac{\text{Tr } Q^2}{\text{Tr } T_C^2} = \frac{\text{Tr } (T_L^3)^2 + \frac{5}{3} \text{Tr } T_Y^2}{\text{Tr } T_C^2} = \frac{8}{3}, \quad (304)$$

where  $Q = T_L^3 + \sqrt{5/3} T_Y$ , in terms of the GUT-normalized hypercharge generator  $T_Y$ . This result follows from the fact that all the generators of the GUT group, and in particular  $T_C, T_L^3$  and  $T_Y$ , have the same normalization.<sup>76</sup>

The Yukawa sector of an axion GUT model is similar (as far as concerns global PQ charges) to that of the DFSZ-I model with Yukawa Lagrangian in Eq. (91). E.g. in minimal  $SU(5)$  one has (neglecting for simplicity neutrino masses and corrections to the charged fermion mass relations)

$$\mathcal{L}_{\text{SU}(5)}^Y \supset -Y_{10} 10_F 10_F \bar{5}_{H_u} - Y_5 \bar{5}_F 10_F \bar{5}_{H_d}, \quad (305)$$

which after projecting onto the SM components matches Eq. (91), with the following GUT-scale boundary values for the Yukawa matrices:  $Y_{10} = Y_U$  and  $Y_5 = Y_E = Y_D^T$ . Hence, we can take over the derivation of the axion couplings to SM fermions in the DFSZ-I model (cf. Eqs. (103)–(105)), which yields

$$c_{u_i}^0 = -\frac{1}{N} \cos^2 \beta, \quad c_{d_i}^0 = -\frac{1}{N} \sin^2 \beta, \quad c_{e_i}^0 = -\frac{1}{N} \sin^2 \beta, \quad (306)$$

where we used  $v_a = f_a(2N)$  and with the important difference (compared to DFSZ-I) that the color anomaly  $N$  is a model-dependent factor that can be computed only after specifying the full GUT model.

While we have exemplified this derivation in the context of  $SU(5)$ , similar results apply to the  $SO(10)$  case, where however care must be taken in order to properly orthogonalize the physical axion field with respect to the Goldstone fields of all the broken gauge generators (see Ref. [683] for a detailed account). Another peculiarity of GUTs like is  $SO(10)$  is also the fact that some vacua of the axion potential can be connected by gauge transformations, and hence the naive identification  $N_{\text{DW}} = 2N$  does not hold [674, 683].

<sup>76</sup>Differ values of  $E/N$  are instead possible in the ‘unificaxion’ framework of Ref. [499], which assumes that the anomaly factors are due to intermediate-scale KSVZ-like fermions which form incomplete GUT multiplets and assist gauge coupling unification. It should be noted, however, that such scenarios are not easily motivated from a UV point of view. Indeed, as long as the  $U(1)_{PQ}$  symmetry commutes with the GUT group, the full GUT representation contributes to the anomaly coefficients, yielding the result in Eq. (304). Moreover, all the fragments of the original GUT multiplet obtain mass of order  $f_a$ , and thus do not improve gauge coupling unification.

## 8. Concluding remarks and *desiderata*

Axion physics is witnessing an exponential growth of interest from the particle physics community. According to the inSPIRE database, during the first lustrum of this millennium less than 250 papers were published containing the word *axion* in the title. In the following years, the number of publications has steadily grown, reaching the stunning number of more than 1,250 papers published in the last quinquennium, and there is no hint that this growth is going to diminish in the forthcoming years. It is an experimental fact that particle physicists interests and wishes do not render a theory correct (as LHC results have recently reconfirmed). However, scientific attention gets naturally focussed by theories that, besides being highly consistent and remarkably elegant, are able to explain some longstanding theoretical conundrums and are also particularly promising as far as regards the possibility of experimental verification. Undoubtedly axion physics belongs to this class of theories. For this reason we are convinced that any effort to develop further crucial theoretical issues in axion physics is soundly justified while, at the same time, experimental axion searches should be pursued along all viable pathways.

A major aim of this Review was that of motivating experimental colleagues to explore all the accessible regions in the axion parameter space. We have shown how axions can hide in regions that lie well beyond the boundaries of canonical windows. Axions can, for example, embody the whole DM also for mass values much larger or much smaller than what it is generally assumed. Axion searches which exploit their couplings to nucleons and electrons are complementary to traditional experimental searches which exploit their coupling to photons. As we have stressed, each type of axion couplings to SM particles could be suppressed well below their benchmark values, while leaving the other couplings substantially unaffected. In particular, it is possible to decouple the axion from the photon, in which case experimental searches that rely on the couplings to nucleons and electrons would play a crucial role. It is also conceivable that a strong suppression would instead occur for the axion-nucleon and axion-electron interactions. This would relax the tightest astrophysical bounds rendering viable regions in the  $m_a$ - $g_{a\gamma}$  parameter space that are generally regarded as excluded. Conversely, large enhancements of a single type of coupling are also possible. For this reason, new leading-edge experiments based on novel search techniques, which in many cases are characterised by limited sensitivities, can still contribute to circumscribe the landscape of phenomenologically viable axion models.

While the current blossoming of the field of axion physics is certainly driven by experiments, there exist important calls also for the theory community. We have collected in a (personal) list of *desiderata* those theoretical advancements that we consider crucial for further developments of axion physics, and that is conceivable that could be accomplished in the forthcoming years.

*Origin of the Peccei-Quinn symmetry.* Undoubtedly the PQ symmetry can be considered the ‘standard model’ for generating in QFT the effective axion-gluon interaction in Eq. (36) needed for solving the strong CP problem. However, a ‘standard model’ for explaining the origin of the PQ symmetry is still missing. The remarkably large number of model realisations that have been reviewed in this work provides the best evidence of this statement. Candidate models should in first place provide a cogent explanation for how a global PQ symmetry arises and should naturally embed some mechanism to preserve it at an exceptionally good level. However, they would acquire real credibility if, with no additional or ad hoc theoretical inputs, they could automatically shed light on some other unsettled issue of the SM, like for example the flavour problem, the origin of neutrino masses, etc. We believe that any progress in this direction would represent an important milestone to improve the plausibility of the axion hypothesis.

*Topological defects.* Assessing the axion contribution to the DM arising from axion-related topological defects (within  $N_{\text{DW}} = 1$  models and post-inflationary PQ breaking scenarios) is, at the time of writing, a major unsettled question. Tackling this problem requires extensive numerical simulations of the string network evolution and an extrapolation through several orders of magnitude between the PQ scale down to the Hubble scale at the time the axion acquires its mass. Although this appears as a remarkably difficult task, the importance of converging towards a reliable estimate cannot be overstated since it would drive the scanning strategy of axion DM experiments.

*Temperature dependence of the axion mass.* Lattice studies of the temperature dependence of the axion mass have made remarkable progresses in the last few years. However, it seems that universal consensus on the behaviour of the mass function  $m_a(T)$  has not yet been established. A final convergence on this issue is highly desirable in order to refine estimates of the VRM contribution to axion DM. We believe that it is realistic to expect that this goal will be achieved in the not so far future.

*Axion emissivity from supernova cores.* Our understanding of nuclear matter in the extreme conditions of proton-neutron stars in the cooling phase, shortly after a SN explosion, is still limited. Also this issue has recently witnessed important advancements, however, a detailed and reliable treatment of axion emissivity is, at least in part, still lacking. Any improvement in this direction will be of utmost importance. In fact, although the bound has been reassessed more than one time since first established, constraints from observed neutrino signal from SN1987A still provide some of the strongest limits for axion models, and this in spite of the fact that the data were very sparse. A new galactic SN explosion would produce an immensely richer data set, which could be optimally interpreted only with a better understanding of this issue.

We do not know if the axion exists. What we do know, is that this hypothetical particle has been able to focus an enormous amount of theoretical and experimental efforts in the attempt of understanding its properties and arrive at its discovery. It might be deemed surprising that so much commitment is devoted to prove what remains, admittedly, essentially a theoretical speculation. We believe that the explanation lies in the beauty and in the elegance of the theoretical construction. Whether these two paradigms can really provide insight into the way nature works, only future experiments will tell. For the moment axion physics, in all its aspects, is healthy and frisky. May it remain so until the axion is discovered.

## Acknowledgments

We thank Claudio Bonati, Andrea Caputo, Luc Darmé, Giovanni Grilli di Cortona, Axel Lindner, David J. E. Marsh, Pablo Quílez and Sunny Vagnozzi, for reviewing parts of the manuscript. We acknowledge Stefano Bertolini, Dmitry Budker, Derek Jackson Kimball, Igor G. Irastorza, Giacomo Landini, Federico Mescia, Alessandro Mirizzi, Fabrizio Nesti, Alessio Notari, Javier Redondo, Andreas Ringwald, Giuseppe Ruoso and Daniele Teresi, for discussions and inputs, and Michael Wiescher for permission for reproducing the left panel in the left panel of Fig. 4. L.D.L., M.G. and L.V. acknowledge the INFN Laboratori Nazionali di Frascati, where this project was first laid down, and where relevant portions of their work was performed, for hospitality and partial financial support. A large part of the work of L.D.L., M.G. and E.N. was performed at the Aspen Center for Physics, which is supported by National Science Foundation grant PHY-1607611. The participation of L.D.L. and E.N. at the Aspen Center for Physics was supported in part by a grant from the Simons Foundation. L.D.L. acknowledges hospitality from the Theoretical Physics Group at the University of Padova during the final stages of this work. E.N. acknowledges hospitality from the Munich Institute for Astro- and Particle Physics (MIAPP) where this project was brought to completion. L.V. thanks the kind hospitality of the Leinweber Center for Theoretical Physics, the University of Michigan, and Barry University, where part of this work was carried out. L.D.L. is supported by the Marie Skłodowska-Curie Individual Fellowship grant AXIONRUSH (GA 840791). E.N. is supported by the Italian Istituto Nazionale di Fisica Nucleare (INFN) through the ‘Theoretical Astroparticle Physics’ project TAsP. L.V. acknowledges support by the Vetenskapsrådet (Swedish Research Council) through contract No. 638-2013-8993 and the Oskar Klein Centre for Cosmoparticle Physics. The work of L.V. is part of the research program ‘The Hidden Universe of Weakly Interacting Particles’ with project number 680.92.18.03 (NWO Vrije Programma), which is (partly) financed by the Dutch Research Council (NWO). L.V. acknowledges support by the Department of Physics and Astronomy, Uppsala University, by Nordita, KTH Royal Institute of Technology and Stockholm University, by GRAPPA University of Amsterdam.

## Appendix A: Tables of notations and of acronyms

Symbol	Meaning	Equation
$\theta$	CP violating QCD angle	1
$\epsilon^{\mu\nu\rho\sigma}$	Levi-Civita symbol ( $\epsilon^{0123} = -1$ )	4
$N$	$U(1)_{\text{PQ}}\text{-}SU(3)_{\text{QCD}}$ anomaly coefficient	70
$E$	$U(1)_{\text{PQ}}\text{-}U(1)_{\text{QED}}$ anomaly coefficient	70
$\Phi$	axion multiplet $\Phi(x) = \frac{1}{\sqrt{2}}(v_a + \rho_a(x)) e^{i\frac{a(x)}{v_a}}$	79
$\rho_a$	axion multiplet radial mode	79
$a$	axion field: axion multiplet orbital mode	79
$v_a$	Peccei-Quinn symmetry breaking VEV $v_a = \sqrt{2}\langle\Phi\rangle$	79
$f_a$	axion decay constant $f_a = v_a/(2N)$	88
$N_{\text{DW}}$	domain wall number $N_{\text{DW}} = 2N$	88
$m_a$	axion mass	108
$C_{a\gamma}$	axion-photon coupling	110
$C_{ap}$	axion-proton coupling	111
$C_{an}$	axion-neutron coupling	112
$C_{ae}$	axion-electron coupling	114
$C_{a\pi}$	axion-pion coupling	115
$C_{an\gamma}$	axion coupling to the neutron EDM	116
$g_{a\gamma}$	dimensional axion-photon coupling ( $\text{GeV}^{-1}$ )	118
$g_{af}$	rescaled axion-fermion coupling	118
$g_d$	rescaled axion coupling to the neutron EDM	118
$g_{aN}^S$	CP-violating scalar axion-nucleon coupling	127
$\chi$	topological susceptibility	131
$R$	cosmological scale factor	139
$H$	Hubble parameter $H = \dot{R}/R$	140
$m_{\text{Pl}}$	Planck mass	140
$\rho, s$	energy and entropy density ( $(\rho, s) \simeq (\rho, s)_{\text{rad}}$ in rad. domination)	145
$g_*, g_S$	effective energy and entropy degrees of freedom	146
$m_a(T)$	axion mass at temperature $T$	149
$t_{\text{osc}}$	time for the onset of axion oscillations	154
$\theta_{\text{PQ}}, \dot{\theta}_{\text{PQ}}$	misalignment angle, axion velocity at the PQ scale	155
$\theta_i, \dot{\theta}_i$	misalignment angle, axion velocity at $t_{\text{osc}}$	158
$\Omega_a^{\text{VRM}}$	fractional axion energy density from VRM	168
$\varepsilon$	energy-loss rate per unit mass	200
$\mathcal{R}$	ratio of number of stars in Horizontal and Red Giant branches	202
$g_{e12}, g_{\gamma10}$	respectively $g_{ae}/10^{-12}$ and $g_{a\gamma}/10^{-10} \text{ GeV}^{-1}$	231

Table 8: Notations introduced in the text, their meaning, and equations where they are defined.

Acronym	Meaning
ABC	Atomic recombination and de-excitation, Bremsstrahlung, Compton
ALP	Axion-like Particle
BBN	Big-Bang Nucleosynthesis
(C)DM	(Cold) Dark Matter
CL	Confidence Level
CMBR	Cosmic Microwave Background Radiation
CMD	Color Magnitude Diagram
CP	Charge Parity
$\chi$ PT	Chiral Perturbation Theory
DFSZ	Dine-Fischler-Srednicki-Zhitnitsky
DIGA	Dilute Instanton Gas Approximation
DW	Domain Wall
EFT	Effective Field Theory
FCNC	Flavour Changing Neutral Currents
FLRW	Friedmann-Lemaître-Robertson-Walker
FV	Flavour Violating
GUT	Grand Unified Theory
HB	Horizontal Branch
HDM	Hot Dark Matter
HR	Hertzsprung-Russell
IILM	Interacting Instanton Liquid Model
IR	Infrared
KK	Kaluza-Klein
KSVZ	Kim-Shifman-Vainshtein-Zakharov
LP	Landau Pole
LSW	Light Shining Through a Wall
(n)EDM	(neutron) Electric Dipole Moment
(p)NGB	(pseudo) Nambu-Goldstone Boson
NMR	Nuclear Magnetic Resonance
(N)LO	(Next-to) Leading Order
NS	Neutron Star
OPE	One Pion Exchange
PQ	Peccei Quinn
QCD	Quantum Chromo Dynamics
QED	Quantum Electro Dynamics
QFT	Quantum Field Theory
RGB	Red Giant Branch
SM	Standard Model
SMASH	Standard Model–Axion–Seesaw–Higgs inflation portal
SN	Supernova
UV	Ultraviolet
VEV	Vacuum Expectation Value
VRM	Vacuum Realignment Mechanism
WD	White Dwarf
WDLF	White Dwarf Luminosity Function
WIMP	Weakly Interacting Massive Particle
WW	Weinberg-Wilczek

Table 9: Acronyms used in the text and their meaning.

Experiment	Meaning
ABRACADABRA [291]	A Broadband/Resonant Approach to Cosmic Axion Detection
ADMX [505]	Axion Dark Matter Experiment
ALPS (II) [504]	Any Light Particle Search (II)
ARGUS [566]	A Russian-German-United States-Swedish Collaboration
ARIADNE [448]	Axion Resonant InterAction Detection Experiment
ATLAS [695]	A Toroidal LHC ApparatuS
AXIOMA [466]	AXION dark MATter detection
BEAST [462]	Broadband Electric Axion Sensing Technique
BELLE II [559]	
CAPP-8TB [433]	Center for Axion and Precision Physics
CASPEr [290]	Cosmic Axion Spin Precession Experiment
CAST [420]	CERN Axion Solar Telescope
CLEO [558]	
CMS [696]	Compact Muon Solenoid
Crystal Box [562]	
CULTASK [697]	CAPP's Ultra Low Temperature Axion Search in Korea
DARWIN [698]	Dark Matter WIMP Search With Liquid Xenon
E949+E787 [555]	
Fermi LAT [453]	Fermi Large Area Telescope
GAIA [394]	Global Astrometric Interferometer for Astrophysics
GNOME [468]	Global Network of Optical Magnetometers for Exotic Physics
HAYSTACK [435]	Haloscope at Yale Sensitive to Axion CDM
IAXO [699]	International Axion Observatory
KLASH [294]	KLoe magnet for Axion Search
LHC [700]	Large Hadron Collider
LSST [377]	Large Synoptic Survey Telescope
LUX [425]	Large Underground Xenon
LZ [425]	LUX-ZEPLIN
MADMAX [300]	MAgnetized Disc and Mirror Axion eXperiment
ORGAN [436]	Oscillating Resonant Group AxioN
ORPHEUS [459]	
OSQAR [445]	Optical Search for QED vacuum birefringence, Axions, and photon Regeneration
PandaX [426]	Particle aND Astrophysical Xenon experiment
PVLAS [446]	Polarisation of Vacuum with LASer
QUAX [440]	QUaerere AXion
RADES [460]	Relic Axion Detector Exploratory Setup
SCSS [701]	SuperCOSMOS Sky Survey
SDSS [702]	Sloan Digital Sky Survey
STAX [463]	Sub-THz-AXion
TASTE [458]	Troitsk Axion Solar Telescope Experiment
TOORAD [439]	Topological Resonant Axion Detection
TRIUMF [560]	TRI University Meson Facility
VMB@CERN [447]	Vacuum Magnetic Birefringence experiment at CERN
XENON100 [424]	100 kg liquid Xenon target

Table 10: Experiment acronyms and their meaning. Blank entries correspond to experiment names that are not acronyms.



## References

## References

- [1] S. Weinberg, Anthropic Bound on the Cosmological Constant, *Phys. Rev. Lett.* 59 (1987) 2607. [doi:10.1103/PhysRevLett.59.2607](#).
- [2] V. Agrawal, S. M. Barr, J. F. Donoghue, D. Seckel, Viable range of the mass scale of the standard model, *Phys. Rev. D* 57 (1998) 5480–5492. [arXiv:hep-ph/9707380](#), [doi:10.1103/PhysRevD.57.5480](#).
- [3] V. Agrawal, S. M. Barr, J. F. Donoghue, D. Seckel, Anthropic considerations in multiple domain theories and the scale of electroweak symmetry breaking, *Phys. Rev. Lett.* 80 (1998) 1822–1825. [arXiv:hep-ph/9801253](#), [doi:10.1103/PhysRevLett.80.1822](#).
- [4] L. Ubaldi, Effects of theta on the deuteron binding energy and the triple-alpha process, *Phys. Rev. D* 81 (2010) 025011. [arXiv:0811.1599](#), [doi:10.1103/PhysRevD.81.025011](#).
- [5] M. Dine, L. Stephenson Haskins, L. Ubaldi, D. Xu, Some Remarks on Anthropic Approaches to the Strong CP Problem, *JHEP* 05 (2018) 171. [arXiv:1801.03466](#), [doi:10.1007/JHEP05\(2018\)171](#).
- [6] P. Minkowski,  $\mu \rightarrow e\gamma$  at a Rate of One Out of  $10^9$  Muon Decays?, *Phys. Lett.* 67B (1977) 421–428. [doi:10.1016/0370-2693\(77\)90435-X](#).
- [7] T. Yanagida, Horizontal gauge symmetry and masses of neutrinos, *Conf. Proc. C7902131* (1979) 95–99.
- [8] M. Gell-Mann, P. Ramond, R. Slansky, Complex Spinors and Unified Theories, *Conf. Proc. C790927* (1979) 315–321. [arXiv:1306.4669](#).
- [9] R. N. Mohapatra, G. Senjanovic, Neutrino Masses and Mixings in Gauge Models with Spontaneous Parity Violation, *Phys. Rev. D* 23 (1981) 165. [doi:10.1103/PhysRevD.23.165](#).
- [10] M. Fukugita, T. Yanagida, Baryogenesis Without Grand Unification, *Phys. Lett. B* 174 (1986) 45–47. [doi:10.1016/0370-2693\(86\)91126-3](#).
- [11] S. Davidson, A. Ibarra, A Lower bound on the right-handed neutrino mass from leptogenesis, *Phys. Lett. B* 535 (2002) 25–32. [arXiv:hep-ph/0202239](#), [doi:10.1016/S0370-2693\(02\)01735-5](#).
- [12] W. Buchmuller, P. Di Bari, M. Plumacher, Leptogenesis for pedestrians, *Annals Phys.* 315 (2005) 305–351. [arXiv:hep-ph/0401240](#), [doi:10.1016/j.aop.2004.02.003](#).
- [13] S. Davidson, E. Nardi, Y. Nir, Leptogenesis, *Phys. Rept.* 466 (2008) 105–177. [arXiv:0802.2962](#), [doi:10.1016/j.physrep.2008.06.002](#).
- [14] C. S. Fong, E. Nardi, A. Riotto, Leptogenesis in the Universe, *Adv. High Energy Phys.* 2012 (2012) 158303. [arXiv:1301.3062](#), [doi:10.1155/2012/158303](#).
- [15] E. J. Chun, et al., Probing Leptogenesis, *Int. J. Mod. Phys. A* 33 (05n06) (2018) 1842005. [arXiv:1711.02865](#), [doi:10.1142/S0217751X18420058](#).
- [16] S. Weinberg, A New Light Boson?, *Phys. Rev. Lett.* 40 (1978) 223–226. [doi:10.1103/PhysRevLett.40.223](#).
- [17] F. Wilczek, Problem of Strong p and t Invariance in the Presence of Instantons, *Phys. Rev. Lett.* 40 (1978) 279–282. [doi:10.1103/PhysRevLett.40.279](#).
- [18] C. Vafa, E. Witten, Parity Conservation in QCD, *Phys. Rev. Lett.* 53 (1984) 535. [doi:10.1103/PhysRevLett.53.535](#).
- [19] R. D. Peccei, H. R. Quinn, CP Conservation in the Presence of Instantons, *Phys. Rev. Lett.* 38 (1977) 1440–1443. [doi:10.1103/PhysRevLett.38.1440](#).
- [20] R. D. Peccei, H. R. Quinn, Constraints Imposed by CP Conservation in the Presence of Instantons, *Phys. Rev. D* 16 (1977) 1791–1797. [doi:10.1103/PhysRevD.16.1791](#).
- [21] S. Coleman, *Aspects of Symmetry*, Cambridge University Press, Cambridge, U.K., 1985. [doi:10.1017/CB09780511565045](#).
- [22] J. E. Kim, Light Pseudoscalars, *Particle Physics and Cosmology*, *Phys. Rept.* 150 (1987) 1–177. [doi:10.1016/0370-1573\(87\)90017-2](#).
- [23] H.-Y. Cheng, The Strong CP Problem Revisited, *Phys. Rept.* 158 (1988) 1. [doi:10.1016/0370-1573\(88\)90135-4](#).
- [24] R. D. Peccei, The Strong CP Problem, *Adv. Ser. Direct. High Energy Phys.* 3 (1989) 503–551. [doi:10.1142/9789814503280\\_0013](#).
- [25] R. D. Peccei, The Strong CP problem and axions, *Lect. Notes Phys.* 741 (2008) 3–17, [3(2006)]. [arXiv:hep-ph/0607268](#), [doi:10.1007/978-3-540-73518-2\\_1](#).
- [26] J. E. Kim, G. Carosi, Axions and the Strong CP Problem, *Rev. Mod. Phys.* 82 (2010) 557–602, [erratum: *Rev. Mod. Phys.* 91, no. 4, 049902 (2019)]. [arXiv:0807.3125](#), [doi:10.1103/RevModPhys.82.557](#), [doi:10.1103/RevModPhys.91.049902](#).
- [27] P. Sikivie, Axion Cosmology, *Lect. Notes Phys.* 741 (2008) 19–50, [19(2006)]. [arXiv:astro-ph/0610440](#), [doi:10.1007/978-3-540-73518-2\\_2](#).
- [28] M. Kawasaki, K. Nakayama, Axions: Theory and Cosmological Role, *Ann. Rev. Nucl. Part. Sci.* 63 (2013) 69–95. [arXiv:1301.1123](#), [doi:10.1146/annurev-nucl-102212-170536](#).
- [29] D. J. E. Marsh, Axion Cosmology, *Phys. Rept.* 643 (2016) 1–79. [arXiv:1510.07633](#), [doi:10.1016/j.physrep.2016.06.005](#).
- [30] M. S. Turner, Windows on the Axion, *Phys. Rept.* 197 (1990) 67–97. [doi:10.1016/0370-1573\(90\)90172-X](#).
- [31] G. G. Raffelt, Astrophysical methods to constrain axions and other novel particle phenomena, *Phys. Rept.* 198 (1990) 1–113. [doi:10.1016/0370-1573\(90\)90054-6](#).
- [32] G. G. Raffelt, Astrophysical axion bounds, *Lect. Notes Phys.* 741 (2008) 51–71, [51(2006)]. [arXiv:hep-ph/0611350](#), [doi:10.1007/978-3-540-73518-2\\_3](#).
- [33] S. J. Asztalos, L. J. Rosenberg, K. van Bibber, P. Sikivie, K. Zioutas, Searches for astrophysical and cosmological axions, *Ann. Rev. Nucl. Part. Sci.* 56 (2006) 293–326. [doi:10.1146/annurev-nucl.56.080805.140513](#).

- [34] M. Giannotti, I. G. Irastorza, J. Redondo, A. Ringwald, K. Saikawa, Stellar Recipes for Axion Hunters, JCAP 1710 (10) (2017) 010. [arXiv:1708.02111](#), [doi:10.1088/1475-7516/2017/10/010](#).
- [35] L. J. Rosenberg, K. A. van Bibber, Searches for invisible axions, Phys. Rept. 325 (2000) 1–39. [doi:10.1016/S0370-1573\(99\)00045-9](#).
- [36] R. Battesti, B. Beltran, H. Davoudiasl, M. Kuster, P. Pagnat, R. Rabadan, A. Ringwald, N. Spooner, K. Zioutas, Axion searches in the past, at present, and in the near future, Lect. Notes Phys. 741 (2008) 199–237, [199(2007)]. [arXiv:0705.0615](#), [doi:10.1007/978-3-540-73518-2\\_10](#).
- [37] P. W. Graham, I. G. Irastorza, S. K. Lamoreaux, A. Lindner, K. A. van Bibber, Experimental Searches for the Axion and Axion-Like Particles, Ann. Rev. Nucl. Part. Sci. 65 (2015) 485–514. [arXiv:1602.00039](#), [doi:10.1146/annurev-nucl-102014-022120](#).
- [38] I. G. Irastorza, J. Redondo, New experimental approaches in the search for axion-like particles, Prog. Part. Nucl. Phys. 102 (2018) 89–159. [arXiv:1801.08127](#), [doi:10.1016/j.pnpnp.2018.05.003](#).
- [39] S. Weinberg, The U(1) Problem, Phys. Rev. D11 (1975) 3583–3593. [doi:10.1103/PhysRevD.11.3583](#).
- [40] D. V. Nanopoulos, Towards a renormalizable unified gauge theory of strong, electromagnetic and weak interactions, Lett. Nuovo Cim. 8S2 (1973) 873–877, [Lett. Nuovo Cim. 8,873(1973)]. [doi:10.1007/BF02727401](#).
- [41] S. Weinberg, Nonabelian Gauge Theories of the Strong Interactions, Phys. Rev. Lett. 31 (1973) 494–497. [doi:10.1103/PhysRevLett.31.494](#).
- [42] A. A. Belavin, A. M. Polyakov, A. S. Schwartz, Yu. S. Tyupkin, Pseudoparticle Solutions of the Yang-Mills Equations, Phys. Lett. B59 (1975) 85–87, [350(1975)]. [doi:10.1016/0370-2693\(75\)90163-X](#).
- [43] C. G. Callan, Jr., R. F. Dashen, D. J. Gross, The Structure of the Gauge Theory Vacuum, Phys. Lett. B63 (1976) 334–340, [357(1976)]. [doi:10.1016/0370-2693\(76\)90277-X](#).
- [44] R. Jackiw, C. Rebbi, Vacuum Periodicity in a Yang-Mills Quantum Theory, Phys. Rev. Lett. 37 (1976) 172–175, [353(1976)]. [doi:10.1103/PhysRevLett.37.172](#).
- [45] G. Grilli di Cortona, E. Hardy, J. Pardo Vega, G. Villadoro, The QCD axion, precisely, JHEP 01 (2016) 034. [arXiv:1511.02867](#), [doi:10.1007/JHEP01\(2016\)034](#).
- [46] R. Bott, On the iteration of closed geodesics and the sturm intersection theory, Communications on Pure and Applied Mathematics 9 (2) (1956) 171–206. [doi:10.1002/cpa.3160090204](#).
- [47] G. 't Hooft, Symmetry Breaking Through Bell-Jackiw Anomalies, Phys. Rev. Lett. 37 (1976) 8–11, [226(1976)]. [doi:10.1103/PhysRevLett.37.8](#).
- [48] G. 't Hooft, Computation of the Quantum Effects Due to a Four-Dimensional Pseudoparticle, Phys. Rev. D14 (1976) 3432–3450, [70(1976)]. [doi:10.1103/PhysRevD.18.2199.3](#), [doi:10.1103/PhysRevD.14.3432](#).
- [49] E. Witten, Some Exact Multi - Instanton Solutions of Classical Yang-Mills Theory, Phys. Rev. Lett. 38 (1977) 121–124, [124(1976)]. [doi:10.1103/PhysRevLett.38.121](#).
- [50] R. Jackiw, C. Nohl, C. Rebbi, Conformal Properties of Pseudoparticle Configurations, Phys. Rev. D15 (1977) 1642, [128(1976)]. [doi:10.1103/PhysRevD.15.1642](#).
- [51] R. Jackiw, Introduction to the Yang-Mills Quantum Theory, Rev. Mod. Phys. 52 (1980) 661–673. [doi:10.1103/RevModPhys.52.661](#).
- [52] S. Weinberg, The quantum theory of fields. Vol. 2: Modern applications, Cambridge University Press, 2013.
- [53] G. 't Hooft, How Instantons Solve the U(1) Problem, Phys. Rept. 142 (1986) 357–387. [doi:10.1016/0370-1573\(86\)90117-1](#).
- [54] D. J. Gross, R. D. Pisarski, L. G. Yaffe, QCD and Instantons at Finite Temperature, Rev. Mod. Phys. 53 (1981) 43. [doi:10.1103/RevModPhys.53.43](#).
- [55] K. Fujikawa, Path Integral Measure for Gauge Invariant Fermion Theories, Phys. Rev. Lett. 42 (1979) 1195–1198. [doi:10.1103/PhysRevLett.42.1195](#).
- [56] C. Vafa, E. Witten, Restrictions on Symmetry Breaking in Vector-Like Gauge Theories, Nucl. Phys. B234 (1984) 173–188. [doi:10.1016/0550-3213\(84\)90230-X](#).
- [57] J. M. Pendlebury, et al., Revised experimental upper limit on the electric dipole moment of the neutron, Phys. Rev. D92 (9) (2015) 092003. [arXiv:1509.04411](#), [doi:10.1103/PhysRevD.92.092003](#).
- [58] C. Abel, et al., Measurement of the permanent electric dipole moment of the neutron. [arXiv:2001.11966](#).
- [59] B. W. Filippone, Worldwide Search for the Neutron EDM, in: 13th Conference on the Intersections of Particle and Nuclear Physics (CIPANP 2018) Palm Springs, California, USA, May 29-June 3, 2018, 2018. [arXiv:1810.03718](#).
- [60] V. Baluni, CP Violating Effects in QCD, Phys. Rev. D19 (1979) 2227–2230. [doi:10.1103/PhysRevD.19.2227](#).
- [61] R. J. Crewther, P. Di Vecchia, G. Veneziano, E. Witten, Chiral Estimate of the Electric Dipole Moment of the Neutron in Quantum Chromodynamics, Phys. Lett. 88B (1979) 123, [Erratum: Phys. Lett. 91B,487(1980)]. [doi:10.1016/0370-2693\(80\)91025-4](#), [doi:10.1016/0370-2693\(79\)90128-X](#).
- [62] A. Pich, E. de Rafael, Strong CP violation in an effective chiral Lagrangian approach, Nucl. Phys. B367 (1991) 313–333. [doi:10.1016/0550-3213\(91\)90019-T](#).
- [63] M. Pospelov, A. Ritz, Theta vacua, QCD sum rules, and the neutron electric dipole moment, Nucl. Phys. B573 (2000) 177–200. [arXiv:hep-ph/9908508](#), [doi:10.1016/S0550-3213\(99\)00817-2](#).
- [64] M. Pospelov, A. Ritz, Electric dipole moments as probes of new physics, Annals Phys. 318 (2005) 119–169. [arXiv:hep-ph/0504231](#), [doi:10.1016/j.aop.2005.04.002](#).
- [65] M. Pospelov, A. Ritz, Probing CP violation with electric dipole moments, Adv. Ser. Direct. High Energy Phys. 20 (2009) 439–518. [doi:10.1142/9789814271844\\_0013](#).
- [66] V. V. Flambaum, M. Pospelov, A. Ritz, Y. V. Stadnik, Sensitivity of EDM experiments in paramagnetic atoms and molecules to hadronic CP violation. [arXiv:1912.13129](#).

- [67] J. R. Ellis, M. K. Gaillard, Strong and Weak CP Violation, Nucl. Phys. B150 (1979) 141–162. [doi:10.1016/0550-3213\(79\)90297-9](#).
- [68] I. B. Khriplovich, A. I. Vainshtein, Infinite renormalization of Theta term and Jarlskog invariant for CP violation, Nucl. Phys. B414 (1994) 27–32. [arXiv:hep-ph/9308334](#), [doi:10.1016/0550-3213\(94\)90419-7](#).
- [69] C. Jarlskog, Commutator of the Quark Mass Matrices in the Standard Electroweak Model and a Measure of Maximal CP Violation, Phys. Rev. Lett. 55 (1985) 1039. [doi:10.1103/PhysRevLett.55.1039](#).
- [70] N. Kaloper, J. Terning, Landscaping the Strong CP Problem, JHEP 03 (2019) 032. [arXiv:1710.01740](#), [doi:10.1007/JHEP03\(2019\)032](#).
- [71] G. Dvali, A Vacuum accumulation solution to the strong CP problem, Phys. Rev. D74 (2006) 025019. [arXiv:hep-th/0510053](#), [doi:10.1103/PhysRevD.74.025019](#).
- [72] D. B. Kaplan, A. V. Manohar, Current Mass Ratios of the Light Quarks, Phys. Rev. Lett. 56 (1986) 2004. [doi:10.1103/PhysRevLett.56.2004](#).
- [73] M. Tanabashi, et al., Review of Particle Physics, Phys. Rev. D98 (3) (2018) 030001. [doi:10.1103/PhysRevD.98.030001](#).
- [74] W. A. Bardeen, Instanton Triggered Chiral Symmetry Breaking, the U(1) Problem and a Possible Solution to the Strong CP Problem. [arXiv:1812.06041](#).
- [75] H. Georgi, I. N. McArthur, Instantons And The Mu Quark Mass.
- [76] M. A. B. Beg, H. S. Tsao, Strong P, T Noninvariances in a Superweak Theory, Phys. Rev. Lett. 41 (1978) 278. [doi:10.1103/PhysRevLett.41.278](#).
- [77] H. Georgi, A Model of Soft CP Violation, Hadronic J. 1 (1978) 155.
- [78] R. N. Mohapatra, G. Senjanovic, Natural Suppression of Strong p and t Noninvariance, Phys. Lett. 79B (1978) 283–286. [doi:10.1016/0370-2693\(78\)90243-5](#).
- [79] A. E. Nelson, Naturally Weak CP Violation, Phys. Lett. B136 (1984) 387–391. [doi:10.1016/0370-2693\(84\)92025-2](#).
- [80] S. M. Barr, Solving the Strong CP Problem Without the Peccei-Quinn Symmetry, Phys. Rev. Lett. 53 (1984) 329. [doi:10.1103/PhysRevLett.53.329](#).
- [81] M. Dine, P. Draper, Challenges for the Nelson-Barr Mechanism, JHEP 08 (2015) 132. [arXiv:1506.05433](#), [doi:10.1007/JHEP08\(2015\)132](#).
- [82] L. Vecchi, Spontaneous CP violation and the strong CP problem, JHEP 04 (2017) 149. [arXiv:1412.3805](#), [doi:10.1007/JHEP04\(2017\)149](#).
- [83] S. Yu. Khlebnikov, M. E. Shaposhnikov, Extra Space-time Dimensions: Towards a Solution to the Strong CP Problem, Phys. Lett. B203 (1988) 121–124. [doi:10.1016/0370-2693\(88\)91582-1](#).
- [84] M. Chaichian, A. Kobakhidze, Extra dimensions and the strong CP problem, Phys. Rev. Lett. 87 (2001) 171601. [arXiv:hep-ph/0104158](#), [doi:10.1103/PhysRevLett.87.171601](#).
- [85] S. Khlebnikov, M. Shaposhnikov, Brane-worlds and theta-vacua, Phys. Rev. D71 (2005) 104024. [arXiv:hep-th/0412306](#), [doi:10.1103/PhysRevD.71.104024](#).
- [86] F. L. Bezrukov, Y. Burnier, Towards a solution of the strong CP problem by compact extra dimensions, Phys. Rev. D80 (2009) 125004. [arXiv:0811.1163](#), [doi:10.1103/PhysRevD.80.125004](#).
- [87] S. Samuel, Does the Yang-Mills theory solve the strong CP problem by itself?, Mod. Phys. Lett. A7 (1992) 2007–2016. [doi:10.1142/S0217732392001737](#).
- [88] N. J. Dowrick, N. A. McDougall, On the Samuel solution to the strong CP problem within QCD, Nucl. Phys. B399 (1993) 426–440. [doi:10.1016/0550-3213\(93\)90503-H](#).
- [89] G. Gabadadze, M. Shifman, QCD vacuum and axions: What’s happening?, Int. J. Mod. Phys. A17 (2002) 3689–3728, [521(2002)]. [arXiv:hep-ph/0206123](#), [doi:10.1142/S0217751X02011357](#).
- [90] V. G. Knizhnik, A. Yu. Morozov, Renormalization of topological charge, JETP Lett. 39 (1984) 240–243, [Pisma Zh. Eksp. Teor. Fiz.39,202(1984)].
- [91] H. Levine, S. B. Libby, Renormalization of the  $\theta$  Angle, the Quantum Hall Effect and the Strong CP Problem, Phys. Lett. 150B (1985) 182–186. [doi:10.1016/0370-2693\(85\)90165-0](#).
- [92] M. Reuter, Renormalization of the topological charge in Yang-Mills theory, Mod. Phys. Lett. A12 (1997) 2777–2802. [arXiv:hep-th/9604124](#), [doi:10.1142/S0217732397002922](#).
- [93] S. M. Apenko, Renormalization of the vacuum angle in quantum mechanics, Berry phase and continuous measurements, J. Phys. A41 (2008) 315301. [arXiv:0710.2769](#), [doi:10.1088/1751-8113/41/31/315301](#).
- [94] Y. Nakamura, G. Schierholz, Does confinement imply CP invariance of the strong interactions?, in: 37th International Symposium on Lattice Field Theory (Lattice 2019) Wuhan, Hubei, China, June 16–22, 2019, 2019. [arXiv:1912.03941](#).
- [95] H. Georgi, D. B. Kaplan, L. Randall, Manifesting the Invisible Axion at Low-energies, Phys. Lett. 169B (1986) 73–78. [doi:10.1016/0370-2693\(86\)90688-X](#).
- [96] J. Kodaira, QCD Higher Order Effects in Polarized Electroproduction: Flavor Singlet Coefficient Functions, Nucl. Phys. B165 (1980) 129–140. [doi:10.1016/0550-3213\(80\)90310-7](#).
- [97] S. A. Larin, The Renormalization of the axial anomaly in dimensional regularization, Phys. Lett. B303 (1993) 113–118. [arXiv:hep-ph/9302240](#), [doi:10.1016/0370-2693\(93\)90053-K](#).
- [98] E. Witten, Large N Chiral Dynamics, Annals Phys. 128 (1980) 363. [doi:10.1016/0003-4916\(80\)90325-5](#).
- [99] P. Di Vecchia, G. Veneziano, Chiral Dynamics in the Large n Limit, Nucl. Phys. B171 (1980) 253–272. [doi:10.1016/0550-3213\(80\)90370-3](#).
- [100] L. Di Luzio, M. Redi, A. Strumia, D. Teresi, Coset Cosmology, JHEP 06 (2019) 110. [arXiv:1902.05933](#), [doi:10.1007/JHEP06\(2019\)110](#).
- [101] S. Chang, K. Choi, Hadronic axion window and the big bang nucleosynthesis, Phys. Lett. B316 (1993) 51–56. [arXiv:hep-ph/9306216](#), [doi:10.1016/0370-2693\(93\)90656-3](#).

- [102] M. Srednicki, Axion Couplings to Matter. 1. CP Conserving Parts, Nucl. Phys. B260 (1985) 689–700. [doi:10.1016/0550-3213\(85\)90054-9](#).
- [103] D. B. Kaplan, Opening the Axion Window, Nucl. Phys. B260 (1985) 215–226. [doi:10.1016/0550-3213\(85\)90319-0](#).
- [104] T. W. Donnelly, S. J. Freedman, R. S. Lytel, R. D. Peccei, M. Schwartz, Do Axions Exist?, Phys. Rev. D18 (1978) 1607. [doi:10.1103/PhysRevD.18.1607](#).
- [105] L. J. Hall, M. B. Wise, Flavor changing Higgs - boson couplings, Nucl. Phys. B187 (1981) 397–408. [doi:10.1016/0550-3213\(81\)90469-7](#).
- [106] F. Wilczek, Decays of Heavy Vector Mesons Into Higgs Particles, Phys. Rev. Lett. 39 (1977) 1304. [doi:10.1103/PhysRevLett.39.1304](#).
- [107] M. Davier, Searches for New Particles, in: Proceedings, 23RD International Conference on High Energy Physics, JULY 16-23, 1986, Berkeley, CA, 1986.
- [108] W. A. Bardeen, R. D. Peccei, T. Yanagida, Constraints on variant axion models, Nucl. Phys. B279 (1987) 401–428. [doi:10.1016/0550-3213\(87\)90003-4](#).
- [109] A. R. Zhitnitsky, On Possible Suppression of the Axion Hadron Interactions. (In Russian), Sov. J. Nucl. Phys. 31 (1980) 260, [Yad. Fiz.31,497(1980)].
- [110] M. Dine, W. Fischler, M. Srednicki, A Simple Solution to the Strong CP Problem with a Harmless Axion, Phys. Lett. B104 (1981) 199–202. [doi:10.1016/0370-2693\(81\)90590-6](#).
- [111] J. E. Kim, Weak Interaction Singlet and Strong CP Invariance, Phys. Rev. Lett. 43 (1979) 103. [doi:10.1103/PhysRevLett.43.103](#).
- [112] M. A. Shifman, A. I. Vainshtein, V. I. Zakharov, Can Confinement Ensure Natural CP Invariance of Strong Interactions?, Nucl. Phys. B166 (1980) 493. [doi:10.1016/0550-3213\(80\)90209-6](#).
- [113] L. Di Luzio, J. F. Kamenik, M. Nardecchia, Implications of perturbative unitarity for scalar di-boson resonance searches at LHC, Eur. Phys. J. C77 (1) (2017) 30. [arXiv:1604.05746](#), [doi:10.1140/epjc/s10052-017-4594-2](#).
- [114] L. Di Luzio, M. Nardecchia, What is the scale of new physics behind the  $B$ -flavour anomalies?, Eur. Phys. J. C77 (8) (2017) 536. [arXiv:1706.01868](#), [doi:10.1140/epjc/s10052-017-5118-9](#).
- [115] F. Bjorkeröth, L. Di Luzio, F. Mescia, E. Nardi, P. Panci, R. Ziegler, Axion-electron decoupling in nucleophobic axion models. [arXiv:1907.06575](#).
- [116] M. Gorghetto, G. Villadoro, Topological Susceptibility and QCD Axion Mass: QED and NNLO corrections, JHEP 03 (2019) 033. [arXiv:1812.01008](#), [doi:10.1007/JHEP03\(2019\)033](#).
- [117] S. Borsanyi, et al., Calculation of the axion mass based on high-temperature lattice quantum chromodynamics, Nature 539 (7627) (2016) 69–71. [arXiv:1606.07494](#), [doi:10.1038/nature20115](#).
- [118] T. Vonk, F.-K. Guo, U.-G. Meissner, Precision calculation of the axion-nucleon coupling in chiral perturbation theory [arXiv:2001.05327](#).
- [119] J. E. Moody, F. Wilczek, New macroscopic forces?, Phys. Rev. D30 (1984) 130. [doi:10.1103/PhysRevD.30.130](#).
- [120] H. Georgi, L. Randall, Flavor Conserving CP Violation in Invisible Axion Models, Nucl. Phys. B276 (1986) 241–252. [doi:10.1016/0550-3213\(86\)90022-2](#).
- [121] M. Pospelov, CP odd interaction of axion with matter, Phys. Rev. D58 (1998) 097703. [arXiv:hep-ph/9707431](#), [doi:10.1103/PhysRevD.58.097703](#).
- [122] H. M. Georgi, L. J. Hall, M. B. Wise, Grand Unified Models With an Automatic Peccei-Quinn Symmetry, Nucl. Phys. B192 (1981) 409–416. [doi:10.1016/0550-3213\(81\)90433-8](#).
- [123] M. Dine, N. Seiberg, String Theory and the Strong CP Problem, Nucl. Phys. B273 (1986) 109–124. [doi:10.1016/0550-3213\(86\)90043-X](#).
- [124] S. M. Barr, D. Seckel, Planck scale corrections to axion models, Phys. Rev. D46 (1992) 539–549. [doi:10.1103/PhysRevD.46.539](#).
- [125] M. Kamionkowski, J. March-Russell, Planck scale physics and the Peccei-Quinn mechanism, Phys. Lett. B282 (1992) 137–141. [arXiv:hep-th/9202003](#), [doi:10.1016/0370-2693\(92\)90492-M](#).
- [126] R. Holman, S. D. H. Hsu, T. W. Kephart, E. W. Kolb, R. Watkins, L. M. Widrow, Solutions to the strong CP problem in a world with gravity, Phys. Lett. B282 (1992) 132–136. [arXiv:hep-ph/9203206](#), [doi:10.1016/0370-2693\(92\)90491-L](#).
- [127] S. Ghigna, M. Lusignoli, M. Roncadelli, Instability of the invisible axion, Phys. Lett. B283 (1992) 278–281. [doi:10.1016/0370-2693\(92\)90019-Z](#).
- [128] S. W. Hawking, Particle Creation by Black Holes, Commun. Math. Phys. 43 (1975) 199–220, [167(1975)]. [doi:10.1007/BF02345020](#), [doi:10.1007/BF01608497](#).
- [129] L. F. Abbott, M. B. Wise, Wormholes and Global Symmetries, Nucl. Phys. B325 (1989) 687–704. [doi:10.1016/0550-3213\(89\)90503-8](#).
- [130] S. R. Coleman, K.-M. Lee, Wormholes made without massless matter fields, Nucl. Phys. B329 (1990) 387–409. [doi:10.1016/0550-3213\(90\)90149-8](#).
- [131] R. Kallosh, A. D. Linde, D. A. Linde, L. Susskind, Gravity and global symmetries, Phys. Rev. D52 (1995) 912–935. [arXiv:hep-th/9502069](#), [doi:10.1103/PhysRevD.52.912](#).
- [132] R. Alonso, A. Urbano, Wormholes and masses for Goldstone bosons, JHEP 02 (2019) 136. [arXiv:1706.07415](#), [doi:10.1007/JHEP02\(2019\)136](#).
- [133] A. G. Dias, V. Pleitez, M. D. Tonasse, Naturally light invisible axion in models with large local discrete symmetries, Phys. Rev. D67 (2003) 095008. [arXiv:hep-ph/0211107](#), [doi:10.1103/PhysRevD.67.095008](#).
- [134] L. M. Carpenter, M. Dine, G. Festuccia, Dynamics of the Peccei Quinn Scale, Phys. Rev. D80 (2009) 125017. [arXiv:0906.1273](#), [doi:10.1103/PhysRevD.80.125017](#).
- [135] K. Harigaya, M. Ibe, K. Schmitz, T. T. Yanagida, Peccei-Quinn symmetry from a gauged discrete R symmetry, Phys.



- Rev. D88 (7) (2013) 075022. [arXiv:1308.1227](#), [doi:10.1103/PhysRevD.88.075022](#).
- [136] A. G. Dias, A. C. B. Machado, C. C. Nishi, A. Ringwald, P. Vaudrevange, The Quest for an Intermediate-Scale Accidental Axion and Further ALPs, JHEP 06 (2014) 037. [arXiv:1403.5760](#), [doi:10.1007/JHEP06\(2014\)037](#).
  - [137] H. Fukuda, M. Ibe, M. Suzuki, T. T. Yanagida, A “gauged”  $U(1)$  Peccei-Quinn symmetry, Phys. Lett. B771 (2017) 327–331. [arXiv:1703.01112](#), [doi:10.1016/j.physletb.2017.05.071](#).
  - [138] M. Duerr, K. Schmidt-Hoberg, J. Unwin, Protecting the Axion with Local Baryon Number, Phys. Lett. B780 (2018) 553–556. [arXiv:1712.01841](#), [doi:10.1016/j.physletb.2018.03.054](#).
  - [139] L. Di Luzio, E. Nardi, L. Ubaldi, Accidental Peccei-Quinn symmetry protected to arbitrary order, Phys. Rev. Lett. 119 (1) (2017) 011801. [arXiv:1704.01122](#), [doi:10.1103/PhysRevLett.119.011801](#).
  - [140] H.-S. Lee, W. Yin, Peccei-Quinn symmetry from a hidden gauge group structure, Phys. Rev. D99 (1) (2019) 015041. [arXiv:1811.04039](#), [doi:10.1103/PhysRevD.99.015041](#).
  - [141] L. Randall, Composite axion models and Planck scale physics, Phys. Lett. B284 (1992) 77–80. [doi:10.1016/0370-2693\(92\)91928-3](#).
  - [142] B. A. Dobrescu, The Strong CP problem versus Planck scale physics, Phys. Rev. D55 (1997) 5826–5833. [arXiv:hep-ph/9609221](#), [doi:10.1103/PhysRevD.55.5826](#).
  - [143] M. Redi, R. Sato, Composite Accidental Axions, JHEP 05 (2016) 104. [arXiv:1602.05427](#), [doi:10.1007/JHEP05\(2016\)104](#).
  - [144] B. Lillard, T. M. P. Tait, A High Quality Composite Axion, JHEP 11 (2018) 199. [arXiv:1811.03089](#), [doi:10.1007/JHEP11\(2018\)199](#).
  - [145] M. B. Gavela, M. Ibe, P. Quilez, T. T. Yanagida, Automatic Peccei-Quinn symmetry, Eur. Phys. J. C79 (6) (2019) 542. [arXiv:1812.08174](#), [doi:10.1140/epjc/s10052-019-7046-3](#).
  - [146] C. Cheung, Axion Protection from Flavor, JHEP 06 (2010) 074. [arXiv:1003.0941](#), [doi:10.1007/JHEP06\(2010\)074](#).
  - [147] C. G. Callan, Jr., R. F. Dashen, D. J. Gross, Toward a Theory of the Strong Interactions, Phys. Rev. D17 (1978) 2717, [36(1977)]. [doi:10.1103/PhysRevD.17.2717](#).
  - [148] C. Bonati, M. D’Elia, M. Mariti, G. Martinelli, M. Mesiti, F. Negro, F. Sanfilippo, G. Villadoro, Axion phenomenology and  $\theta$ -dependence from  $N_f = 2+1$  lattice QCD, JHEP 03 (2016) 155. [arXiv:1512.06746](#), [doi:10.1007/JHEP03\(2016\)155](#).
  - [149] O. Wantz, E. P. S. Shellard, The Topological susceptibility from grand canonical simulations in the interacting instanton liquid model: Chiral phase transition and axion mass, Nucl. Phys. B829 (2010) 110–160. [arXiv:0908.0324](#), [doi:10.1016/j.nuclphysb.2009.12.005](#).
  - [150] O. Wantz, E. P. S. Shellard, Axion Cosmology Revisited, Phys. Rev. D82 (2010) 123508. [arXiv:0910.1066](#), [doi:10.1103/PhysRevD.82.123508](#).
  - [151] P. Petreczky, H.-P. Schadler, S. Sharma, The topological susceptibility in finite temperature QCD and axion cosmology, Phys. Lett. B762 (2016) 498–505. [arXiv:1606.03145](#), [doi:10.1016/j.physletb.2016.09.063](#).
  - [152] C. Bonati, M. D’Elia, G. Martinelli, F. Negro, F. Sanfilippo, A. Todaro, Topology in full QCD at high temperature: a multicanonical approach, JHEP 11 (2018) 170. [arXiv:1807.07954](#), [doi:10.1007/JHEP11\(2018\)170](#).
  - [153] F. Burger, E.-M. Ilgenfritz, M. P. Lombardo, A. Trunin, Chiral observables and topology in hot QCD with two families of quarks, Phys. Rev. D98 (9) (2018) 094501. [arXiv:1805.06001](#), [doi:10.1103/PhysRevD.98.094501](#).
  - [154] A. Bazavov, et al., The chiral and deconfinement aspects of the QCD transition, Phys. Rev. D85 (2012) 054503. [arXiv:1111.1710](#), [doi:10.1103/PhysRevD.85.054503](#).
  - [155] M. S. Turner, Cosmic and Local Mass Density of Invisible Axions, Phys. Rev. D33 (1986) 889–896. [doi:10.1103/PhysRevD.33.889](#).
  - [156] L. F. Abbott, P. Sikivie, A Cosmological Bound on the Invisible Axion, Phys. Lett. B120 (1983) 133–136. [doi:10.1016/0370-2693\(83\)90638-X](#).
  - [157] M. Dine, W. Fischler, The Not So Harmless Axion, Phys. Lett. B120 (1983) 137–141. [doi:10.1016/0370-2693\(83\)90639-1](#).
  - [158] J. Preskill, M. B. Wise, F. Wilczek, Cosmology of the Invisible Axion, Phys. Lett. B120 (1983) 127–132. [doi:10.1016/0370-2693\(83\)90637-8](#).
  - [159] A. D. Linde, Generation of Isothermal Density Perturbations in the Inflationary Universe, Phys. Lett. 158B (1985) 375–380. [doi:10.1016/0370-2693\(85\)90436-8](#).
  - [160] D. Seckel, M. S. Turner, “isothermal” density perturbations in an axion-dominated inflationary universe, Phys. Rev. D 32 (1985) 3178–3183. [doi:10.1103/PhysRevD.32.3178](#).  
URL <https://link.aps.org/doi/10.1103/PhysRevD.32.3178>
  - [161] D. H. Lyth, A limit on the inflationary energy density from axion isocurvature fluctuations, Physics Letters B 236 (4) (1990) 408 – 410. [doi:http://dx.doi.org/10.1016/0370-2693\(90\)90374-F](#).  
URL <http://www.sciencedirect.com/science/article/pii/037026939090374F>
  - [162] A. D. Linde, D. H. Lyth, Axionic domain wall production during inflation, Phys. Lett. B246 (1990) 353–358. [doi:10.1016/0370-2693\(90\)90613-B](#).
  - [163] M. S. Turner, F. Wilczek, Inflationary axion cosmology, Phys. Rev. Lett. 66 (1991) 5–8. [doi:10.1103/PhysRevLett.66.5](#).  
URL <https://link.aps.org/doi/10.1103/PhysRevLett.66.5>
  - [164] D. H. Lyth, Axions and inflation: Vacuum fluctuations, Phys. Rev. D 45 (1992) 3394–3404. [doi:10.1103/PhysRevD.45.3394](#).  
URL <http://link.aps.org/doi/10.1103/PhysRevD.45.3394>
  - [165] D. H. Lyth, E. D. Stewart, Constraining the inflationary energy scale from axion cosmology, Physics Letters B 283 (3) (1992) 189 – 193. [doi:http://dx.doi.org/10.1016/0370-2693\(92\)90006-P](#).  
URL <http://www.sciencedirect.com/science/article/pii/037026939290006P>
  - [166] G. F. Giudice, E. W. Kolb, A. Riotto, Largest temperature of the radiation era and its cosmological implications, Phys.

- Rev. D64 (2001) 023508. [arXiv:hep-ph/0005123](#), [doi:10.1103/PhysRevD.64.023508](#).
- [167] P. Crotty, J. Garcia-Bellido, J. Lesgourgues, A. Riazuelo, Bounds on isocurvature perturbations from CMB and LSS data, *Phys. Rev. Lett.* 91 (2003) 171301. [arXiv:astro-ph/0306286](#), [doi:10.1103/PhysRevLett.91.171301](#).
  - [168] M. Beltran, J. Garcia-Bellido, J. Lesgourgues, A. R. Liddle, A. Slosar, Bayesian model selection and isocurvature perturbations, *Phys. Rev. D* 71 (2005) 063532. [arXiv:astro-ph/0501477](#), [doi:10.1103/PhysRevD.71.063532](#).
  - [169] M. Beltran, J. Garcia-Bellido, J. Lesgourgues, Isocurvature bounds on axions revisited, *Phys. Rev. D* 75 (2007) 103507. [arXiv:hep-ph/0606107](#), [doi:10.1103/PhysRevD.75.103507](#).
  - [170] D. H. Lyth, Axions and inflation: Sitting in the vacuum, *Phys. Rev. D* 45 (1992) 3394–3404. [doi:10.1103/PhysRevD.45.3394](#).
  - [171] K. Strobl, T. J. Weiler, Anharmonic evolution of the cosmic axion density spectrum, *Phys. Rev. D* 50 (1994) 7690–7702. [arXiv:astro-ph/9405028](#), [doi:10.1103/PhysRevD.50.7690](#).
  - [172] K. J. Bae, J.-H. Huh, J. E. Kim, Update of axion CDM energy, *JCAP* 0809 (2008) 005. [arXiv:0806.0497](#), [doi:10.1088/1475-7516/2008/09/005](#).
  - [173] L. Visinelli, P. Gondolo, Dark Matter Axions Revisited, *Phys. Rev. D* 80 (2009) 035024. [arXiv:0903.4377](#), [doi:10.1103/PhysRevD.80.035024](#).
  - [174] V. Poulin, T. L. Smith, D. Grin, T. Karwal, M. Kamionkowski, Cosmological implications of ultralight axionlike fields, *Phys. Rev. D* 98 (8) (2018) 083525. [arXiv:1806.10608](#), [doi:10.1103/PhysRevD.98.083525](#).
  - [175] J. Cookmeyer, D. Grin, T. L. Smith, How sound are our ultra-light axion approximations?, *Phys. Rev. D* 101 (2) (2020) 023501. [arXiv:1909.11094](#), [doi:10.1103/PhysRevD.101.023501](#).
  - [176] E. Di Valentino, R. Z. Ferreira, L. Visinelli, U. Danielsson, Late time transitions in the quintessence field and the  $H_0$  tension, *Phys. Dark Univ.* 26 (2019) 100385. [arXiv:1906.11255](#), [doi:10.1016/j.dark.2019.100385](#).
  - [177] K. Freese, J. A. Frieman, A. V. Olinto, Natural inflation with pseudo - Nambu-Goldstone bosons, *Phys. Rev. Lett.* 65 (1990) 3233–3236. [doi:10.1103/PhysRevLett.65.3233](#).
  - [178] F. C. Adams, J. R. Bond, K. Freese, J. A. Frieman, A. V. Olinto, Natural inflation: Particle physics models, power law spectra for large scale structure, and constraints from COBE, *Phys. Rev. D* 47 (1993) 426–455. [arXiv:hep-ph/9207245](#), [doi:10.1103/PhysRevD.47.426](#).
  - [179] A. Vilenkin, E. P. S. Shellard, *Cosmic Strings and Other Topological Defects*, Cambridge University Press, 2000. URL <http://www.cambridge.org/mw/academic/subjects/physics/theoretical-physics-and-mathematical-physics/cosmic-strings-and-other-topological-defects?format=PB>
  - [180] T. W. B. Kibble, Topology of cosmic domains and strings, *Journal of Physics A Mathematical General* 9 (1976) 1387–1398. [doi:10.1088/0305-4470/9/8/029](#).
  - [181] T. W. B. Kibble, G. Lazarides, Q. Shafi, Walls Bounded by Strings, *Phys. Rev. D* 26 (1982) 435. [doi:10.1103/PhysRevD.26.435](#).
  - [182] A. Vilenkin, Cosmic Strings, *Phys. Rev. D* 24 (1981) 2082–2089. [doi:10.1103/PhysRevD.24.2082](#).
  - [183] R. L. Davis, Goldstone Bosons in String Models of Galaxy Formation, *Phys. Rev. D* 32 (1985) 3172. [doi:10.1103/PhysRevD.32.3172](#).
  - [184] R. L. Davis, Cosmic Axions from Cosmic Strings, *Phys. Lett. B* 180 (1986) 225–230. [doi:10.1016/0370-2693\(86\)90300-X](#).
  - [185] D. H. Lyth, *Estimates of the cosmological axion density*, *Physics Letters B* 275 (3) (1992) 279 – 283. [doi:https://doi.org/10.1016/0370-2693\(92\)91590-6](#). URL <http://www.sciencedirect.com/science/article/pii/0370269392915906>
  - [186] A. Vilenkin, A. E. Everett, Cosmic Strings and Domain Walls in Models with Goldstone and PseudoGoldstone Bosons, *Phys. Rev. Lett.* 48 (1982) 1867–1870. [doi:10.1103/PhysRevLett.48.1867](#).
  - [187] A. Vilenkin, T. Vachaspati, Radiation of Goldstone Bosons From Cosmic Strings, *Phys. Rev. D* 35 (1987) 1138. [doi:10.1103/PhysRevD.35.1138](#).
  - [188] D. Harari, P. Sikivie, On the Evolution of Global Strings in the Early Universe, *Phys. Lett. B* 195 (1987) 361–365. [doi:10.1016/0370-2693\(87\)90032-3](#).
  - [189] R. L. Davis, E. P. S. Shellard, Do Axions Need Inflation?, *Nucl. Phys. B* 324 (1989) 167–186. [doi:10.1016/0550-3213\(89\)90187-9](#).
  - [190] R. A. Battye, E. P. S. Shellard, Global string radiation, *Nucl. Phys. B* 423 (1994) 260–304. [arXiv:astro-ph/9311017](#), [doi:10.1016/0550-3213\(94\)90573-8](#).
  - [191] R. A. Battye, E. P. S. Shellard, Axion string constraints, *Phys. Rev. Lett.* 73 (1994) 2954–2957, [Erratum: *Phys. Rev. Lett.* 76,2203(1996)]. [arXiv:astro-ph/9403018](#), [doi:10.1103/PhysRevLett.73.2954](#), [doi:10.1103/PhysRevLett.76.2203](#).
  - [192] M. Yamaguchi, M. Kawasaki, J. Yokoyama, Evolution of axionic strings and spectrum of axions radiated from them, *Phys. Rev. Lett.* 82 (1999) 4578–4581. [arXiv:hep-ph/9811311](#), [doi:10.1103/PhysRevLett.82.4578](#).
  - [193] M. Yamaguchi, J. Yokoyama, M. Kawasaki, Evolution of a global string network in a matter dominated universe, *Phys. Rev. D* 61 (2000) 061301. [arXiv:hep-ph/9910352](#), [doi:10.1103/PhysRevD.61.061301](#).
  - [194] T. Hiramatsu, M. Kawasaki, T. Sekiguchi, M. Yamaguchi, J. Yokoyama, Improved estimation of radiated axions from cosmological axionic strings, *Phys. Rev. D* 83 (2011) 123531. [arXiv:1012.5502](#), [doi:10.1103/PhysRevD.83.123531](#).
  - [195] T. Hiramatsu, M. Kawasaki, K. Saikawa, Evolution of String-Wall Networks and Axionic Domain Wall Problem, *JCAP* 1108 (2011) 030. [arXiv:1012.4558](#), [doi:10.1088/1475-7516/2011/08/030](#).
  - [196] T. Hiramatsu, M. Kawasaki, K. Saikawa, T. Sekiguchi, Axion cosmology with long-lived domain walls, *JCAP* 1301 (2013) 001. [arXiv:1207.3166](#), [doi:10.1088/1475-7516/2013/01/001](#).
  - [197] T. Hiramatsu, M. Kawasaki, K. Saikawa, T. Sekiguchi, Production of dark matter axions from collapse of string-wall systems, *Phys. Rev. D* 85 (2012) 105020, [Erratum: *Phys. Rev. D* 86,089902(2012)]. [arXiv:1202.5851](#), [doi:10.1103/PhysRevD.86.089902](#), [doi:10.1103/PhysRevD.85.105020](#).

- [198] V. B. Klaer, G. D. Moore, How to simulate global cosmic strings with large string tension, JCAP 1710 (2017) 043. [arXiv:1707.05566](#), [doi:10.1088/1475-7516/2017/10/043](#).
- [199] V. B. Klaer, G. D. Moore, The dark-matter axion mass, JCAP 1711 (11) (2017) 049. [arXiv:1708.07521](#), [doi:10.1088/1475-7516/2017/11/049](#).
- [200] M. Gorghetto, E. Hardy, G. Villadoro, Axions from Strings: the Attractive Solution, JHEP 07 (2018) 151. [arXiv:1806.04677](#), [doi:10.1007/JHEP07\(2018\)151](#).
- [201] A. Vaquero, J. Redondo, J. Stadler, Early seeds of axion miniclusters, JCAP 1904 (04) (2019) 012. [arXiv:1809.09241](#), [doi:10.1088/1475-7516/2019/04/012](#).
- [202] M. Buschmann, J. W. Foster, B. R. Safdi, Early-Universe Simulations of the Cosmological Axion. [arXiv:1906.00967](#).
- [203] Ya. B. Zeldovich, M. Yu. Khlopov, On the Concentration of Relic Magnetic Monopoles in the Universe, Phys. Lett. 79B (1978) 239–241. [doi:10.1016/0370-2693\(78\)90232-0](#).
- [204] J. Preskill, Cosmological Production of Superheavy Magnetic Monopoles, Phys. Rev. Lett. 43 (1979) 1365. [doi:10.1103/PhysRevLett.43.1365](#).
- [205] A. H. Guth, S. H. H. Tye, Phase Transitions and Magnetic Monopole Production in the Very Early Universe, Phys. Rev. Lett. 44 (1980) 631, [Erratum: Phys. Rev. Lett. 44, 963 (1980)]. [doi:10.1103/PhysRevLett.44.631](#), [doi:10.1103/PhysRevLett.44.963.2](#).
- [206] A. Albrecht, N. Turok, Evolution of Cosmic String Networks, Phys. Rev. D40 (1989) 973–1001. [doi:10.1103/PhysRevD.40.973](#).
- [207] C. J. A. P. Martins, E. P. S. Shellard, Quantitative string evolution, Phys. Rev. D54 (1996) 2535–2556. [arXiv:hep-ph/9602271](#), [doi:10.1103/PhysRevD.54.2535](#).
- [208] C. J. A. P. Martins, E. P. S. Shellard, Extending the velocity dependent one scale string evolution model, Phys. Rev. D65 (2002) 043514. [arXiv:hep-ph/0003298](#), [doi:10.1103/PhysRevD.65.043514](#).
- [209] C. J. A. P. Martins, J. N. Moore, E. P. S. Shellard, A Unified model for vortex string network evolution, Phys. Rev. Lett. 92 (2004) 251601. [arXiv:hep-ph/0310255](#), [doi:10.1103/PhysRevLett.92.251601](#).
- [210] A. Vilenkin, Cosmic Strings and Domain Walls, Phys. Rept. 121 (1985) 263–315. [doi:10.1016/0370-1573\(85\)90033-X](#).
- [211] C. J. A. P. Martins, E. P. S. Shellard, String evolution with friction, Phys. Rev. D53 (1996) 575–579. [arXiv:hep-ph/9507335](#), [doi:10.1103/PhysRevD.53.R575](#).
- [212] T. Vachaspati, A. Vilenkin, Evolution of cosmic networks, Phys. Rev. D35 (1987) 1131. [doi:10.1103/PhysRevD.35.1131](#).
- [213] D. P. Bennett, F. R. Bouchet, Evidence for a Scaling Solution in Cosmic String Evolution, Phys. Rev. Lett. 60 (1988) 257. [doi:10.1103/PhysRevLett.60.257](#).
- [214] L. Fleury, G. D. Moore, Axion dark matter: strings and their cores, JCAP 1601 (2016) 004. [arXiv:1509.00026](#), [doi:10.1088/1475-7516/2016/01/004](#).
- [215] C. J. A. P. Martins, Scaling properties of cosmological axion strings, Phys. Lett. B788 (2019) 147–151. [arXiv:1811.12678](#), [doi:10.1016/j.physletb.2018.11.031](#).
- [216] R. A. Battye, E. P. S. Shellard, String radiative back reaction, Phys. Rev. Lett. 75 (1995) 4354–4357. [arXiv:astro-ph/9408078](#), [doi:10.1103/PhysRevLett.75.4354](#).
- [217] M. Sakellariadou, Gravitational waves emitted from infinite strings, Phys. Rev. D42 (1990) 354–360, [Erratum: Phys. Rev. D43, 4150 (1991)]. [doi:10.1103/PhysRevD.42.354](#), [doi:10.1103/PhysRevD.43.4150.2](#).
- [218] M. Sakellariadou, Radiation of Nambu-Goldstone bosons from infinitely long cosmic strings, Phys. Rev. D44 (1991) 3767–3773. [doi:10.1103/PhysRevD.44.3767](#).
- [219] V. Vanchurin, K. D. Olum, A. Vilenkin, Scaling of cosmic string loops, Phys. Rev. D74 (2006) 063527. [arXiv:gr-qc/0511159](#), [doi:10.1103/PhysRevD.74.063527](#).
- [220] C. J. A. P. Martins, E. P. S. Shellard, Fractal properties and small-scale structure of cosmic string networks, Phys. Rev. D73 (2006) 043515. [arXiv:astro-ph/0511792](#), [doi:10.1103/PhysRevD.73.043515](#).
- [221] C. Ringeval, M. Sakellariadou, F. Bouchet, Cosmological evolution of cosmic string loops, JCAP 0702 (2007) 023. [arXiv:astro-ph/0511646](#), [doi:10.1088/1475-7516/2007/02/023](#).
- [222] K. D. Olum, V. Vanchurin, Cosmic string loops in the expanding Universe, Phys. Rev. D75 (2007) 063521. [arXiv:astro-ph/0610419](#), [doi:10.1103/PhysRevD.75.063521](#).
- [223] J. J. Blanco-Pillado, K. D. Olum, B. Shlaer, Large parallel cosmic string simulations: New results on loop production, Phys. Rev. D83 (2011) 083514. [arXiv:1101.5173](#), [doi:10.1103/PhysRevD.83.083514](#).
- [224] J. J. Blanco-Pillado, K. D. Olum, Stochastic gravitational wave background from smoothed cosmic string loops, Phys. Rev. D96 (10) (2017) 104046. [arXiv:1709.02693](#), [doi:10.1103/PhysRevD.96.104046](#).
- [225] T. W. B. Kibble, Evolution of a system of cosmic strings, Nucl. Phys. B252 (1985) 227, [Erratum: Nucl. Phys. B261, 750 (1985)]. [doi:10.1016/0550-3213\(85\)90439-0](#), [doi:10.1016/0550-3213\(85\)90596-6](#).
- [226] Y. Cui, D. E. Morrissey, Non-Thermal Dark Matter from Cosmic Strings, Phys. Rev. D79 (2009) 083532. [arXiv:0805.1060](#), [doi:10.1103/PhysRevD.79.083532](#).
- [227] C. Hagmann, P. Sikivie, Computer simulations of the motion and decay of global strings, Nucl. Phys. B363 (1991) 247–280. [doi:10.1016/0550-3213\(91\)90243-Q](#).
- [228] S. Chang, C. Hagmann, P. Sikivie, Studies of the motion and decay of axion walls bounded by strings, Phys. Rev. D59 (1999) 023505. [arXiv:hep-ph/9807374](#), [doi:10.1103/PhysRevD.59.023505](#).
- [229] S. M. Barr, K. Choi, J. E. Kim, Axion Cosmology in Superstring Models, Nucl. Phys. B283 (1987) 591–604. [doi:10.1016/0550-3213\(87\)90288-4](#).
- [230] P. Sikivie, Of Axions, Domain Walls and the Early Universe, Phys. Rev. Lett. 48 (1982) 1156–1159. [doi:10.1103/PhysRevLett.48.1156](#).
- [231] V. F. Mukhanov, G. V. Chibisov, Quantum Fluctuations and a Nonsingular Universe, JETP Lett. 33 (1981) 532–535,



- [Pisma Zh. Eksp. Teor. Fiz.33,549(1981)].
- [232] A. H. Guth, S. Y. Pi, Fluctuations in the New Inflationary Universe, Phys. Rev. Lett. 49 (1982) 1110–1113. [doi:10.1103/PhysRevLett.49.1110](#).
  - [233] S. W. Hawking, The Development of Irregularities in a Single Bubble Inflationary Universe, Phys. Lett. 115B (1982) 295. [doi:10.1016/0370-2693\(82\)90373-2](#).
  - [234] A. A. Starobinsky, Dynamics of Phase Transition in the New Inflationary Universe Scenario and Generation of Perturbations, Phys. Lett. 117B (1982) 175–178. [doi:10.1016/0370-2693\(82\)90541-X](#).
  - [235] J. M. Bardeen, P. J. Steinhardt, M. S. Turner, Spontaneous Creation of Almost Scale - Free Density Perturbations in an Inflationary Universe, Phys. Rev. D28 (1983) 679. [doi:10.1103/PhysRevD.28.679](#).
  - [236] P. J. Steinhardt, M. S. Turner, A Prescription for Successful New Inflation, Phys. Rev. D29 (1984) 2162–2171. [doi:10.1103/PhysRevD.29.2162](#).
  - [237] Y. Akrami, et al., Planck 2018 results. I. Overview and the cosmological legacy of Planck. [arXiv:1807.06205](#).
  - [238] N. Aghanim, et al., Planck 2018 results. VI. Cosmological parameters. [arXiv:1807.06209](#).
  - [239] Y. Akrami, et al., Planck 2018 results. X. Constraints on inflation. [arXiv:1807.06211](#).
  - [240] A. Kosowsky, M. S. Turner, CBR anisotropy and the running of the scalar spectral index, Phys. Rev. D52 (1995) R1739–R1743. [arXiv:astro-ph/9504071](#), [doi:10.1103/PhysRevD.52.R1739](#).
  - [241] S. M. Leach, A. R. Liddle, Microwave background constraints on inflationary parameters, Mon. Not. Roy. Astron. Soc. 341 (2003) 1151. [arXiv:astro-ph/0207213](#), [doi:10.1046/j.1365-8711.2003.06445.x](#).
  - [242] A. R. Liddle, S. M. Leach, How long before the end of inflation were observable perturbations produced?, Phys. Rev. D68 (2003) 103503. [arXiv:astro-ph/0305263](#), [doi:10.1103/PhysRevD.68.103503](#).
  - [243] A. Riotto, Inflation and the theory of cosmological perturbations, ICTP Lect. Notes Ser. 14 (2003) 317–413. [arXiv:hep-ph/0210162](#).
  - [244] V. Bozza, M. Gasperini, M. Giovannini, G. Veneziano, Assisting pre - big bang phenomenology through short lived axions, Phys. Lett. B543 (2002) 14–22. [arXiv:hep-ph/0206131](#), [doi:10.1016/S0370-2693\(02\)02387-0](#).
  - [245] V. Bozza, M. Gasperini, M. Giovannini, G. Veneziano, Constraints on pre big bang parameter space from CMBR anisotropies, Phys. Rev. D67 (2003) 063514. [arXiv:hep-ph/0212112](#), [doi:10.1103/PhysRevD.67.063514](#).
  - [246] T. Kobayashi, R. Kurematsu, F. Takahashi, Isocurvature Constraints and Anharmonic Effects on QCD Axion Dark Matter, JCAP 1309 (2013) 032. [arXiv:1304.0922](#), [doi:10.1088/1475-7516/2013/09/032](#).
  - [247] P. A. R. Ade, et al., Planck 2013 results. XVI. Cosmological parameters, Astron. Astrophys. 571 (2014) A16. [arXiv:1303.5076](#), [doi:10.1051/0004-6361/201321591](#).
  - [248] P. A. R. Ade, et al., Planck 2013 results. XXII. Constraints on inflation, Astron. Astrophys. 571 (2014) A22. [arXiv:1303.5082](#), [doi:10.1051/0004-6361/201321569](#).
  - [249] D. Barkats, et al., Degree-Scale CMB Polarization Measurements from Three Years of BICEP1 Data, Astrophys. J. 783 (2014) 67. [arXiv:1310.1422](#), [doi:10.1088/0004-637X/783/2/67](#).
  - [250] P. A. R. Ade, et al., Joint Analysis of BICEP2/KeckArray and Planck Data, Phys. Rev. Lett. 114 (2015) 101301. [arXiv:1502.00612](#), [doi:10.1103/PhysRevLett.114.101301](#).
  - [251] P. A. R. Ade, et al., Planck 2015 results. XX. Constraints on inflation, Astron. Astrophys. 594 (2016) A20. [arXiv:1502.02114](#), [doi:10.1051/0004-6361/201525898](#).
  - [252] P. A. R. Ade, et al., BICEP2 / Keck Array x: Constraints on Primordial Gravitational Waves using Planck, WMAP, and New BICEP2/Keck Observations through the 2015 Season, Phys. Rev. Lett. 121 (2018) 221301. [arXiv:1810.05216](#), [doi:10.1103/PhysRevLett.121.221301](#).
  - [253] J. E. Kim, H. P. Nilles, M. Peloso, Completing natural inflation, JCAP 0501 (2005) 005. [arXiv:hep-ph/0409138](#), [doi:10.1088/1475-7516/2005/01/005](#).
  - [254] S. Hannestad, A. Mirizzi, G. G. Raffelt, Y. Y. Y. Wong, Neutrino and axion hot dark matter bounds after WMAP-7, JCAP 1008 (2010) 001. [arXiv:1004.0695](#), [doi:10.1088/1475-7516/2010/08/001](#).
  - [255] E. Di Valentino, E. Giusarma, M. Lattanzi, O. Mena, A. Melchiorri, J. Silk, Cosmological Axion and neutrino mass constraints from Planck 2015 temperature and polarization data, Phys. Lett. B752 (2016) 182–185. [arXiv:1507.08665](#), [doi:10.1016/j.physletb.2015.11.025](#).
  - [256] E. Masso, R. Toldra, New constraints on a light spinless particle coupled to photons, Phys. Rev. D55 (1997) 7967–7969. [arXiv:hep-ph/9702275](#), [doi:10.1103/PhysRevD.55.7967](#).
  - [257] D. Cadamuro, S. Hannestad, G. Raffelt, J. Redondo, Cosmological bounds on sub-MeV mass axions, JCAP 1102 (2011) 003. [arXiv:1011.3694](#), [doi:10.1088/1475-7516/2011/02/003](#).
  - [258] M. Millea, L. Knox, B. Fields, New Bounds for Axions and Axion-Like Particles with keV-GeV Masses, Phys. Rev. D92 (2) (2015) 023010. [arXiv:1501.04097](#), [doi:10.1103/PhysRevD.92.023010](#).
  - [259] P. F. Depta, M. Hufnagel, K. Schmidt-Hoberg, Robust cosmological constraints on axion-like particles [arXiv:2002.08370](#).
  - [260] K. Mimasu, V. Sanz, ALPs at Colliders, JHEP 06 (2015) 173. [arXiv:1409.4792](#), [doi:10.1007/JHEP06\(2015\)173](#).
  - [261] J. Jaeckel, M. Spannowsky, Probing MeV to 90 GeV axion-like particles with LEP and LHC, Phys. Lett. B753 (2016) 482–487. [arXiv:1509.00476](#), [doi:10.1016/j.physletb.2015.12.037](#).
  - [262] B. Döbrich, J. Jaeckel, F. Kahlhoefer, A. Ringwald, K. Schmidt-Hoberg, ALPtraum: ALP production in proton beam dump experiments, JHEP 02 (2016) 018, [JHEP02,018(2016)]. [arXiv:1512.03069](#), [doi:10.1007/JHEP02\(2016\)018](#).
  - [263] S. Knapen, T. Lin, H. K. Lou, T. Melia, Searching for Axionlike Particles with Ultraperipheral Heavy-Ion Collisions, Phys. Rev. Lett. 118 (17) (2017) 171801. [arXiv:1607.06083](#), [doi:10.1103/PhysRevLett.118.171801](#).
  - [264] I. Brivio, M. B. Gavela, L. Merlo, K. Mimasu, J. M. No, R. del Rey, V. Sanz, ALPs Effective Field Theory and Collider Signatures, Eur. Phys. J. C77 (8) (2017) 572. [arXiv:1701.05379](#), [doi:10.1140/epjc/s10052-017-5111-3](#).
  - [265] M. Bauer, M. Neubert, A. Thamm, Collider Probes of Axion-Like Particles, JHEP 12 (2017) 044. [arXiv:1708.00443](#),

- doi:10.1007/JHEP12(2017)044.
- [266] M. J. Dolan, T. Ferber, C. Hearty, F. Kahlhoefer, K. Schmidt-Hoberg, Revised constraints and Belle II sensitivity for visible and invisible axion-like particles, JHEP 12 (2017) 094. [arXiv:1709.00009](#), doi:10.1007/JHEP12(2017)094.
  - [267] E. Di Valentino, E. Giusarma, M. Lattanzi, A. Melchiorri, O. Mena, Axion cold dark matter: status after Planck and BICEP2, Phys. Rev. D90 (4) (2014) 043534. [arXiv:1405.1860](#), doi:10.1103/PhysRevD.90.043534.
  - [268] P. Gondolo, L. Visinelli, Axion cold dark matter in view of BICEP2 results, Phys. Rev. Lett. 113 (2014) 011802. [arXiv:1403.4594](#), doi:10.1103/PhysRevLett.113.011802.
  - [269] L. M. Fleury, G. D. Moore, Axion String Dynamics I: 2+1D, JCAP 1605 (05) (2016) 005. [arXiv:1602.04818](#), doi:10.1088/1475-7516/2016/05/005.
  - [270] M. Kawasaki, K. Saikawa, T. Sekiguchi, Axion dark matter from topological defects, Phys. Rev. D91 (6) (2015) 065014. [arXiv:1412.0789](#), doi:10.1103/PhysRevD.91.065014.
  - [271] J. N. Moore, E. P. S. Shellard, C. J. A. P. Martins, On the evolution of Abelian-Higgs string networks, Phys. Rev. D65 (2002) 023503. [arXiv:hep-ph/0107171](#), doi:10.1103/PhysRevD.65.023503.
  - [272] S. Hoof, F. Kahlhoefer, P. Scott, C. Weniger, M. White, Axion global fits with Peccei-Quinn symmetry breaking before inflation using GAMBIT, JHEP 03 (2019) 191. [arXiv:1810.07192](#), doi:10.1007/JHEP03(2019)191.
  - [273] T. Bringmann, et al., DarkBit: A GAMBIT module for computing dark matter observables and likelihoods, Eur. Phys. J. C77 (12) (2017) 831. [arXiv:1705.07920](#), doi:10.1140/epjc/s10052-017-5155-4.
  - [274] P. Athron, et al., GAMBIT: The Global and Modular Beyond-the-Standard-Model Inference Tool, Eur. Phys. J. C77 (11) (2017) 784, [Addendum: Eur. Phys. J.C78,no.2,98(2018)]. [arXiv:1705.07908](#), doi:10.1140/epjc/s10052-017-5513-2, 10.1140/epjc/s10052-017-5321-8.
  - [275] P. W. Graham, A. Scherlis, Stochastic axion scenario, Phys. Rev. D98 (3) (2018) 035017. [arXiv:1805.07362](#), doi:10.1103/PhysRevD.98.035017.
  - [276] F. Takahashi, W. Yin, A. H. Guth, QCD axion window and low-scale inflation, Phys. Rev. D98 (1) (2018) 015042. [arXiv:1805.08763](#), doi:10.1103/PhysRevD.98.015042.
  - [277] R. T. Co, E. Gonzalez, K. Harigaya, Axion Misalignment Driven to the Hilltop, JHEP 05 (2019) 163. [arXiv:1812.11192](#), doi:10.1007/JHEP05(2019)163.
  - [278] G. G. Raffelt, Axion constraints from white dwarf cooling times, Physics Letters B 166 (4) (1986) 402 – 406. doi:[https://doi.org/10.1016/0370-2693\(86\)91588-1](#).  
URL <http://www.sciencedirect.com/science/article/pii/0370269386915881>
  - [279] N. Viaux, M. Catelan, P. B. Stetson, G. Raffelt, J. Redondo, A. A. R. Valcarce, A. Weiss, Neutrino and axion bounds from the globular cluster M5 (NGC 5904), Phys. Rev. Lett. 111 (2013) 231301. [arXiv:1311.1669](#), doi:10.1103/PhysRevLett.111.231301.
  - [280] A. Arvanitaki, S. Dubovsky, Exploring the String Axiverse with Precision Black Hole Physics, Phys. Rev. D83 (2011) 044026. [arXiv:1004.3558](#), doi:10.1103/PhysRevD.83.044026.
  - [281] A. Arvanitaki, M. Baryakhtar, X. Huang, Discovering the QCD Axion with Black Holes and Gravitational Waves, Phys. Rev. D91 (8) (2015) 084011. [arXiv:1411.2263](#), doi:10.1103/PhysRevD.91.084011.
  - [282] P. A. R. Ade, et al., Planck 2015 results. XIII. Cosmological parameters, Astron. Astrophys. 594 (2016) A13. [arXiv:1502.01589](#), doi:10.1051/0004-6361/201525830.
  - [283] G. Ballesteros, J. Redondo, A. Ringwald, C. Tamarit, Unifying inflation with the axion, dark matter, baryogenesis and the seesaw mechanism, Phys. Rev. Lett. 118 (7) (2017) 071802. [arXiv:1608.05414](#), doi:10.1103/PhysRevLett.118.071802.
  - [284] G. Ballesteros, J. Redondo, A. Ringwald, C. Tamarit, Standard Model—axion—seesaw—Higgs portal inflation. Five problems of particle physics and cosmology solved in one stroke, JCAP 1708 (08) (2017) 001. [arXiv:1610.01639](#), doi:10.1088/1475-7516/2017/08/001.
  - [285] G. Ballesteros, J. Redondo, A. Ringwald, C. Tamarit, Several Problems in Particle Physics and Cosmology Solved in One SMASH, Front. Astron. Space Sci. 6 (2019) 55. [arXiv:1904.05594](#), doi:10.3389/fspas.2019.00055.
  - [286] N. Kitajima, F. Takahashi, Resonant conversions of QCD axions into hidden axions and suppressed isocurvature perturbations, JCAP 1501 (01) (2015) 032. [arXiv:1411.2011](#), doi:10.1088/1475-7516/2015/01/032.
  - [287] M. Fairbairn, R. Hogan, D. J. E. Marsh, Unifying inflation and dark matter with the Peccei-Quinn field: observable axions and observable tensors, Phys. Rev. D91 (2) (2015) 023509. [arXiv:1410.1752](#), doi:10.1103/PhysRevD.91.023509.
  - [288] K. N. Abazajian, et al., CMB-S4 Science Book, First Edition. [arXiv:1610.02743](#).
  - [289] T. Tenkanen, L. Visinelli, Axion dark matter from Higgs inflation with an intermediate  $H_*$ , JCAP 1908 (08) (2019) 033. [arXiv:1906.11837](#), doi:10.1088/1475-7516/2019/08/033.
  - [290] D. Budker, P. W. Graham, M. Ledbetter, S. Rajendran, A. Sushkov, Proposal for a Cosmic Axion Spin Precession Experiment (CASPER), Phys. Rev. X4 (2) (2014) 021030. [arXiv:1306.6089](#), doi:10.1103/PhysRevX.4.021030.
  - [291] Y. Kahn, B. R. Safdi, J. Thaler, Broadband and Resonant Approaches to Axion Dark Matter Detection, Phys. Rev. Lett. 117 (14) (2016) 141801. [arXiv:1602.01086](#), doi:10.1103/PhysRevLett.117.141801.
  - [292] J. L. Ouellet, et al., First Results from ABRACADABRA-10 cm: A Search for Sub- $\mu$ eV Axion Dark Matter, Phys. Rev. Lett. 122 (12) (2019) 121802. [arXiv:1810.12257](#), doi:10.1103/PhysRevLett.122.121802.
  - [293] D. Alesini, D. Babusci, D. Di Gioacchino, C. Gatti, G. Lamanna, C. Ligi, The KLASH Proposal. [arXiv:1707.06010](#).
  - [294] D. Babusci, et al., KLASH Conceptual Design Report. [arXiv:1911.02427](#).
  - [295] L. D. Duffy, P. Sikivie, D. B. Tanner, S. J. Asztalos, C. Hagmann, D. Kinion, L. J. Rosenberg, K. van Bibber, D. B. Yu, R. F. Bradley, A high resolution search for dark-matter axions, Phys. Rev. D74 (2006) 012006. [arXiv:astro-ph/0603108](#), doi:10.1103/PhysRevD.74.012006.
  - [296] S. J. Asztalos, et al., A SQUID-based microwave cavity search for dark-matter axions, Phys. Rev. Lett. 104 (2010) 041301. [arXiv:0910.5914](#), doi:10.1103/PhysRevLett.104.041301.

- [297] S. J. Asztalos, et al., Design and performance of the ADMX SQUID-based microwave receiver, Nucl. Instrum. Meth. A656 (2011) 39–44. [arXiv:1105.4203](#), [doi:10.1016/j.nima.2011.07.019](#).
- [298] I. Stern, ADMX Status, PoS ICHEP2016 (2016) 198. [arXiv:1612.08296](#).
- [299] T. Braine, et al., Extended Search for the Invisible Axion with the Axion Dark Matter Experiment. [arXiv:1910.08638](#).
- [300] A. Caldwell, G. Dvali, B. Majorovits, A. Millar, G. Raffelt, J. Redondo, O. Reimann, F. Simon, F. Steffen, Dielectric Haloscopes: A New Way to Detect Axion Dark Matter, Phys. Rev. Lett. 118 (9) (2017) 091801. [arXiv:1611.05865](#), [doi:10.1103/PhysRevLett.118.091801](#).
- [301] J. K. Vogel, et al., IAXO - The International Axion Observatory, in: 8th Patras Workshop on Axions, WIMPs and WISPs (AXION-WIMP 2012) Chicago, Illinois, July 18–22, 2012, 2013. [arXiv:1302.3273](#). URL <http://lss.fnal.gov/archive/2013/pub/fermilab-pub-13-699-a.pdf>
- [302] J. K. Vogel, et al., The Next Generation of Axion Helioscopes: The International Axion Observatory (IA XO), Phys. Procedia 61 (2015) 193–200. [doi:10.1016/j.phpro.2014.12.031](#).
- [303] E. Armengaud, et al., Physics potential of the International Axion Observatory (IA XO), JCAP 1906 (06) (2019) 047. [arXiv:1904.09155](#), [doi:10.1088/1475-7516/2019/06/047](#).
- [304] P. F. de Salas, S. Pastor, Relic neutrino decoupling with flavour oscillations revisited, JCAP 1607 (07) (2016) 051. [arXiv:1606.06986](#), [doi:10.1088/1475-7516/2016/07/051](#).
- [305] G. Mangano, G. Miele, S. Pastor, T. Pinto, O. Pisanti, P. D. Serpico, Relic neutrino decoupling including flavor oscillations, Nucl. Phys. B729 (2005) 221–234. [arXiv:hep-ph/0506164](#), [doi:10.1016/j.nuclphysb.2005.09.041](#).
- [306] S. Dodelson, M. S. Turner, Nonequilibrium neutrino statistical mechanics in the expanding universe, Phys. Rev. D46 (1992) 3372–3387. [doi:10.1103/PhysRevD.46.3372](#).
- [307] S. Hannestad, J. Madsen, Neutrino decoupling in the early universe, Phys. Rev. D52 (1995) 1764–1769. [arXiv:astro-ph/9506015](#), [doi:10.1103/PhysRevD.52.1764](#).
- [308] A. D. Dolgov, S. H. Hansen, D. V. Semikoz, Nonequilibrium corrections to the spectra of massless neutrinos in the early universe, Nucl. Phys. B503 (1997) 426–444. [arXiv:hep-ph/9703315](#), [doi:10.1016/S0550-3213\(97\)00479-3](#).
- [309] M. Gerbino, K. Freese, S. Vagnozzi, M. Lattanzi, O. Mena, E. Giusarma, S. Ho, Impact of neutrino properties on the estimation of inflationary parameters from current and future observations, Phys. Rev. D 95 (4) (2017) 043512. [arXiv:1610.08830](#), [doi:10.1103/PhysRevD.95.043512](#).
- [310] M. Archidiacono, E. Giusarma, S. Hannestad, O. Mena, Cosmic dark radiation and neutrinos, Adv. High Energy Phys. 2013 (2013) 191047. [arXiv:1307.0637](#), [doi:10.1155/2013/191047](#).
- [311] J. Lesgourgues, S. Pastor, Neutrino cosmology and Planck, New J. Phys. 16 (2014) 065002. [arXiv:1404.1740](#), [doi:10.1088/1367-2630/16/6/065002](#).
- [312] F. D’Eramo, R. Z. Ferreira, A. Notari, J. L. Bernal, Hot Axions and the  $H_0$  tension, JCAP 1811 (11) (2018) 014. [arXiv:1808.07430](#), [doi:10.1088/1475-7516/2018/11/014](#).
- [313] D. Baumann, D. Green, B. Wallisch, New Target for Cosmic Axion Searches, Phys. Rev. Lett. 117 (17) (2016) 171301. [arXiv:1604.08614](#), [doi:10.1103/PhysRevLett.117.171301](#).
- [314] E. Mazzo, F. Rota, G. Zsembinszki, On axion thermalization in the early universe, Phys. Rev. D66 (2002) 023004. [arXiv:hep-ph/0203221](#), [doi:10.1103/PhysRevD.66.023004](#).
- [315] P. Graf, F. D. Steffen, Thermal axion production in the primordial quark-gluon plasma, Phys. Rev. D83 (2011) 075011. [arXiv:1008.4528](#), [doi:10.1103/PhysRevD.83.075011](#).
- [316] A. Salvio, A. Strumia, W. Xue, Thermal axion production, JCAP 1401 (2014) 011. [arXiv:1310.6982](#), [doi:10.1088/1475-7516/2014/01/011](#).
- [317] M. S. Turner, Thermal Production of Not SO Invisible Axions in the Early Universe, Phys. Rev. Lett. 59 (1987) 2489, [Erratum: Phys. Rev. Lett. 60, 1101 (1988)]. [doi:10.1103/PhysRevLett.59.2489](#), [doi:10.1103/PhysRevLett.60.1101.3](#).
- [318] R. Z. Ferreira, A. Notari, Observable Windows for the QCD Axion Through the Number of Relativistic Species, Phys. Rev. Lett. 120 (19) (2018) 191301. [arXiv:1801.06090](#), [doi:10.1103/PhysRevLett.120.191301](#).
- [319] J. L. Bernal, L. Verde, A. G. Riess, The trouble with  $H_0$ , JCAP 1610 (10) (2016) 019. [arXiv:1607.05617](#), [doi:10.1088/1475-7516/2016/10/019](#).
- [320] A. G. Riess, S. Casertano, W. Yuan, L. M. Macri, D. Scolnic, Large Magellanic Cloud Cepheid Standards Provide a 1% Foundation for the Determination of the Hubble Constant and Stronger Evidence for Physics beyond  $\Lambda$ CDM, Astrophys. J. 876 (1) (2019) 85. [arXiv:1903.07603](#), [doi:10.3847/1538-4357/ab1422](#).
- [321] S. Vagnozzi, New physics in light of the  $H_0$  tension: an alternative view. [arXiv:1907.07569](#).
- [322] A. Melchiorri, O. Mena, A. Slosar, An improved cosmological bound on the thermal axion mass, Phys. Rev. D76 (2007) 041303. [arXiv:0705.2695](#), [doi:10.1103/PhysRevD.76.041303](#).
- [323] E. Di Valentino, S. Gariazzo, E. Giusarma, O. Mena, Robustness of cosmological axion mass limits, Phys. Rev. D91 (12) (2015) 123505. [arXiv:1503.00911](#), [doi:10.1103/PhysRevD.91.123505](#).
- [324] R. Mayle, J. R. Wilson, J. R. Ellis, K. A. Olive, D. N. Schramm, G. Steigman, Constraints on Axions from SN 1987a, Phys. Lett. B203 (1988) 188–196. [doi:10.1016/0370-2693\(88\)91595-X](#).
- [325] M. S. Turner, Axions from SN 1987a, Phys. Rev. Lett. 60 (1988) 1797. [doi:10.1103/PhysRevLett.60.1797](#).
- [326] G. Raffelt, D. Seckel, Bounds on Exotic Particle Interactions from SN 1987a, Phys. Rev. Lett. 60 (1988) 1793. [doi:10.1103/PhysRevLett.60.1793](#).
- [327] R. Mayle, J. R. Wilson, J. R. Ellis, K. A. Olive, D. N. Schramm, G. Steigman, Updated Constraints on Axions from SN 1987a, Phys. Lett. B219 (1989) 515, [188(1989)]. [doi:10.1016/0370-2693\(89\)91104-0](#).
- [328] C. J. Hogan, M. J. Rees, Axion Miniclusters, Phys. Lett. B205 (1988) 228–230. [doi:10.1016/0370-2693\(88\)91655-3](#).
- [329] E. W. Kolb, I. I. Tkachev, Axion miniclusters and Bose stars, Phys. Rev. Lett. 71 (1993) 3051–3054. [arXiv:hep-ph/9303313](#), [doi:10.1103/PhysRevLett.71.3051](#).

- [330] E. W. Kolb, I. I. Tkachev, Nonlinear axion dynamics and formation of cosmological pseudosolitons, *Phys. Rev. D* 49 (1994) 5040–5051. [arXiv:astro-ph/9311037](#), [doi:10.1103/PhysRevD.49.5040](#).
- [331] E. W. Kolb, I. I. Tkachev, Large amplitude isothermal fluctuations and high density dark matter clumps, *Phys. Rev. D* 50 (1994) 769–773. [arXiv:astro-ph/9403011](#), [doi:10.1103/PhysRevD.50.769](#).
- [332] V. S. Berezhinsky, V. I. Dokuchaev, Yu. N. Eroshenko, Formation and internal structure of superdense dark matter clumps and ultracompact minihaloes, *JCAP* 1311 (2013) 059. [arXiv:1308.6742](#), [doi:10.1088/1475-7516/2013/11/059](#).
- [333] E. Hardy, Miniclusters in the Axiverse, *JHEP* 02 (2017) 046. [arXiv:1609.00208](#), [doi:10.1007/JHEP02\(2017\)046](#).
- [334] M. Reig, J. W. F. Valle, M. Yamada, Light majoron cold dark matter from topological defects and the formation of boson stars, *JCAP* 1909 (09) (2019) 029. [arXiv:1905.01287](#), [doi:10.1088/1475-7516/2019/09/029](#).
- [335] M. Fairbairn, D. J. E. Marsh, J. Quevillon, S. Rozier, Structure formation and microlensing with axion miniclusters, *Phys. Rev. D* 97 (8) (2018) 083502. [arXiv:1707.03310](#), [doi:10.1103/PhysRevD.97.083502](#).
- [336] M. Fairbairn, D. J. E. Marsh, J. Quevillon, Searching for the QCD Axion with Gravitational Microlensing, *Phys. Rev. Lett.* 119 (2) (2017) 021101. [arXiv:1701.04787](#), [doi:10.1103/PhysRevLett.119.021101](#).
- [337] J. Enander, A. Pargner, T. Schwetz, Axion minicluster power spectrum and mass function, *JCAP* 1712 (12) (2017) 038. [arXiv:1708.04466](#), [doi:10.1088/1475-7516/2017/12/038](#).
- [338] L. Visinelli, J. Redondo, Axion Miniclusters in Modified Cosmological Histories, *Phys. Rev. D* 101 (2) (2020) 023008. [arXiv:1808.01879](#), [doi:10.1103/PhysRevD.101.023008](#).
- [339] A. K. Drukier, K. Freese, D. N. Spergel, Detecting Cold Dark Matter Candidates, *Phys. Rev. D* 33 (1986) 3495–3508. [doi:10.1103/PhysRevD.33.3495](#).
- [340] S. Knirck, A. J. Millar, C. A. J. O’Hare, J. Redondo, F. D. Steffen, Directional axion detection, *JCAP* 1811 (11) (2018) 051. [arXiv:1806.05927](#), [doi:10.1088/1475-7516/2018/11/051](#).
- [341] E. W. Kolb, I. I. Tkachev, Femtolensing and picolensing by axion miniclusters, *Astrophys. J.* 460 (1996) L25–L28. [arXiv:astro-ph/9510043](#), [doi:10.1086/309962](#).
- [342] P. Tinyakov, I. Tkachev, K. Zioutas, Tidal streams from axion miniclusters and direct axion searches, *JCAP* 1601 (01) (2016) 035. [arXiv:1512.02884](#), [doi:10.1088/1475-7516/2016/01/035](#).
- [343] I. I. Tkachev, On the possibility of Bose star formation, *Phys. Lett. B* 261 (1991) 289–293. [doi:10.1016/0370-2693\(91\)90330-S](#).
- [344] H.-Y. Schive, T. Chiueh, T. Broadhurst, Cosmic Structure as the Quantum Interference of a Coherent Dark Wave, *Nature Phys.* 10 (2014) 496–499. [arXiv:1406.6586](#), [doi:10.1038/nphys2996](#).
- [345] B. Eggemeier, J. C. Niemeyer, Formation and mass growth of axion stars in axion miniclusters, *Phys. Rev. D* 100 (6) (2019) 063528. [arXiv:1906.01348](#), [doi:10.1103/PhysRevD.100.063528](#).
- [346] D. J. Kaup, Klein-Gordon Geon, *Phys. Rev.* 172 (1968) 1331–1342. [doi:10.1103/PhysRev.172.1331](#).
- [347] R. Ruffini, S. Bonazzola, Systems of selfgravitating particles in general relativity and the concept of an equation of state, *Phys. Rev.* 187 (1969) 1767–1783. [doi:10.1103/PhysRev.187.1767](#).
- [348] J. D. Breit, S. Gupta, A. Zaks, Cold Bose Stars, *Phys. Lett. B* 140B (1984) 329–332. [doi:10.1016/0370-2693\(84\)90764-0](#).
- [349] L. A. Urena-Lopez, T. Matos, R. Becerril, Inside oscillatons, *Class. Quant. Grav.* 19 (2002) 6259–6277. [doi:10.1088/0264-9381/19/23/320](#).
- [350] T. Helfer, D. J. E. Marsh, K. Clough, M. Fairbairn, E. A. Lim, R. Becerril, Black hole formation from axion stars, *JCAP* 1703 (03) (2017) 055. [arXiv:1609.04724](#), [doi:10.1088/1475-7516/2017/03/055](#).
- [351] E. Seidel, W.-M. Suen, Formation of solitonic stars through gravitational cooling, *Phys. Rev. Lett.* 72 (1994) 2516–2519. [arXiv:gr-qc/9309015](#), [doi:10.1103/PhysRevLett.72.2516](#).
- [352] F. S. Guzman, L. A. Urena-Lopez, Gravitational cooling of self-gravitating Bose-Condensates, *Astrophys. J.* 645 (2006) 814–819. [arXiv:astro-ph/0603613](#), [doi:10.1086/504508](#).
- [353] D. G. Levkov, A. G. Panin, I. I. Tkachev, Gravitational Bose-Einstein condensation in the kinetic regime, *Phys. Rev. Lett.* 121 (15) (2018) 151301. [arXiv:1804.05857](#), [doi:10.1103/PhysRevLett.121.151301](#).
- [354] P.-H. Chavanis, Mass-radius relation of Newtonian self-gravitating Bose-Einstein condensates with short-range interactions: I. Analytical results, *Phys. Rev. D* 84 (2011) 043531. [arXiv:1103.2050](#), [doi:10.1103/PhysRevD.84.043531](#).
- [355] P. H. Chavanis, L. Delfini, Mass-radius relation of Newtonian self-gravitating Bose-Einstein condensates with short-range interactions: II. Numerical results, *Phys. Rev. D* 84 (2011) 043532. [arXiv:1103.2054](#), [doi:10.1103/PhysRevD.84.043532](#).
- [356] L. Visinelli, S. Baum, J. Redondo, K. Freese, F. Wilczek, Dilute and dense axion stars, *Phys. Lett. B* 777 (2018) 64–72. [arXiv:1710.08910](#), [doi:10.1016/j.physletb.2017.12.010](#).
- [357] D. G. Levkov, A. G. Panin, I. I. Tkachev, Relativistic axions from collapsing Bose stars, *Phys. Rev. Lett.* 118 (1) (2017) 011301. [arXiv:1609.03611](#), [doi:10.1103/PhysRevLett.118.011301](#).
- [358] G. G. Raffelt, *Stars as laboratories for fundamental physics*, 1996. URL <http://wwwth.mpp.mpg.de/members/raffelt/mypapers/199613.pdf>
- [359] P. Di Vecchia, M. Giannotti, M. Lattanzi, A. Lindner, Round Table on Axions and Axion-like Particles, in: 13th Conference on Quark Confinement and the Hadron Spectrum (Confinement XIII) Maynooth, Ireland, July 31–August 6, 2018, 2019. [arXiv:1902.06567](#).
- [360] A. Friedland, M. Giannotti, M. Wise, Constraining the Axion-Photon Coupling with Massive Stars., *Phys.Rev.Lett.* 110 (2013) 061101. [arXiv:1210.1271](#), [doi:10.1103/PhysRevLett.110.061101](#).
- [361] A. Ayala, I. Dominguez, M. Giannotti, A. Mirizzi, O. Straniero, Revisiting the bound on axion-photon coupling from Globular Clusters, *Phys. Rev. Lett.* 113 (19) (2014) 191302. [arXiv:1406.6053](#), [doi:10.1103/PhysRevLett.113.191302](#).
- [362] O. Straniero, A. Ayala, M. Giannotti, A. Mirizzi, I. Dominguez, Axion-Photon Coupling: Astrophysical Constraints, in: Proceedings, 11th Patras Workshop on Axions, WIMPs and WISPs (Axion-WIMP 2015): Zaragoza, Spain, June 22–26, 2015, 2015, pp. 77–81. [doi:10.3204/DESY-PROC-2015-02/straniero\\_oscar](#).



- [363] N. Vinyoles, A. M. Serenelli, F. L. Villante, S. Basu, J. Bergström, M. C. Gonzalez-Garcia, M. Maltoni, C. Peña-Garay, N. Song, A new Generation of Standard Solar Models, *Astrophys. J.* 835 (2) (2017) 202. [arXiv:1611.09867](#), [doi:10.3847/1538-4357/835/2/202](#).
- [364] O. Straniero, I. Dominguez, L. Piersanti, M. Giannotti, A. Mirizzi, The Initial Mass–Final Luminosity Relation of Type II Supernova Progenitors: Hints of New Physics?, *Astrophys. J.* 881 (2) (2019) 158. [arXiv:1907.06367](#), [doi:10.3847/1538-4357/ab3222](#).
- [365] G. G. Raffelt, D. S. P. Dearborn, Bounds on Hadronic Axions From Stellar Evolution, *Phys. Rev. D* 36 (1987) 2211. [doi:10.1103/PhysRevD.36.2211](#).
- [366] H. Schlattl, A. Weiss, G. Raffelt, Helioseismological constraint on solar axion emission, *Astropart. Phys.* 10 (1999) 353–359. [arXiv:hep-ph/9807476](#), [doi:10.1016/S0927-6505\(98\)00063-2](#).
- [367] N. Vinyoles, A. Serenelli, F. L. Villante, S. Basu, J. Redondo, J. Isern, New axion and hidden photon constraints from a solar data global fit, *JCAP* 1510 (10) (2015) 015. [arXiv:1501.01639](#), [doi:10.1088/1475-7516/2015/10/015](#).
- [368] P. Gondolo, G. G. Raffelt, Solar neutrino limit on axions and keV-mass bosons, *Phys. Rev. D* 79 (2009) 107301. [arXiv:0807.2926](#), [doi:10.1103/PhysRevD.79.107301](#).
- [369] M. Giannotti, I. Irastorza, J. Redondo, A. Ringwald, Cool WISPs for stellar cooling excesses, *JCAP* 1605 (05) (2016) 057. [arXiv:1512.08108](#), [doi:10.1088/1475-7516/2016/05/057](#).
- [370] Y. I. Izotov, G. Stasinska, N. G. Guseva, Primordial 4He abundance: a determination based on the largest sample of HII regions with a methodology tested on model HII regions, *Astron. Astrophys.* 558 (2013) A57. [arXiv:1308.2100](#), [doi:10.1051/0004-6361/201220782](#).
- [371] Y. I. Izotov, T. X. Thuan, N. G. Guseva, A new determination of the primordial He abundance using the He I  $\lambda$ 10830 Å emission line: cosmological implications, *Mon. Not. Roy. Astron. Soc.* 445 (1) (2014) 778–793. [arXiv:1408.6953](#), [doi:10.1093/mnras/stu1771](#).
- [372] E. Aver, K. A. Olive, E. D. Skillman, The effects of He I  $\lambda$  10830 on helium abundance determinations, *JCAP* 1507 (07) (2015) 011. [arXiv:1503.08146](#), [doi:10.1088/1475-7516/2015/07/011](#).
- [373] G. Carosi, A. Friedland, M. Giannotti, M. Pivovarov, J. Ruz, et al., Probing the axion-photon coupling: phenomenological and experimental perspectives. A snowmass white paper. [arXiv:1309.7035](#).
- [374] R. Kippenhahn, A. Weigert, *Stellar Structure and Evolution.*, Springer-Verlag, 1994.
- [375] K. B. McQuinn, E. D. Skillman, J. J. Dalcanton, A. E. Dolphin, J. Holtzman, et al., Observational Constraints on Red and Blue Helium Burning Sequences., *Astrophys. J.* 740 (2011) 48. [arXiv:1108.1405](#), [doi:10.1088/0004-637X/740/1/48](#).
- [376] M. Giannotti, ALP hints from cooling anomalies, in: *Proceedings, 11th Patras Workshop on Axions, WIMPs and WISPs (Axion-WIMP 2015): Zaragoza, Spain, June 22-26, 2015*, 2015, pp. 26–30. [arXiv:1508.07576](#), [doi:10.3204/DESY-PROC-2015-02/giannotti\\_maurizio](#).
- [377] LSST Science Collaboration, P. A. Abell, J. Allison, S. F. Anderson, J. R. Andrew, J. R. P. Angel, L. Armus, D. Arnett, S. J. Asztalos, T. S. Axelrod, *LSST Science Book, Version 2.0*. [arXiv:0912.0201](#).
- [378] A. Drlica-Wagner, et al., Probing the Fundamental Nature of Dark Matter with the Large Synoptic Survey Telescope. [arXiv:1902.01055](#).
- [379] A. Pantziris, K. Kang, Axion Emission Rates in Stars and Constraints on Its Mass, *Phys. Rev. D* 33 (1986) 3509. [doi:10.1103/PhysRevD.33.3509](#).
- [380] J. Redondo, Solar axion flux from the axion-electron coupling, *JCAP* 1312 (2013) 008. [arXiv:1310.0823](#), [doi:10.1088/1475-7516/2013/12/008](#).
- [381] G. Raffelt, A. Weiss, Red giant bound on the axion - electron coupling revisited, *Phys. Rev. D* 51 (1995) 1495–1498. [arXiv:hep-ph/9410205](#), [doi:10.1103/PhysRevD.51.1495](#).
- [382] M. Giannotti, Hints of new physics from stars., *PoS ICHEP2016* (2016) 076. [arXiv:1611.04651](#), [doi:10.22323/1.282.0076](#).
- [383] A. H. Córscico, L. G. Althaus, M. M. Miller Bertolami, S. O. Kepler, Pulsating white dwarfs: new insights, *Astron. Astrophys. Rev.* 27 (1) (2019) 7. [arXiv:1907.00115](#), [doi:10.1007/s00159-019-0118-4](#).
- [384] M. M. Miller Bertolami, B. E. Melendez, L. G. Althaus, J. Isern, Revisiting the axion bounds from the Galactic white dwarf luminosity function, *JCAP* 1410 (10) (2014) 069. [arXiv:1406.7712](#), [doi:10.1088/1475-7516/2014/10/069](#).
- [385] C.-F. Chang, Hidden Photon Compton and Bremsstrahlung in White Dwarf Anomalous Cooling and Luminosity Functions. [arXiv:1607.03347](#).
- [386] M. M. Miller Bertolami, Limits on the neutrino magnetic dipole moment from the luminosity function of hot white dwarfs, *Astron. Astrophys.* 562 (2014) A123. [arXiv:1407.1404](#), [doi:10.1051/0004-6361/201322641](#).
- [387] J. Isern, E. Garcia-Berro, S. Torres, R. Cojocaru, S. Catalan, Axions and the luminosity function of white dwarfs: the thin and thick discs, and the halo, *Mon. Not. Roy. Astron. Soc.* 478 (2) (2018) 2569–2575. [arXiv:1805.00135](#), [doi:10.1093/mnras/sty1162](#).
- [388] M. Kilic, N. C. Hambly, P. Bergeron, C. Genest-Beaulieu, N. Rowell, Gaia reveals evidence for merged white dwarfs, *MNRAS* 479 (1) (2018) L113–L117. [arXiv:1805.01227](#), [doi:10.1093/mnrasl/sly110](#).
- [389] N. P. Gentile Fusillo, P.-E. Tremblay, B. T. Gänsicke, C. J. Manser, T. Cunningham, E. Cukanovaite, M. Hollands, T. Marsh, R. Raddi, S. Jordan, A Gaia Data Release 2 catalogue of white dwarfs and a comparison with SDSS, *MNRAS* 482 (4) (2019) 4570–4591. [arXiv:1807.03315](#), [doi:10.1093/mnras/sty3016](#).
- [390] S. A. Díaz, K.-P. Schröder, K. Zuber, D. Jack, E. E. B. Barrios, Constraint on the axion-electron coupling constant and the neutrino magnetic dipole moment by using the tip-RGB luminosity of fifty globular clusters. [arXiv:1910.10568](#).
- [391] O. Straniero, I. Dominguez, M. Giannotti, A. Mirizzi, Axion-electron coupling from the RGB tip of Globular Clusters, in: *Proceedings, 13th Patras Workshop on Axions, WIMPs and WISPs, (PATRAS 2017): Thessaloniki, Greece, 15 May 2017 - 19, 2017, 2018*, pp. 172–176. [arXiv:1802.10357](#), [doi:10.3204/DESY-PROC-2017-02/straniero\\_oscar](#).

- [392] A. Serenelli, A. Weiss, S. Cassisi, M. Salaris, A. Pietrinferni, *The brightness of the red giant branch tip*, *Astronomy & Astrophysics* 606 (2017) A33. doi:[10.1051/0004-6361/201731004](https://doi.org/10.1051/0004-6361/201731004). URL <http://dx.doi.org/10.1051/0004-6361/201731004>
- [393] N. Viaux, M. Catelan, P. B. Stetson, G. Raffelt, J. Redondo, A. A. R. Valcarce, A. Weiss, Particle-physics constraints from the globular cluster M5: Neutrino Dipole Moments, *Astron. Astrophys.* 558 (2013) A12. arXiv:[1308.4627](https://arxiv.org/abs/1308.4627), doi:[10.1051/0004-6361/201322004](https://doi.org/10.1051/0004-6361/201322004).
- [394] E. Pancino, M. Bellazzini, G. Giuffrida, S. Marinoni, Globular clusters with Gaia, *Monthly Notices of the Royal Astronomical Society* 467 (2017) 412–427. arXiv:[1701.03003](https://arxiv.org/abs/1701.03003).
- [395] C. Hanhart, D. R. Phillips, S. Reddy, Neutrino and axion emissivities of neutron stars from nucleon-nucleon scattering data, *Phys. Lett. B* 499 (2001) 9–15. arXiv:[astro-ph/0003445](https://arxiv.org/abs/astro-ph/0003445), doi:[10.1016/S0370-2693\(00\)01382-4](https://doi.org/10.1016/S0370-2693(00)01382-4).
- [396] P. Carenza, T. Fischer, M. Giannotti, G. Guo, G. Martinez-Pinedo, A. Mirizzi, Improved axion emissivity from a supernova via nucleon-nucleon bremsstrahlung, *JCAP* 1910 (10) (2019) 016. arXiv:[1906.11844](https://arxiv.org/abs/1906.11844), doi:[10.1088/1475-7516/2019/10/016](https://doi.org/10.1088/1475-7516/2019/10/016).
- [397] A. Burrows, M. S. Turner, R. P. Brinkmann, Axions and SN 1987a, *Phys. Rev. D* 39 (1989) 1020. doi:[10.1103/PhysRevD.39.1020](https://doi.org/10.1103/PhysRevD.39.1020).
- [398] L. B. Leinson, Axion mass limit from observations of the neutron star in Cassiopeia A, *JCAP* 1408 (2014) 031. arXiv:[1405.6873](https://arxiv.org/abs/1405.6873), doi:[10.1088/1475-7516/2014/08/031](https://doi.org/10.1088/1475-7516/2014/08/031).
- [399] L. B. Leinson, Superfluid phases of triplet pairing and rapid cooling of the neutron star in Cassiopeia A, *Phys. Lett. B* 741 (2015) 87–91. arXiv:[1411.6833](https://arxiv.org/abs/1411.6833), doi:[10.1016/j.physletb.2014.12.017](https://doi.org/10.1016/j.physletb.2014.12.017).
- [400] K. Hamaguchi, N. Nagata, K. Yanagi, J. Zheng, Limit on the Axion Decay Constant from the Cooling Neutron Star in Cassiopeia A, *Phys. Rev. D* 98 (10) (2018) 103015. arXiv:[1806.07151](https://arxiv.org/abs/1806.07151), doi:[10.1103/PhysRevD.98.103015](https://doi.org/10.1103/PhysRevD.98.103015).
- [401] M. V. Beznogov, E. Rrapaj, D. Page, S. Reddy, Constraints on Axion-like Particles and Nucleon Pairing in Dense Matter from the Hot Neutron Star in HESS J1731-347, *Phys. Rev. C* 98 (3) (2018) 035802. arXiv:[1806.07991](https://arxiv.org/abs/1806.07991), doi:[10.1103/PhysRevC.98.035802](https://doi.org/10.1103/PhysRevC.98.035802).
- [402] P. W. Graham, S. Rajendran, New Observables for Direct Detection of Axion Dark Matter, *Phys. Rev. D* 88 (2013) 035023. arXiv:[1306.6088](https://arxiv.org/abs/1306.6088), doi:[10.1103/PhysRevD.88.035023](https://doi.org/10.1103/PhysRevD.88.035023).
- [403] G. Raffelt, Limits on a CP-violating scalar axion-nucleon interaction, *Phys. Rev. D* 86 (2012) 015001. arXiv:[1205.1776](https://arxiv.org/abs/1205.1776), doi:[10.1103/PhysRevD.86.015001](https://doi.org/10.1103/PhysRevD.86.015001).
- [404] E. Hardy, R. Lasenby, Stellar cooling bounds on new light particles: plasma mixing effects, *JHEP* 02 (2017) 033. arXiv:[1611.05852](https://arxiv.org/abs/1611.05852), doi:[10.1007/JHEP02\(2017\)033](https://doi.org/10.1007/JHEP02(2017)033).
- [405] R. Penrose, Gravitational collapse: The role of general relativity, *Riv. Nuovo Cim.* 1 (1969) 252–276, [Gen. Rel. Grav. 34,1141(2002)].
- [406] V. Cardoso, Ó. J. C. Dias, G. S. Hartnett, M. Middleton, P. Pani, J. E. Santos, Constraining the mass of dark photons and axion-like particles through black-hole superradiance, *JCAP* 1803 (03) (2018) 043. arXiv:[1801.01420](https://arxiv.org/abs/1801.01420), doi:[10.1088/1475-7516/2018/03/043](https://doi.org/10.1088/1475-7516/2018/03/043).
- [407] A. Arvanitaki, M. Baryakhtar, S. Dimopoulos, S. Dubovsky, R. Lasenby, Black Hole Mergers and the QCD Axion at Advanced LIGO, *Phys. Rev. D* 95 (4) (2017) 043001. arXiv:[1604.03958](https://arxiv.org/abs/1604.03958), doi:[10.1103/PhysRevD.95.043001](https://doi.org/10.1103/PhysRevD.95.043001).
- [408] T. Fischer, S. Chakraborty, M. Giannotti, A. Mirizzi, A. Payez, A. Ringwald, Probing axions with the neutrino signal from the next galactic supernova, *Phys. Rev. D* 94 (8) (2016) 085012. arXiv:[1605.08780](https://arxiv.org/abs/1605.08780), doi:[10.1103/PhysRevD.94.085012](https://doi.org/10.1103/PhysRevD.94.085012).
- [409] M. Archidiacono, S. Hannestad, A. Mirizzi, G. Raffelt, Y. Y. Y. Wong, Axion hot dark matter bounds after Planck, *JCAP* 1310 (2013) 020. arXiv:[1307.0615](https://arxiv.org/abs/1307.0615), doi:[10.1088/1475-7516/2013/10/020](https://doi.org/10.1088/1475-7516/2013/10/020).
- [410] S. Andriamonje, et al., An Improved limit on the axion-photon coupling from the CAST experiment, *JCAP* 0704 (2007) 010. arXiv:[hep-ex/0702006](https://arxiv.org/abs/hep-ex/0702006), doi:[10.1088/1475-7516/2007/04/010](https://doi.org/10.1088/1475-7516/2007/04/010).
- [411] K. Barth, et al., CAST constraints on the axion-electron coupling, *JCAP* 1305 (2013) 010. arXiv:[1302.6283](https://arxiv.org/abs/1302.6283), doi:[10.1088/1475-7516/2013/05/010](https://doi.org/10.1088/1475-7516/2013/05/010).
- [412] J. Jaeckel, L. J. Thormaehlen, Distinguishing Axion Models with IAXO, *JCAP* 1903 (03) (2019) 039. arXiv:[1811.09278](https://arxiv.org/abs/1811.09278), doi:[10.1088/1475-7516/2019/03/039](https://doi.org/10.1088/1475-7516/2019/03/039).
- [413] P. Sikivie, Experimental Tests of the Invisible Axion, *Phys. Rev. Lett.* 51 (1983) 1415–1417, [,321(1983)]. doi:[10.1103/PhysRevLett.51.1415](https://doi.org/10.1103/PhysRevLett.51.1415), doi:[10.1103/PhysRevLett.52.695.2](https://doi.org/10.1103/PhysRevLett.52.695.2).
- [414] E. A. Paschos, K. Zioutas, A Proposal for solar axion detection via Bragg scattering, *Phys. Lett. B* 323 (1994) 367–372. doi:[10.1016/0370-2693\(94\)91233-5](https://doi.org/10.1016/0370-2693(94)91233-5).
- [415] A. V. Derbin, A. S. Kayunov, V. N. Muratova, D. A. Semenov, E. V. Unzhakov, Constraints on the axion-electron coupling for solar axions produced by Compton process and bremsstrahlung, *Phys. Rev. D* 83 (2011) 023505. arXiv:[1101.2290](https://arxiv.org/abs/1101.2290), doi:[10.1103/PhysRevD.83.023505](https://doi.org/10.1103/PhysRevD.83.023505).
- [416] K. Arisaka, P. Beltrame, C. Ghag, J. Kaidi, K. Lung, A. Lyashenko, R. D. Peccei, P. Smith, K. Ye, Expected Sensitivity to Galactic/Solar Axions and Bosonic Super-WIMPs based on the Axio-electric Effect in Liquid Xenon Dark Matter Detectors, *Astropart. Phys.* 44 (2013) 59–67. arXiv:[1209.3810](https://arxiv.org/abs/1209.3810), doi:[10.1016/j.astropartphys.2012.12.009](https://doi.org/10.1016/j.astropartphys.2012.12.009).
- [417] T. Dafni, C. A. J. O’Hare, B. Lakić, J. Galán, F. J. Iguaz, I. G. Irastorza, K. Jakovčić, G. Luzón, J. Redondo, E. Ruiz Chóliz, Weighing the solar axion, *Phys. Rev. D* 99 (3) (2019) 035037. arXiv:[1811.09290](https://arxiv.org/abs/1811.09290), doi:[10.1103/PhysRevD.99.035037](https://doi.org/10.1103/PhysRevD.99.035037).
- [418] K. van Bibber, P. M. McIntyre, D. E. Morris, G. G. Raffelt, A Practical Laboratory Detector for Solar Axions, *Phys. Rev. D* 39 (1989) 2089. doi:[10.1103/PhysRevD.39.2089](https://doi.org/10.1103/PhysRevD.39.2089).
- [419] K. Zioutas, et al., A Decommissioned LHC model magnet as an axion telescope, *Nucl. Instrum. Meth. A* 425 (1999) 480–489. arXiv:[astro-ph/9801176](https://arxiv.org/abs/astro-ph/9801176), doi:[10.1016/S0168-9002\(98\)01442-9](https://doi.org/10.1016/S0168-9002(98)01442-9).
- [420] V. Anastassopoulos, et al., New CAST Limit on the Axion-Photon Interaction, *Nature Phys.* 13 (2017) 584–590. arXiv:



- 1705.02290, doi:10.1038/nphys4109.
- [421] S. Hannestad, A. Mirizzi, G. Raffelt, New cosmological mass limit on thermal relic axions, JCAP 0507 (2005) 002. [arXiv:hep-ph/0504059](#), doi:10.1088/1475-7516/2005/07/002.
  - [422] I. G. Irastorza, et al., Towards a new generation axion helioscope, JCAP 1106 (2011) 013. [arXiv:1103.5334](#), doi:10.1088/1475-7516/2011/06/013.
  - [423] F. T. Avignone, III, et al., Experimental search for solar axions via coherent Primakoff conversion in a germanium spectrometer, Phys. Rev. Lett. 81 (1998) 5068–5071. [arXiv:astro-ph/9708008](#), doi:10.1103/PhysRevLett.81.5068.
  - [424] E. Aprile, et al., First Axion Results from the XENON100 Experiment, Phys. Rev. D90 (6) (2014) 062009, [Erratum: Phys. Rev.D95,no.2,029904(2017)]. [arXiv:1404.1455](#), doi:10.1103/PhysRevD.90.062009, doi:10.1103/PhysRevD.95.029904.
  - [425] D. S. Akerib, et al., First Searches for Axions and Axionlike Particles with the LUX Experiment, Phys. Rev. Lett. 118 (26) (2017) 261301. [arXiv:1704.02297](#), doi:10.1103/PhysRevLett.118.261301.
  - [426] C. Fu, et al., Limits on Axion Couplings from the First 80 Days of Data of the PandaX-II Experiment, Phys. Rev. Lett. 119 (18) (2017) 181806. [arXiv:1707.07921](#), doi:10.1103/PhysRevLett.119.181806.
  - [427] S. Dimopoulos, G. D. Starkman, B. W. Lynn, Atomic Enhancements in the Detection of Axions, Mod. Phys. Lett. A1 (1986) 491–500. doi:10.1142/S0217732386000622.
  - [428] M. Pospelov, A. Ritz, M. B. Voloshin, Bosonic super-WIMPs as keV-scale dark matter, Phys. Rev. D78 (2008) 115012. [arXiv:0807.3279](#), doi:10.1103/PhysRevD.78.115012.
  - [429] A. Derevianko, V. A. Dzuba, V. V. Flambaum, M. Pospelov, Axio-electric effect, Phys. Rev. D82 (2010) 065006. [arXiv:1007.1833](#), doi:10.1103/PhysRevD.82.065006.
  - [430] N. Du, et al., A Search for Invisible Axion Dark Matter with the Axion Dark Matter Experiment, Phys. Rev. Lett. 120 (15) (2018) 151301. [arXiv:1804.05750](#), doi:10.1103/PhysRevLett.120.151301.
  - [431] R. Dicke, The Measurement of Thermal Radiation at Microwave Frequencies, Rev.of.Sci.Instr. 17 (1946) 268–275. doi:10.1063/1.1770483.
  - [432] J. Kim, S. Youn, J. Jeong, W. Chung, O. Kwon, Y. K. Semertzidis, Exploiting higher-order resonant modes for axion haloscopes. [arXiv:1910.00793](#).
  - [433] S. Lee, S. Ahn, J. Choi, B. R. Ko, Y. K. Semertzidis, CAPP-8TB: Search for Axion Dark Matter in a Mass Range of 6.62 to 7.04  $\mu\text{eV}$ , 2019. [arXiv:1910.00047](#).
  - [434] Y. K. Semertzidis, et al., Axion Dark Matter Research with IBS/CAPP. [arXiv:1910.11591](#).
  - [435] B. M. Brubaker, et al., First results from a microwave cavity axion search at 24  $\mu\text{eV}$ , Phys. Rev. Lett. 118 (6) (2017) 061302. [arXiv:1610.02580](#), doi:10.1103/PhysRevLett.118.061302.
  - [436] B. T. McAllister, G. Flower, E. N. Ivanov, M. Goryachev, J. Bourhill, M. E. Tobar, The ORGAN Experiment: An axion haloscope above 15 GHz, Phys. Dark Univ. 18 (2017) 67–72. [arXiv:1706.00209](#), doi:10.1016/j.dark.2017.09.010.
  - [437] P. Brun, et al., A new experimental approach to probe QCD axion dark matter in the mass range above 40  $\mu\text{eV}$ , Eur. Phys. J. C79 (3) (2019) 186. [arXiv:1901.07401](#), doi:10.1140/epjc/s10052-019-6683-x.
  - [438] M. Lawson, A. J. Millar, M. Pancaldi, E. Vitagliano, F. Wilczek, Tunable axion plasma haloscopes, Phys. Rev. Lett. 123 (2019) 141802. [arXiv:1904.11872](#), doi:10.1103/PhysRevLett.123.141802.
  - [439] D. J. E. Marsh, K.-C. Fong, E. W. Lentz, L. Smejkal, M. N. Ali, Proposal to Detect Dark Matter using Axionic Topological Antiferromagnets, Phys. Rev. Lett. 123 (12) (2019) 121601. [arXiv:1807.08810](#), doi:10.1103/PhysRevLett.123.121601.
  - [440] R. Barbieri, C. Braggio, G. Carugno, C. S. Gallo, A. Lombardi, A. Ortolan, R. Pengo, G. Ruoso, C. C. Speake, Searching for galactic axions through magnetized media: the QUAX proposal, Phys. Dark Univ. 15 (2017) 135–141. [arXiv:1606.02201](#), doi:10.1016/j.dark.2017.01.003.
  - [441] N. Crescini, et al., Operation of a ferromagnetic axion haloscope at  $m_a = 58 \mu\text{eV}$ , Eur. Phys. J. C78 (9) (2018) 703, [Erratum: Eur. Phys. J.C78,no.9,813(2018)]. [arXiv:1806.00310](#), doi:10.1140/epjc/s10052-018-6262-6, doi:10.1140/epjc/s10052-018-6163-8.
  - [442] A. Hook, Y. Kahn, B. R. Safdi, Z. Sun, Radio Signals from Axion Dark Matter Conversion in Neutron Star Magnetospheres, Phys. Rev. Lett. 121 (24) (2018) 241102. [arXiv:1804.03145](#), doi:10.1103/PhysRevLett.121.241102.
  - [443] D. F. Jackson Kimball, et al., Overview of the Cosmic Axion Spin Precession Experiment (CASPER). [arXiv:1711.08999](#).
  - [444] K. Van Bibber, N. R. Dagdeviren, S. E. Koonin, A. Kerman, H. N. Nelson, Proposed experiment to produce and detect light pseudoscalars, Phys. Rev. Lett. 59 (1987) 759–762. doi:10.1103/PhysRevLett.59.759.
  - [445] R. Ballou, et al., New exclusion limits on scalar and pseudoscalar axionlike particles from light shining through a wall, Phys. Rev. D92 (9) (2015) 092002. [arXiv:1506.08082](#), doi:10.1103/PhysRevD.92.092002.
  - [446] F. Della Valle, A. Ejlli, U. Gastaldi, G. Messineo, E. Milotti, R. Pengo, G. Ruoso, G. Zavattini, The PVLAS experiment: measuring vacuum magnetic birefringence and dichroism with a birefringent Fabry–Perot cavity, Eur. Phys. J. C76 (1) (2016) 24. [arXiv:1510.08052](#), doi:10.1140/epjc/s10052-015-3869-8.
  - [447] R. Ballou, F. Della Valle, A. Ejlli, U. Gastaldi, H. Grote, S. Kunc, K. Meissner, E. Milotti, W.-T. Ni, S.-s. Pan, R. Pengo, P. Pugnat, G. Ruoso, A. Siemko, M. Sulc, G. Zavattini, Letter of Intent to measure Vacuum Magnetic Birefringence: the VMB@CERN experiment, Tech. Rep. CERN-SPSC-2018-036. SPSC-I-249, CERN, Geneva (Dec 2018). URL <https://cds.cern.ch/record/2649744>
  - [448] A. Arvanitaki, A. A. Geraci, Resonantly Detecting Axion-Mediated Forces with Nuclear Magnetic Resonance, Phys. Rev. Lett. 113 (16) (2014) 161801. [arXiv:1403.1290](#), doi:10.1103/PhysRevLett.113.161801.
  - [449] A. A. Geraci, et al., Progress on the ARIADNE axion experiment, Springer Proc. Phys. 211 (2018) 151–161. [arXiv:1710.05413](#), doi:10.1007/978-3-319-92726-8\_18.
  - [450] N. Crescini, C. Braggio, G. Carugno, P. Falferi, A. Ortolan, G. Ruoso, Improved constraints on monopole-dipole interaction mediated by pseudo-scalar bosons, Phys. Lett. B773 (2017) 677–680. [arXiv:1705.06044](#), doi:10.1016/j.physletb.2017.09.019.

- [451] M. Ajello, et al., Search for Spectral Irregularities due to Photon–Axionlike-Particle Oscillations with the Fermi Large Area Telescope, *Phys. Rev. Lett.* 116 (16) (2016) 161101. [arXiv:1603.06978](#), [doi:10.1103/PhysRevLett.116.161101](#).
- [452] A. Payez, C. Evoli, T. Fischer, M. Giannotti, A. Mirizzi, A. Ringwald, Revisiting the SN1987A gamma-ray limit on ultralight axion-like particles, *JCAP* 1502 (02) (2015) 006. [arXiv:1410.3747](#), [doi:10.1088/1475-7516/2015/02/006](#).
- [453] M. Meyer, M. Giannotti, A. Mirizzi, J. Conrad, M. A. Sánchez-Conde, Fermi Large Area Telescope as a Galactic Supernovae Axionscope, *Phys. Rev. Lett.* 118 (1) (2017) 011103. [arXiv:1609.02350](#), [doi:10.1103/PhysRevLett.118.011103](#).
- [454] T. Schmidt, Über die magnetischen Momente der Atomkerne. , *Zeitschrift für Physik* 106 (5-6) (1937) 358–361. [doi:10.1007/BF01338744](#).
- [455] D. F. Jackson Kimball, Nuclear spin content and constraints on exotic spin-dependent couplings. , *New J. Phys.* 17 (7) (2015) 073008. [arXiv:1407.2671](#), [doi:10.1088/1367-2630/17/7/073008](#).
- [456] T. Wu, et al., Search for Axionlike Dark Matter with a Liquid-State Nuclear Spin Comagnetometer. , *Phys. Rev. Lett.* 122 (19) (2019) 191302. [arXiv:1901.10843](#), [doi:10.1103/PhysRevLett.123.169002](#), [doi:10.1103/PhysRevLett.122.191302](#).
- [457] N. Crisosto, G. Rybka, P. Sikivie, N. S. Sullivan, D. B. Tanner, J. Yang, ADMX SLIC: Results from a Superconducting LC Circuit Investigating Cold Axions [arXiv:1911.05772](#).
- [458] V. Anastassopoulos, et al., Towards a medium-scale axion helioscope and haloscope, *JINST* 12 (11) (2017) P11019. [arXiv:1706.09378](#), [doi:10.1088/1748-0221/12/11/P11019](#).
- [459] G. Rybka, A. Wagner, A. Brill, K. Ramos, R. Percival, K. Patel, Search for dark matter axions with the Orpheus experiment, *Phys. Rev. D* 91 (1) (2015) 011701. [arXiv:1403.3121](#), [doi:10.1103/PhysRevD.91.011701](#).
- [460] A. Á. Melcón, et al., Axion Searches with Microwave Filters: the RADES project, *JCAP* 1805 (05) (2018) 040. [arXiv:1803.01243](#), [doi:10.1088/1475-7516/2018/05/040](#).
- [461] M. Baryakhtar, J. Huang, R. Lasenby, Axion and hidden photon dark matter detection with multilayer optical haloscopes, *Phys. Rev. D* 98 (3) (2018) 035006. [arXiv:1803.11455](#), [doi:10.1103/PhysRevD.98.035006](#).
- [462] B. T. McAllister, M. Goryachev, J. Bourhill, E. N. Ivanov, M. E. Tobar, Broadband Axion Dark Matter Haloscopes via Electric Sensing [arXiv:1803.07755](#).
- [463] L. Capparelli, G. Cavoto, J. Ferretti, F. Giazotto, A. D. Polosa, P. Spagnolo, Axion-like particle searches with sub-THz photons, *Phys. Dark Univ.* 12 (2016) 37–44. [arXiv:1510.06892](#), [doi:10.1016/j.dark.2016.01.003](#).
- [464] P. Spagnolo, STAX: a new technique for detecting Axions, *PoS ICHEP2016* (2016) 207. [doi:10.22323/1.282.0207](#).
- [465] J. Ferretti, STAX. An Axion-like Particle Search with Microwave Photons, in: *Proceedings, 12th Patras Workshop on Axions, WIMPs and WISPs (PATRAS 2016): Jeju Island, South Korea, June 20-24, 2016, 2017*, pp. 35–38. [arXiv:1609.05105](#), [doi:10.3204/DESY-PROC-2009-03/Ferretti\\_Jacopo](#).
- [466] L. Santamaria, C. Braggio, G. Carugno, V. D. Sarno, P. Maddaloni, G. Ruoso, [Axion dark matter detection by laser spectroscopy of ultracold molecular oxygen: a proposal](#), *New Journal of Physics* 17 (11) (2015) 113025. [doi:10.1088/1367-2630/17/11/113025](#).  
URL <https://doi.org/10.1088/2F1367-2630%2F17%2F11%2F113025>
- [467] C. Braggio, et al., New detectors for axions, *PoS IFD2015* (2017) 032. [doi:10.22323/1.266.0032](#).
- [468] S. Pustelny, et al., The Global Network of Optical Magnetometers for Exotic physics (GNOME): A novel scheme to search for physics beyond the Standard Model, *Annalen Phys.* 525 (8-9) (2013) 659–670. [arXiv:1303.5524](#), [doi:10.1002/andp.201300061](#).
- [469] E. Farhi, L. Susskind, Technicolor, *Phys. Rept.* 74 (1981) 277. [doi:10.1016/0370-1573\(81\)90173-3](#).
- [470] J. E. Kim, A composite invisible axion, *Phys. Rev. D* 31 (1985) 1733. [doi:10.1103/PhysRevD.31.1733](#).
- [471] S. L. Cheng, C. Q. Geng, W. T. Ni, Axion - photon couplings in invisible axion models, *Phys. Rev. D* 52 (1995) 3132–3135. [arXiv:hep-ph/9506295](#), [doi:10.1103/PhysRevD.52.3132](#).
- [472] L. Di Luzio, F. Mescia, E. Nardi, Redefining the Axion Window, *Phys. Rev. Lett.* 118 (2017) 031801. [arXiv:1610.07593](#), [doi:10.1103/PhysRevLett.118.031801](#).
- [473] K. Choi, J. E. Kim, DYNAMICAL AXION, *Phys. Rev. D* 32 (1985) 1828. [doi:10.1103/PhysRevD.32.1828](#).
- [474] L. Di Luzio, F. Mescia, E. Nardi, Window for preferred axion models, *Phys. Rev. D* 96 (7) (2017) 075003. [arXiv:1705.05370](#), [doi:10.1103/PhysRevD.96.075003](#).
- [475] S. P. Robinson, F. Wilczek, Gravitational correction to running of gauge couplings, *Phys. Rev. Lett.* 96 (2006) 231601. [arXiv:hep-th/0509050](#), [doi:10.1103/PhysRevLett.96.231601](#).
- [476] L. Di Luzio, R. Grober, J. F. Kamenik, M. Nardecchia, Accidental matter at the LHC, *JHEP* 07 (2015) 074. [arXiv:1504.00359](#), [doi:10.1007/JHEP07\(2015\)074](#).
- [477] M. L. Perl, E. R. Lee, D. Loomba, Searches for fractionally charged particles, *Ann. Rev. Nucl. Part. Sci.* 59 (2009) 47–65. [doi:10.1146/annurev-nucl-121908-122035](#).
- [478] C. B. Dover, T. K. Gaisser, G. Steigman, Cosmological constraints on new stable hadrons, *Phys. Rev. Lett.* 42 (1979) 1117. [doi:10.1103/PhysRevLett.42.1117](#).
- [479] E. Nardi, E. Roulet, Are exotic stable quarks cosmologically allowed?, *Phys. Lett. B* 245 (1990) 105–110. [doi:10.1016/0370-2693\(90\)90172-3](#).
- [480] A. Arvanitaki, C. Davis, P. W. Graham, A. Pierce, J. G. Wacker, Limits on split supersymmetry from gluino cosmology, *Phys. Rev. D* 72 (2005) 075011. [arXiv:hep-ph/0504210](#), [doi:10.1103/PhysRevD.72.075011](#).
- [481] J. Kang, M. A. Luty, S. Nasri, The Relic abundance of long-lived heavy colored particles, *JHEP* 09 (2008) 086. [arXiv:hep-ph/0611322](#), [doi:10.1088/1126-6708/2008/09/086](#).
- [482] C. Jacoby, S. Nussinov, The Relic Abundance of Massive Colored Particles after a Late Hadronic Annihilation Stage. [arXiv:0712.2681](#).
- [483] M. Kusakabe, T. Takesako, Resonant annihilation of long-lived massive colored particles through hadronic collisions,

- Phys. Rev. D85 (2012) 015005. [arXiv:1112.0860](#), [doi:10.1103/PhysRevD.85.015005](#).
- [484] S. Dimopoulos, D. Eichler, R. Esmailzadeh, G. D. Starkman, Getting a Charge Out of Dark Matter, Phys. Rev. D41 (1990) 2388. [doi:10.1103/PhysRevD.41.2388](#).
  - [485] L. Chuzhoy, E. W. Kolb, Reopening the window on charged dark matter, JCAP 0907 (2009) 014. [arXiv:0809.0436](#), [doi:10.1088/1475-7516/2009/07/014](#).
  - [486] S. Burdin, M. Fairbairn, P. Mermod, D. Milstead, J. Pinfold, T. Sloan, W. Taylor, Non-collider searches for stable massive particles, Phys. Rept. 582 (2015) 1–52. [arXiv:1410.1374](#), [doi:10.1016/j.physrep.2015.03.004](#).
  - [487] M. P. Hertzberg, A. Masoumi, Astrophysical Constraints on Singlet Scalars at LHC, JCAP 1704 (04) (2017) 028. [arXiv:1607.06445](#), [doi:10.1088/1475-7516/2017/04/028](#).
  - [488] A. Gould, B. T. Draine, R. W. Romani, S. Nussinov, Neutron Stars: Graveyard of Charged Dark Matter, Phys. Lett. B238 (1990) 337. [doi:10.1016/0370-2693\(90\)91745-W](#).
  - [489] G. D. Mack, J. F. Beacom, G. Bertone, Towards Closing the Window on Strongly Interacting Dark Matter: Far-Reaching Constraints from Earth’s Heat Flow, Phys. Rev. D76 (2007) 043523. [arXiv:0705.4298](#), [doi:10.1103/PhysRevD.76.043523](#).
  - [490] M. Kawasaki, K. Kohri, T. Moroi, Big-Bang nucleosynthesis and hadronic decay of long-lived massive particles, Phys. Rev. D71 (2005) 083502. [arXiv:astro-ph/0408426](#), [doi:10.1103/PhysRevD.71.083502](#).
  - [491] K. Jedamzik, Big bang nucleosynthesis constraints on hadronically and electromagnetically decaying relic neutral particles, Phys. Rev. D74 (2006) 103509. [arXiv:hep-ph/0604251](#), [doi:10.1103/PhysRevD.74.103509](#).
  - [492] K. Jedamzik, Bounds on long-lived charged massive particles from Big Bang nucleosynthesis, JCAP 0803 (2008) 008. [arXiv:0710.5153](#), [doi:10.1088/1475-7516/2008/03/008](#).
  - [493] M. Kawasaki, K. Kohri, T. Moroi, Y. Takaesu, Revisiting Big-Bang Nucleosynthesis Constraints on Long-Lived Decaying Particles, Phys. Rev. D97 (2) (2018) 023502. [arXiv:1709.01211](#), [doi:10.1103/PhysRevD.97.023502](#).
  - [494] W. Hu, J. Silk, Thermalization constraints and spectral distortions for massive unstable relic particles, Phys. Rev. Lett. 70 (1993) 2661–2664. [doi:10.1103/PhysRevLett.70.2661](#).
  - [495] J. Chluba, R. A. Sunyaev, The evolution of CMB spectral distortions in the early Universe, Mon. Not. Roy. Astron. Soc. 419 (2012) 1294–1314. [arXiv:1109.6552](#), [doi:10.1111/j.1365-2966.2011.19786.x](#).
  - [496] J. Chluba, Distinguishing different scenarios of early energy release with spectral distortions of the cosmic microwave background, Mon. Not. Roy. Astron. Soc. 436 (2013) 2232–2243. [arXiv:1304.6121](#), [doi:10.1093/mnras/stt1733](#).
  - [497] G. D. Kribs, I. Z. Rothstein, Bounds on longlived relics from diffuse gamma-ray observations, Phys. Rev. D55 (1997) 4435–4449, [Erratum: Phys. Rev.D56,1822(1997)]. [arXiv:hep-ph/9610468](#), [doi:10.1103/PhysRevD.56.1822](#), [doi:10.1103/PhysRevD.55.4435](#).
  - [498] M. Ackermann, et al., Fermi LAT Search for Dark Matter in Gamma-ray Lines and the Inclusive Photon Spectrum, Phys. Rev. D86 (2012) 022002. [arXiv:1205.2739](#), [doi:10.1103/PhysRevD.86.022002](#).
  - [499] G. F. Giudice, R. Rattazzi, A. Strumia, Unificaxion, Phys. Lett. B715 (2012) 142–148. [arXiv:1204.5465](#), [doi:10.1016/j.physletb.2012.07.028](#).
  - [500] S. De Panfilis, A. C. Melissinos, B. E. Moskowitz, J. T. Rogers, Y. K. Semertzidis, W. Wuensch, H. J. Halama, A. G. Prodell, W. B. Fowler, F. A. Nezrick, Limits on the Abundance and Coupling of Cosmic Axions at 4.5-Microev  $< m(a) < 5.0$ -Microev, Phys. Rev. Lett. 59 (1987) 839. [doi:10.1103/PhysRevLett.59.839](#).
  - [501] W. Wuensch, S. De Panfilis-Wuensch, Y. K. Semertzidis, J. T. Rogers, A. C. Melissinos, H. J. Halama, B. E. Moskowitz, A. G. Prodell, W. B. Fowler, F. A. Nezrick, Results of a Laboratory Search for Cosmic Axions and Other Weakly Coupled Light Particles, Phys. Rev. D40 (1989) 3153. [doi:10.1103/PhysRevD.40.3153](#).
  - [502] C. Hagmann, P. Sikivie, N. S. Sullivan, D. B. Tanner, Results from a search for cosmic axions, Phys. Rev. D42 (1990) 1297–1300. [doi:10.1103/PhysRevD.42.1297](#).
  - [503] C. Patrignani, et al., Review of Particle Physics, Chin. Phys. C40 (10) (2016) 100001. [doi:10.1088/1674-1137/40/10/100001](#).
  - [504] R. Bähre, et al., Any light particle search II —Technical Design Report, JINST 8 (2013) T09001. [arXiv:1302.5647](#), [doi:10.1088/1748-0221/8/09/T09001](#).
  - [505] S. J. Asztalos, et al., An Improved RF cavity search for halo axions, Phys. Rev. D69 (2004) 011101. [arXiv:astro-ph/0310042](#), [doi:10.1103/PhysRevD.69.011101](#).
  - [506] J. E. Kim, Constraints on very light axions from cavity experiments, Phys. Rev. D58 (1998) 055006. [arXiv:hep-ph/9802220](#), [doi:10.1103/PhysRevD.58.055006](#).
  - [507] K. Choi, S. H. Im, Realizing the relaxation from multiple axions and its UV completion with high scale supersymmetry, JHEP 01 (2016) 149. [arXiv:1511.00132](#), [doi:10.1007/JHEP01\(2016\)149](#).
  - [508] D. E. Kaplan, R. Rattazzi, Large field excursions and approximate discrete symmetries from a clockwork axion, Phys. Rev. D93 (8) (2016) 085007. [arXiv:1511.01827](#), [doi:10.1103/PhysRevD.93.085007](#).
  - [509] G. F. Giudice, M. McCullough, A Clockwork Theory, JHEP 02 (2017) 036. [arXiv:1610.07962](#), [doi:10.1007/JHEP02\(2017\)036](#).
  - [510] M. Farina, D. Papadopoulos, F. Rompineve, A. Tesi, The photo-philic QCD axion, JHEP 01 (2017) 095. [arXiv:1611.09855](#), [doi:10.1007/JHEP01\(2017\)095](#).
  - [511] A. J. Long, Cosmological Aspects of the Clockwork Axion, JHEP 07 (2018) 066. [arXiv:1803.07086](#), [doi:10.1007/JHEP07\(2018\)066](#).
  - [512] P. Agrawal, J. Fan, M. Reece, L.-T. Wang, Experimental Targets for Photon Couplings of the QCD Axion, JHEP 02 (2018) 006. [arXiv:1709.06085](#), [doi:10.1007/JHEP02\(2018\)006](#).
  - [513] M. Shin, Light Neutrino Masses and Strong CP Problem, Phys. Rev. Lett. 59 (1987) 2515, [Erratum: Phys. Rev. Lett.60,383(1988)]. [doi:10.1103/PhysRevLett.60.383](#), [doi:10.1103/PhysRevLett.59.2515](#).

- [514] A. Pilaftsis, Astrophysical and terrestrial constraints on singlet Majoron models, *Phys. Rev. D* 49 (1994) 2398–2404. [arXiv:hep-ph/9308258](#), [doi:10.1103/PhysRevD.49.2398](#).
- [515] C. Garcia-Cely, J. Heeck, Neutrino Lines from Majoron Dark Matter, *JHEP* 05 (2017) 102. [arXiv:1701.07209](#), [doi:10.1007/JHEP05\(2017\)102](#).
- [516] L. Di Luzio, F. Mescia, E. Nardi, P. Panci, R. Ziegler, Astrophobic Axions, *Phys. Rev. Lett.* 120 (26) (2018) 261803. [arXiv:1712.04940](#), [doi:10.1103/PhysRevLett.120.261803](#).
- [517] G. Marques-Tavares, M. Teo, Light axions with large hadronic couplings, *JHEP* 05 (2018) 180. [arXiv:1803.07575](#), [doi:10.1007/JHEP05\(2018\)180](#).
- [518] L. Darmé, L. Di Luzio, E. Nardi, Exponential enhancements of the axion couplings to nucleons. In preparation, *Phys. Rev. D* XX (2020) 1. [arXiv:2003.xxxxx](#), [doi:XX](#).
- [519] L. M. Krauss, D. J. Nash, A viable weak interaction axion?, *Phys. Lett. B* 202 (1988) 560–567. [doi:10.1016/0370-2693\(88\)91864-3](#).
- [520] M. Hindmarsh, P. Moulatsiotis, Constraints on variant axion models, *Phys. Rev. D* 56 (1997) 8074–8081. [arXiv:hep-ph/9708281](#), [doi:10.1103/PhysRevD.56.8074](#).
- [521] K. Saikawa, T. T. Yanagida, Stellar cooling anomalies and variant axion models. [arXiv:1907.07662](#).
- [522] F. Björkeröth, L. Di Luzio, F. Mescia, E. Nardi,  $U(1)$  flavour symmetries as Peccei-Quinn symmetries, *JHEP* 02 (2019) 133. [arXiv:1811.09637](#), [doi:10.1007/JHEP02\(2019\)133](#).
- [523] F. Björkeröth, L. Di Luzio, F. Mescia, E. Nardi, Covert symmetries in the neutrino mass matrix. [arXiv:1910.00576](#).
- [524] M. Buschmann, R. T. Co, C. Dessert, B. R. Safdi, X-ray Search for Axions from Nearby Isolated Neutron Stars [arXiv:1910.04164](#).
- [525] W. A. Bardeen, S. H. H. Tye, Current Algebra Applied to Properties of the Light Higgs Boson, *Phys. Lett.* 74B (1978) 229–232. [doi:10.1016/0370-2693\(78\)90560-9](#).
- [526] F. Wilczek, Axions and Family Symmetry Breaking, *Phys. Rev. Lett.* 49 (1982) 1549–1552. [doi:10.1103/PhysRevLett.49.1549](#).
- [527] J. Schweppe, et al., Observation of a peak structure in positron spectra from  $U + Cm$  collisions, *Phys. Rev. Lett.* 51 (1983) 2261–2264. [doi:10.1103/PhysRevLett.51.2261](#).
- [528] M. Clemente, E. Berdermann, P. Kienle, H. Tsertos, W. Wagner, C. Kozhuharov, F. Bosch, W. König, Narrow positron lines from  $U - U$  and  $U - Th$  collisions, *Phys. Lett.* 137B (1984) 41–46. [doi:10.1016/0370-2693\(84\)91102-X](#).
- [529] T. Cowan, et al., Anomalous positron peaks from supercritical collisions systems, *Phys. Rev. Lett.* 54 (1985) 1761–1764. [doi:10.1103/PhysRevLett.54.1761](#).
- [530] T. Cowan, et al., Observation of Correlated Narrow Peak Structures in Positron and electron Spectra from Superheavy Collision Systems, *Phys. Rev. Lett.* 56 (1986) 444–447. [doi:10.1103/PhysRevLett.56.444](#).
- [531] A. Schafer, J. Reinhardt, B. Müller, W. Greiner, G. Soff, IS THERE EVIDENCE FOR THE PRODUCTION OF A NEW PARTICLE IN HEAVY ION COLLISIONS?, *J. Phys. G* 11 (1985) L69–L74. [doi:10.1088/0305-4616/11/5/001](#).
- [532] A. B. Balantekin, C. Bottcher, M. R. Strayer, S. J. Lee, Phenomenology of New Particle Production in Heavy Ion Collisions, *Phys. Rev. Lett.* 55 (1985) 461. [doi:10.1103/PhysRevLett.55.461](#).
- [533] R. D. Peccei, T. T. Wu, T. Yanagida, A viable axion model, *Phys. Lett. B* 172 (1986) 435–440. [doi:10.1016/0370-2693\(86\)90284-4](#).
- [534] L. M. Krauss, F. Wilczek, A short lived axion variant, *Phys. Lett. B* 173 (1986) 189–192. [doi:10.1016/0370-2693\(86\)90244-3](#).
- [535] C. Q. Geng, J. N. Ng, Flavor Connections and Neutrino Mass Hierarchy Invariant Invisible Axion Models Without Domain Wall Problem, *Phys. Rev. D* 39 (1989) 1449. [doi:10.1103/PhysRevD.39.1449](#).
- [536] G. Mageras, P. Franzini, P. M. Tuts, S. Youssef, T. Zhao, J. Lee-Franzini, R. D. Schamberger, Search for Shortlived Axions in Radiative  $\Upsilon$  Decays, *Phys. Rev. Lett.* 56 (1986) 2672–2675. [doi:10.1103/PhysRevLett.56.2672](#).
- [537] T. J. V. Bowcock, et al., Upper Limits for the Production of Light Shortlived Neutral Particles in Radiative  $\Upsilon$  Decay, *Phys. Rev. Lett.* 56 (1986) 2676. [doi:10.1103/PhysRevLett.56.2676](#).
- [538] C. N. Brown, et al., A New Limit on Axion Production in 800-GeV Hadronic Showers, *Phys. Rev. Lett.* 57 (1986) 2101. [doi:10.1103/PhysRevLett.57.2101](#).
- [539] A. L. Hallin, F. P. Calaprice, R. W. Dunford, A. B. McDonald, Restrictions on a 1.7-MeV Axion From Nuclear Pair Transitions, *Phys. Rev. Lett.* 57 (1986) 2105–2108. [doi:10.1103/PhysRevLett.57.2105](#).
- [540] M. Davier, J. Jeanjean, H. Nguyen Ngoc, Search for Axions in Electron Bremsstrahlung, *Phys. Lett. B* 180 (1986) 295–298. [doi:10.1016/0370-2693\(86\)90313-8](#).
- [541] E. M. Riordan, et al., A Search for Short Lived Axions in an Electron Beam Dump Experiment, *Phys. Rev. Lett.* 59 (1987) 755. [doi:10.1103/PhysRevLett.59.755](#).
- [542] A. Davidson, K. C. Wali, Minimal flavor unification via multigenerational peccei-quinn symmetry, *Phys. Rev. Lett.* 48 (1982) 11. [doi:10.1103/PhysRevLett.48.11](#).
- [543] A. Davidson, V. P. Nair, K. C. Wali, Peccei-Quinn Symmetry as Flavor Symmetry and Grand Unification, *Phys. Rev. D* 29 (1984) 1504. [doi:10.1103/PhysRevD.29.1504](#).
- [544] A. Davidson, M. A. H. Vozmediano, The Horizontal Axion Alternative: The Interplay of Vacuum Structure and Flavor Interactions, *Nucl. Phys. B* 248 (1984) 647–670. [doi:10.1016/0550-3213\(84\)90616-3](#).
- [545] C. D. Froggatt, H. B. Nielsen, Hierarchy of Quark Masses, Cabibbo Angles and CP Violation, *Nucl. Phys. B* 147 (1979) 277–298. [doi:10.1016/0550-3213\(79\)90316-X](#).
- [546] Y. Ema, K. Hamaguchi, T. Moroi, K. Nakayama, Flaxion: a minimal extension to solve puzzles in the standard model, *JHEP* 01 (2017) 096. [arXiv:1612.05492](#), [doi:10.1007/JHEP01\(2017\)096](#).
- [547] L. Calibbi, F. Goertz, D. Redigolo, R. Ziegler, J. Zupan, Minimal axion model from flavor, *Phys. Rev. D* 95 (9) (2017)



095009. [arXiv:1612.08040](#), [doi:10.1103/PhysRevD.95.095009](#).
- [548] Z. G. Berezhiani, Horizontal Symmetry and Quark - Lepton Mass Spectrum: The  $SU(5) \times SU(3)$ -h Model, *Phys. Lett.* 150B (1985) 177–181. [doi:10.1016/0370-2693\(85\)90164-9](#).
  - [549] Z. G. Berezhiani, M. Yu. Khlopov, Cosmology of Spontaneously Broken Gauge Family Symmetry, *Z. Phys. C*49 (1991) 73–78. [doi:10.1007/BF01570798](#).
  - [550] J. L. Feng, T. Moroi, H. Murayama, E. Schnapka, Third generation familons, b factories, and neutrino cosmology, *Phys. Rev. D*57 (1998) 5875–5892. [arXiv:hep-ph/9709411](#), [doi:10.1103/PhysRevD.57.5875](#).
  - [551] F. Bjorkerth, E. J. Chun, S. F. King, Flavourful Axion Phenomenology, *JHEP* 08 (2018) 117. [arXiv:1806.00660](#), [doi:10.1007/JHEP08\(2018\)117](#).
  - [552] R. Ziegler, Flavored Axions, *PoS CORFU2018* (2019) 035. [arXiv:1905.01084](#), [doi:10.22323/1.347.0035](#).
  - [553] L. Di Luzio, Flavour Violating Axions, in: Workshop on Flavour changing and conserving processes (FCCP2019) Anacapri, Capri Island, Italy, August 29-31, 2019, 2019. [arXiv:1911.02591](#).
  - [554] J. Martin Camalich, M. Pospelov, P. N. H. Vuong, R. Ziegler, J. Zupan, Quark Flavor Phenomenology of the QCD Axion. [arXiv:2002.04623](#).
  - [555] S. Adler, et al., Measurement of the  $K^+ \rightarrow \pi^+ \nu \nu$  branching ratio, *Phys. Rev. D*77 (2008) 052003. [arXiv:0709.1000](#), [doi:10.1103/PhysRevD.77.052003](#).
  - [556] G. Anelli, et al., Proposal to measure the rare decay  $K^+ \rightarrow \pi^+ \nu \text{ anti-}\nu$  at the CERN SPS.
  - [557] R. Fantechi, The NA62 experiment at CERN: status and perspectives, in: 12th Conference on Flavor Physics and CP Violation (FPCP 2014) Marseille, France, May 26-30, 2014, 2014. [arXiv:1407.8213](#).
  - [558] R. Ammar, et al., Search for the familon via  $B^{+-} \rightarrow \pi^{+-} X^0$ ,  $B^{+-} \rightarrow K^{+-} X^0$ , and  $B^0 \rightarrow K^0(S)X^0$  decays, *Phys. Rev. Lett.* 87 (2001) 271801. [arXiv:hep-ex/0106038](#), [doi:10.1103/PhysRevLett.87.271801](#).
  - [559] T. Abe, et al., Belle II Technical Design Report [arXiv:1011.0352](#).
  - [560] A. Jodidio, et al., Search for Right-Handed Currents in Muon Decay, *Phys. Rev. D*34 (1986) 1967, [Erratum: *Phys. Rev. D*37,237(1988)]. [doi:10.1103/PhysRevD.34.1967](#), [doi:10.1103/PhysRevD.37.237](#).
  - [561] J. T. Goldman, et al., Light Boson Emission in the Decay of the  $\mu^+$ , *Phys. Rev. D*36 (1987) 1543–1546. [doi:10.1103/PhysRevD.36.1543](#).
  - [562] R. D. Bolton, et al., Search for Rare Muon Decays with the Crystal Box Detector, *Phys. Rev. D*38 (1988) 2077. [doi:10.1103/PhysRevD.38.2077](#).
  - [563] R. Bayes, et al., Search for two body muon decay signals, *Phys. Rev. D*91 (5) (2015) 052020. [arXiv:1409.0638](#), [doi:10.1103/PhysRevD.91.052020](#).
  - [564] F. Renga, The quest for  $\mu \rightarrow e\gamma$ : present and future, *Hyperfine Interact.* 239 (1) (2018) 58. [arXiv:1811.05921](#), [doi:10.1007/s10751-018-1534-y](#).
  - [565] A. Blondel, et al., Research Proposal for an Experiment to Search for the Decay  $\mu \rightarrow eee$ . [arXiv:1301.6113](#).
  - [566] H. Albrecht, et al., A Search for lepton flavor violating decays  $\tau \rightarrow e\alpha$ ,  $\tau \rightarrow \mu\alpha$ , *Z. Phys. C*68 (1995) 25–28. [doi:10.1007/BF01579801](#).
  - [567] P. J. Steinhardt, M. S. Turner, Saving the invisible axion, *Phys. Lett. B*129 (1983) 51. [doi:10.1016/0370-2693\(83\)90727-X](#).
  - [568] G. Lazarides, C. Panagiotakopoulos, Q. Shafi, Relaxing the cosmological bound on axions, *Phys. Lett. B*192 (1987) 323. [doi:10.1016/0370-2693\(87\)90115-8](#).
  - [569] G. Lazarides, R. K. Schaefer, D. Seckel, Q. Shafi, Dilution of Cosmological Axions by Entropy Production, *Nucl. Phys. B*346 (1990) 193–212. [doi:10.1016/0550-3213\(90\)90244-8](#).
  - [570] M. Kawasaki, T. Moroi, T. Yanagida, Can decaying particles raise the upper bound on the Peccei-Quinn scale?, *Phys. Lett. B*383 (1996) 313–316. [arXiv:hep-ph/9510461](#), [doi:10.1016/0370-2693\(96\)00743-5](#).
  - [571] P. Jordan, *Schwerkraft und Weltall: Grundlagen der theoretische Kosmologie*, Vol. 107, Vieweg. (Braunschweig: und Sohns), 1955.
  - [572] M. Fierz, On the physical interpretation of P.Jordan’s extended theory of gravitation, *Helv. Phys. Acta* 29 (1956) 128–134.
  - [573] C. Brans, R. H. Dicke, Mach’s principle and a relativistic theory of gravitation, *Phys. Rev.* 124 (1961) 925–935. [doi:10.1103/PhysRev.124.925](#).
  - [574] R. Catena, N. Fornengo, A. Masiero, M. Pietroni, F. Rosati, Dark matter relic abundance and scalar - tensor dark energy, *Phys. Rev. D*70 (2004) 063519. [arXiv:astro-ph/0403614](#), [doi:10.1103/PhysRevD.70.063519](#).
  - [575] R. Catena, N. Fornengo, M. Pato, L. Pieri, A. Masiero, Thermal Relics in Modified Cosmologies: Bounds on Evolution Histories of the Early Universe and Cosmological Boosts for PAMELA, *Phys. Rev. D*81 (2010) 123522. [arXiv:0912.4421](#), [doi:10.1103/PhysRevD.81.123522](#).
  - [576] M. T. Meehan, I. B. Whittingham, Dark matter relic density in scalar-tensor gravity revisited, *JCAP* 1512 (12) (2015) 011. [arXiv:1508.05174](#), [doi:10.1088/1475-7516/2015/12/011](#).
  - [577] B. Dutta, E. Jimenez, I. Zavala, Dark Matter Relics and the Expansion Rate in Scalar-Tensor Theories, *JCAP* 1706 (06) (2017) 032. [arXiv:1612.05553](#), [doi:10.1088/1475-7516/2017/06/032](#).
  - [578] B. Dutta, E. Jimenez, I. Zavala, D-brane Disformal Coupling and Thermal Dark Matter, *Phys. Rev. D*96 (10) (2017) 103506. [arXiv:1708.07153](#), [doi:10.1103/PhysRevD.96.103506](#).
  - [579] B. Dutta, C. S. Fong, E. Jimenez, E. Nardi, A cosmological pathway to testable leptogenesis, *JCAP* 1810 (10) (2018) 025. [arXiv:1804.07676](#), [doi:10.1088/1475-7516/2018/10/025](#).
  - [580] G. Gelmini, P. Gondolo, A. Soldatenko, C. E. Yaguna, The Effect of a late decaying scalar on the neutralino relic density, *Phys. Rev. D*74 (2006) 083514. [arXiv:hep-ph/0605016](#), [doi:10.1103/PhysRevD.74.083514](#).
  - [581] G. B. Gelmini, P. Gondolo, A. Soldatenko, C. E. Yaguna, Direct detection of neutralino dark matter in non-standard cosmologies, *Phys. Rev. D*76 (2007) 015010. [arXiv:hep-ph/0610379](#), [doi:10.1103/PhysRevD.76.015010](#).

- [582] G. B. Gelmini, P. Gondolo, Ultra-cold WIMPs: relics of non-standard pre-BBN cosmologies, JCAP 0810 (2008) 002. [arXiv:0803.2349](#), [doi:10.1088/1475-7516/2008/10/002](#).
- [583] A. L. Erickcek, K. Sigurdson, Reheating Effects in the Matter Power Spectrum and Implications for Substructure, Phys. Rev. D84 (2011) 083503. [arXiv:1106.0536](#), [doi:10.1103/PhysRevD.84.083503](#).
- [584] K. Redmond, A. L. Erickcek, New Constraints on Dark Matter Production during Kination, Phys. Rev. D96 (4) (2017) 043511. [arXiv:1704.01056](#), [doi:10.1103/PhysRevD.96.043511](#).
- [585] L. Visinelli, (Non-)thermal production of WIMPs during kination, Symmetry 10 (11) (2018) 546. [arXiv:1710.11006](#), [doi:10.3390/sym10110546](#).
- [586] L. Visinelli, P. Gondolo, Kinetic decoupling of WIMPs: analytic expressions, Phys. Rev. D91 (8) (2015) 083526. [arXiv:1501.02233](#), [doi:10.1103/PhysRevD.91.083526](#).
- [587] D. Grin, T. L. Smith, M. Kamionkowski, Axion constraints in non-standard thermal histories, Phys. Rev. D77 (2008) 085020. [arXiv:0711.1352](#), [doi:10.1103/PhysRevD.77.085020](#).
- [588] L. Visinelli, P. Gondolo, Axion cold dark matter in non-standard cosmologies, Phys. Rev. D81 (2010) 063508. [arXiv:0912.0015](#), [doi:10.1103/PhysRevD.81.063508](#).
- [589] L. Visinelli, Light axion-like dark matter must be present during inflation, Phys. Rev. D96 (2) (2017) 023013. [arXiv:1703.08798](#), [doi:10.1103/PhysRevD.96.023013](#).
- [590] P. Draper, J. Kozaczuk, J.-H. Yu, Theta in new QCD-like sectors, Phys. Rev. D98 (1) (2018) 015028. [arXiv:1803.00015](#), [doi:10.1103/PhysRevD.98.015028](#).
- [591] N. Ramberg, L. Visinelli, Probing the Early Universe with Axion Physics and Gravitational Waves, Phys. Rev. D99 (12) (2019) 123513. [arXiv:1904.05707](#), [doi:10.1103/PhysRevD.99.123513](#).
- [592] N. Blinov, M. J. Dolan, P. Draper, J. Kozaczuk, Dark matter targets for axionlike particle searches, Phys. Rev. D100 (1) (2019) 015049. [arXiv:1905.06952](#), [doi:10.1103/PhysRevD.100.015049](#).
- [593] M. S. Turner, Coherent Scalar Field Oscillations in an Expanding Universe, Phys. Rev. D28 (1983) 1243. [doi:10.1103/PhysRevD.28.1243](#).
- [594] R. J. Scherrer, M. S. Turner, Decaying Particles Do Not Heat Up the Universe, Phys. Rev. D31 (1985) 681. [doi:10.1103/PhysRevD.31.681](#).
- [595] J. D. Barrow, Massive Particles As A Probe Of The Early Universe, Nucl. Phys. B208 (1982) 501–508. [doi:10.1016/0550-3213\(82\)90233-4](#).
- [596] L. H. Ford, Gravitational Particle Creation and Inflation, Phys. Rev. D35 (1987) 2955. [doi:10.1103/PhysRevD.35.2955](#).
- [597] A. Hook, Solving the Hierarchy Problem Discretely, Phys. Rev. Lett. 120 (26) (2018) 261802. [arXiv:1802.10093](#), [doi:10.1103/PhysRevLett.120.261802](#).
- [598] Z. Berezhiani, D. Comelli, F. L. Villante, The Early mirror universe: Inflation, baryogenesis, nucleosynthesis and dark matter, Phys. Lett. B503 (2001) 362–375. [arXiv:hep-ph/0008105](#), [doi:10.1016/S0370-2693\(01\)00217-9](#).
- [599] M. Giannotti, Mirror world and axion: Relaxing cosmological bounds, Int. J. Mod. Phys. A20 (2005) 2454–2458. [arXiv:astro-ph/0504636](#), [doi:10.1142/S0217751X05024766](#).
- [600] T. D. Lee, C.-N. Yang, Question of Parity Conservation in Weak Interactions, Phys. Rev. 104 (1956) 254–258. [doi:10.1103/PhysRev.104.254](#).
- [601] B. Holdom, Two U(1)’s and Epsilon Charge Shifts, Phys. Lett. 166B (1986) 196–198. [doi:10.1016/0370-2693\(86\)91377-8](#).
- [602] S. L. Glashow, Positronium Versus the Mirror Universe, Phys. Lett. 167B (1986) 35–36. [doi:10.1016/0370-2693\(86\)90540-X](#).
- [603] M. Yu. Khlopov, G. M. Beskin, N. E. Bochkarev, L. A. Pustynnik, S. A. Pustynnik, Observational Physics of Mirror World, Sov. Astron. 35 (1991) 21, [Astron. Zh.68,42(1991)].
- [604] J.-S. Roux, J. M. Cline, Constraining galactic structures of mirror dark matter. [arXiv:2001.11504](#).
- [605] V. A. Rubakov, Grand unification and heavy axion, JETP Lett. 65 (1997) 621–624. [arXiv:hep-ph/9703409](#), [doi:10.1134/1.567390](#).
- [606] Z. Berezhiani, L. Gianfagna, M. Giannotti, Strong CP problem and mirror world: The Weinberg-Wilczek axion revisited, Phys. Lett. B500 (2001) 286–296. [arXiv:hep-ph/0009290](#), [doi:10.1016/S0370-2693\(00\)01392-7](#).
- [607] L. Gianfagna, M. Giannotti, F. Nesti, Mirror world, supersymmetric axion and gamma ray bursts, JHEP 10 (2004) 044. [arXiv:hep-ph/0409185](#), [doi:10.1088/1126-6708/2004/10/044](#).
- [608] P. Agrawal, G. Marques-Tavares, W. Xue, Opening up the QCD axion window, JHEP 03 (2018) 049. [arXiv:1708.05008](#), [doi:10.1007/JHEP03\(2018\)049](#).
- [609] E. Witten, Dyons of Charge  $e\theta/2\pi$ , Phys. Lett. B86 (1979) 283–287, [,283(1979)]. [doi:10.1016/0370-2693\(79\)90838-4](#).
- [610] W. Fischler, J. Preskill, Dyon-axion dynamics, Phys. Lett. 125B (1983) 165–170. [doi:10.1016/0370-2693\(83\)91260-1](#).
- [611] M. Kawasaki, F. Takahashi, M. Yamada, Suppressing the QCD Axion Abundance by Hidden Monopoles, Phys. Lett. B753 (2016) 677–681. [arXiv:1511.05030](#), [doi:10.1016/j.physletb.2015.12.075](#).
- [612] M. Kawasaki, F. Takahashi, M. Yamada, Adiabatic suppression of the axion abundance and isocurvature due to coupling to hidden monopoles, JHEP 01 (2018) 053. [arXiv:1708.06047](#), [doi:10.1007/JHEP01\(2018\)053](#).
- [613] R. T. Co, L. J. Hall, K. Harigaya, Kinetic Misalignment Mechanism. [arXiv:1910.14152](#).
- [614] C.-F. Chang, Y. Cui, New Perspectives on Axion Misalignment Mechanism. [arXiv:1911.11885](#).
- [615] T. C. Yang, Gauge Chiral U(1) Symmetry and CP Invariance in the Presence of Instantons, Phys. Rev. Lett. 41 (1978) 523–526. [doi:10.1103/PhysRevLett.41.523](#).
- [616] S. Dimopoulos, A Solution of the Strong CP Problem in Models With Scalars, Phys. Lett. 84B (1979) 435–439. [doi:10.1016/0370-2693\(79\)91233-4](#).



- [617] S. H. H. Tye, A Superstrong Force With a Heavy Axion, *Phys. Rev. Lett.* 47 (1981) 1035. [doi:10.1103/PhysRevLett.47.1035](#).
- [618] B. Holdom, Strong QCD at High-energies and a Heavy Axion, *Phys. Lett.* 154B (1985) 316, [Erratum: *Phys. Lett.* 156B, 452 (1985)]. [doi:10.1016/0370-2693\(85\)90371-5](#).
- [619] J. M. Flynn, L. Randall, A Computation of the Small Instanton Contribution to the Axion Potential, *Nucl. Phys.* B293 (1987) 731–739. [doi:10.1016/0550-3213\(87\)90089-7](#).
- [620] D. S. M. Alves, N. Weiner, A viable QCD axion in the MeV mass range, *JHEP* 07 (2018) 092. [arXiv:1710.03764](#), [doi:10.1007/JHEP07\(2018\)092](#).
- [621] Z. Berezhiani, A. Drago, Gamma-ray bursts via emission of axion - like particles, *Phys. Lett.* B473 (2000) 281–290. [arXiv:hep-ph/9911333](#), [doi:10.1016/S0370-2693\(99\)01449-5](#).
- [622] X. Cid Vidal, A. Mariotti, D. Redigolo, F. Sala, K. Tobioka, New Axion Searches at Flavor Factories, *JHEP* 01 (2019) 113. [arXiv:1810.09452](#), [doi:10.1007/JHEP01\(2019\)113](#).
- [623] A. Hook, Anomalous solutions to the strong CP problem, *Phys. Rev. Lett.* 114 (14) (2015) 141801. [arXiv:1411.3325](#), [doi:10.1103/PhysRevLett.114.141801](#).
- [624] S. Dimopoulos, A. Hook, J. Huang, G. Marques-Tavares, A collider observable QCD axion, *JHEP* 11 (2016) 052. [arXiv:1606.03097](#), [doi:10.1007/JHEP11\(2016\)052](#).
- [625] P. Agrawal, K. Howe, Factoring the Strong CP Problem, *JHEP* 12 (2018) 029. [arXiv:1710.04213](#), [doi:10.1007/JHEP12\(2018\)029](#).
- [626] P. Agrawal, K. Howe, A Flavorful Factoring of the Strong CP Problem, *JHEP* 12 (2018) 035. [arXiv:1712.05803](#), [doi:10.1007/JHEP12\(2018\)035](#).
- [627] C. Csaki, M. Ruhdorfer, Y. Shirman, UV Sensitivity of the Axion Mass from Instantons in Partially Broken Gauge Groups. [arXiv:1912.02197](#).
- [628] M. K. Gaillard, M. B. Gavela, R. Houtz, P. Quilez, R. Del Rey, Color unified dynamical axion, *Eur. Phys. J.* C78 (11) (2018) 972. [arXiv:1805.06465](#), [doi:10.1140/epjc/s10052-018-6396-6](#).
- [629] J. E. Kim, Reason for SU(6) Grand Unification, *Phys. Lett.* 107B (1981) 69–72. [doi:10.1016/0370-2693\(81\)91149-7](#).
- [630] R. N. Mohapatra, G. Senjanovic, The Superlight Axion and Neutrino Masses, *Z. Phys.* C17 (1983) 53–56. [doi:10.1007/BF01577819](#).
- [631] Q. Shafi, F. W. Stecker, Implications of a Class of Grand Unified Theories for Large Scale Structure in the Universe, *Phys. Rev. Lett.* 53 (1984) 1292. [doi:10.1103/PhysRevLett.53.1292](#).
- [632] P. Langacker, R. D. Peccei, T. Yanagida, Invisible Axions and Light Neutrinos: Are They Connected?, *Mod. Phys. Lett.* A1 (1986) 541. [doi:10.1142/S0217732386000683](#).
- [633] X. G. He, R. R. Volkas, Models Featuring Spontaneous CP Violation: An Invisible Axion and Light Neutrino Masses, *Phys. Lett.* B208 (1988) 261, [Erratum: *Phys. Lett.* B218, 508 (1989)]. [doi:10.1016/0370-2693\(88\)90427-3](#), [doi:10.1016/0370-2693\(88\)90427-3](#).
- [634] A. G. Dias, V. Pleitez, The Invisible axion and neutrino masses, *Phys. Rev.* D73 (2006) 017701. [arXiv:hep-ph/0511104](#), [doi:10.1103/PhysRevD.73.017701](#).
- [635] A. Salvio, A Simple Motivated Completion of the Standard Model below the Planck Scale: Axions and Right-Handed Neutrinos, *Phys. Lett.* B743 (2015) 428–434. [arXiv:1501.03781](#), [doi:10.1016/j.physletb.2015.03.015](#).
- [636] J. D. Clarke, R. R. Volkas, Technically natural nonsupersymmetric model of neutrino masses, baryogenesis, the strong CP problem, and dark matter, *Phys. Rev.* D93 (3) (2016) 035001, [*Phys. Rev.* D93, 035001 (2016)]. [arXiv:1509.07243](#), [doi:10.1103/PhysRevD.93.035001](#).
- [637] S. Bertolini, A. Santamaria, The Strong CP problem and the solar neutrino puzzle: Are they related?, *Nucl. Phys.* B357 (1991) 222–240. [doi:10.1016/0550-3213\(91\)90467-C](#).
- [638] H. Arason, P. Ramond, B. D. Wright, A Standard model extension with neutrino masses and an invisible axion, *Phys. Rev.* D43 (1991) 2337–2350. [doi:10.1103/PhysRevD.43.2337](#).
- [639] S. Bertolini, L. Di Luzio, H. Kolesová, M. Malinský, Massive neutrinos and invisible axion minimally connected, *Phys. Rev.* D91 (5) (2015) 055014. [arXiv:1412.7105](#), [doi:10.1103/PhysRevD.91.055014](#).
- [640] Y. H. Ahn, E. J. Chun, Minimal Models for Axion and Neutrino, *Phys. Lett.* B752 (2016) 333–337. [arXiv:1510.01015](#), [doi:10.1016/j.physletb.2015.11.067](#).
- [641] S. Bertolini, L. Di Luzio, H. Kolesova, M. Malinsky, J. C. Vazquez, Neutrino-axion-dilaton interconnection, *Phys. Rev.* D93 (1) (2016) 015009. [arXiv:1510.03668](#), [doi:10.1103/PhysRevD.93.015009](#).
- [642] C.-S. Chen, L.-H. Tsai, Peccei-Quinn symmetry as the origin of Dirac Neutrino Masses, *Phys. Rev.* D88 (5) (2013) 055015. [arXiv:1210.6264](#), [doi:10.1103/PhysRevD.88.055015](#).
- [643] P.-H. Gu, Peccei-Quinn symmetry for Dirac seesaw and leptogenesis, *JCAP* 1607 (07) (2016) 004. [arXiv:1603.05070](#), [doi:10.1088/1475-7516/2016/07/004](#).
- [644] C. D. R. Carvalho, Ó. Zapata, One-loop Dirac neutrino mass and mixed axion-WIMP dark matter, *Phys. Rev.* D99 (7) (2019) 075009. [arXiv:1812.06364](#), [doi:10.1103/PhysRevD.99.075009](#).
- [645] E. Peinado, M. Reig, R. Srivastava, J. W. F. Valle, Dirac neutrinos from Peccei-Quinn symmetry: a fresh look at the axion. [arXiv:1910.02961](#).
- [646] V. A. Kuzmin, M. E. Shaposhnikov, I. I. Tkachev, Strong CP violation, electroweak baryogenesis, and axionic dark matter, *Phys. Rev.* D45 (1992) 466–475. [doi:10.1103/PhysRevD.45.466](#).
- [647] G. Servant, Baryogenesis from Strong CP Violation and the QCD Axion, *Phys. Rev. Lett.* 113 (17) (2014) 171803. [arXiv:1407.0030](#), [doi:10.1103/PhysRevLett.113.171803](#).
- [648] J. Garcia-Bellido, M. Garcia-Perez, A. Gonzalez-Arroyo, Chern-Simons production during preheating in hybrid inflation models, *Phys. Rev.* D69 (2004) 023504. [arXiv:hep-ph/0304285](#), [doi:10.1103/PhysRevD.69.023504](#).

- [649] A. Tranberg, J. Smit, Baryon asymmetry from electroweak tachyonic preheating, JHEP 11 (2003) 016. [arXiv:hep-ph/0310342](#), [doi:10.1088/1126-6708/2003/11/016](#).
- [650] S. Ipek, T. M. P. Tait, Early Cosmological Period of QCD Confinement, Phys. Rev. Lett. 122 (11) (2019) 112001. [arXiv:1811.00559](#), [doi:10.1103/PhysRevLett.122.112001](#).
- [651] D. Croon, J. N. Howard, S. Ipek, T. M. P. Tait, QCD Baryogenesis. [arXiv:1911.01432](#).
- [652] R. T. Co, K. Harigaya, Axiogenesis [arXiv:1910.02080](#).
- [653] A. A. Starobinsky, A New Type of Isotropic Cosmological Models Without Singularity, Phys. Lett. B91 (1980) 99–102, [771(1980)]. [doi:10.1016/0370-2693\(80\)90670-X](#).
- [654] A. H. Guth, The Inflationary Universe: A Possible Solution to the Horizon and Flatness Problems, Phys. Rev. D23 (1981) 347–356. [doi:10.1103/PhysRevD.23.347](#).
- [655] M. B. Einhorn, K. Sato, Monopole Production in the Very Early Universe in a First Order Phase Transition, Nucl. Phys. B180 (1981) 385–404. [doi:10.1016/0550-3213\(81\)90057-2](#).
- [656] K. Sato, Cosmological Baryon Number Domain Structure and the First Order Phase Transition of a Vacuum, Phys. Lett. 99B (1981) 66–70, [Adv. Ser. Astrophys. Cosmol.3,134(1987)]. [doi:10.1016/0370-2693\(81\)90805-4](#).
- [657] D. Kazanas, Dynamics of the Universe and Spontaneous Symmetry Breaking, Astrophys. J. 241 (1980) L59–L63. [doi:10.1086/183361](#).
- [658] J. Martin, C. Ringeval, R. Trotta, V. Vennin, The Best Inflationary Models After Planck, JCAP 1403 (2014) 039. [arXiv:1312.3529](#), [doi:10.1088/1475-7516/2014/03/039](#).
- [659] W. H. Kinney, S. Vagnozzi, L. Visinelli, The zoo plot meets the swampland: mutual (in)consistency of single-field inflation, string conjectures, and cosmological data, Class. Quant. Grav. 36 (11) (2019) 117001. [arXiv:1808.06424](#), [doi:10.1088/1361-6382/ab1d87](#).
- [660] A. Linde, M. Noorbala, A. Westphal, Observational consequences of chaotic inflation with nonminimal coupling to gravity, JCAP 1103 (2011) 013. [arXiv:1101.2652](#), [doi:10.1088/1475-7516/2011/03/013](#).
- [661] F. L. Bezrukov, M. Shaposhnikov, The Standard Model Higgs boson as the inflaton, Phys. Lett. B659 (2008) 703–706. [arXiv:0710.3755](#), [doi:10.1016/j.physletb.2007.11.072](#).
- [662] C. P. Burgess, H. M. Lee, M. Trott, Power-counting and the Validity of the Classical Approximation During Inflation, JHEP 09 (2009) 103. [arXiv:0902.4465](#), [doi:10.1088/1126-6708/2009/09/103](#).
- [663] J. L. F. Barbon, J. R. Espinosa, On the Naturalness of Higgs Inflation, Phys. Rev. D79 (2009) 081302. [arXiv:0903.0355](#), [doi:10.1103/PhysRevD.79.081302](#).
- [664] P. Fox, A. Pierce, S. D. Thomas, Probing a QCD string axion with precision cosmological measurements, [arXiv:hep-th/0409059](#).
- [665] M. P. Hertzberg, M. Tegmark, F. Wilczek, Axion Cosmology and the Energy Scale of Inflation, Phys. Rev. D78 (2008) 083507. [arXiv:0807.1726](#), [doi:10.1103/PhysRevD.78.083507](#).
- [666] D. J. E. Marsh, D. Grin, R. Hlozek, P. G. Ferreira, Tensor Interpretation of BICEP2 Results Severely Constrains Axion Dark Matter, Phys. Rev. Lett. 113 (1) (2014) 011801. [arXiv:1403.4216](#), [doi:10.1103/PhysRevLett.113.011801](#).
- [667] F. Bauer, D. A. Demir, Inflation with Non-Minimal Coupling: Metric versus Palatini Formulations, Phys. Lett. B665 (2008) 222–226. [arXiv:0803.2664](#), [doi:10.1016/j.physletb.2008.06.014](#).
- [668] K. Freese, D. Spolyar, Chain inflation: ‘Bubble bubble toil and trouble’, JCAP 0507 (2005) 007. [arXiv:hep-ph/0412145](#), [doi:10.1088/1475-7516/2005/07/007](#).
- [669] K. Freese, J. T. Liu, D. Spolyar, Inflating with the QCD axion, Phys. Rev. D72 (2005) 123521. [arXiv:hep-ph/0502177](#), [doi:10.1103/PhysRevD.72.123521](#).
- [670] D. Chialva, U. H. Danielsson, Chain inflation revisited, JCAP 0810 (2008) 012. [arXiv:0804.2846](#), [doi:10.1088/1475-7516/2008/10/012](#).
- [671] D. Chialva, U. H. Danielsson, Chain inflation and the imprint of fundamental physics in the CMBR, JCAP 0903 (2009) 007. [arXiv:0809.2707](#), [doi:10.1088/1475-7516/2009/03/007](#).
- [672] J. M. Cline, G. D. Moore, Y. Wang, Chain Inflation Reconsidered, JCAP 1108 (2011) 032. [arXiv:1106.2188](#), [doi:10.1088/1475-7516/2011/08/032](#).
- [673] H. Georgi, M. B. Wise, Hiding the Invisible Axion, Phys. Lett. 116B (1982) 123–126. [doi:10.1016/0370-2693\(82\)90989-3](#).
- [674] G. Lazarides, Q. Shafi, Axion Models with No Domain Wall Problem, Phys. Lett. 115B (1982) 21–25. [doi:10.1016/0370-2693\(82\)90506-8](#).
- [675] S. M. Barr, D. B. Reiss, A. Zee, Families, the Invisible Axion, and Domain Walls, Phys. Lett. 116B (1982) 227–230. [doi:10.1016/0370-2693\(82\)90331-8](#).
- [676] S. M. Barr, X. C. Gao, D. Reiss, PECEI-QUINN SYMMETRIES WITHOUT DOMAINS, Phys. Rev. D26 (1982) 2176. [doi:10.1103/PhysRevD.26.2176](#).
- [677] A. Davidson, M. A. H. Vozmediano, Domain Walls: Horizontal Epilogue, Phys. Lett. 141B (1984) 177–180. [doi:10.1016/0370-2693\(84\)90198-9](#).
- [678] L. M. Krauss, F. Wilczek, Discrete Gauge Symmetry in Continuum Theories, Phys. Rev. Lett. 62 (1989) 1221. [doi:10.1103/PhysRevLett.62.1221](#).
- [679] E. Nardi, Naturally large yukawa hierarchies, Phys. Rev. D 84 (2011) 036008. [arXiv:1105.1770](#), [doi:10.1103/PhysRevD.84.036008](#).
- [680] D. Buttazzo, L. Di Luzio, P. Ghorbani, C. Gross, G. Landini, A. Strumia, D. Teresi, J.-W. Wang, Scalar gauge dynamics and Dark Matter, JHEP 01 (2020) 130. [arXiv:1911.04502](#), [doi:10.1007/JHEP01\(2020\)130](#).
- [681] M. B. Wise, H. Georgi, S. L. Glashow, SU(5) and the Invisible Axion, Phys. Rev. Lett. 47 (1981) 402. [doi:10.1103/PhysRevLett.47.402](#).

- [682] G. Lazarides, SO(10) and the Invisible Axion, Phys. Rev. D25 (1982) 2425. [doi:10.1103/PhysRevD.25.2425](#).
- [683] A. Ernst, A. Ringwald, C. Tamarit, Axion Predictions in  $SO(10) \times U(1)_{PQ}$  Models, JHEP 02 (2018) 103. [arXiv:1801.04906](#), [doi:10.1007/JHEP02\(2018\)103](#).
- [684] L. Di Luzio, A. Ringwald, C. Tamarit, Axion mass prediction from minimal grand unification, Phys. Rev. D98 (9) (2018) 095011. [arXiv:1807.09769](#), [doi:10.1103/PhysRevD.98.095011](#).
- [685] A. Ernst, L. Di Luzio, A. Ringwald, C. Tamarit, Axion properties in GUTs, PoS CORFU2018 (2019) 054. [arXiv:1811.11860](#), [doi:10.22323/1.347.0054](#).
- [686] P. Fileviez Pérez, C. Murgui, A. D. Plascencia, The QCD Axion and Unification, JHEP 11 (2019) 093. [arXiv:1908.01772](#), [doi:10.1007/JHEP11\(2019\)093](#).
- [687] H. Georgi, S. L. Glashow, Unity of All Elementary Particle Forces, Phys. Rev. Lett. 32 (1974) 438–441. [doi:10.1103/PhysRevLett.32.438](#).
- [688] B. Bajc, G. Senjanovic, Seesaw at LHC, JHEP 08 (2007) 014. [arXiv:hep-ph/0612029](#), [doi:10.1088/1126-6708/2007/08/014](#).
- [689] B. Bajc, M. Nemevsek, G. Senjanovic, Probing seesaw at LHC, Phys. Rev. D76 (2007) 055011. [arXiv:hep-ph/0703080](#), [doi:10.1103/PhysRevD.76.055011](#).
- [690] L. Di Luzio, L. Mihaila, Unification scale vs. electroweak-triplet mass in the  $SU(5) + 24_F$  model at three loops, Phys. Rev. D87 (2013) 115025. [arXiv:1305.2850](#), [doi:10.1103/PhysRevD.87.115025](#).
- [691] R. Holman, G. Lazarides, Q. Shafi, Axions and the Dark Matter of the Universe, Phys. Rev. D27 (1983) 995. [doi:10.1103/PhysRevD.27.995](#).
- [692] B. Bajc, A. Melfo, G. Senjanovic, F. Vissani, Yukawa sector in non-supersymmetric renormalizable SO(10), Phys. Rev. D73 (2006) 055001. [arXiv:hep-ph/0510139](#), [doi:10.1103/PhysRevD.73.055001](#).
- [693] S. Bertolini, L. Di Luzio, M. Malinsky, Light color octet scalars in the minimal SO(10) grand unification, Phys. Rev. D87 (8) (2013) 085020. [arXiv:1302.3401](#), [doi:10.1103/PhysRevD.87.085020](#).
- [694] G. Altarelli, D. Meloni, A non supersymmetric SO(10) grand unified model for all the physics below  $M_{GUT}$ , JHEP 08 (2013) 021. [arXiv:1305.1001](#), [doi:10.1007/JHEP08\(2013\)021](#).
- [695] G. Aad, et al., The ATLAS Experiment at the CERN Large Hadron Collider, JINST 3 (2008) S08003. [doi:10.1088/1748-0221/3/08/S08003](#).
- [696] S. Chatrchyan, et al., The CMS Experiment at the CERN LHC, JINST 3 (2008) S08004. [doi:10.1088/1748-0221/3/08/S08004](#).
- [697] W. Chung, CULTASK, The Coldest Axion Experiment at CAPP/IBS in Korea, PoS CORFU2015 (2016) 047.
- [698] J. Aalbers, et al., DARWIN: towards the ultimate dark matter detector, JCAP 1611 (2016) 017. [arXiv:1606.07001](#), [doi:10.1088/1475-7516/2016/11/017](#).
- [699] E. Armengaud, et al., Conceptual Design of the International Axion Observatory (IAXO), JINST 9 (2014) T05002. [arXiv:1401.3233](#), [doi:10.1088/1748-0221/9/05/T05002](#).
- [700] L. Evans, P. Bryant, LHC Machine, JINST 3 (2008) S08001. [doi:10.1088/1748-0221/3/08/S08001](#).
- [701] N. Rowell, N. Hambly, White Dwarfs in the SuperCOSMOS Sky Survey: the Thin Disk, Thick Disk and Spheroid Luminosity Functions [arXiv:1102.3193](#).
- [702] S. DeGennaro, T. von Hippel, D. E. Winget, S. O. Kepler, A. Nitta, D. Koester, L. Althaus, White Dwarf Luminosity and Mass Functions from Sloan Digital Sky Survey Spectra, Astron. J. 135 (2008) 1–9. [arXiv:0709.2190](#), [doi:10.1088/0004-6256/135/1/1](#).